

AD A 122 373

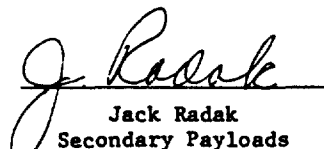
2

SSD 82-0165

GPS / IGS DESIGN
ANALYSIS REPORT
VOLUME I

NOVEMBER 15, 1982

Contract F04701-76-C-0216
CDRL 008A4


Jack Radak
Secondary Payloads
Program Manager

DTIC
ELECTE
DEC 15 1982
S B D

DTIC FILE COPY



Rockwell International
Space Operations/Integration &
Satellite Systems Division

DISTRIBUTION STATEMENT A

Approved for public release;
Distribution Unlimited

82 12 02 029

Best Available Copy

FOREWORD

The results of the GPS secondary payloads, Integrated Operational Nuclear Detection System (IONDS) design analysis task, performed by Rockwell International Space Operations/Integration and Satellite Systems Division for the USAF Space and Missile Systems Organization under contract number F04701-76-C-0216, are documented in this report. Much of the effort that led to the results presented in this report originated with the IONDS legacy task defined in contract amendment P00072 to GPS contract F04701-74-C-0527. The report, published in two volumes (Volume I, GPS/IGS Design Analysis; and Volume II, GPS Spacecraft Impacts), has also been summarized in the "GPS Secondary Payloads Executive Summary Update," dated Feb. 20, 1978. The GPS/IONDS interfaces developed through this effort are documented in:

- GPS Secondary Payloads RF Compatibility Test Report (SD 77-GP-0046)
- GPS Secondary Payloads IGS Component Integration Test Report (SD 78-GP-0010)
- GPS Secondary Payloads Integrated System Test Report (SD 78-GP-0012-1)

The IONDS subsystem described in this report is the basic design tested on the Engineering Test Vehicle (ETV). This GPS/IGS Design Analysis Report summarizes the design and validation testing performed on the IGS payload to demonstrate the projected capability of IGS and assure compatibility with GPS. It is the culmination of several previous editions as draft copies for internal program reviews and references. The report is intended to describe the design/validation phase of the IGS program and therefore reflects the status of the program as of September 1978. Subsequently, several changes have occurred in the program, including incorporation of some of the recommended changes contained in this report. However, these changes are not part of the design/validation phase of the program and were not described in this report.

The analysis and testing efforts for the above tasks were managed by R.F. D'Ausilio and J.A. Canaday. Technical direction was provided by D.S. Mercadante. This report was compiled by E.J. Dryer and P.J. Berndsen, with major contributions from R. Feldt, T.H. Moore, W.D. Eden, R.A. Gronlund, A.C. Goo, F. Knowlden, and C.W. Huston. The radio astronomy analysis, contained in the appendix, was prepared by Dr. L.O. Krause.

U.S. Air Force personnel who coordinated the tests included Lt. Col. A.H. Hayden, Capt. H. Hatlelid, R. Rennard, and B. Shelton, and Lt. Marilyn Jowdy of SAMSO.



<input checked="" type="checkbox"/> <input type="checkbox"/> <input type="checkbox"/>		PER LETTER	
		By _____	
Distribution/		Availability Codes	
Dist		Avail and/or Special	
A			

CONTENTS

Section		Page
1	INTRODUCTION AND SUMMARY	1
	1.1 Introduction	1
	1.2 Program Summary	9
2	NAVSTAR GLOBAL POSITIONING SYSTEM (GPS)	17
	2.1 GPS Objectives	17
	2.2 GPS System Description	18
	2.3 GPS/IGS Interfacing Subsystems	19
3	IONDS GLOBAL SEGMENT (IGS)	27
	3.1 IGS Objective	27
	3.2 IGS System Description	27
	3.3 IGS User Operations	35
	3.4 GPS Time and Frequency Synthesis	39
	3.5 Code Characteristics	39
	3.6 Downlink System Data	42
4	GPS/IGS SUBSYSTEM DESIGN	59
	4.1 Requirements and Constraints	59
	4.2 IGS Design	59
	4.3 IGS/GPS Design Integration	92
5	RELIABILITY	111
	5.1 Reliability/Compatibility Analysis	111
	5.2 Reliability Predictions and Failure Mode Effects Analysis	112
	5.3 Critical Item List	117
	5.4 Parts, Materials, and Processes	118
6	TEST PROGRAM	119
	6.1 Test Plan	119
	6.2 Component Tests	119
	6.3 L3 Subsystem Tests	128
	6.4 IGS System Tests	132
	6.5 GPS Integration Tests	152
	6.6 GPS/SPL Thermal Control Tests	204
7	CONCLUSIONS AND RECOMMENDATIONS	217
	7.1 Conclusions	217
	7.2 Recommendations	218
	APPENDIX	
	RADIO ASTRONOMY INTERFERENCE STUDY	219

ILLUSTRATIONS

Figure		Page
1	GPS-SPL Configuration	5
2	IGS Functional Block Diagram	5
3	IGS/GPS Components	7
4	IGS L ₃ Transmitter Chain	8
5	L ₃ Encoder	8
6	L ₃ Encoder Circuit Board	9
7	IGS Development Schedule	10
8	FSV 6 Schedule	12
9	GPS Program Plan	17
10	GPS Space Vehicle Subsystems	21
11	Navigation Subsystem	22
12	TT&C External Interface	23
13	Functional Flow Diagram	27
14	Installation of IGS Components on GPS Vehicle	29
15	IONDS Data Coding	30
16	Baseband Interface Timing Relationship	30
17	IGS Data Format	31
18	Encoder Timing Diagram	32
19	IONDS/GPS Receiving Terminals	33
20	IONDS Receive Block Diagram	34
21	IONDS Receiving Terminal Processing Functions	34
22	Global Burst Detection Parameters	36
23	Relationship Between SV Times	36
24	P Code Generation	41
25	L ₁ P Signal - Flux Density at Ground Versus Frequency	44
26	L ₃ P Signal - Flux Density at Ground Versus Frequency	45
27	Typical Transmitted Carrier Phase Noise Spectral Density Versus Offset Frequency at 10.23 MHz	46
28	GPS Received Power Versus User Elevation Angle, L ₁ and L ₂	47
29	Flow Chart for User Implementation of Parity Algorithm	57
30	IONDS/GPS Overall Block Diagram	60
31	GBD Block Diagram	62
32	Baseband/Processor Functional Block Diagram	64
33	IONDS Modified Baseband	65
34	Baseband Board 2 With SPL Components Added	67
35	L ₃ Encoder Block Diagram	68
36	Block Encoder/Sync Detector Block Diagram	68
37	Differential Encoder Block Diagram	69
38	Convolutional Encoder Block Diagram	69
39	L ₃ Transmitter and Encoder Schematic	71
40	L ₃ Transmitter Characteristics (EDM)	72
41	L ₃ Switch and Power Divider (EDM)	72
42	L ₃ Encoder	73

Figure		Page
43	L ₃ Transmitter Assembly Block Diagram	73
44	L ₃ Synthesizer Mechanization	74
45	Loop Logic Schematic	76
46	Loop Filter and VCO Schematic	76
47	X ₉ Frequency Multiplier Schematic	78
48	AGC Amplifier Schematic	78
49	BPSK/QPSK Modulator Diagram	79
50	Quadruphase Modulator Diagram	79
51	IPA/HPA Block Diagram	81
52	IPA/HPA Schematic	81
53	Power Monitor Block Diagram	83
54	Power Monitor Schematic	83
55	Coaxial Switch Latching Drive Assembly	84
56	Power Supply Block Diagram	85
57	Dc/dc Converter Schematic	86
58	+20 Volt Series Regulator Schematic	87
59	Diplexer Schematic Diagram	88
60	Triplexer Schematic Diagram	88
61	Triplexer Frequency Response Characteristics	89
62	Triplexer Block Diagram	89
63	IGS Diplexer/Triplexer Modification	90
64	GPS/SPL Antenna	90
65	Principal Plane Radiation Pattern	91
66	Timing Interface Box	92
67	Magnitude Command Format	95
68	Magnitude Command Data, Clock and Enable Signal Phase Relationships	96
69	Discrete and SOH Telemetry Interface Schematic (Reference)	98
70	Encoder Interface Timing Relationship	100
71	Sensor Processor/Load Control Unit Interface Simplified Schematic (Reference)	101
72	IGS Grounding Schematic	103
73	X-Sensor (BDX) Field of View	104
74	Integrated SV/PSE Configuration	105
75	GBD Test Set Interface	106
76	L ₃ Transmitter and Encoder Reliability Logic Diagrams	113
77	Baseband Processor Reliability Logic Diagram	114
78	Triplexer Reliability Logic Diagram	115
79	L ₁ , L ₂ , and L ₃ Reliability Logic Diagrams	116
80	L ₁ , L ₂ , and L ₃ Reliability Comparison	117
81	IGS Parts Selection Process	118
82	GPS Pull-Up Antenna Configuration	120
83	L ₁ Gain Impact	120
84	L ₁ Ellipticity Impact	121
85	L ₂ Gain Impact	122
86	L ₂ Ellipticity Impact	122
87	Triplexer VSWR Plot, Port 1 to Port 4	124
88	Triplexer Loss Plot, Port 1 to Port 4	124
89	Triplexer VSWR Plot, Port 2 to Port 4	125



Figure		Page
90	Triplexer Loss Plot, Port 2 to Port 4	125
91	Triplexer VSWR Plot, Port 3 to Port 4	126
92	Triplexer Loss Plot, Port 3 to Port 4	126
93	Triplexer Loss Plot, Port 3 to Port 1	127
94	Triplexer Loss Plot, Port 3 to Port 2	127
95	L3 Transmitter and Encoder Development Procedure	129
96	L3 Transmitter and Encoder Engineering Model Test Summary	129
97	Prototype Circuit Data	133
98	Junction Temperature	134
99	L3 Transmitter Power Loss Distribution	134
100	1381-MHz Filter Response	135
101	Breadboard Tests - Encoder	136
102	Breadboard Tests - Squaring Amplifier	137
103	Baseband Processor Readiness Test	137
104	Encoder Readiness Test	138
105	BDP Readiness Test	139
106	Baseband/Encoder Readiness Test	141
107	EDC Overall Test Configuration	143
108	Block Diagram - Final ICI	145
109	ICI Overall Test Setup	145
110	Final ICI ETV Configuration	146
111	GBD Test Set (CANOE)	147
112	Checkout Equipment for the ICI Test	151
113	IGS Control and Monitor Test Set Equipment Layout	153
114	ETV RF Compatibility Test Configuration	155
115	Electrical Test Vehicle Installed in Anechoic Chamber	156
116	Signal Compatibility Test System	156
117	L1 User Impact	157
118	L2 User Impact	158
119	Intermod Test Equipment on ETV	159
120	IGS Telecom Test Set	160
121	Data Acquisition, Control, and Processing Test Set	161
122	DACP Peripheral Equipment	161
123	TT&C Intermodulation Noise Test Results	162
124	Cross-Strapping	165
125	IGS Test Configuration	185
126	10.23 MHz Distribution	185
127	Cross-Strapping Results	186
128	IONDS Receiver Threshold Sensitivity Test Setup	189
129	Delay Offset Correlation Loss	189
130	DTV With Secondary Payload Hardware on Forward Bulkhead	192
131	Alternative Sunshade Mountings	194
132	IGS X-Sensor Random Vibration Qualification Levels (X-Axis)	195
133	IGS X-Sensor Random Vibration Qualification Levels (Y- and Z Axes)	196
134	IGS Y-Sensor Random Vibration Qualification Levels (Y-Axis)	197
135	IGS Y-Sensor Random Vibration Qualification Levels (X- and Z-Axes)	198

Figure		Page
136	BDP Y-Sensor Random Vibration Qualification Levels (X-, Y-, and Z-Axes)	199
137	L3 Transmitter and Encoder Random Vibration Qualification Levels (Y-Axis)	200
138	L3 Transmitter and Encoder Random Vibration Qualification Levels (X- and Z-Axes)	201
139	Triplexer Random Vibration Qualification Levels (X-, Y-, and Z-Axes)	202
140	SPL Doubler Requirements	207
141	SPL Equipment Nodal Location - Forward Face, Forward Bulkhead	209
142	SPL Equipment Nodal Location - +Y Shear Panel	210
143	SPL Equipment Nodal Location - -Y Shear Panel	210
144	SPL Equipment Nodal Location - Forward Face, Aft Bulkhead	211
145	Proposed SPL Radiator Addition	211

TABLES

Table		Page
1	IGS ETV System Parameters	6
2	IGS Analyses and Investigations	13
3	IGS Documentation - Rockwell Reports	14
4	IGS Documentation - Rockwell Specifications and Interface Control Documents	14
5	IGS Test Summary	15
6	GPS Launching Schedule	18
7	Navigation Subsystem Requirement Summary	22
8	NAV System Operating Modes	43
9	FSV 6 EIRP at Channel Center Frequency	44
10	Composite L ₁ Transmitted Signal Phase and Code State Relationship for Normal Mode	48
11	Subframe Identification	49
12	Elements to Earth-Fixed Coordinates	51
13	Data Block II Definitions	52
14	Data Block II Parameters	53
15	Data Block III Content	54
16	Burst Detection Sensor Spacecraft Requirements	61
17	L ₃ Frequency Synthesizer Characteristics	74
18	Loop Filter/VCO Performance Data	77
19	X ₉ Frequency Multiplier	77
20	Teledyne CS33S6-C-Coaxial Switch	83
21	Power Supply Output Requirements	84
22	Sensor Processor Telemetry Outputs	97
23	L ₃ Hardware MIL-STD Compliance Summary	107
24	IGS Weight Summary	108
25	IGS Prime Power Summary	109
26	Diplexer/Triplexer Comparison	123
27	L ₃ Transmitter and Encoder Functional Testing	130
28	L ₃ Transmitter and Functional Test Parameters	130
29	L ₃ Encoder Test Parameters	131
30	Environmental Test Conditions - Transmitter and Encoder	131
31	GPS and IGS Transmitter Characteristics	132
32	HPA Output Transistor Power Consumption	132
33	Thermal Design Analysis for Transistor TRW-1417-11	133
34	BPSK Modulator Prototype Test Data	138
35	ICI Console Operations	153
36	Integration Test Overview	154
37	GPS/SPL Signal Compatibility Parameters	157
38	TT&C Key Parameters	159
39	IGS Telecom Test Set Functions	160
40	L ₃ Transmission Tests	163
41	Interface Verification	164
42	Cross-Strapping Matrix	165

Table		Page
43	IGS Checkout Test Run	166
44	SOH Readout	176
45	X and Y Calibration Readout	181
46	Interface Verification Test Anomalies	186
47	Data Transmission Matrix	187
48	ETV Cross-Strapping Problems.	187
49	Threshold Test Summary	192
50	Summary of Secondary Payloads Acoustic Testing	193
51	Summary of IGS Component G rms Test Results	203
52	Comparison of IGS Test G rms Values	204
53	SPL Nodal Inputs	208
54	SPL Equipment Power Dissipation	209
55	IGS Equipment Temperature - On-Orbit Steady-State Cold Case	212
56	IGS Equipment Temperatures - On-Orbit Steady-State Hot Case	212
57	GPS Component Temperatures - Hot Case (IGS Configuration)	213
58	SCT/IGS Equipment Temperatures - On-Orbit Steady-State Cold Case	214
59	SCT/IGS Equipment Temperatures - On-Orbit Steady State Hot Case	214
60	GPS Component Temperatures - Hot Case (IGS/SCT Configuration)	215

LIST OF ACRONYMS AND ABBREVIATIONS

AFSCF	Air Force Satellite Control Facility
AGC	Automatic Gain Control
AIL	Airborne Instrument Lab
AKM	Apogee Kick Motor
AODC	Age of Data (Clock)
AODE	Age of Data (Ephemeris)
ATA	Acceptance Test Analyzer
AVCS	Attitude and Velocity Control Subsystem
BBP	Baseband Processor
BDP	Burst Detector Processor
BER	Bit Error Rate
bps	Bits per Second
BPSK	Bi-Phase Shift Key
C/A	Clear/Acquisition
CANOE	GBD Test Set
CCIR	International Radio Consultative Committee
CONUS	Continental U.S.
DACP	Data Acquisition, Control, and Processing
dBc	Decibel Referred to Carrier
dB _i	Decibel Referred to Isotropic
dB _m	Decibel Referred to One Milliwatt
dBW	Decibel Referred to One Watt
DCD	Dual Command Decoder
DLL	Delay Lock Loop
DRS	Delta Range Sigma
DTV	Development Test Vehicle
EDC	Engineering Data Compatibility
EDM	Engineering Development Model
EIRP	Effective Isotropic Radiated Power
EMC	Electromagnetic Compatibility
EMI	Electromagnetic Interference
EOE	Edge of Earth
EPS	Electrical Power Subsystem
ETV	Electrical Test Vehicle
FMEA	Failure Mode Effects Analysis
FSV	Flight Space Vehicle
GFE	Government Furnished Equipment
GPS	Global Positioning System
GSE	Ground Support Equipment

HOW	Handover Word
HP	Hewlett Packard
HPA	High Power Amplifier
HUL	Hardware Utilization List
IAM	Incidental Amplitude Modulation
ICI	IGS Component Integration
IGS	IONDS Global Segment
IONDS	Integrated Operational Nudet Detection System
IPA	Intermediate Power Amplifier
IST	Integrated System Test
IUS	IONDS User Segment
JCS	Joint Chiefs of Staff
LCU	Load Control Unit
MCEB	Military Communications Electronics Board
MCS	Master Control Station
MDM	Mission Data Message
MSB	Most Significant Bit
NAV	Navigation
NDS	Navigation Development Satellite
NTS	Navigation Technology Satellite
NWS	Naval Weapons Station
NUDET	Nuclear Detonation
P	Precision
PCM	Pulse Code Modulation
PCU	Power Control Unit
PLL	Phase Lock Loop
PMPCB	Parts, Materials, and Processes Control Board
PPPL	Program Preferred Parts List
PRN	Pseudo-Random Noise
PSE	Peculiar Support Equipment
QPSK	Quadrature Phase (or Quadri Phase) Shift Key
QTV	Qualification Test Vehicle
RAF	Radio Astronomy Filter
RAS	Radio Astronomy Service
RCS	Reaction Control System
RF	Radio Frequency
RTS	Remote Tracking Station
SAMSO	Space and Missile Systems Office
SCD	Specification Control Drawing
SCF	Satellite Control Facility
SCT	Single-Channel Transponder
SCU	Signal Conditioning Unit
SGLS	Space Ground Link System

SHB Shaped Hemispherical Beam
SOH State of Health
SPG Single Point Ground
SPL Secondary Payload
SPS Samples per Second
STC Satellite Test Center
STI Stanford Telecommunications, Inc.

TCS Thermal Control Subsystem
TDOA Time Difference of Arrival
TIE Timing Interface and Encoder
TLM Telemetry
TOA Time of Arrival
TT&C Telemetry, Tracking, and Command

ULS Upload Station

VCO Voltage Controlled Oscillator

WER Word Error Rate

1. INTRODUCTION AND SUMMARY

1.1 INTRODUCTION

1.1.1 Background

Recent and projected changes in the nuclear posture of the major countries of the world have significantly increased the requirements for timely nuclear detonation (NUDET) surveillance. To fulfill these requirements the Department of Defense and the U.S. Air Force initiated studies that led to the establishment of the Integrated Operational NUDET Detection System (IONDS).

These studies suggested that many of these detection and location requirements could be accomplished by including a NUDET sensor on the Navstar satellite since the successful development of the Navstar Global Positioning System (GPS) had provided advancements in the state-of-the-art precision time and frequency standards. The precision navigation capability provided by these time and frequency standards through precise transit time measurements also makes the implementation of a precise NUDET location system feasible. This, plus the worldwide coverage afforded by the GPS satellites, makes the GPS an ideal host for the NUDET surveillance mission.

Feasibility studies investigating the concept of implementing a global burst detector (GBD) on the GPS satellite were performed by Rockwell and subsequently verified by Ford Aerospace and Communication Corporation, the IONDS system engineering contractor. Following these studies, the development of the IONDS global segment (IGS) was initiated with Rockwell in mid-1976. Subcontracts were awarded to ITT to develop the modified baseband/processor and the triplexer for the IGS, to Autonetics for the L₃ transmitter and L₃ encoder, and to Stanford Telecommunications for a compatible test receiver. At the same time Sandia Laboratories and Los Alamos Scientific Laboratory started development of the sensors and processor that are government-furnished equipment (GFE) provided by the Department of Energy (DOE).

The IONDS program was structured to provide an orderly progression of analysis and tests to validate the projected capability of the IGS and its compatibility with the GPS satellite. A series of tests ranging from component acceptance tests through integrated system functional tests was performed resulting in the evolution of an optimum hardware and system interface toward a flight configuration.

The data derived from this series of tests demonstrated that the system mechanization and hardware satisfied the IONDS mission requirement. Further, these tests demonstrated that these IONDS requirements can be achieved on the GPS host vehicle without introducing any deleterious effects on the prime GPS navigation mission. As a result, the USAF has directed that the IONDS subsystem be incorporated into and flown on the Navigation Development Satellite (NDS) 6 GPS Phase I satellite.

1.1.1.1 Objectives. The objectives of the program were as follows:

1. Develop IONDS hardware: Design, fabricate, and test each subsystem at the box, subsystem, and integrated levels.
2. Develop GPS/IGS interfaces: Design, fabricate, and test the box-level interfaces and perform a working interface test between the modified GPS boxes and the IGS hardware. This includes identifying and resolving any condition that could potentially impact GPS operation.
3. Develop an IGS maturity: Provide an overall emphasis in the IONDS program to develop maturity via detailed ground tests, part and component selection, and design equivalent to that being achieved by the GPS satellite in its Phase I program.

1.1.1.2 Ground Rules. The following ground rules were established.

1. IONDS must be implemented without an impact on the navigation mission as determined by measurements of navigation performance parameters that can resolve system degradation within 1/4 dB.
2. IONDS implementation must result in minimum spacecraft modifications by using a basic design approach that incorporates as much of the interface design into the secondary payload (SPL) hardware as possible.
3. IONDS implementation must maintain the total satellite weight so that it remains within the boost capability of the Atlas F.

1.1.2 Alternate Approaches

Various alternative concepts that could accomplish the IONDS mission were analyzed early in the program. Several of the more significant considerations are summarized below.

1.1.2.1 Selection of the L₃ Frequency for IONDS. Two L-band downlinks (L₁ and L₂) have been implemented to provide mission data to GPS users. These two GPS data streams are multiplexed together and transmitted from a common L-band antenna. To minimize the IONDS impact to the GPS system and to reduce the cost and risk, a third L-band link (L₃) was selected with its frequency located about midway between the L₁ and L₂ frequencies. This frequency selection allows the existing GPS L-band antenna to be used for IONDS data transmission. Further, the selection of the L₃ link permits the use of the proven GPS L-band RF link approach and its associated receiver technology for IONDS. The L₃ frequency selected was 1381.05 MHz. The choice was the result of a tradeoff analysis of (1) L-band antenna pattern, (2) intermodulation interference, (3) triplexer design, (4) ease of frequency synthesis, and (5) radio astronomy considerations.

The GPS spacecraft's L-band antenna was designed to satisfy requirements imposed by the navigation mission on the L₁ and L₂ downlinks. Tests have verified that the gain and pattern coverage of this L-band antenna were relatively constant between the designated L₁ and L₂ frequencies. The selection of the L₃ frequency of 1381.05 MHz satisfied IONDS antenna performance

requirements and other requirements imposed by such elements as frequency synthesis and intermodulation interference.

1.1.2.2 Radio Astronomy Interference. Two of the assigned radio astronomy frequency bands are in or near the GPS L-band spectrum (1400 to 1427 MHz and 1664.4 to 1668.4 MHz). There is a potential for interference between the 1400- to 1427-MHz band and the IONDS L₃ frequency assignment. A radio astronomy study was performed to predict the energy in the radio astronomy band due to IGS L-band transmissions. This included a spectrum analysis that was verified by testing at full power. This test indicated that some low-level energy from L₃ falls within the radio astronomy band. However, in the normal mode, the L₃ transmitter operates only when it detects an event, and then only long enough to get the data to the ground. Normally, this will require less than one minute of transmission. Random triggers from cosmic particles and very powerful lightning strikes can trigger the system but are expected to be quite infrequent. There will also be a test/calibrate mode that will be used approximately weekly when the system is established. Considering all modes, there should be on the average less than five minutes of transmission per day per satellite. Due to the unusual energy and low-duty factor (the time L₃ is transmitting divided by the typical radio astronomy integration time), there should be no interference with the Radio Astronomy Service (RAS). This is to be demonstrated by NDS 6 in a test fully coordinated with the RAS. An in-line L₃ filter, which would decrease the L₃ signal level in the 1400- to 1427-MHz band by approximately 27 dB, is being considered to eliminate potential L₃/RAS interference even with extended L₃ transmission time.

The Radio Astronomy Technical Report has been included in this document as an appendix.

1.1.2.3 Existing GPS Data Links. Using the existing GPS L-band navigation and S-band telemetry data links simultaneously was considered for IONDS data links. None of the existing GPS data links investigated for the IONDS system could provide the data rate or the receiving terminal flexibility necessary to satisfy IONDS user requirements. The existing L₁ and L₂ data capacity was insufficient to meet IONDS requirements. Using the GPS L₂ downlink frequency in a quadrature phase shift keyed (QPSK) mode was analyzed and found capable of providing the necessary data rate and user terminal flexibility required for the IONDS mission. However, this segment of the L₂ channel has been reserved for possible expansion of the GPS navigation mission. For that reason, further consideration of the L₂ link for IONDS was terminated. The GPS S-band downlink for IONDS was not feasible since it would involve the use of a large, fixed ground site.

1.1.2.4 Electromagnetic Compatibility (EMC). The electromagnetic environment on the GPS spacecraft has been analyzed to assure a minimum impact to the GPS system and mission from adding the IONDS hardware. The EMC hardware test performed in late 1977 and early 1978 verified that the IONDS system did not impact or interfere with GPS operation or the GPS navigation mission. The operation of the IONDS L₃ system was also verified during the radio frequency interference (RFI) testing using an L₃ transmitter operating into an L₃ test receiver.

1.1.2.5 The IGS System. The IGS is made up of space and ground segments. It has been developed to the point that space-related hardware has been integrated with the GPS system and thoroughly evaluated by numerous tests which demonstrated that there was no GPS navigation mission impact and that the IGS system exceeded performance specifications over the full MIL-STD-1540 range.

The GPS/SPL configuration is shown in Figure 1. This secondary payload configuration includes IGS and the AFSATCOM single-channel transponder (SCT). This SPL on-orbit external configuration is characterized by additions on the forward bulkhead. All of the telemetry, tracking, and command (TT&C), navigation (NAV), IGS, and SCT devices on the bulkhead have fixed optical and electrical axes aligned parallel to the spacecraft's local vertical. The SPL units are the IGS optical (BDY) sensor and sunshade, the X-ray (BDX) sensor, and the SCT UHF and SHF antennas. The IGS shares the GPS L-band mission antenna, eliminating the requirement for a separate antenna that would have significantly complicated the earth-pointing forward bulkhead. The sunshade material and paints are nonconductive, thus the sunshade is transparent at microwave frequencies and does not create radiation pattern blockages.

A functional block diagram of the IGS is shown in Figure 2.

The IGS system consists of BDX and BDY sensors located on the GPS forward bulkhead, a sensor processor, an encoder, and a separate L-band transmitter all supported by GPS subsystems. The system has been designed to accomplish its mission objectives and function on a noninterfering basis with the GPS system.

Nuclear burst detection and location are determined from optical and X-ray signals received by the sensors. Sensor data are fed to the burst detector processor (BDP) where they are processed and synchronized to the GPS clock. The BDP enables the L₃ encoder and provides event data for encoding. The L₃ encoder uses the 10.23-MHz reference frequency and the GPS P code to provide modulated data to the L₃ transmitter. The L₃ transmitter uses a frequency midway between the GPS L₁ and L₂ channels for transmitting event data. These three L-band channels are combined in the GPS triplexer and fed to a common L-band antenna for transmission to the ground terminals.

The IGS employs the GPS precision time capability to measure the time of arrival (TOA) of the nuclear burst signal. Using TOA data from several GPS satellites, IONDS can accurately determine event locations. IGS system parameters are summarized in Table 1. The L₃ transmitter chain equipment is illustrated in Figures 3 through 6.

Figure 3 shows the five new units in the IGS subsystem and the two key GPS units modified to accept the secondary payload. In the upper left are the Sandia X-ray (BDX) and optical (BDY) sensors. Data from these units are processed in the Sandia data processor (BDP) shown in the lower left corner. All three Sandia units are internally redundant for reliability.

Pictured in the bottom center and right corner of Figure 3 and in Figures 4, 5, and 6 are the encoder and transmitter built by Rockwell Autonetics for the IONDS dedicated downlink.

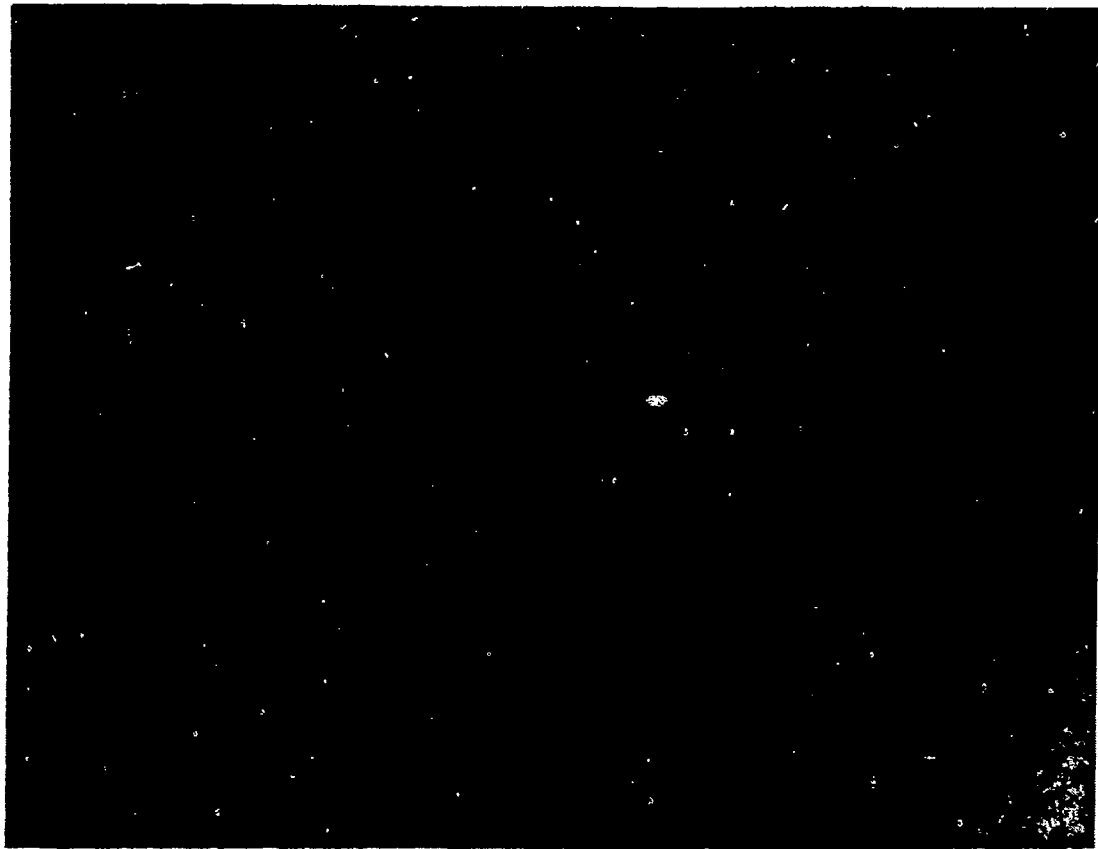


Figure 1. GPS-SPL Configuration

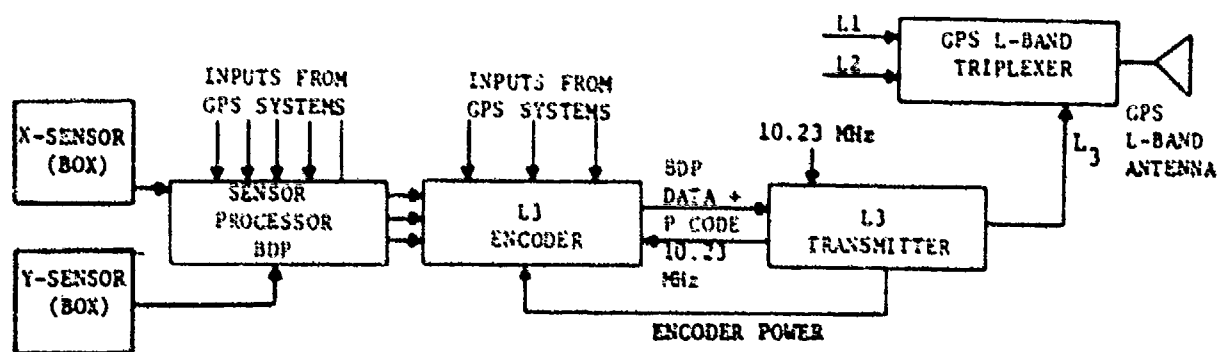


Figure 2. IGS Functional Block Diagram

Table 1. IGS ETV System Parameters

Parameter	Value
L ₃ frequency	1381.05 MHz (nominal)*
L ₃ transmitter power	18.5 watts (measured)
Antenna gain on axis	9.9 dB (measured)
Antenna gain at 5 degrees elevation	11.4 dB (measured)
Worst-case system margin	2.2 dB (predicted)
IGS power required (total)	92.2 watts (measured)
IGS system weight (total)	61.2 lb (measured)
L ₃ /L ₁ timing error	100 nanoseconds (predicted)
*Refer to Section 3.6	

The encoder has several functions, one of which is to reduce the power demand for a 200-bps data rate from the spacecraft by differential and block encoding. The overall bandwidth gain obtained by this process is 5 dB (a factor of 3.16 power reduction). The encoder also contains a Modulo 2 adder that combines the coded data with the GPS P code. The resultant signal permits the identification of each satellite on a single carrier frequency by GPS code division multiple-access techniques. The encoder is internally redundant to provide reliable operation for at least five years.

Redundant transmitter units (A and B) are used for high reliability. Transmitter A is identical to transmitter B, except for an RF transfer switch module to couple either transmitter to the triplexer. One of the two IGS transmitters is shown. IGS transmitters A and B are never operated simultaneously. Transmitter output is 17 watts minimum at a center of frequency of 1381.05 MHz. This frequency is derived from the NAV frequency standard via a voltage-controlled oscillator (VCO) and a frequency multiplier chain that multiplies the frequency standard output (10.23 MHz) by a factor of 135.

In the upper right corner of Figure 3 are the GPS/ITT units that were modified to support the IONDS payload. The larger unit is the baseband processor, which will have a minor modification to provide the GPS timing signal for IGS use. A third port was added to the existing diplexer, providing a triplexer function to couple the two GPS signals at L₁ and L₂ and the IONDS signal at L₃. This triplexer enables IONDS to use the existing GPS mission antenna (top center).

IGS system-level testing was successfully accomplished in March 1978 while operating at full power on the Engineering Test Vehicle in an anechoic chamber.

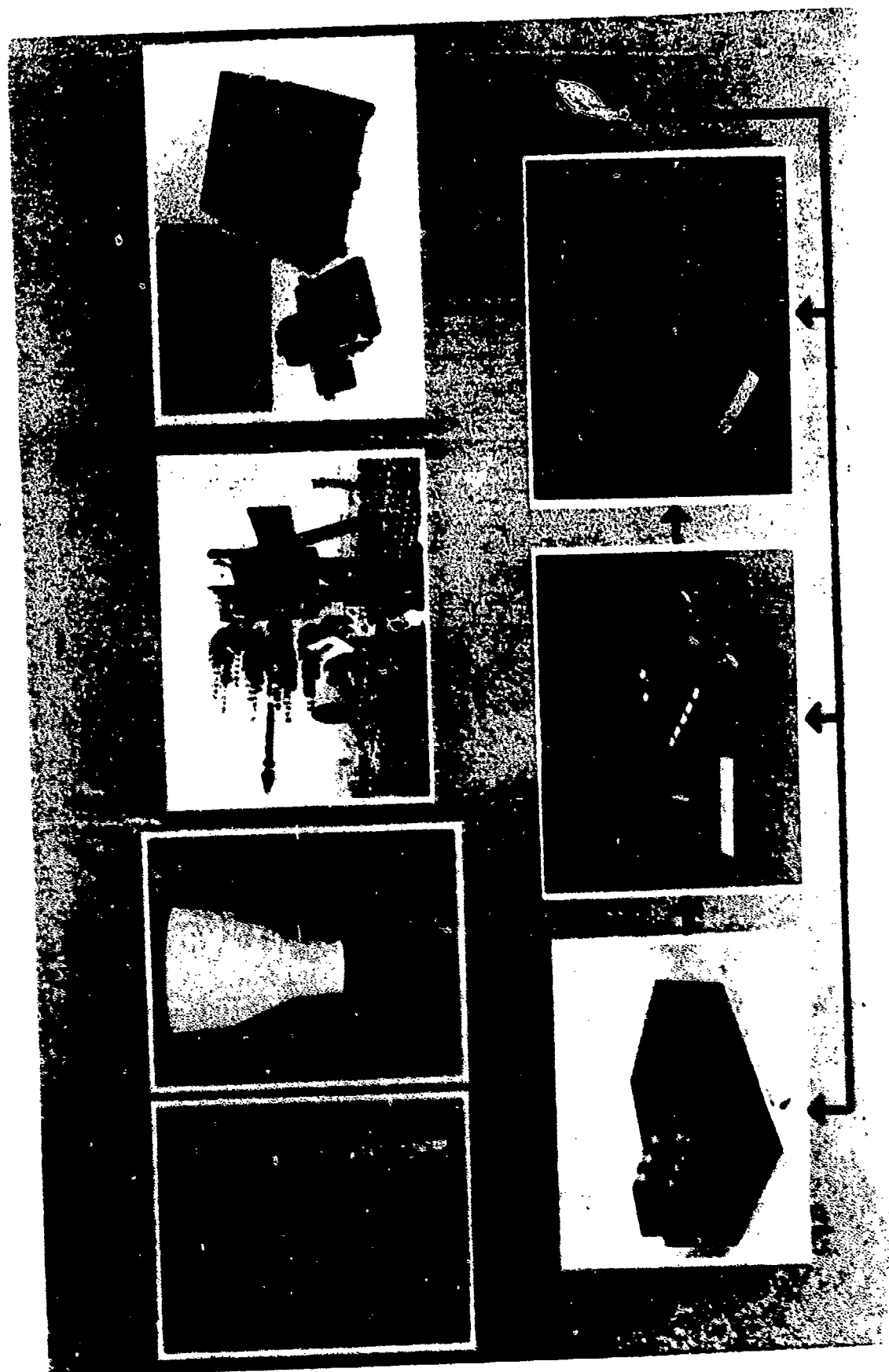


Figure 3. ICS/GPS Components

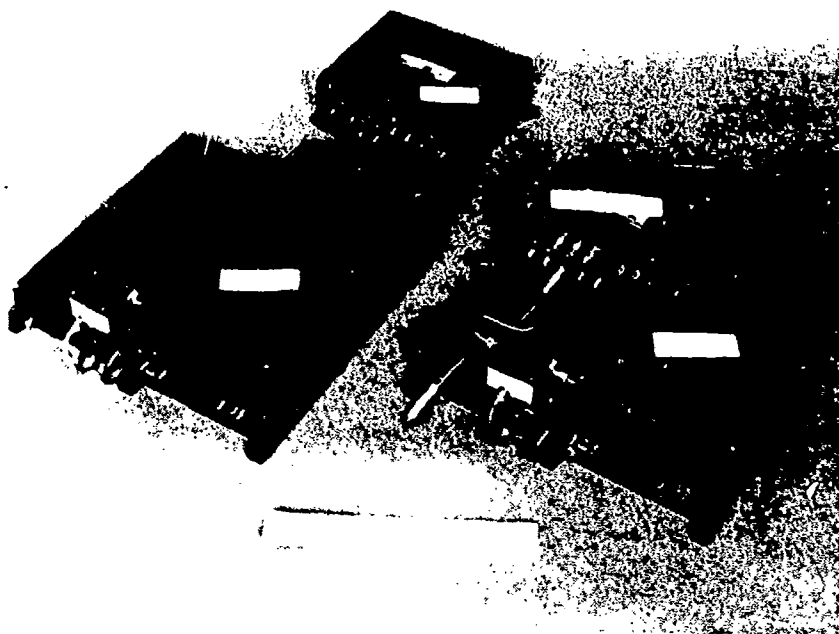


Figure 4. IGS L_3 Transmitter Chain

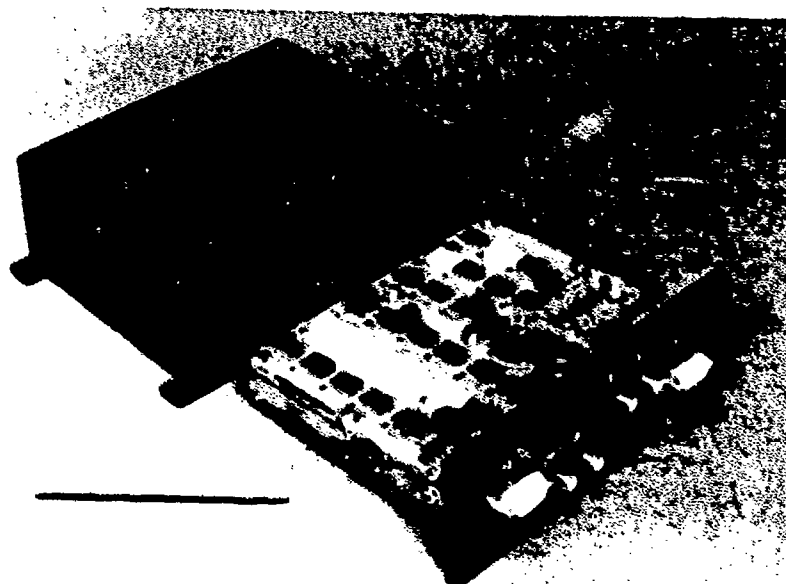


Figure 5. L_3 Encoder

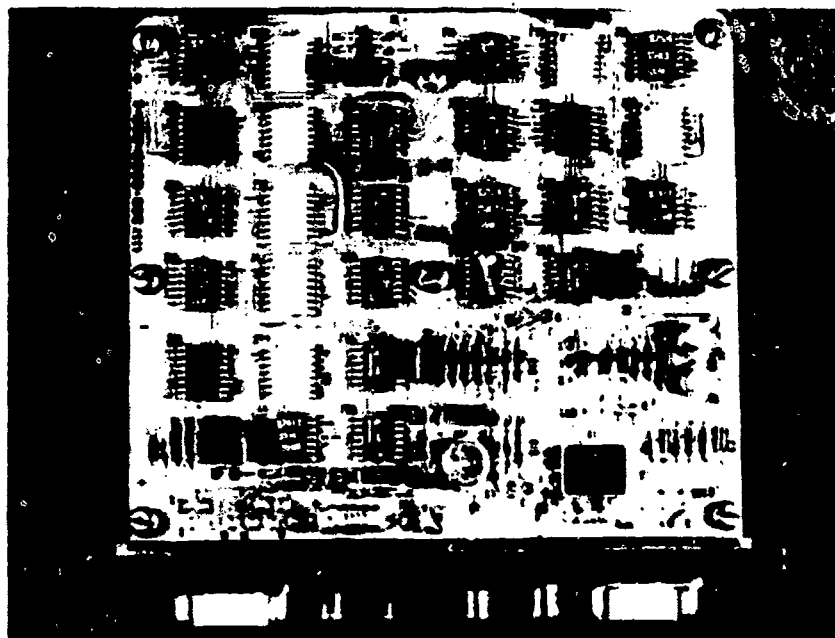


Figure 6. L₃ Encoder Circuit Board

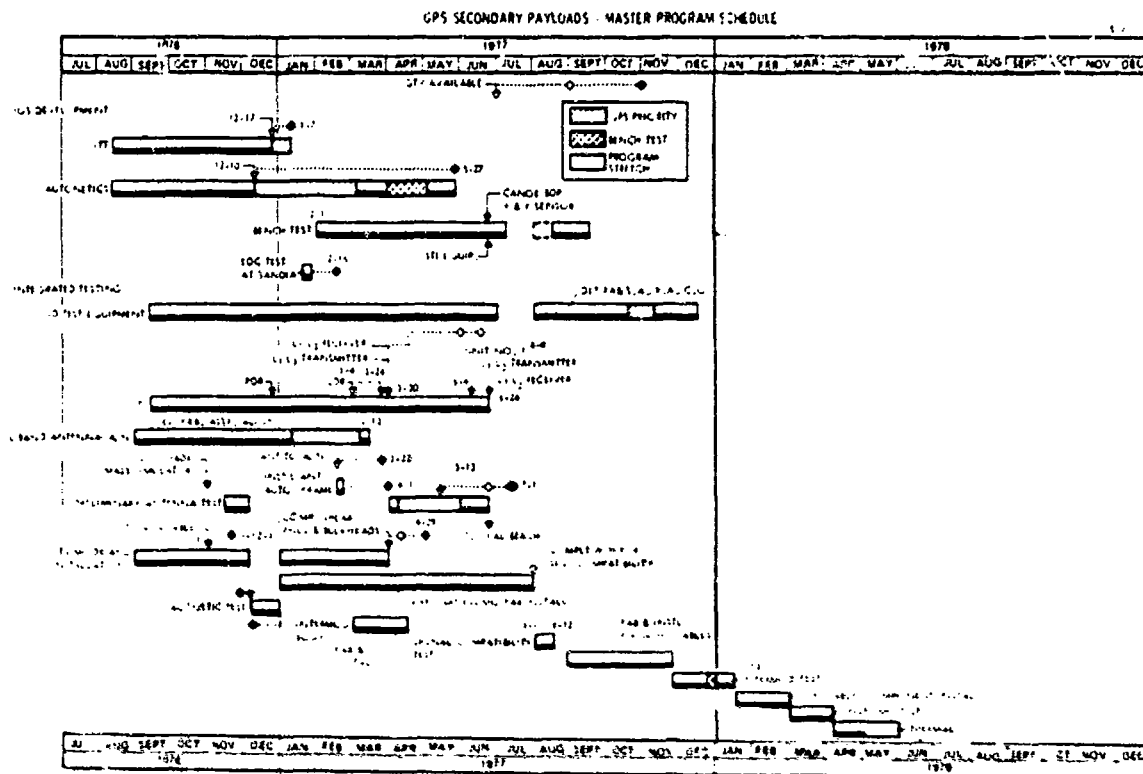
1.2 PROGRAM SUMMARY

1.2.1 IGS Program Overview

The IGS system has been designed to be transparent to the basic GPS navigation function, and if implemented as planned, it will be essentially a no-risk program. These two desirable objectives have been achieved by in-depth analysis and trade studies, by following rigorous engineering standards coupled with intensive verification testing, and by using space-qualified components.

The IGS hardware has been designed, fabricated, and tested to MIL-STD-1540/1541 requirements in accordance with the schedule shown in Figure 7. The initial flight-type engineering models were subjected to full functional and limited qualification tests at the component level. The L₃ encoder, L₃ transmitter, triplexer, and baseband demonstrated full compliance in the areas tested. The IGS hardware was integrated with the SCT, NAV, TT&C, and electrical power subsystem (EPS) hardware and subjected to numerous tests to verify performance compliance and GPS compatibility. Tests were performed in an anechoic chamber at full RF power to investigate intermodulation noise, threshold sensitivity, and EMC. The results of these tests demonstrated that there was no GPS navigation impact and that the IGS system exceeds performance specifications over the entire MIL-STD-1540 range.

The IGS hardware was designed to stringent radiation hardening requirements and made maximum use of parts that had already been tested as part of the GPS program. The IGS radiation hardening test program includes Joint Chiefs of Staff (JCS) and natural environmental total dose testing on 21 selected parts and dose rate testing for the Sandia components and Autonetics transmitter and timing interface and encoder (TIE) units.



Analysis, development, and testing have shown that IONDS equipment can be successfully integrated with the GPS vehicle, in the FSV 6 time frame, without excessive changes to the vehicle. The added IGS weight can be accommodated by the Atlas F launch vehicle and by the apogee kick motor (AKM) by upgrading the perigee kick motors in the stage vehicle. There is adequate power margin to support the IGS payload. Minor revisions required in the NAV, EPS, and TT&C to support SPL operations have been validated to verify the compatibility of the SPL with GPS mission functions. As a result, the Air Force directed in January 1978 that the IGS be incorporated in NDS 6 during its refurbishment from the Phase I Qualification Test Vehicle (QTV) into a flight vehicle.

Full-up testing on an actual satellite (NDS 6) will conclusively prove there is no performance, cost, or schedule risk in incorporating IGS in the GPS vehicle. At the completion of the NDS 6 test sequence, a full set of validated test procedures will exist for use on future satellites. On-orbit test operations with IGS's installed will certify the operational performance of IGS and result in space-proven components being available for future vehicles.

The NDS 6/QTV-type modification can be accomplished economically and be interchangeable with unmodified units. Added wiring may be removed with SPL components or added with SPL components.

The extensive testing and handling of the NDS 6 as the Phase I QTV would normally be expected to shorten its useful life. This is the primary reason NDS 6 is the only GPS not covered by on-orbit incentives. As a result, certain

key areas (i.e., earth sensor) require refurbishment to assure long life. Since NDS 6 is to have an operational IGS payload, these areas are being refurbished to assure a useful life on the order of five years.

A mid-1980 launch data is the earliest feasible because of modifications and refurbishment lead times. However, the modification and testing are sufficiently early to minimize the procurement risk for FSV 9 through 12. Similar low-risk refurbishment of any other available Phase I vehicle is technically feasible and could provide additional IONDS capability in the 1980's.

1.2.2 Program Schedule

The NDS 6 program schedule shown in Figure 8 calls for launching of the satellite in the summer of 1980. This schedule identifies each IGS flight hardware item and its relationship to the present qualification program and shows that each item will be available for subsystem installation in time to support NDS 6 acceptance testing.

Following the initial IGS development phase, several functions were incorporated into the TIE to minimize the modifications required in the GPS NAV hardware to support IGS. The TIE assembly performs data encoding with the same redundant encoder mechanization employed during the development phase. The qualification TIE unit incorporates the added functions of 10.23 MHz distribution amplifiers, timing interface circuits, and a low-voltage power supply. These circuits are contained on four multilayer printed circuit boards (PCM's) with a master interconnect board. The TIE qualification program was structured to provide time to breadboard and test the added functions before the fabrication of the qualification hardware.

The transmitter assembly consists of redundant transmitters and an RF switch. The transmitter includes a power supply, frequency synthesizer, modulator, and RF amplifiers. The power supply is constructed with conventional discrete components, while the RF portions use microwave integrated circuitry (MIC) and hybrid technology. The components include 3 printed circuit boards (one 2-sided board for the synthesizer and two 4-layer printed circuit boards for the power supply), 15 MIC's, and 2 hybrid assemblies. The qualification transmitter to be tested is the A configuration, which includes an RF switch differentiating it from the B configuration, and is virtually identical to the development model.

The ITT qualification program consists of completing the qualification of the IGS triplexer and modified baseband. The original engineering development model (EDM) units were new units built to the latest GPS flight design and modified for IGS use. The triplexer qualification was completed by performing qualification-level tests on the EDM triplexer in the areas of vibration and pyrotechnic shock, which had not been done in the original test program. The qualification of the baseband includes the development of a modified baseband 2 board and performance of a complete qualification test equivalent to the original GPS qualification test.

The NDS 6 schedule shows the time spans required to refurbish to an IGS configuration plus subsystem installation, acceptance testing, and launch

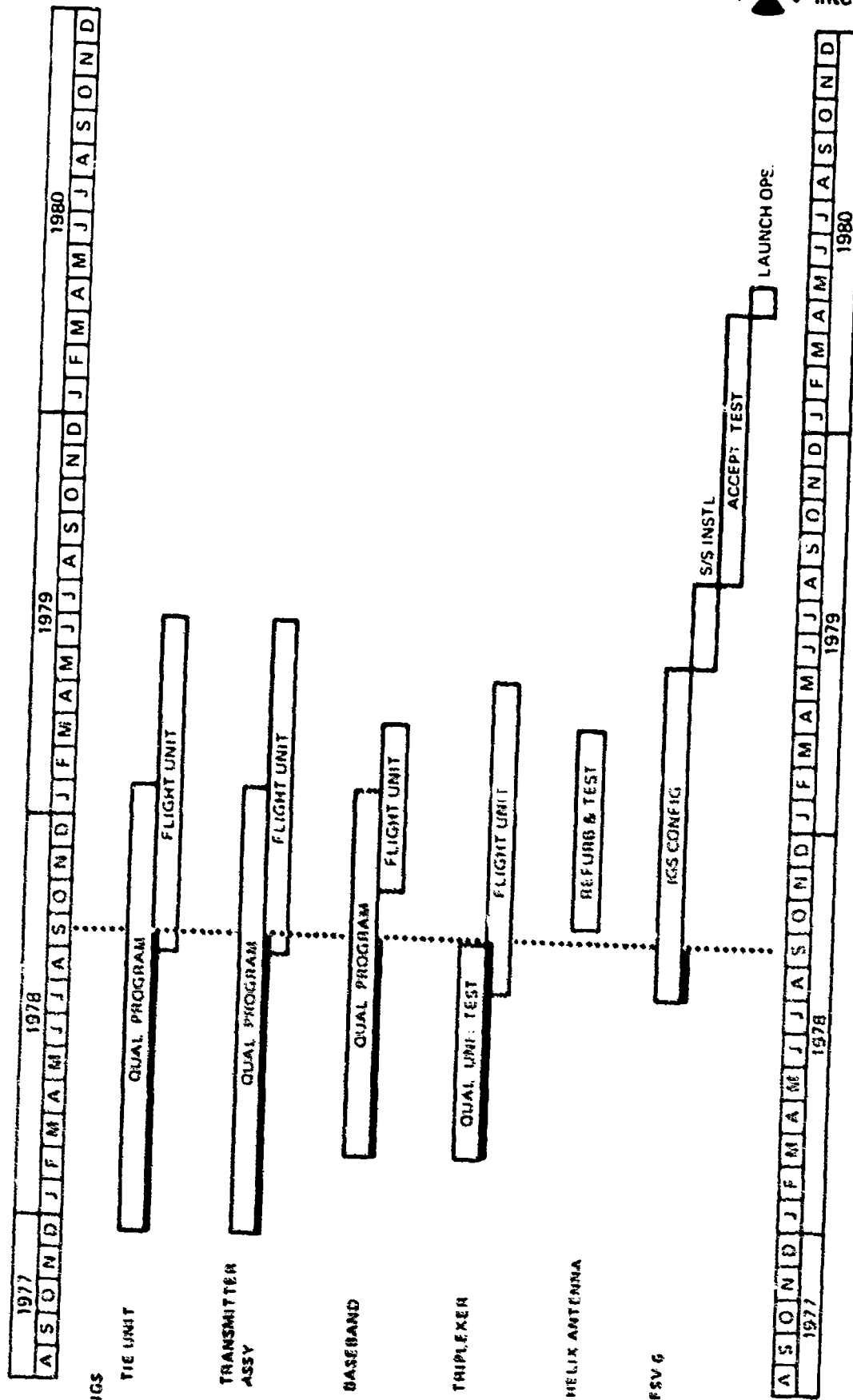


Figure 8. FSV 6 Schedule

operations. Detailed refurbishment plans of hardware items used in QTV testing have been developed and summarized in the NDS 6 hardware utilization list (HUL).

1.2.3 IGS Program Documentation

This report documents the analysis and testing accomplished to establish the feasibility of implementing IGS as a secondary and noninterfering payload on the GPS satellite. The impact of implementing IGS on the GPS space vehicle has been detailed in Volume II of this report. The analysis presented in Volume II clearly indicates that the GPS spacecraft is an ideal host for the NUDET detection and location system. The IGS system can be implemented without interference to the GPS mission and with only a small impact on the GPS supporting subsystems.

Feasibility investigations, analyses, and studies performed in support of IGS development are listed in Table 2. Documentation of these studies and other IGS reports published by Rockwell are listed in Tables 3 and 4.

The testing accomplished on the GPS vehicle and on IONDS has created an extremely optimistic projection of IONDS operational capabilities. The performance of the GPS clock on NDS 1 and NDS 2 in orbital operations is proving by demonstration that it exceeds all estimates of accuracy (about

Table 2. IGS Analyses and Investigations

Analysis	Objective	Results
Initial GPS/IONDS feasibility study	Establish feasibility of GPS/IGS	GPS/IGS configuration found to be feasible
Ford Aerospace and Communication Corp. concept definition study (WDS-TR7035)	Verify Rockwell GPS/IGS feasibility study and define system concept	Results of Rockwell study verified and concept defined
Reliability analysis	Establish IGS reliability and identify single-point failures	Single-point failure points identified; IGS reliability performance predictions indicate reliability requirements will be satisfied
IGS downlink frequency selection tradeoff study	Find optimum downlink frequency	L ₃ frequency (1381.05 MHz) found to be optimum for IGS
Radio-astronomy interference study	Determine radio-astronomy background noise due to IGS	Defined bandstop filter for the L ₃ transmitter which could be included to permit extended L ₃ transmission without RAS interference

Table 3. IGS Documentation - Rockwell Reports

Title	Date	Report Number
RF Signal Compatible Test Report	13 August 1977	SD 77-GP-0046
Intermodulation Noise Test	23 December 1977	SD 78-GP-0007
IGS System Test	21 March 1978	SD 78-GP-0012
IGS EMC Test	31 March 1978	SD 78-GP-0012
IGS Threshold Sensitivity Test	21 March 1978	SD 78-GP-0012
IGS/GPS Acoustic Test	1 October 1976	SD 77-GP-0010 Vols. 1,2,3,&4
GPS-NBRS Design Analysis Report, Vol. II, GPS Spacecraft Impacts	12 August 1976	SD 78-GP-0018-1 & 2
IGS Reliability Analysis	15 June 1977	SD 77-GP-0035
GPS/SPL Antenna Compatibility Tests	September 1977	SD 77-GP-0034
Baseband/GBD Processor/L3 Encoder EDC Tests	13 May 1977	SD 77-GP-0028
GPS/SPL Thermal Control	15 June 1978	SD 78-GP-0020

Table 4. IGS Documentation - Rockwell Specifications
and Interface Control Documents

Title	Document No.
Specifications	
Antenna Coupler and Absorber Housing	MC483-0010
IONDS Baseband Assembly	MC409-0097
PRN Signal Assembly	MC409-0018
Antenna, Helix Array	MC481-0077
Rubidium Frequency Standard	MC474-0030
L3 Transmitter	MC476-0171
L3 Encoder	MC476-0175
L3 Triplexer, Antenna	MC476-0174
IONDS Test Receiver	MC476-0180
L3 Timing Interface and Encoder	MC409-0099
Interface Control Documents (ICD's)	
Encoder and L3 Transmitter	MH08-00002-200
Cesium Frequency Standard	MH08-00010-400 Current Issue
L3 System/Global Positioning System	MH08-00016-400 Current Issue
Space Vehicle Integrated Global Segments Subsystem/Integrated Operational NUDET Detection System	MH08-00014-400 Current Issue
L3 Subsystem Physical and Functional	MH08-00013-400
GPS/Global Burst Detector Interfaces	MH08-00012-400

1 microsecond/year) and should lead to precision three-dimensional burst location data. The IGS sensors' similarity to space-proven capabilities will assure that nuclear burst data will be received as expected for TOA transmissions. Verification that the GPS and IGS systems will function on a noninterfering basis has been demonstrated in an electrical test vehicle (ETV) which closely approximated the GPS flight vehicle. In summary, the information contained in this technical report indicates that:

1. GPS is an ideal vehicle for IGS implementation.
2. IGS will have no impact on GPS navigation.
3. IGS can be implemented in the GPS spacecraft with a small impact on vehicle design.
4. IGS presents no risk to the GPS program because of extensive testing and by designing IGS components to MIL-STD-1540 and MIL-STD-1541.

1.2.4 IGS Program Test Summary

The testing that verified the program objectives listed above is summarized in Table 5. Each of the tests listed in the table is summarized in Section 6, IGS Test Program. The initial testing was aimed at verifying the functional operation of IGS components. Other tests were performed to determine any IGS impact on the satellite system or mission and to demonstrate system compatibility. The test program has successfully verified IGS system operation and its compatibility with GPS and has indicated that the IGS implementation will be a low-risk program.

Table 5. IGS Test Summary

Test	Objective	Results
IGS component testing GSD subsystem L ₁ transmitter L ₁ encoder Baseband TI box Triplexer	Verify functional operation Verify functional operation Verify functional operation Verify functional operation Verify functional operation Verify functional operation	All IGS components functionally operational
Sunshade tests	Find optimal sunshade location and size	An optimal sunshade size and location established
GPS secondary payloads DTV acoustic test	Verify acoustic design of GPS vehicle with secondary payloads and establish unit vibro-acoustic specification	GPS vibration levels found to be within specified tolerances and SPL levels identified
GPS/IGS intermodulation noise test	Determine impact of IGS transmissions on GPS system, GPS users, and TTAC	GPS and IGS systems found to be compatible
GPS/IGS antenna compatibility test	Demonstrate compatibility of GPS antenna system with IGS sunshade	GPS L ₁ antenna pattern not degraded; L ₂ antenna pattern slightly degraded. Determined that IGS was compatible with the GPS antenna system
GPS/IGS RF compatibility test	Establish compatibility of IGS transmissions with NAV system users	GPS/IGS RF transmissions found compatible with GPS receiver operation

Table 5. IGS Test Summary (Cont)

Test	Objective	Results
Triplexer tests	Verify triplexer functional compatibility for L ₁ , L ₂ , and L ₃	Triplexer performance found equivalent to GPS diplexer
EMC tests	Determine electromagnetic compatibility between IGS and GPS subsystems	GPS/IGS found to be compatible
Bench test IGS system	Demonstrate functional compatibility between the baseband processor, BDP, and L ₃ encoder	IGS components found to be electrically compatible
GPS/SPL thermal control analysis	Verify GPS/SPL thermal control capability	Minor GPS equipment temperature increases over qual test results. Impact of IGS on GPS minor, requiring no requalification of GPS equipment and minimal thermal control design changes
GPS/IGS signal compatibility test KTV	Demonstrate IGS transmissions do not degrade GPS navigation signal	IGS transmissions did not degrade GPS navigation signal or mission
System-level intermodulation test	Demonstrate system-level intermodulation capability	IGS systems intermodulation found to be EMC-compatible
System functional EMC test	Demonstrate compatibility between IGS components in a system configuration	IGS components found to be EMC-compatible
GPS/IGS thermal-vacuum test	Demonstrate systems thermal-vacuum operational capability	Analysis based on GPS QTV test at AEDC and initial GPS flight results indicates no problems. Full thermal-vacuum test to be accomplished on MDS 6
Baseband processor acceptance test	Demonstrate BBP compliance to specifications	Baseband processor accepted
Triplexer acceptance test	Demonstrate triplexer compliance to specifications	Triplexer accepted
L ₃ transmitter acceptance test	Demonstrate L ₃ transmitter compliance to specification	L ₃ transmitter accepted
Y-sensor grounding and threshold sensitivity tests	Demonstrate Y-sensor grounding and threshold sensitivity	Background noise approximately 150 mV p-p. Threshold sensitivity approximately same as bench test
IONDS receiver threshold sensitivity tests	Determine IGS system threshold with STI receiver	See Table 43
PCM enable tests	Demonstrate the PCM function	PCM function operation verified
IGS component ICI tests	<ol style="list-style-type: none"> 1. Demonstrate compatibility between IGS components in system configuration 2. Measure on-off characteristics 3. Verify readiness for signal compatibility, functional compatibility, and EMC tests 	<ol style="list-style-type: none"> 1. Overall compatibility demonstrated 2. All voltages normal 3. IGS system rated ready for signal and functional compatibility and EMC tests

2. NAVSTAR GLOBAL POSITIONING SYSTEM (GPS)

2.1 GPS OBJECTIVES

The Navstar GPS is a satellite navigation system under development to provide space, air, sea, and land users with position information to an accuracy of 15 to 30 feet. Eight developmental space vehicles are being produced by Rockwell under funding from the joint Army, Navy, Air Force, Marine Corps program, managed by SAMS0.

The program plan is illustrated in Figure 9. Scheduled launching dates for the flight vehicles are listed in Table 6. By the end of 1978, enough data from the space vehicles will be available for DSARC-II (the Department of Defense decision point to enter production for Phase III) in May 1979.

Full, three-dimensional coverage by 24 spacecraft will occur at the beginning of 1986. The operational phase constellation will consist of 24 satellites in 12-hour orbits with 8 satellites in 3 orbital planes inclined ≥ 55 degrees.

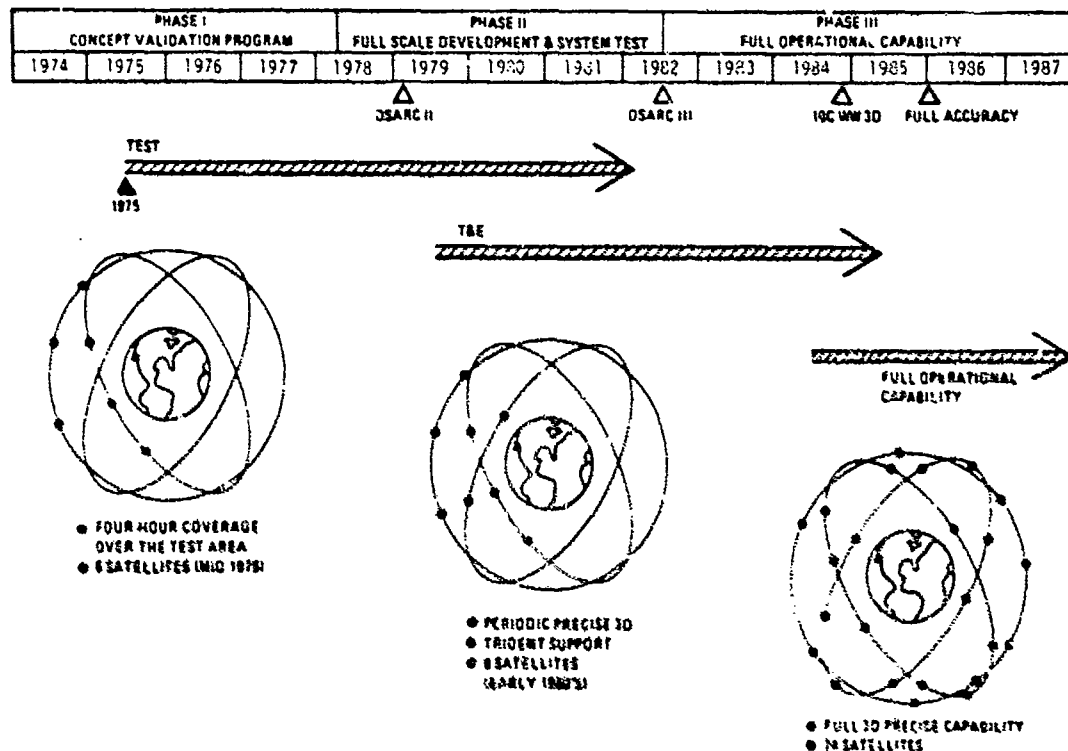


Figure 9. GPS Program Plan

Table 6. GPS Launching Schedule.

Flight Vehicle	Launch Date
FSV 1 (Navstar 1)	Feb. 22, 1978
FSV 2 (Navstar 2)	May 13, 1978
FSV 3 (Navstar 3)	Oct. 6, 1978
FSV 4 (Navstar 4)	Dec. 10, 1978
FSV 5	TBD
FSV 7	TBD
FSV 8	TBD
FSV 6 (QTV vehicle)	TBD

2.2 GPS SYSTEM DESCRIPTION

2.2.1 GPS User Segment

A GPS user requires pseudo-range measurements from four GPS satellites to obtain a three-dimensional navigation fix, with time being the fourth solution variable. Pseudo-range is defined as the transit times of the satellite-generated signals as observed by the user and scaled to the speed of light. Using GPS time as a reference, the true transit times are those between the GPS transit times and the GPS receive times. These transit times represent the true slant ranges except for propagation delays.

In the solution for pseudo-range, the satellite transmits a pseudo-random noise (PRN) code and a navigation message. The satellites radiate these signals on two frequencies, L_1 and L_2 , to correct for ionospheric delays. Tropospheric delays are estimated, based on prevailing atmospheric conditions, geometry, and altitude.

The GPS navigation message is the information supplied to the GPS users from a GPS space vehicle (SV). It is in the form of a 50-bit-per-second data bit stream that is modulated on the GPS navigation signals. This signal carries SV ephemerides, system time, SV clock behavior data, transmitter status information, and C/A (clear/acquisition) to P (precision) signal handover information. The data stream is common to both the P and C/A signal on both the L_1 and L_2 frequencies.

The data message is contained in a data frame that is 1,500 bits long. It has five subframes, each of which contains system time and the C/A to P handover information. The first subframe contains the SV's clock correction parameters and ionospheric propagation delay model parameters. The second and third

subframes contain the SV's ephemeris. The fourth subframe contains a message of alphanumeric characters. The fifth subframe is a cycling of the almanacs of all SV's (one per frame), containing their ephemerides, clock correction parameters, and health. This almanac information is for user acquisition of yet-to-be-acquired SV's.

The user system segment includes the hardware and computer programs necessary to receive and process navigation signals and output the results as three-dimensional position and velocity. It is capable of displaying system time to users who require it. A user equipment set is the appropriate combination of elements that are required to convert the available C/A navigation signals into usable navigation data under the operating conditions associated with the host vehicle. The elements of a user equipment set include an antenna assembly, receiver, data processor, control/display unit, power supply unit, and interface units.

When a user wants to establish his position, he must acquire at least four satellites. Since all of the satellites transmit on the same frequency and the user equipment receives energy from all satellites within view, the user's receiver employs correlation techniques to recover the desired data.

The receiver equipment selects four of the satellites within view and provides instructions for acquisition and data recovery (i.e., codes and predicted doppler). The acquisition sequence consists of a carrier acquisition, C/A code acquisition, and P code acquisition. Nonprotected receivers omit the P code acquisition and use the less accurate C/A code.

To select a satellite, the user receiver generates a predetermined C/A code (one of 32 codes selected before launch). This code is used as a reference and compared with the received signal. A PN signal search is performed by shifting the reference PRN code until a correlation peak exceeds an acquisition threshold. This correlation peak occurs when the reference code and the received code are synchronized in both frequency and time. After the C/A code has been acquired, data can be extracted. The extracted data contain SV ephemerides, system time of day, SV clock data, system status messages, and C/A to P handover information. This handover information is then used to provide the *a priori* information necessary to code-lock the receiver to the higher chipping rate (10.23 MHz), long-term P code.

A sophisticated user receiver will perform this sequence simultaneously for four satellites. The receiving craft will use its own special clock, updated regularly by one of the atomic clocks in orbit, and calculate, by computer, the time required for transmission of the space vehicle signals and the range and direction involved. From this information, the receiving equipment will calculate the user's position within tens of feet in three dimensions in a few seconds.

2.3 GPS/ICS INTERFACING SUBSYSTEMS

The navigation and NUDET surveillance missions are separate functions but use some common elements that operate on a noninterfering basis. The IONDS subsystem has been constrained to cause no GPS performance degradation, even

though its implementation is functionally dependent on the navigation, TT&C, EPS, and other GPS subsystems. Similarly, no unique NUDET data are included in the navigation message although the IONDS system depends on the data contained in the L₁ and L₂ data message. The organization of these GPS subsystems is illustrated in Figure 10.

2.3.1 Navigation Subsystem

The GPS global segment navigation subsystem block diagram is shown in Figure 11. The subsystem provides for the simultaneous downlink generation of two L-band carriers: L₁ at 1575.42 MHz and L₂ at 1227.60 MHz. The L₁ carrier is biphas-modulated with two codes: a 10.23-MHz PRN precision code and a 1.023 MHz (C/A) PRN code for acquisition. The C/A signal is modulated in quadrature to the P signal.

The second carrier, L₂, is biphas-modulated with the 10.23 MHz PRN P code only. The C/A signal may be used by some users for limited precision ranging and is used by all users for acquisition. The P signal, which cannot be used for rapid direct acquisition, is used for precision ranging. Table 7 summarizes the navigation subsystem characteristics.

2.3.2 Telemetry, Tracking, and Command (TT&C) Subsystem

The TT&C subsystem provides telemetry, tracking, command, and navigation upload capabilities to support GPS space vehicle operations in conjunction with the Air Force Satellite Control Facility (AFSCF) and the Master Control Station (MCS) (see Figure 12).

2.3.3 Subsystem Functions

The TT&C subsystem is designed to support the following functions:

1. Primary navigation upload from the upload station (ULS) and backup from the AFSCF
2. Alternate navigation encrypted or bypass upload from the AFSCF via the command decoder
3. TT&C commands from the AFSCF in either the bypass or the encrypted format
4. Space ground link system (SGLS) telemetry to the AFSCF at either 4,000 or 500 bps
5. PRN turn-around ranging (tracking) from the AFSCF

The navigation upload has three modes, i.e., primary, backup, and alternate. In the primary mode, navigation data are routed from the MCS/ULS via the TT&C receiver/demodulators and signal conditioning unit (SCU) to the baseband processor. The ULS does not have the capability to send discrete or magnitude commands in the TT&C encrypted or bypass modes. The primary mode applies to the NDS and the Navigation Technology Satellite and to the ULS. The backup mode is

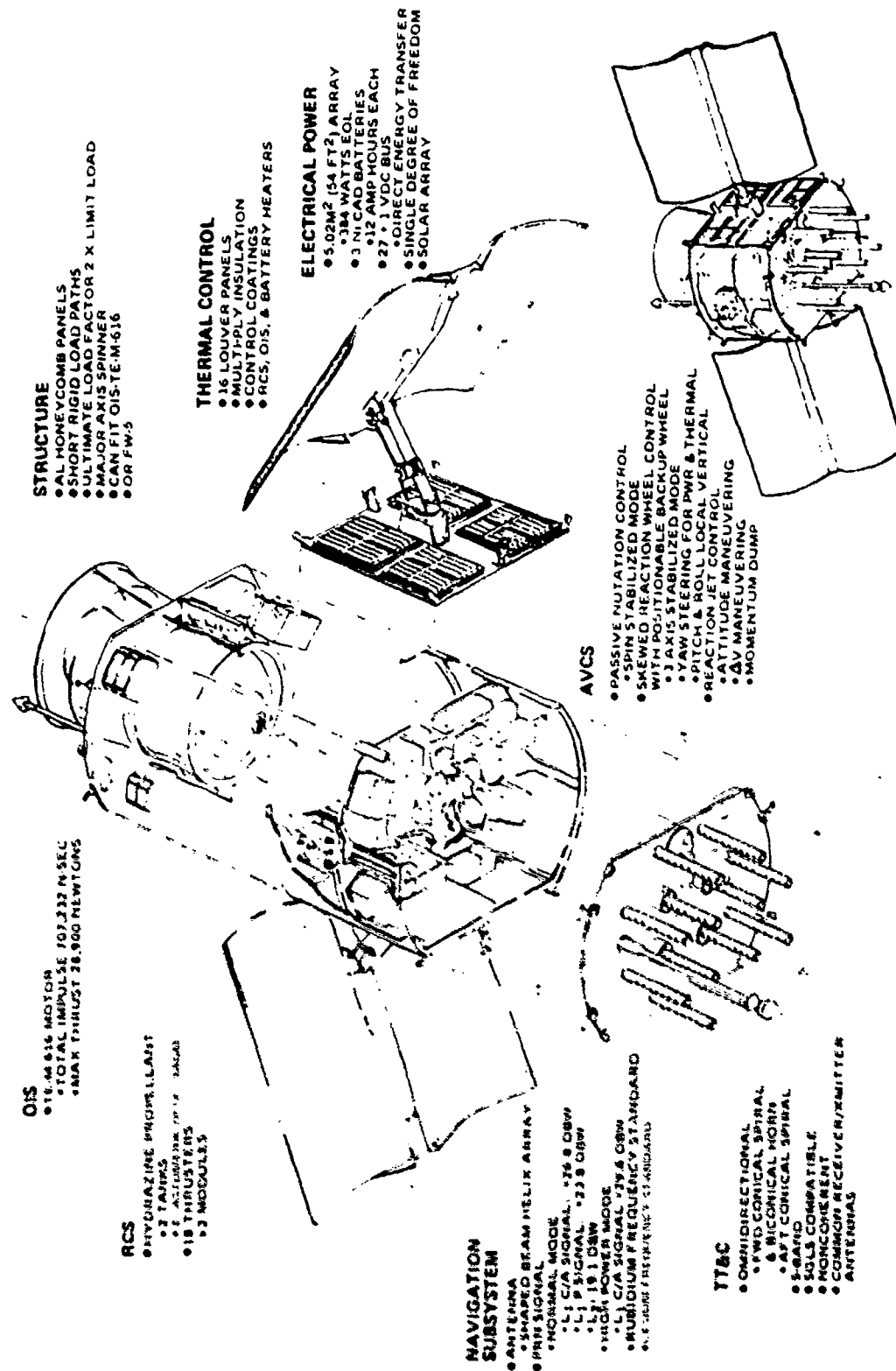


Figure 10. GPS Space Vehicle Subsystems

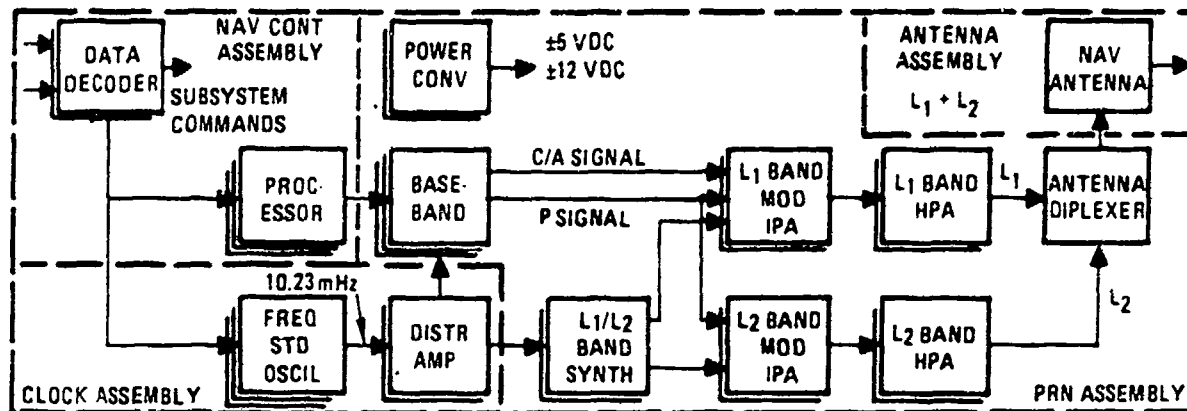


Figure 11. Navigation Subsystem

Table 7. Navigation Subsystem Requirement Summary

<u>Frequencies</u>	<u>C/A Signal Structure</u>
L ₁ : 1,575.42 MHz L ₂ : 1,227.60 MHz	Chipping rate: 1.023 Mbps Data Rate: 50 bps Biphase-modulated: modulo 2 sum of data and code
<u>User Receiver RF Signal Levels</u> (minimum)	<u>Combined Signals</u>
-163 dBW: P at L ₁ (normal power mode) -160 dBW: C/A at L ₁ (normal power mode) -158 dBW: C/A at L ₁ (high power mode) -166 dBW: P or C/A at L ₂	P and C/A cross-talk: ≤ -20 dB Correlation loss (P and C/A): ≤ -0.6 dB AM (composite carrier): ≤ 1.0 dB
<u>Equipment Group Delay Uncertainty</u>	<u>Frequency Standard Accuracy</u> (10.23 MHz Nominal)
Normal: 3 ns (2 sigma) Eclipse: 5 ns (2 sigma)	Frequency stability: < 1 × 10 ⁻¹³ Δf/f Reset resolution: < 2 × 10 ⁻¹³ Δf/f Reset Range: > 1 × 10 ⁻¹¹ Δf/f
<u>P Signal Structure (L₁/L₂)</u>	<u>L-Band antenna</u>
Chipping rate: 10.23 Mbps Data rate: 50 bps Biphase-modulated: Modulo 2 sum of data and PRN code	RHCP transmission off-axis coverage: 14.3 deg Antenna gain at 14.3 deg: +12.8 dB (L ₁) and +11.3 dB (L ₂)

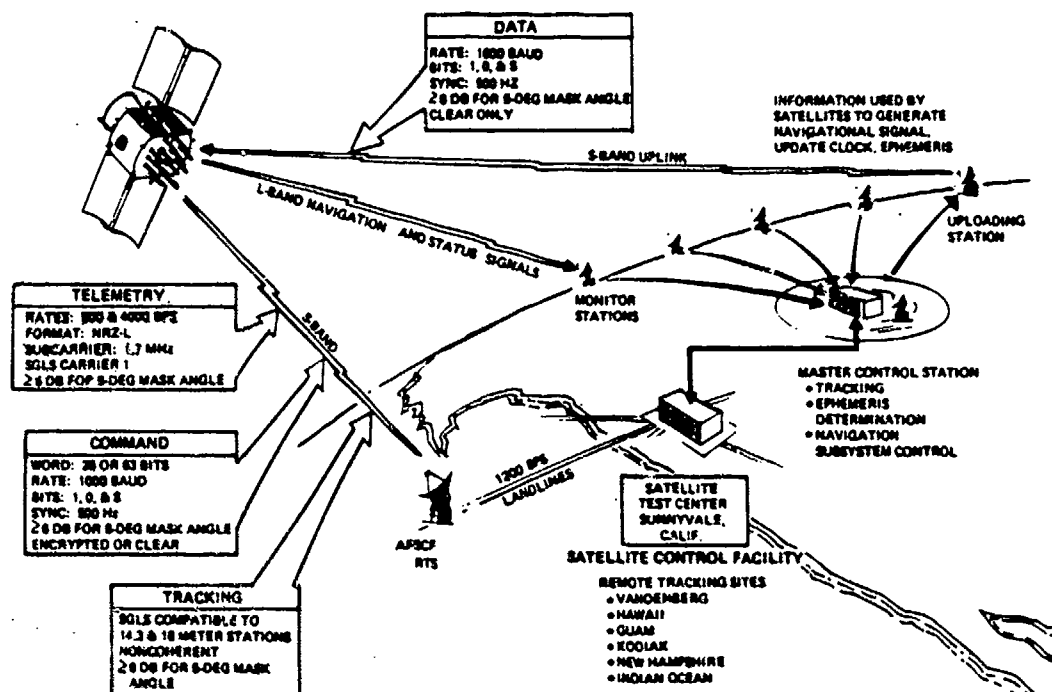


Figure 12. TT&C External Interface

identical with the primary mode except that the signal is transmitted by the AFSCF. The alternate mode (NDS only), a secondary backup mode, routes navigation data via the encrypted or bypass TT&C path in command format. In the primary and backup upload modes, the data rate is 1,000 bps. For a maximum upload, the time required is approximately two minutes. The alternate upload data rate is also 1,000 bps with a maximum upload time of two minutes.

The TT&C commands have two modes: secure (encrypted) or bypass. Normally, the encrypted mode is used. The bypass mode is either selected automatically if a command verification is not initiated after eight days, or by ground command. Turn-around ranging (tracking) can be combined with the command modes. In this case, link margin considerations limit operations to the 46-foot or 60-foot remote tracking station (RTS) tracking and telemetry antennas.

The telemetry function has two modes, 500 or 4,000 bps, which can be combined with tracking. The data are currently unencrypted but are to be encrypted in the Phase III operational satellites.

The 500-bps telemetry mode provides SV housekeeping functions, command accept and reject outputs, KIR-23 authentication, and navigation subsystem readouts. The 500-bps mode is selected by ground command. If PRN ranging is present on the uplink, one receiver/demodulator PRN output is inhibited. The mode can be used with 14-, 46-, or 60-foot antennas.

The 4,000-bps telemetry mode transmits the same information as the 500-bps telemetry mode at a faster rate. Link margin considerations may restrict its use to 46-foot or 60-foot antennas during transfer orbit conditions.

2.3.4 Attitude and Velocity Control Subsystem (AVCS)

The AVCS provides the sensing, logic, and control torques necessary to perform velocity maneuvers and maintain desired space vehicle orientation. This system must maintain spacecraft pointing to within \pm (TBD) degrees and not cause spacecraft pointing movement greater than (TBD) degrees per second to preclude interference with IONDS.

2.3.5 Reaction Control Subsystem (RCS)

The RCS is a simple blowdown, monopropellant system using two 22.2-N and sixteen 0.44-N catalytic thrusters.

2.3.6 Electrical Power Subsystem (EPS)

The EPS consists of a 5.02 m² solar array with single-degree-of-freedom drives. The solar array, in conjunction with the batteries, forms a direct energy transfer system to supply 27 ± 1 Vdc to all GPS space vehicle systems. The EPS operates autonomously, providing battery charge and discharge logic and overload protection for every load.

2.3.7 Solar Arrays

The solar array consists of a series/parallel matrix of N-P silicon solar cells, which convert incident solar energy into electrical power. These cells are arranged on 2 wings, each with 18 parallel-connected diode-isolated solar cell circuits. Each circuit is composed of 81 series-connected submodules of 2 parallel 2-cm by 4-cm cells.

2.3.8 Batteries

Three 16-cell, 12-amp-hour Ni-Cd batteries perform the energy storage function. The battery module is a modification of the 10-cell lunar orbiter module with 3 cells added to each row to obtain the required 16 cells. The battery capacity and number of batteries provide high confidence that the five-year life can be achieved. The average in-orbit battery temperature will be maintained between 0 and 20°C.

2.3.9 Power Conditioning Unit (PCU)

The PCU supports a single bus system and detects the difference between bus and nominal voltage levels. This difference error is amplified and used in the central power control to drive the system functions (i.e., supply regulated power, control battery charging, boost battery discharge voltage, and dispose of excess array power). At the nominal voltage sufficient power is generated from the solar array to support all loads and provide power for battery charging. With a positive deviation from the nominal voltage, the central power control unit within the PCU senses the error voltage and amplifies it to drive the shunt dissipators sequentially on to dissipate excess solar array-generated power and to reduce the voltage toward the nominal.

2.3.10 Other GPS Subsystems

The orbit injection subsystem, structural subsystem, and thermal control subsystem do not interact with IONDS to an extent that would require them to be described in this volume. Further information on these subsystems can be obtained from Volume II.

3. IONDS GLOBAL SEGMENT (IGS)

3.1 IGS OBJECTIVE

The functional objective of IGS is to provide global NUDET surveillance coverage. The objectives of the IGS development program at Rockwell included the definition of a subsystem with maximum political and military value and which, at the same time, has an insignificant impact on the basic GPS mission.

3.2 IGS SYSTEM DESCRIPTION

The baseline GPS/IONDS system consists of two elements: a satellite subsystem carried aboard a GPS satellite and a ground/airborne user terminal. The basic elements of the global subsystem are X and Y sensors, a sensor data processor, an encoder, and an L-band transmitter. The global subsystem is supported by the GPS satellite with time, P and C/A codes, power, commands, state of health (SOH) measurements, and antennas. The user segment consists of an antenna, receiver, processor, and display unit. A top-level functional flow diagram of the IGS/GPS system is shown in Figure 13. The IGS space segment is controlled and monitored by the control system segment of the system. The space segment broadcasts precision time and ephemeris data to both the navigation and IGS user segments on L₁ and L₂ channels. IGS transmits nuclear event data on L₃ to the IGS user segment.

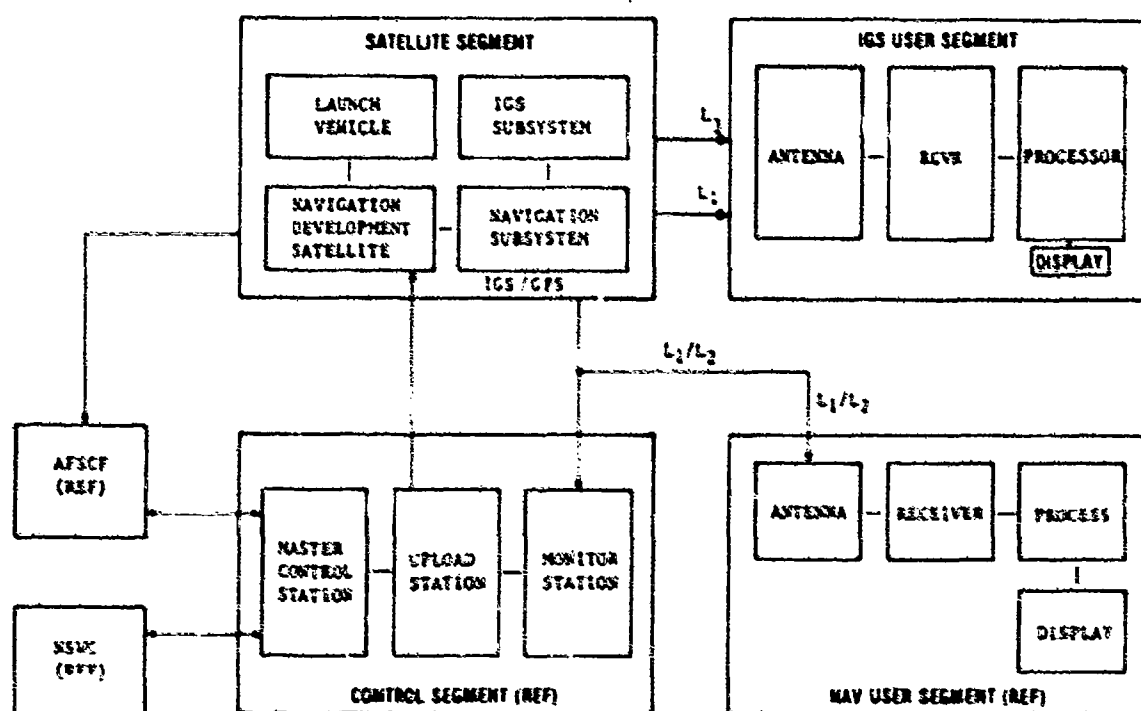


Figure 13. Functional Flow Diagram

3.2.1 IGS System Operation

The IGS system, when operational, will become a significant part of the total IONDS, and the data will be used in conjunction with data obtained from other sources. NUDET information obtained from IGS will have some inherent advantages over counterpart systems in that (1) complete global coverage will be accomplished, (2) better location information will result from the precision time available from GPS, and (3) burst altitude can be accurately determined. In addition to the above advantages, the probability of successfully detecting low yield devices will be enhanced since four or more GPS/IGS satellites will be in view of any global nuclear event simultaneously.

During nuclear event surveillance operations, the IGS X and Y sensors will be operating continuously on each GPS vehicle. If a nuclear burst were to occur, these optical (Y) and X-ray (X) sensors on-board at least four GPS/IGS satellites would be in position to receive event data. The event yield and altitude determine the characteristics of the burst's optical and X-ray signatures. If these signals pass the selection criteria, the NUDET data will be processed and a time tag assigned to each event.

The data from the sensors are digitized and stored in the BDP. The IGS L₃ transmitter is then activated by the BDP, and a prescribed data format is transmitted. After one transmission of the contents of the BDP memory, the L₃ transmitter is turned off. The IGS event memory has the capacity to store data from multiple nuclear events and the stored information will be available for transmission upon command from an appropriate ground station.

3.2.2 IGS Control Segment

The control and monitoring of the IGS operation is accomplished through the GPS TT&C subsystem. Figure 12 illustrates the interface between the GPS TT&C and the Satellite Control Station Network. The GPS command decoder produces both momentary (discrete pulse) commands and a serial command data stream of 14 bits.

The IGS subsystem is provided with eight discrete pulse commands and one 14-bit serial command with clock and enable signals. An IONDS user can communicate with one of the satellite control stations for special IGS commands. Normally, each IGS space vehicle transmits sensor status once a day and nuclear event data in real or delayed time.

The IONDS SOH data are presented to the GPS telemetry (pulse code modulator [PCM]) in digital form. The SOH data are transmitted at a rate of 4,000 or 500 bps. Two 8-bit parallel words are available for outputting sensor SOH to the PCM memory for transmission to the control station.

3.2.3 IONDS Global Segment

Figure 14 illustrates the location of IONDS components with the X-ray (X) sensor and the optical (Y) sensor on the GPS vehicle. The sunshade on the Y sensor is made of RF transparent material to prevent degradation of GPS L-band antenna performance. The X sensor will detect X-rays from exoatmospheric nuclear

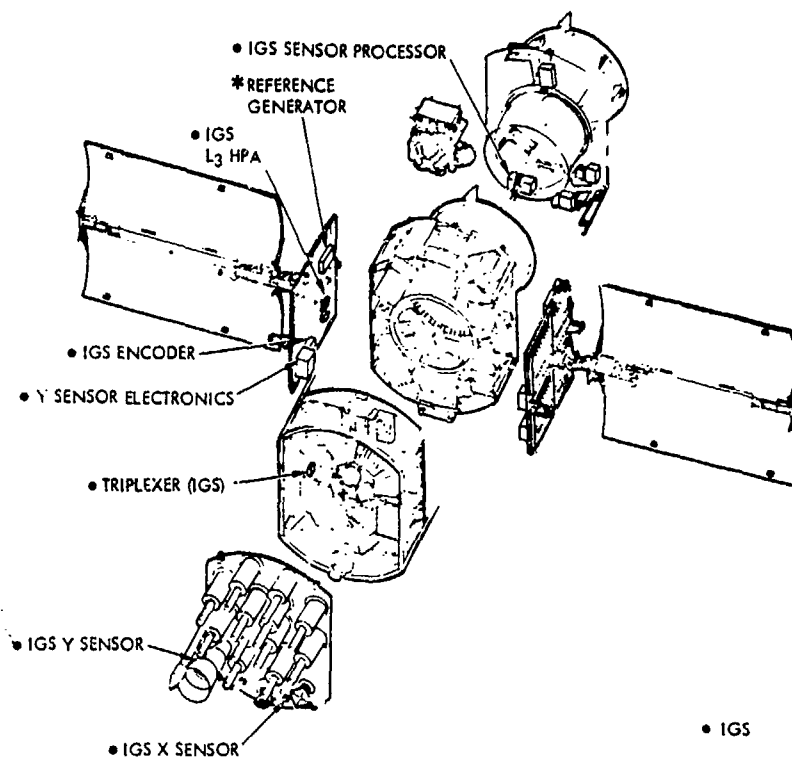


Figure 14. Installation of IGS Components on GPS Vehicle

events. Similarly, the Y sensor will detect the optical signature of an atmospheric nuclear event. Time of arrival from the sensors will be used to determine event location.

3.2.4 IGS Data

The IGS data are provided after a nuclear event to all operational user sites. The sensor data in the initial encoder design was block, differential, and convolutional encoded in that order. Operational satellite encoding is planned to be in the block/convolutional/interleave/differential sequence. The coded data are Modulo-2 added to the P code and transmitted over the L₃ link. Figure 15 shows the overall IONDS coding for the IGS data.

Nuclear event data are time-referenced to GPS system time by using baseband timing information as shown in Figure 16. The baseband/processor provides the Z-count, X1 epoch, and 10.23-MHz timing signal established by the satellite's atomic standard frequency relationship between the signals and the coherent clock used to transfer the Z-count. The X1 epoch provides a time mark to initialize a fine count to achieve nuclear event TOA at the spacecraft. The rise time of less than 100 nanoseconds for the leading edge of the X1 epoch is used to achieve this performance. The 10.23-MHz signal provides the precision clock for fine time counting.

The IGS data format is shown in Figure 17. The encoder provides concatenation coding of the nuclear event data. This coding consists of a block

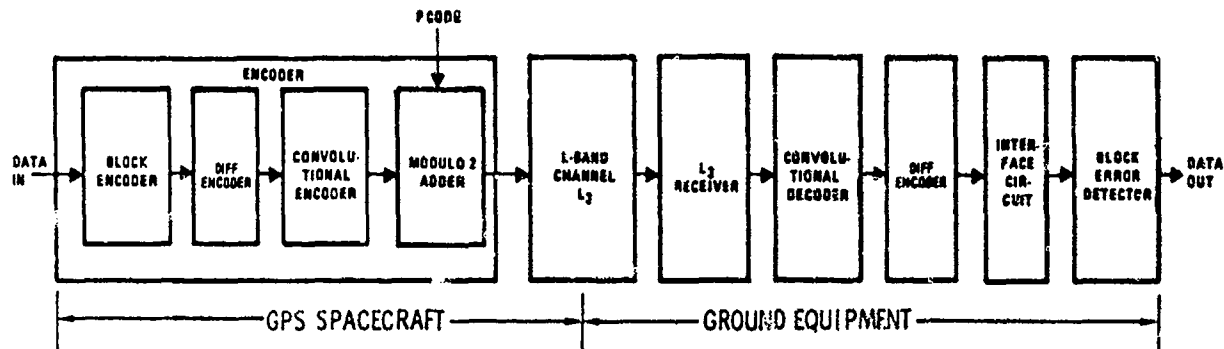


Figure 15. IONDS Data Coding

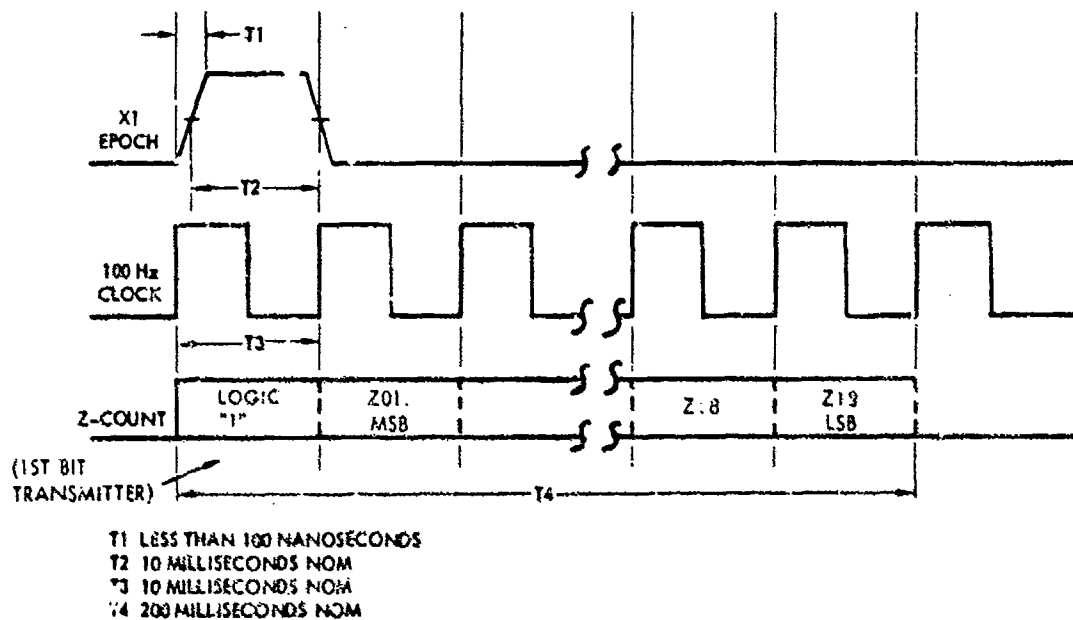


Figure 16. Baseband Interface Timing Relationship

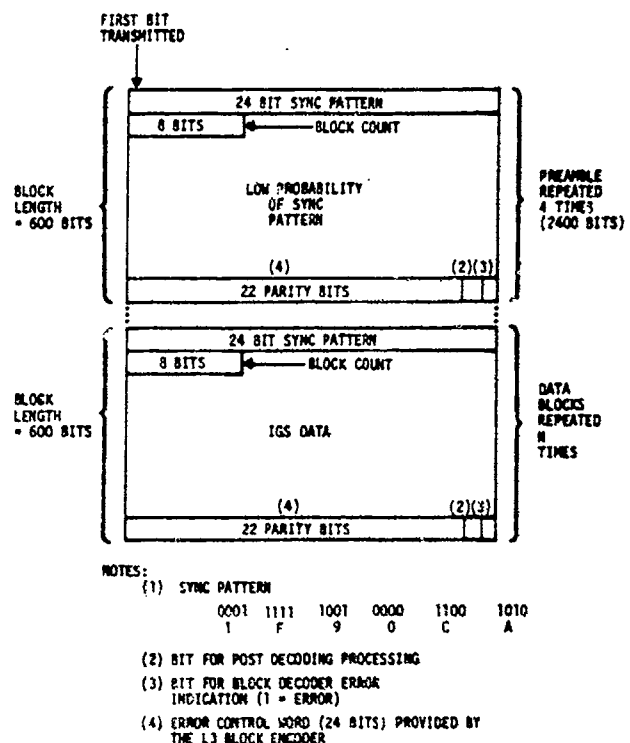


Figure 17. IGS Data Format

code and convolutional code whose characteristics are described below. The block coding provides error detection with a block length of 600 bits.

The differential/convolutional encoding are shown in Figure 18. The 24-bit sync word and the data words are provided by the burst detection processor. The 22-bit error control word is supplied by the encoder. The remaining two bits are used by the decoder and postdecoding processing.

A differential code provides transparency to 180-degree carrier phase ambiguities that give reversals in data logic states. This encoding precedes the convolutional encoding.

The convolutional encoder provides error correcting data encoding. The convolutional code has a constraint length of seven. The code rate is 1/2 with two code bits transmitted for each input bit. Soft quantizing of the received data stream is performed before convolutional decoding. The encoder input is 200 bps with an encoder output of 400 symbols per second. The concatenated-coded data are then Modulo-2 added to the P code to achieve spectrum spreading. The P code is extracted from the data stream by the receiver. The convolution decoder receives data at 400 bps and outputs at 200 bps.

The error control word is generated by division of the input data block by the polynomial

$$G(x) = x^{22} + x^{20} + x^{14} + x^{13} + x^{12} + x^{11} + x^8 + x^7 + x^5 + x^3 + x + 1$$

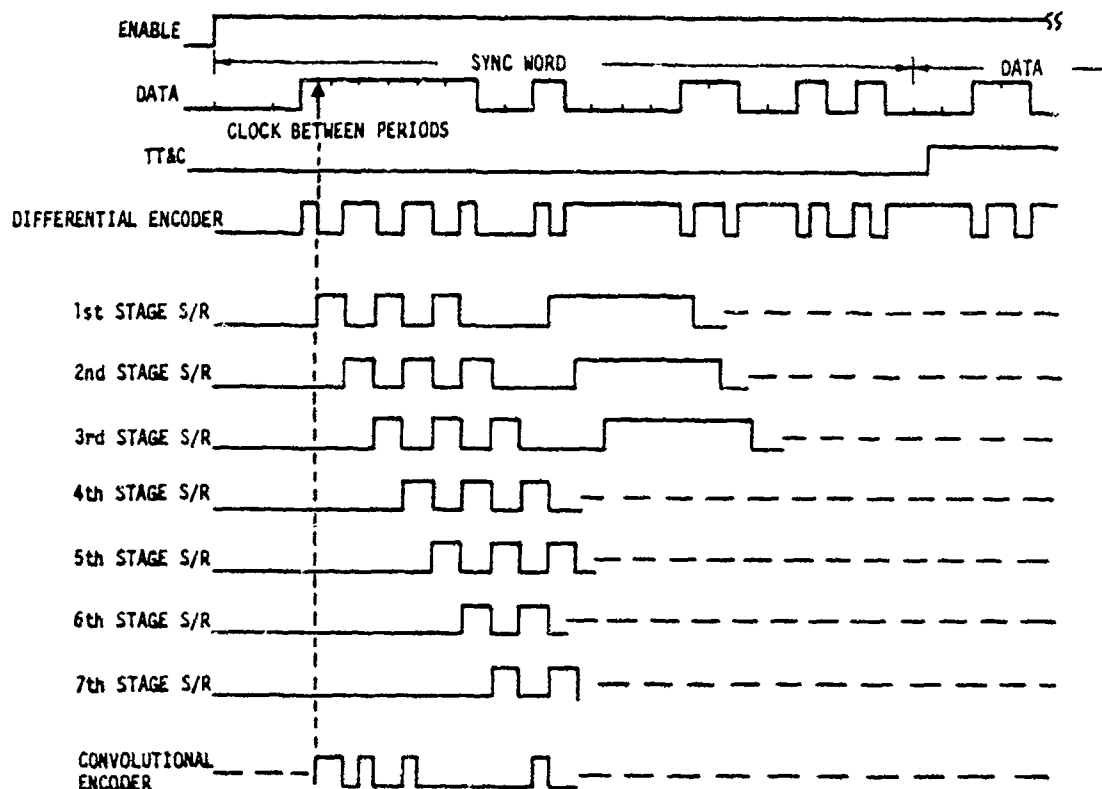


Figure 18. Encoder Timing Diagram

The probability of detecting the presence of random data in the input block at the decoder is 2.4×10^{-7} . The data rate is 200 bps. The encoder delay is 1 bit while the decoder delay is 25 bits.

3.2.5 IONDS User Segment (IUS)

The IONDS user segment consists of a passive receiving and processor station. The receiving terminals can be part of a global receiving terminal, a tactical, or an airborne terminal (see Figure 19).

The theater/global receiving terminal may use a 6-foot shaped hemispherical beam (SHB) antenna, a one-bay 19-inch rack, and an output printing device. The racks contain two four-channel receivers, decoders, a computer, data storage device, and a communications interface.

The tactical terminal will consist of a half-rack for a four-channel receiver, decoders, computer, and power supply. The terminal will not use a communications interface, and the data are printed at the output terminal. The antenna is a mast-mounted 11-inch volute array.

The airborne terminal is basically identical to the theater/global terminal. To ensure full antenna coverage during airplane maneuvers, two 4-inch-diameter turnstile-monopole antennas will be mounted on the top of the fuselage. The preamplifiers will be co-located with the antennas for optimum receiver performance.

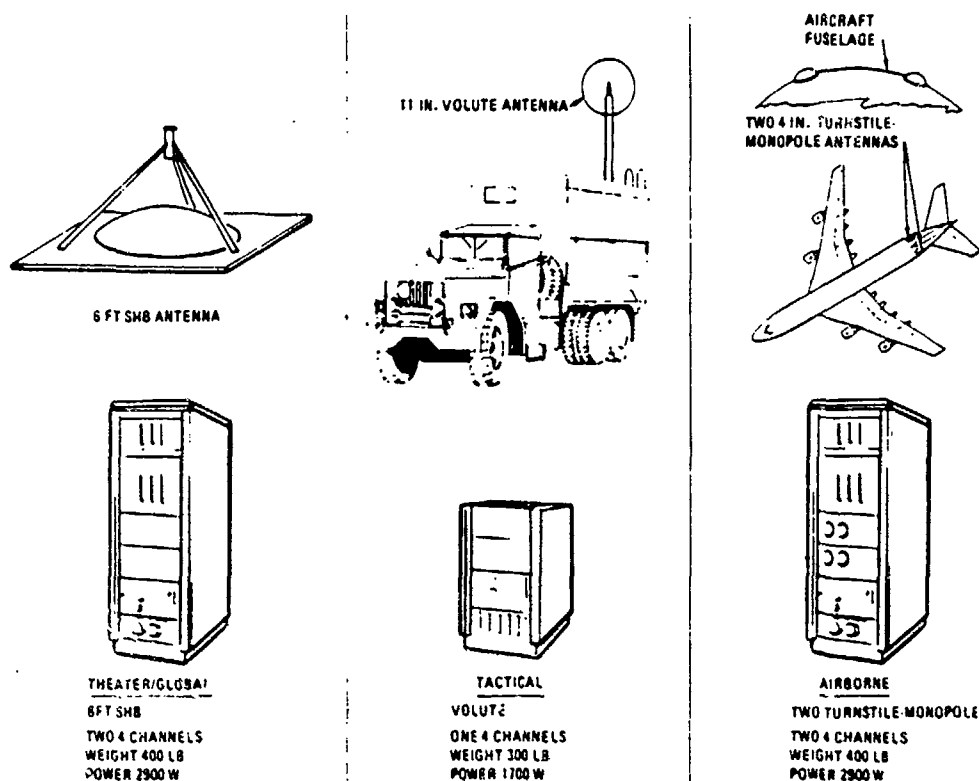


Figure 19. IONDS/GPS Receiving Terminals

An IONDS/GPS receiver set can receive data from four GPS satellites simultaneously. The set has five channels which can monitor either Link 1 or Link 3. A code channel is used to initially search for and acquire Link 1 and then to continuously search for a Link 3 signal. The carrier channels monitor Link 1 to obtain clock correction and satellite position data and to maintain synchronization on the GPS P code while the code channel searches for a Link 3 signal. When any Link 3 signal is detected, the appropriate carrier channel is switched from Link 1 to Link 3 to receive IONDS data messages. Since the channel has previously locked on to the Link 1 P code and Link 3 also carries the P code, Link 3 synchronization is attained within a few seconds. After all data have been transmitted and Link 3 is turned off, the receiver channel switches back to Link 1 to maintain P code synchronization for rapid acquisition of subsequent Link 3 transmissions.

Figure 20 illustrates a typical four-channel IONDS receiver that is expected to be a modified version of the GPS operational receiver that performs similar L_1/L_2 functions.

Figure 21 lists receiving terminal processing functions which determine the NUDET event parameters. Mission data messages (NDM's) are formatted for local user display and/or transmission to other users.

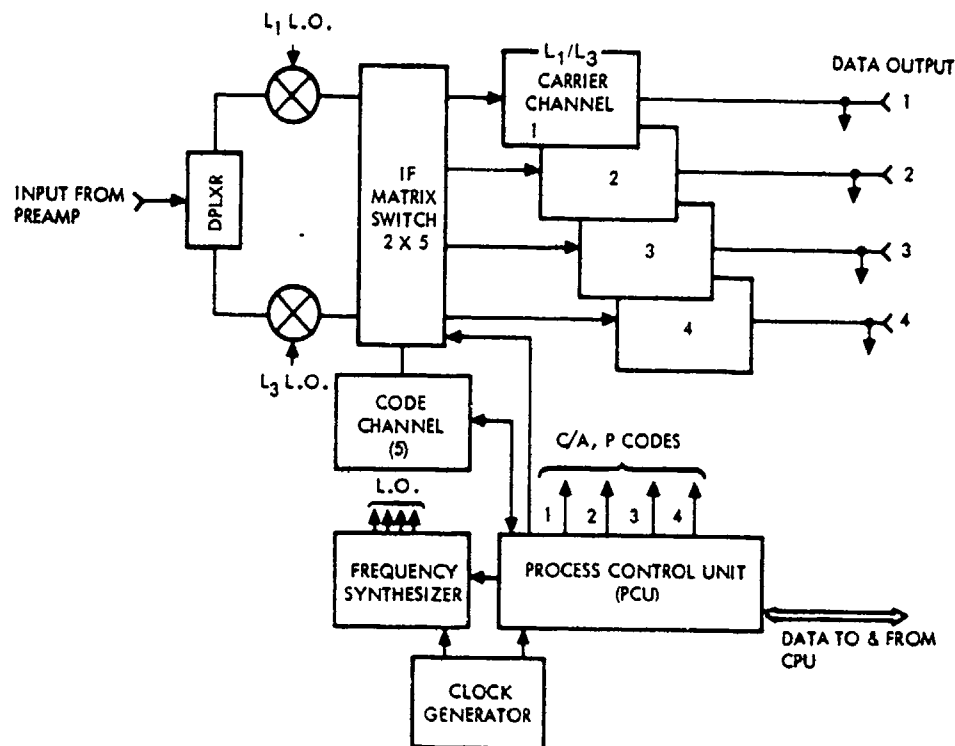


Figure 20. IONDS Receive Block Diagram

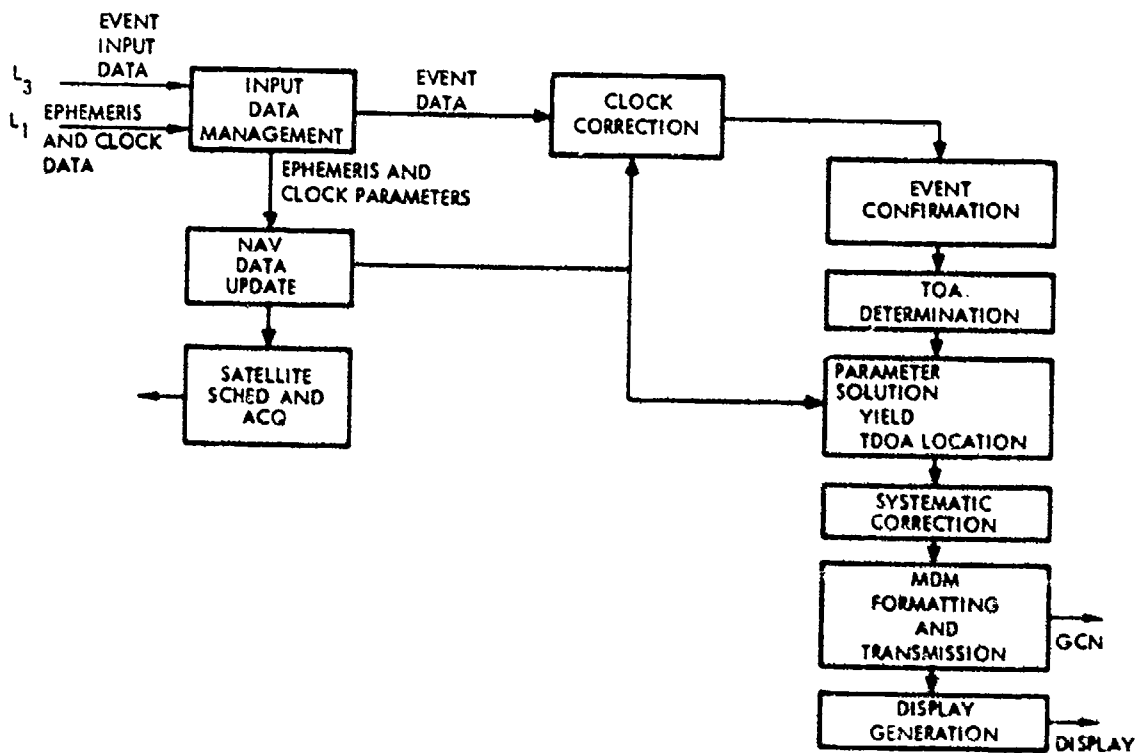


Figure 21. IONDS Receiving Terminal Processing Functions

3.3 IGS USER OPERATIONS

3.3.1 NUDET Position Determination

A NUDET may be detected by multiple sensors on GPS SV's. The times of these detections (t_{GBD_i}) are transmitted to the stations computing the position of the burst via the L_3 signal. The parameters for computing the SV positions are X_{S_i} , Y_{S_i} , Z_{S_i} .¹ The SV clock offsets (Δt_{SV_i} , T_{GD_i}) are also transmitted to the same stations via the L_1 GPS signal. Calibration parameters (Δt_{BBL_i} , Δt_{GBD_i}) are measured on the SV's before their launch and are stored at the stations. Delays through the ionosphere atmosphere (Δt_{A_i}), if any, are expected to be estimated at each terminal. However, continuous monitoring of such data using L_1 and L_2 could be provided for. The position and time of the burst (X_B , Y_B , Z_B , t_B) are computed from these parameters, as illustrated in Figure 22.

The relationships between the various times within a given SV that are pertinent to computing the true GPS time of the burst detection at a given SV are illustrated in Figure 23. The time of interest is t_i , the true GPS time of burst detection, although the tagged time of detection is t_{GBD_i} . This time t_i is related to SV time, t_{SV_i} , as derived in the GPS system as

$$t_i = t_{SV_i} - \Delta t_{SV_i} \quad (1)$$

where, in terms of the parameters in the GPS navigation message,

$$t_{SV_i} = a_{0i} + a_{1i} (t_{SV_i} - t_{oc_i}) + a_{2i} (t_{SV_i} - t_{oc_i})^2 \quad (2)$$

However, the SV time, t_{SV} , is, in general, neither the L_1 signal time nor the L_2 signal time. This is because the clock correction parameters are estimated in the GPS system based on two frequency transit time measurements corrected for ionospheric delay. A possible group delay differential between the transmitted L_1 and L_2 signals causes the correction of Equation 2 to be in error by the amount T_{GD_i} on L_1 and by χT_{GD_i} on L_2 . This is of no consequence to two frequency users, since it performs the same two-frequency corrections. However, for single-frequency users, a correction should be made if accuracies are desired to that level.

The same is true for relating GPS time to the SV baseband processor time, t_{BB_i} . This can be done by relating that baseband time to the time at the phase center of the L_1 transmitting antenna, since that time is related to the SV time as

$$t_{SVL_i} = t_{SV_i} + T_{GD_i} = t_i + \Delta t_{SV_i} + T_{GD_i} \quad (3)$$

If the delay between the baseband processor and the L_1 antenna (Δt_{BBL_i}) is measured before the launch of the SV, so that

$$t_{BB_i} = t_{SVL_i} + \Delta t_{BBL_i} \quad (4)$$

¹At GPS time of detection.

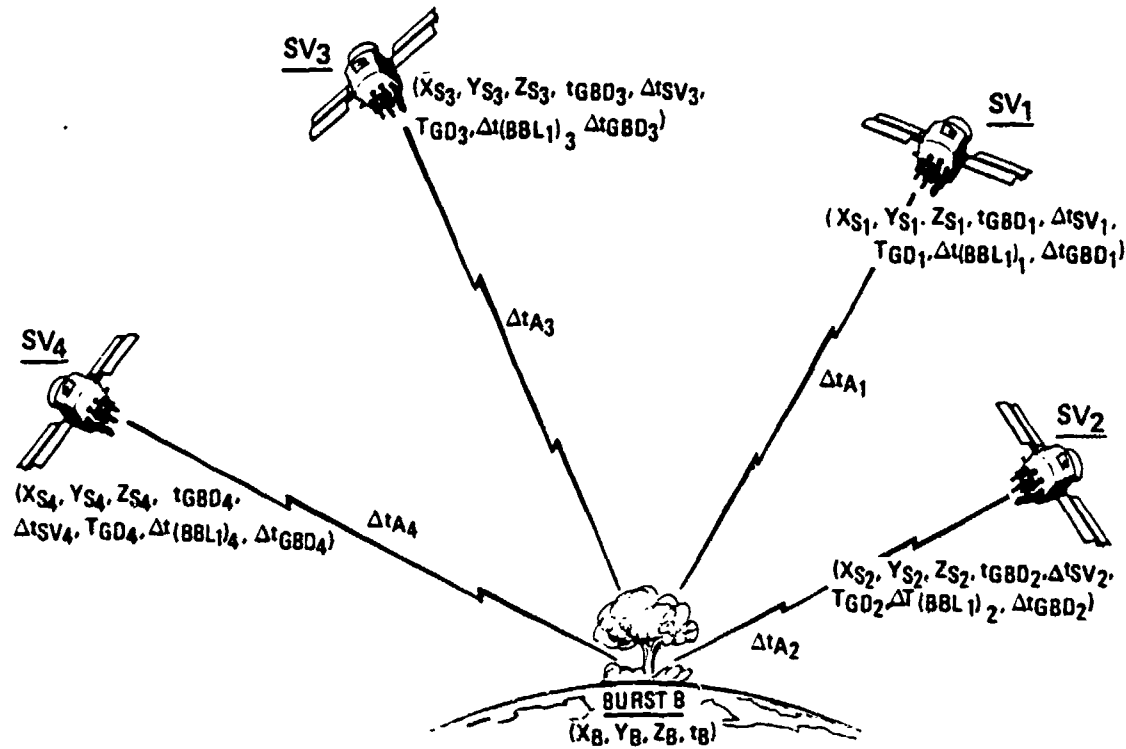
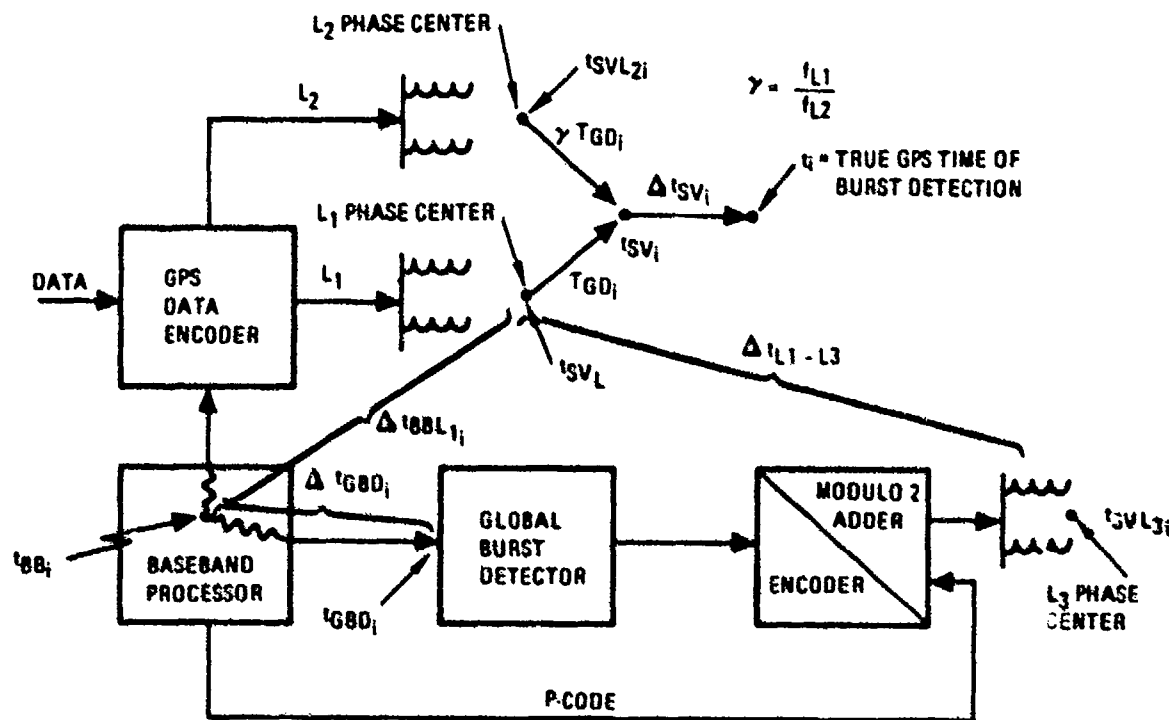


Figure 22. Global Burst Detection Parameters



* POSITIVE t 'S INDICATE TIME IF FAST

Figure 23. Relationship Between SV Times

this baseband time is related to GPS time t_i as

$$t_{BB_i} = t_i + \Delta t_{SV_{1_i}} + T_{GD_i} + \Delta t_{BBL_{1_i}} \quad (5)$$

(An epoch at the baseband occurs earlier than in GPS time by the amount $\Delta t_{SV_i} + T_{GD_i} + \Delta t_{BBL_{1_i}}$.)

Likewise, the delay between the baseband processor and the global burst detector (Δt_{GBD_i}) can be measured before the launch of the SV so that

$$t_{GBD_i} = t_{BB_i} - \Delta t_{GBD_i} \quad (6)$$

The relationship of that time to GPS time is found by combining Equations 5 and 6 so that

$$t_{GBD_i} = t_i + \Delta t_{SV_i} + T_{GD_i} + \Delta t_{BBL_{1_i}} - \Delta t_{GBD_i} \quad (7)$$

or, conversely, the GPS time of a burst time tagged with t_{GBD} is

$$t_i = t_{GBD_i} - \Delta t_{SV_i} - T_{GD_i} - \Delta t_{BBL_{1_i}} + \Delta t_{GBD_i} \quad (8)$$

It is conceivable that the delay between the burst detector and the L_1 antenna could be measured before launch so that

$$\Delta t_{GBDL_{1_i}} = t_{GBD_i} - t_{SVL_{1_i}} \quad (9)$$

Eliminating the baseband time and combining Equations 4 and 6 yield

$$\Delta t_{GBDL_{1_i}} = \Delta t_{BBL_{1_i}} - \Delta t_{GBD_i} \quad (10)$$

so that Equation 8 becomes

$$t_i = t_{GBD_i} - \Delta t_{SV_i} - T_{GD_i} - \Delta t_{GBDL_{1_i}} \quad (11)$$

solving for the NUDET location and time.

The ranges from the burst to the four SV's are

$$R_i = \sqrt{(X_{S_i} - X_B)^2 + (Y_{S_i} - Y_B)^2 + (Z_{S_i} - Z_B)^2}; i = 1, \dots, 4 \quad (12)$$

which is related to the transit times (Δt_{T_i}) of the detected wave front by

$$t_{T_i} = t_i - t_B = \frac{R_i}{C} + \Delta t_{A_i}; i = 1, \dots, 4 \quad (13)$$

where C is the speed of light, so that

$$R_i = Ct_i - C \Delta t_{A_i} - Ct_{B_i}; i = 1, \dots, 4 \quad (14)$$

where t_i is already corrected by Equations 8 or 11. Thus, we have four equations with four unknowns (X_B , Y_B , Z_B , and t_B). The fact that these equations are nonlinear only requires that they be solved in an iterative manner. One approach is to guess a solution (t_B should be about 60 milliseconds earlier than the t_i) and to linearize about the guessed solution and solutions of subsequent iterations. (This is called quasilinearization.) That is, solve for a solution vector

$$U_k = (X_{B_k}, Y_{B_k}, Z_{B_k}, t_{B_k})^T \quad (15)$$

where $()^T$ means transpose, and the k represents the k^{th} iteration ($k = 1, 2, 3, \dots$), from the equation

$$U_k = A_{k-1}^{-1} V \quad (16)$$

where the i^{th} row of the 4×4 matrix A_k is

$$A_{k,i} = \begin{bmatrix} X_{B_k} - 2X_{s_i}, & Y_{B_k} - 2Y_{s_i}, & Z_{B_k} - 2Z_{s_i}, & 2C^2 - C^2 t_{B_k} (t_i - \Delta t_{A_i}) \end{bmatrix} \quad (17)$$

and the i^{th} component of the 4×1 vector V is

$$V_i = C^2 (t_i - \Delta t_{A_i})^2 - X_{s_i}^2 - Y_{s_i}^2 - Z_{s_i}^2 \quad (18)$$

The iterations should be continued until there are no significant changes in the solution.

3.3.2 NUDET Time of Arrival (TOA) Error Sources

The one-sigma error in the computation of the GPS time of burst detection is simply the RSS of the errors in the terms of Equation 8 (or 11). This is, for Equation 8

$$\sigma_{t_i} = \sqrt{\sigma_{t_{GBD_i}}^2 + \sigma_{\Delta t_{SV_i}}^2 + \sigma_{T_{GD_i}}^2 + \sigma_{\Delta t_{BBL_i}}^2 + \sigma_{\Delta t_{GBD_i}}^2} \quad (19)$$

since they are probably, but not necessarily, independent of each other. In this equation $\sigma_{t_{GBD_i}}$ is the one-sigma error in time tagging the event given

that the time tag was supplied perfectly to the GBD. $\sigma_{\Delta t_{SV_i}}$ is the one-sigma

error of the SV clock correction, which for Phase 1 GPS is budgeted to be less than 9 nanoseconds for two hours after upload. $\sigma_{T_{GD_i}}$ is related to the error (or

drift) in the calibration of the L_2 group delay to L_1 group delay in the SV and the GPS control segments' ability to estimate it, which can occur only when the ionospheric delay is thought to be negligible. This error should be as low as 2 to 3 nanoseconds but could be as large as 22.5 nanoseconds $[1/(1-Y) \Delta(L_1 - L_2)]$ before it is estimated. The $\sigma_{\Delta t_{BBL_1}}$ and $\sigma_{\Delta t_{GBD_1}}$ are functions of the ability

to measure these delays and how they drift after launch.

3.3.3 Relativity Effects

The clock correction parameters received from an SV for computing Δt_{SV} include the effects of general relativity on the SV clock as it is observed from the surface of the earth. A question has arisen concerning these effects on the determination of the burst position and time. The position and time solution is identical to that of a GPS user on the surface of the earth except that the signal paths are reversed from those in GPS. Since the time of the burst, t_B , is the time on the surface of the earth, the relativity corrections for the SV times, as related to that time, are identical to those of the GPS user. Therefore, no additional relativity corrections are required.

3.4 GPS TIME AND FREQUENCY SYNTHESIS

The space vehicle navigation system provides continuous earth coverage for a navigational signal comprised of both a C/A signal and a P signal on one L-band carrier, and a P or a C/A signal on a second L-band carrier. The navigation signal is composed of PRN ranging code signals. Superimposed data provide satellite system time for acquisition aiding, the space vehicle ephemerides, and clock correction. The IONDS user will use the L_1 signal for P code tracking and for satellite timing and position data.

The PRN phase-modulated signals are radiated in three bands, L_1 , L_2 , and L_3 . The L_1 carrier component is quadriphase shift key (QPSK) modulated by separate PRN codes that contain the required navigation information. One carrier component is a precision navigation signal and the other a clear/acquisition signal. The P and C/A carrier components' relative RF power levels depend on which of two operating modes is used. The L_2 carrier signal is biphase-modulated by the same P or C/A signals used to modulate L_1 , selectable by ground command. The L_3 carrier signal is biphase-modulated by the P signal used to modulate L_1 , with IGS data added to the P code. The L_1 , L_2 , and L_3 carriers and all modulation rates are derived from one of the three 10.23-MHz frequency sources.

3.5 CODE CHARACTERISTICS

Characteristics of P and C/A codes are as follows, with the frequency and time tolerances being controlled by the SV frequency standard:

Characteristics	P	C/A
Chipping rate (Mbps)	10.23	1.023
Code epoch	7 days	1 ms
Data rate (bps)	50	50
Frame length (bits)	1,500	1,500

3.5.1 PRN P Code

The PRN P code is a ranging code, $XP_i(t)$, of 7 days in length at a chipping rate of 10.23 Mbps. The code generation technique has the capability of generating a set of 37 sequences of 7 days' length. Each of the sequences will be mutually exclusive. The space vehicle code generators are capable of generating a set of 32 sequences of 7 days' length and are selectable before launch. The remaining five sequences are reserved for other transmitters. The 7-day sequence is the Modulo-2 sum of two subsequences called X1 and X2. The X1 sequence is 15,345,000 chips (1.5 seconds) long. The X2 sequence is 15,345,037 chips long.

The P digital stream is the Modulo-2 sum of the data bit stream clocked at 50 Hz and two extended patterns clocked at 10.23 MHz (X1 and X2). X1 is generated by the Modulo-2 sum of the output of two 12-stage registers (X1A and X1B) short cycled to 4,092 and 4,093 chips, respectively. When the X1A short cycles are counted to 3,750, the X1 epoch is generated. The X1 epoch occurs each 1.5 seconds, after 15,345,000 chips of the X1 pattern.

The polynomials for X1A and X1B, as referenced to the shift register input, are as follows:

$$X1A: 1 + x^6 + x^8 + x^{11} + x^{12}$$

$$X1B: 1 + x^1 + x^2 + x^5 + x^8 + x^9 + x^{10} + x^{11} + x^{12}$$

Following the X1 epoch the first 12 chips of X1A contained in stages 1 and 12 (left to right) are 000100100100. The last three chips, 001, of the 4,095 sequence corresponding to this polynomial are omitted in shortening the sequence. The first 12 chips of X1B contained in stages 1 and 12 (left to right) are 001010101010. The last two chips of the 4,095 sequence corresponding to this polynomial, 01, are omitted in shortening the sequence.

At the occurrence of each epoch, X1A and X1B begin at the first chip of their respective sequences. Shortly before X1A completes the 3,750th (last) cycle of each 1.5-second epoch interval, X1B completes its 3,749th cycle. Then X1B is stopped at the final chip of its cycle until X1A completes its cycle, whereupon both begin a new epoch at the first chip of their respective sequences.

X2 is similarly generated by the Modulo-2 sum of the output of two 12-stage registers (X2A and X2B) short cycled to 4,092 and 4,093 chips respectively. The polynomials for X2A and X2B are as referenced to the shift register input:

$$X2A: 1 + x^1 + x^3 + x^4 + x^5 + x^7 + x^8 + x^9 + x^{10} + x^{11} + x^{12}$$

$$X2B: 1 + x^2 + x^3 + x^4 + x^8 + x^9 + x^{12}$$

The first 12 chips of X2A in stages 1 through 12 (left to right) are 101001001001. The last three chips, 100, of the 4,095 sequence corresponding to this polynomial, are omitted in shortening the sequence. The first 12 chips of X2B in stages 1 through 12 (left to right) are 001010101010. The last two chips of the 4,095 sequence, 01, are omitted in shortening the sequence. At the beginning of each one-week interval, all four 12-stage coders begin their sequences together. Thereafter, each time that X2A is in its 3,750th cycle, X2B is stopped until X2A completes its 3,750th cycle when X2B completes its 3,749th cycle. Then both X2A and X2B remain in their final state for 37 more of the 10.23-MHz pulses, and then both begin at the first chip of their respective sequences. The period of X2 is, accordingly, 15,345,037 chips. During the last cycle of X1A of a one-week interval, X1B, X2A, and X2B are halted upon reaching the last chip of their respective sequences until X1A completes its cycle and all four registers begin their sequences together. The X2 sequence is delayed by a selected integer number of chips, i , ranging from 1 to 32 and then is added Modulo-2 to the X1 sequence to produce $XP_i(t)$. The spacecraft P code mechanization is shown in Figure 24. (The end-of-week signal occurs 400 microseconds before the state-of-week signal.)

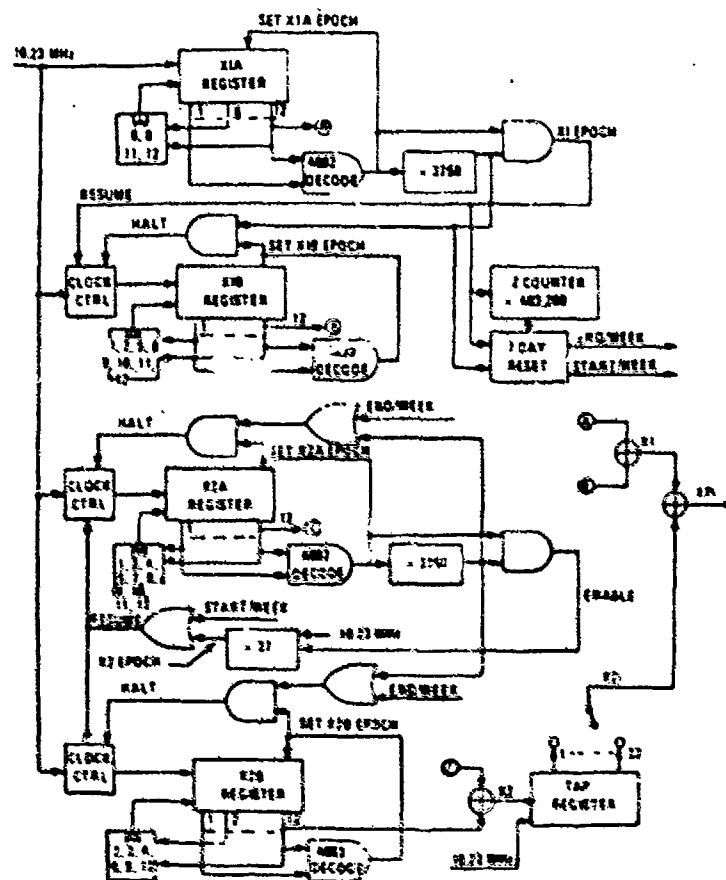


Figure 24. P Code Generation

The L_1 and L_3 codes and the X_1 epochs are synchronous with the same 10.23-MHz clock. The Z-count is defined as the 19-bit binary number that is equal to the number of X_1 epochs that have occurred since the end of the previous week. The range of the Z-count is from 0 to 403,199. The epoch coincident with the start of the present week is defined as the zero state of the Z counter.

3.5.2 PRN C/A Code

The PRN C/A code shall be a ranging code, $X_{Ci}(t)$, at a chipping rate of 1.023 MHz, and it shall be made up of a 1,023-bit Gold code. The epochs of the Gold code shall be synchronized with the X_1 epochs. One of the 32 different codes shall be hardwired at the time of production of each NAV subsystem. Each of the 32 codes shall have a low envelope cross-correlation with any other of the set. The polynomials and phases of the 32 codes shall be selected in accordance with ICD-MH08-00002. The C/A digital stream is a Modulo-2 sum of the data bit stream of 50 Hz (D), and a 1,023-bit linear pattern of 1.023 MHz (G). Epochs of the G code and transitions of the D train are aligned with the X_1 epochs of the P code. The G code is the Modulo-2 sum of two 1,023-bit linear patterns generated by means of the following polynomials

$$G_1 = x^{10} + x^3 + 1$$

$$G_2 = x^{10} + x^9 + x^8 + x^6 + x^3 + x^2 + 1$$

G_2 phases are selectable to provide 36 derived codes. Each of the 36 codes contains 512 ones and 511 zeros. The polynomial exponents are referred to the input end of the shift register.

3.6 DOWNLINK SYSTEM DATA

The transmitted system data $D(t)$ carry space vehicle ephemerides, system time, space vehicle clock behavior data, and system status messages. The data stream $D(t)$ is common to both the P and C/A signals on L_1 and L_2 . IGS data are transmitted on L_3 . Both user system segments use the navigation signal L_1 for acquisition, for P code tracking, and for determining system time and satellite position. The IONDS user receives the IGS signal transmitted on L_3 by the SV.

An antenna triplexer unit in the SV subsystem accepts three separate phase-modulated carrier signals (L_1 , L_2 , L_3), provides spectrum filtering to minimize out-of-band emissions, and combines these signals into a common port for simultaneous transmission to the antennas. The SV antenna radiates the GPS and IONDS signals.

The RF-radiated navigation signals are provided by a PRN assembly on the NAV subsystem on board each SV. Navigation data required by the NAV user will be updated by the MCS through the ULS. These data are stored in the NAV memory/processor module of the baseband processor.

The NAV subsystem is capable of operating in the nine modes shown in Table 6. The modes are differentiated by the specific combinations of P and C/A signals on L_1 and L_2 . Modes 7 and 8 are for ground checkout. The normal

Table 8. NAV System Operating Modes

Mode	L ₁ Link		L ₂ Link (Reference Only)	
	P	C/A	P	C/A
1	Normal	Normal	Normal	Note 4
2	Normal	Normal	Note 4	Normal
3	Normal	High	Normal	Note 4
4	Normal	High	Note 4	Normal
5	Normal	Normal	Note 3	Note 3
6	Normal	High	Note 3	Note 3
7	Note 3	Note 3	Normal	Note 4
8	Note 3	Note 3	Note 4	Normal
Standby	Note 3	Note 3	Note 3	Note 3
Notes: 1. L ₂ link modes are limited to normal P-code or standby 2. Mode control is effected through the TT&C system. 3. No RF carrier is transmitted. 4. Modulation not present.				

effective isotropic radiated power (EIRP) for L₃ is without a radio astronomy filter. Adding such a filter will drop the L₃ output power level due to the filter loss. These power levels are developed as shown in Table 9 and Figure 25. Note that the principal plane cut is deliberately shaped as shown to provide uniform signals to the user after atmospheric attenuation is considered.

The carrier frequencies for the L₁ and L₃ signals are coherently derived from the (nominal) 10.23-MHz oscillator frequency. To compensate for general relativistic effects, the actual SV standard frequency is 10.22999999545 MHz. The nominal carrier frequencies are 1575.42 MHz for L₁ and 1381.05 MHz for L₃.

A radio astronomy study was performed to predict the energy in the radio astronomy band due to IGS L-band transmission. The envelopes of the L₁ and L₃ spectra are shown in Figures 25 and 26, respectively. The analysis, verified by test in an anechoic chamber at full power, indicated that using the current triplexer L₃ filter allowed some low-level energy from L₃ to fall within the radio astronomy band. However, interference with the radio astronomy service (RAS) will be minimal due to the low L₃ duty factor (one time L₃ is transmitting divided by the radio astronomy integration time).

The transmitted spectrum, using an in-line filter (which may be added to the L₃ transmitter output if required), is illustrated in Figure 26. This in-line L₃ filter would decrease the L₃ signal in the 1400- to 1427-MHz band by approximately 27 dB beyond the levels achieved by the current triplexer, virtually assuring no RAS interference even with an increased L₃ duty cycle. Such a filter is not required by the L₃ frequency developmental authorization but may be included on NDS 6 if available.

Table 9. FSV 6 EIRP at Channel Center Frequency

Characteristics		L ₁	L ₂	L ₃
Transmitter total output power level	(dBW)	17.1	10.4	11.76
Losses				
Transmitter to triplexer cable				
Triplexer insertion loss	(dB)	-0.9	-0.9	-1.92
Triplexer to antenna cable				
RF power level at antenna input	(dBW)	16.2	9.5	9.84
Antenna gain*	(dB)	12.8	11.3	11.3
EIRP	(dFW)	29.0	20.8	21.14
*Worst case at EOE				

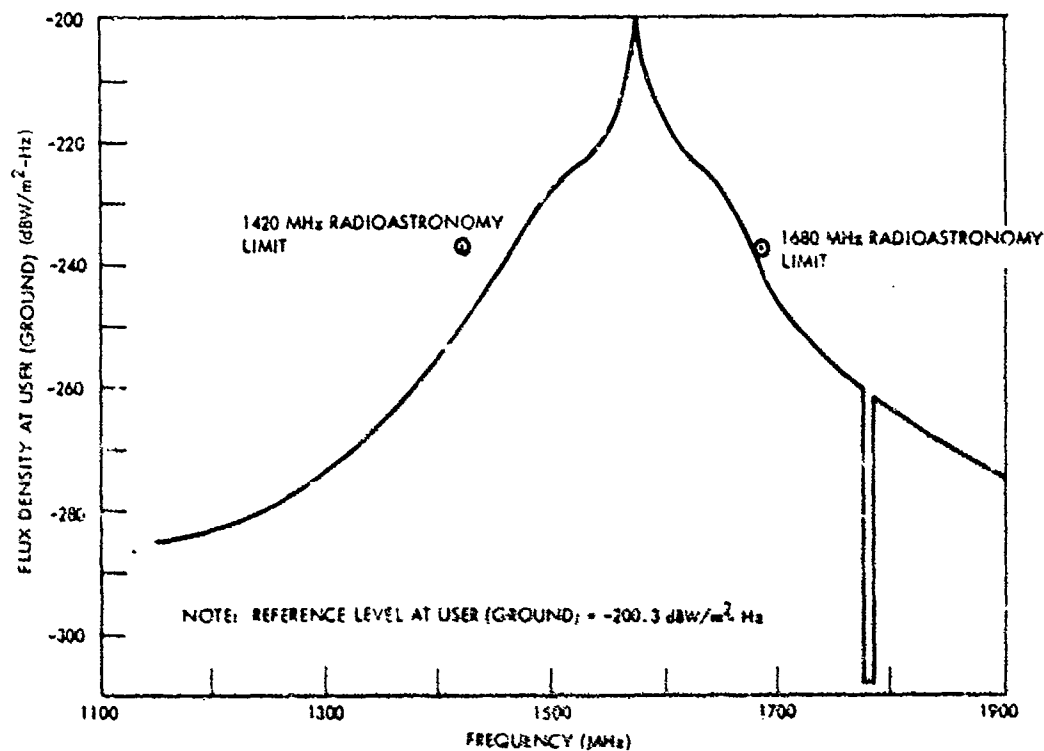


Figure 25. L₁ P Signal - Flux Density at Ground Versus Frequency

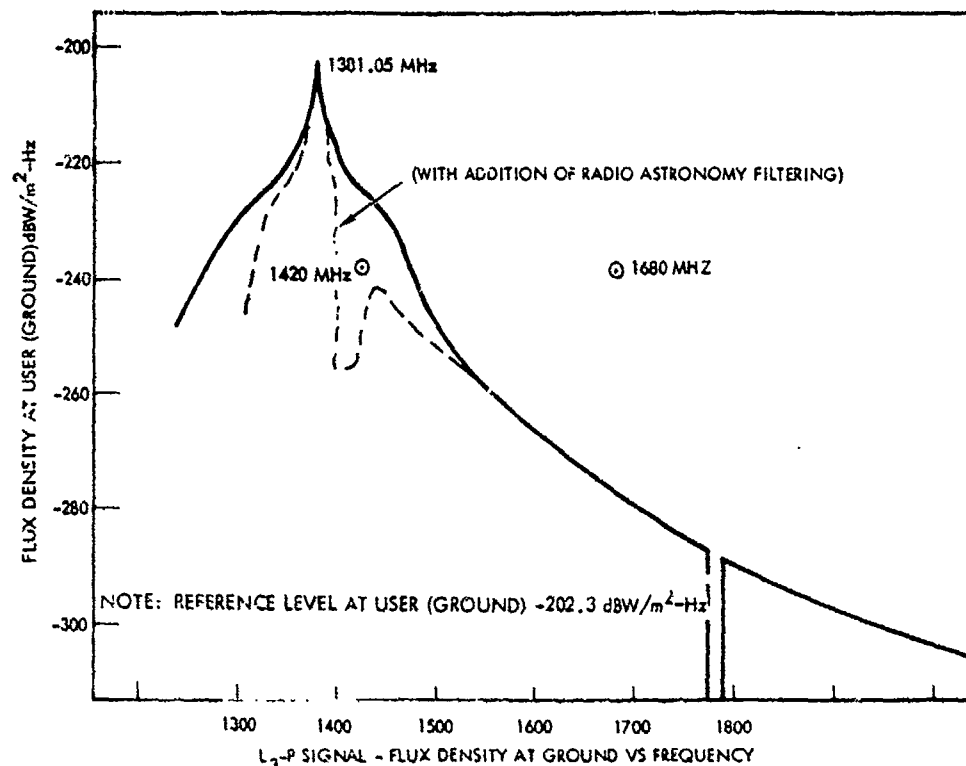


Figure 26. L₃ P Signal - Flux Density at Ground Versus Frequency

3.6.1 Code Waveform Characteristics

The phase noise spectral density of the unmodulated carrier is such that a phase-locked loop of 10-Hz one-sided noise bandwidth will be able to track the carrier to an accuracy of 0.1 radian rms. The typical transmitted carrier phase noise spectral density versus frequency is given in Figure 27.

In-band spurious transmission is less than -50 dB referred to the unmodulated carrier level. The definition of in-band channel allocation for both the L₁ and L₃ carriers is ± 10.23 MHz about the center frequency.

3.6.1.1 Equipment Group Delay Variation. Equipment group delay variation is the uncertainty in group delay as observed at the L₁ radiated output. The effective group delay uncertainty of L₁ does not exceed 3.0 nanoseconds (2 sigma) in noneclipse orbits or 5.0 nanoseconds (2 sigma) during eclipse conditions.

3.6.1.2 Timing Accuracy. The codes will always be maintained by the control segment within 976 microseconds of system time for each SV. In addition, the effective time difference between space vehicle time and system time is maintained within 10 microseconds. Space vehicle time is the mathematical combination of the PRN code phase and the time synchronization terms in the space vehicle almanac.

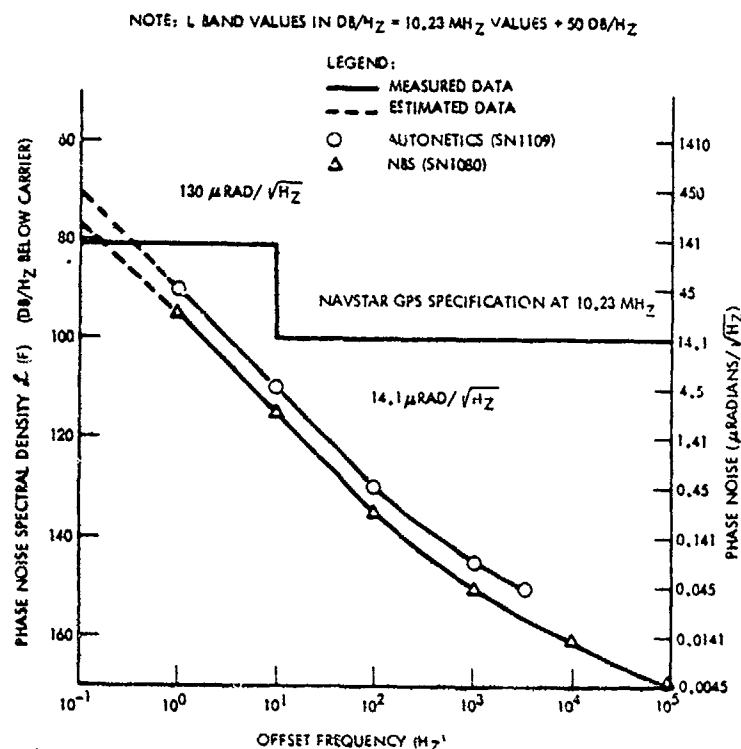


Figure 27. Typical Transmitted Carrier Phase Noise Spectral Density Versus Offset Frequency at 10.23 MHz

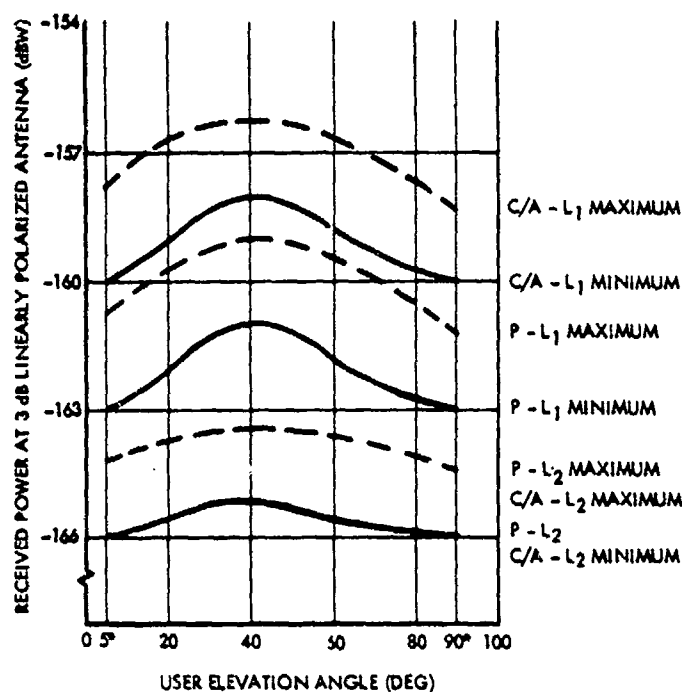
3.6.1.3 Antenna Polarization. All transmitted signals (L_1 , L_2 , L_3) are right-hand circularly polarized.

3.6.2 User-Received RF Signal Levels

3.6.2.1 Minimum GPS Signal Levels. Whenever the SV is above a 5-degree elevation angle, the user-received RF signal levels on L_1 and L_2 , as a function of elevation angle, at the output of a 3-dBi (above an isotropic) linearly polarized receiving antenna (worst orientation), will be above the levels in Figure 28. A maximum atmospheric path loss of 2 dB is included. User-received RF signal levels given are observed within the in-band channel allocation. A worst-case SV attitude error of +0.5 degree for signal level reduction was used. The minimum L_3 received signal strength under similar conditions is -163 dBW, which includes a coding gain not available to L_1 and L_2 .

3.6.2.2 L_1 Navigation Signal. The primary navigation signal at the L_1 frequency consists of the composite P and C/A signals in phase quadrature. These signals also carry digital navigation data.

The P signal is a continuous carrier biphase-modulated by a 10.23-Mbps PRN ranging code. Each SV radiates on the same frequency but is differentiated by code-division-multiplexing techniques. System data are transmitted by Modulo-2 addition of a 50-bps digital stream with the ranging code before carrier modulation.



NOTE: NOT VALID DURING MOMENTUM DUMP.

Figure 28. GPS Received Power Versus User Elevation Angle, L₁ and L₂

The C/A signal (acquisition) consists of a PRN/BPSK carrier with a chipping rate of 1.023 kbps. Navigation data are Modulo-2 added with the ranging code and one identical to that carried on the P signal.

P and C/A signals are transmitted on the same L₁ carrier in phase quadrature ± 100 m (peak); the relations between composite signal phase and code states are shown in Table 10. Crosstalk between the P and C/A signals is less than -20 dB. The total amplitude modulation (AM) on the total composite carrier observed in the middle 50-nanosecond portion of each chip is less than 1 dB.

Correlation loss is defined as the difference between the radiated SV power in a 20.46-MHz bandwidth and the signal power recovered in an ideal 20.46-MHz bandwidth correlation receiver. The correlation loss apportionment is:

- SV modulation imperfections 0.6 dB
- Ideal UE receiver waveform distortion (due to 20.46-MHz filter) 0.4 dB

3.6.2.3 L₂ Navigation Signal. The secondary navigation signal generation, modulation, and data of the L₂ navigation signal are identical to those of the L₁ P and C/A signals. Upon command, either the P or C/A signal is transmitted, but not both.

Table 10. Composite L₁ Transmitted
Signal Phase and Code State Relationship for Normal Mode

Composite L ₁ Signal Phase (deg)	Code State	
	P	C/A
0	0	0
-70.5	1	0
+109.5	0	1
180	1	1

3.6.2.4 L₃ IGS Signal. The IGS signal at the L₃ frequency consists of the biphas-modulated P signal. This signal carries the digital IGS data. The P signal is a continuous carrier biphas-modulated by a 10.23-Mbps PRN code. Each SV radiates on the same frequency but is differentiated by GPS code-division-multiplexing techniques. IGS data are transmitted by Modulo-2 addition of a 200-bps digital stream with the PRN code before carrier modulation. Insertion of a radio astronomy filter will cause some added correlation loss above that discussed for L₁.

3.6.2.5 Frequency Standard. An accurate frequency standard is provided as part of the NAV subsystem as a common source for coherently deriving carrier RF signals and for clocking the PRN generators. The frequency is adjustable via the TT&C in steps of 4×10^{-12} delta-f/f over a range of $\pm 2 \times 10^{-9}$ delta-f/f. The nominal output frequency is 10.23 MHz. Linear frequency drift does not exceed 1×10^{-12} per day after 24 hours of continuous operation. The exact output frequency of the frequency standard adjusted for relativistic effects is 10.22999999545 MHz plus or minus one part in 10^{11} as maintained by the control segment.

3.6.2.6 NAV Data Signal. The NAV data are nonreturn to zero at 50 bps. The complete data message is called a frame, which has a length of 1,500 bits. Each frame is made up of five subframes, each subframe being 300 bits long. Each subframe consists of 10 words, each of which is 30 bits long. The most significant bit (MSB) of all words is transmitted first.

Each data frame contains telemetry (TLM) words and handover words (HOW), both generated by the SV and data blocks generated by the control segment. The data blocks are distributed within the subframes. Each subframe contains a TLM word and a HOW and starts with the TLM/HOW pair. The TLM word is transmitted first, immediately followed by the HOW. The latter is followed by the data blocks. Thus, a TLM/HOW pair occurs every six seconds in the data frame.

3.6.3 Telemetry Word

Each TLM word is 30 bits long, occurs every six seconds in the data frame, and is the first word in each subframe. Bit 1 is transmitted first. Each TLM word begins with a preamble followed by the TLM message and six parity bits. Notification of a roll momentum dump is provided by a roll momentum dump flag in the HOW, a five-bit function code, and eight bits of the truncated Z-count contained in the Z-count buffer of the SV processor at the initialization of the

roll momentum dump. These eight bits are obtained as follows. Of the 19-bit Z-count, the 3 most significant bits and the 8 least significant bits are truncated. The remaining 8 bits are placed in bit positions 15 through 22 of the TLM word. Of any number of roll momentum dumps, the last one will be recorded. After a momentum dump has taken place, the truncated Z-count for the momentum dump is overwritten when any other telemetry request has been processed.

3.6.4 Handover Word

The HOW is 30 bits long and is the second word in each subframe immediately following the TLM word. A HOW occurs every six seconds in the data frame. The MSB is transmitted first. The HOW begins with the uppermost significant 17 bits of the Z-count. These 17 bits correspond to the Z-count at the X1 epoch which occurs at the start (leading edge) of the next subframe. Bit 18 is reserved for the roll momentum dump flag and Bit 19 for a synchronization flag. The roll momentum dump flag (a "1" in Bit 18) indicates that a roll momentum dump has occurred since the last upload. This flag is reset at a new end-of-message transmission at the conclusion of the next upload. When Bit 19 is 0, the SV is in synchronization. Synchronization is defined as the condition in which the leading edge of the TLM word is coincident with the X1 epoch. If Bit 19 is a 1, this condition does not exist (i.e., the SV is not in synchronization and further data may be erroneous). Bits 20 through 22 contain the subframe identification. These three bits show which subframe is within the frame (see Table 11).

3.6.5 Data Block I

The content of Data Block I is the SV clock correction parameters. These parameters are the three polynomial coefficients, a_0 , a_1 , and a_2 ; the L_1/L_2 correction term for the L_1 user, T_{GP} ; the eight ionospheric correction parameters α_n and β_n , $n = 0, 1, 2, 3$; a reference GPS time since weekly epoch, t_{OC} ; and the age of data (clock), AODC. The GPS weekly epoch occurs at midnight Saturday night, Sunday morning.

The polynomial describes the SV PRN code phase offset, Δt_{SV} , with respect to GPS system time, t , at the time of data transmission. These coefficients describe the offset for the interval of time (one hour as a minimum) in which the parameters are transmitted. The polynomial also describes the offset for an additional half hour (i.e., half an hour after the beginning of transmission of the next set of coefficients) to allow the user time to receive the message for

Table 11. Subframe Identification

Bit →	20	21	22	Subframe ↓
	0	0	1	1
	0	1	0	2
	0	1	1	3
	1	0	0	4
	1	0	1	5

the new interval of time (one hour minimum). The AODC indicates the GPS time of week at which the correction parameters were estimated to provide the user with a confidence level in the SV clock correction.

3.6.6 Data Block II

The content of Data Block II is the ephemeris representation parameters. These parameters are an extension to Keplerian orbital parameters describing the orbit during the interval of time (nominally one hour) for which the parameters are transmitted. They also describe the orbit for an additional half hour to allow the user time to receive the message for the new interval of time (one hour). The definitions of the parameters are given in Table 12. The age of data parameters indicates the time of week at which the parameters were estimated.

3.6.6.1 User Algorithm for SV Ephemeris Determination. The user computes the earth-fixed coordinates of position of the SV with a variation of the equations shown in Table 13. Data Block II parameters are Keplerian in appearance. The values of these parameters, however, are obtained via a nonlinear least-squares curve fit of the predicted SV ephemeris (time-position quadruples t, x, y, z).

3.6.6.2 Block II Format. Data Block II occupies the third through tenth 30-bit words (including parity) of the second and third subframes. Values for Data Block II parameters are given in Table 14.

3.6.7 Data Block III

The content of Data Block III consists of almanac data for 25 SV's. When required, the almanac message for dummy SV's is transmitted to maintain 25 pages within the almanac table. The dummy SV's are designated as the 0th SV. Identification is via the SV-ID parameter (i.e., bits 61 through 66 in the third word of the fifth subframe will contain zeros). The almanac message for the dummy SV's contains a simple bit pattern. For 12 or fewer SV's, almanacs may be repeated within the table. The almanac is transmitted on a rotating page basis. The control segment schedules almanac transmission on a per vehicle basis in such a manner as to allow for recovery of the almanac table.

3.6.7.1 Almanac. The almanac is a subset of the Data Block I and II parameters with reduced precision plus SV health and identification. The user algorithm is essentially the same as the one used to compute the precise ephemeris from Data Block II parameters (see Table 14). The almanac content for one SV is given in Table 15. All parameters appearing in the equations not included in the content of the almanac are assumed to be zero. A close inspection of Table 15 will reveal that the parameter δ_1 is transmitted, as opposed to the indication in Table 13 that the value is computed. In this respect, the application of Table 13 equations differs between the almanac and the ephemeris.

3.6.7.2 Almanac Reference Time. The almanac reference time, t_{0a} , is the multiple of 2^{17} seconds truncated from 3.5 days after the time that this applicable almanac begins transmission. The almanac will be renewed every six days at a minimum. Therefore, the almanac reference time is not ambiguous.

Table 12. Elements to Earth-Fixed Coordinates

M_0	Mean anomaly at reference time
Δn	Mean motion difference from computed value
e	Eccentricity
\sqrt{A}	Square root of the semi-major axis
Ω_0	Right ascension at reference time
I_0	Inclination angle at reference time
ω	Argument of perigee
$\dot{\Omega}$	Rate of right ascension
C_{uc}	Amplitude of the cosine harmonic correction term to the argument of latitude
C_{us}	Amplitude of the sine harmonic correction term to the argument of latitude
C_{rc}	Amplitude of the cosine harmonic correction term to the orbit radius
C_{rs}	Amplitude of the sine harmonic correction term to the orbit radius
C_{ic}	Amplitude of the cosine harmonic correction term to the angle of inclination
C_{is}	Amplitude to the sine harmonic correction term to the angle of inclination
t_{oe}	Reference time ephemeris
AODE	Age of data (ephemeris)

Table 13. Data Block II Definitions

$\mu = 3.956008 \times 10^{14} \frac{\text{meters}^3}{\text{sec}^2}$	WGS 72 value of the earth's universal gravitational parameter
$\dot{\Omega}_e = 7.292115855 \times 10^{-5} \frac{\text{rad}}{\text{sec}}$	WGS 72 value of the earth's rotation rate
$A = (\sqrt{A})^2$	Semi-major axis
$n_o = \sqrt{\frac{\mu}{A^3}}$	Computed mean motion
$t_k = t - t_{oe}^*$	Time from epoch
$n = n_o + \Delta n$	Corrected mean motion
$M_k = M_o + nt_k$	Mean anomaly
$M_k = E_k - e \sin E_k$	Kepler's equation for eccentric anomaly
$\cos v_k = (\cos E_k - e)/(1 - e \cos E_k)$ $\sin v_k = \sqrt{1 - e^2} \sin E_k / (1 - e \cos E_k)$	True anomaly
$\phi_k = v_k + \omega$	Argument of latitude
$\delta u_k = C_{us} \sin 2\phi_k + C_{uc} \cos 2\phi_k$	Second harmonic perturbations
$\delta r_k = C_{rc} \cos 2\phi_k + C_{rs} \sin 2\phi_k$	
$\delta i_k = C_{ic} \cos 2\phi_k + C_{is} \sin 2\phi_k$	
$u_k = \phi_k + \delta u_k$	Corrected argument of latitude
$r_k = A (1 - e \cos E_k) + \delta r_k$	Corrected radius
$i_k = i_o + \delta i_k$	Corrected inclination
$x'_k = r_k \cos u_k$ $y'_k = r_k \sin u_k$	Positions in orbital plane
$\Omega_k = \Omega_o + (\dot{\Omega} - \dot{\Omega}_e) t_k - \dot{\Omega}_e t_{oe}$	Corrected longitude of ascending node
$x_k = x'_k \cos \Omega_k - y'_k \sin \Omega_k$ $y_k = x'_k \sin \Omega_k + y'_k \cos \Omega_k$ $z_k = y'_k \sin i_k$	Earth fixed coordinates

*Asterisk indicates GPS system time at time of transmission, i.e., GPS time corrected for transit time (range/speed of light)

Table 14. Data Block II Parameters

Parameter	No. of Bits	Scale Factor (LSB)	Range*	Units
AODE	8	2^{11}	524,288	seconds
C_{rs}	16	2^{-5}	± 1024	meters
Δn	16	2^{-43}	$\pm 4E-9$	semicircles/sec
M_0	32	2^{-31}	± 1	semicircles
C_{uc}	16	2^{-29}	$\pm 6E-5$	radians
e	32	2^{-33}	0.5	dimensionless
C_{us}	16	2^{-29}	$\pm 6E-5$	radians
\sqrt{A}	32	2^{-19}	8192	meters ^{1/2}
t_{oe}	16	2^4	604,784	seconds
Spare	6	-	-	-
C_{ic}	16	2^{-29}	$\pm 6E-5$	radians
Ω_0	32	2^{-31}	± 1	semicircles
C_{is}	16	2^{-29}	$\pm 6E-5$	radians
i_0	32	2^{-31}	± 1	semicircles
C_{rc}	16	2^{-5}	± 1024	meters
ω	32	2^{-31}	± 1	semicircles
Ω	24	2^{-43}	$5E-5$	semicircles/sec
Spare	22	-	-	-

*(+) indicates that the sign bit will occupy the most significant bit (MSB).

GPS time, t , never differs from t_{oa} by more than 3.5 days. If the magnitude of $t - t_{oa}$ is less than 302,400 seconds, t_{oa} will be used as is. If $t - t_{oa} \geq 302,400$, add 604,800 seconds to t_{oa} before use. Similarly, if $t - t_{oa} \leq -302,400$, subtract 604,800 from t_{oa} before use.

3.6.7.3 Aging Parameters. The clock aging parameters consist of a first-order polynomial, which when used to adjust SV time, provides time to within 10 microseconds of GPS time. The polynomial is described by an eight-bit constant term, a_0 , and an eight-bit first-order term, a_1 . The clock correction to the SV PRN code phase time, t_{sv} , is applied as follows

$$t = t_{sv} - \Delta t_{sv}$$

where

t ~ GPS time (seconds)

Table 15. Data Block III Content

Parameter	No. of Bits	Scale Factor (LSB)	Range*	Units
ID	8	1	255	discretes
e	16	2^{-21}	2^{-5}	dimensionless
t_{oa}	8	2^{12}	602,112	seconds
i	16	2^{-20}	$\pm 2^{-5}$	semicircles
SV health	8	1	255	discretes
$\dot{\Omega}$	16	2^{-38}	$\pm 2^{-23}$	semicircles/sec
\sqrt{A}	24	2^{-11}	2^{13}	meters ^{1/2}
Ω_0	24	2^{-23}	± 1	semicircles
ω	24	2^{-23}	± 1	semicircles
M_0	24	2^{-23}	± 1	semicircles
a_0	8	2^{-17}	$\pm 2^{-10}$	sec
a_1	8	2^{-35}	$\pm 2^{-28}$	sec/sec
Spare	6	-	-	-

*(+) indicates that the sign bit will occupy the most significant bit (MSB).
 $i_0 = 0.349609375$ semicircles .33333... = 60-degree inclination.
 Note: All binary numbers will be two's complement.

$t_{gv} \sim$ SV PRN code phase time at transmission (seconds)

and

$$\Delta t_{gv} = a_0 + a_1 (t - t_{oa})$$

where

t_{oa} = almanac reference time (GPS time value)

3.6.7.4 SV Health and Status. The satellite health word occupies bits 137 through 144 of the fifth subframe. The three most significant bits (i.e., bits 137, 138, and 139) indicate the health of the navigation data. The remaining five bits indicate the health of the signal components. The format of the satellite health word follows:

Bits

137 138 139

0 0 0 All data OK

0 0 1 Parity failure--some or all parity bad

Bits			
137	138	139	
0	1	0	TLM/HOW format problem--any departure from standard format (e.g., preamble misplaced and/or incorrect, etc.) except for incorrect Z-count as reported in HOW
0	1	1	Z-count in HOW bad--any problem with Z-count value not reflecting actual code phase
1	0	0	Data Block I and/or II--one or more elements in Data Block I and/or II are bad
1	0	1	Data Block III--one or more elements in Data Block III are bad
1	1	0	All uploaded data bad--one or more elements of Data Block I and/or II and III are bad. Note that this could be used to preclude erroneous use of a vehicle not being serviced by the MCS.
1	1	1	All data bad--TLM and/or HOW and one or more elements in Data Blocks I and/or II and III are bad

Bits					
140	141	142	143	144	
0	0	0	0	0	All signals OK
0	0	0	0	1	All signals weak (i.e., 3 to 6 dB below specified power level due to reduced power output, excess phase noise, SV attitude, etc.)
0	0	0	1	0	All signals dead
0	0	0	1	1	All signals have no data modulation
0	0	1	0	0	L ₁ P signal weak
0	0	1	0	1	L ₁ P signal dead
0	0	1	1	0	L ₁ P signal has no data modulation
0	0	1	1	1	L ₂ P signal weak
0	1	0	0	0	L ₂ P signal dead
0	1	0	0	1	L ₂ P signal has no data modulation
0	1	0	1	0	L ₁ C signal weak
0	1	0	1	1	L ₁ C signal dead

Bits					
140	141	142	143	144	
0	1	1	0	0	L ₁ C signal has no data modulation
0	1	1	0	1	L ₂ C signal weak
0	1	1	1	0	L ₂ C signal dead
0	1	1	1	1	L ₂ C signal has no data modulation
1	0	0	0	0	P signal weak
1	0	0	0	1	P signal dead
1	0	0	1	0	P signal has no data modulation
1	0	0	1	1	C signal weak
1	0	1	0	0	C signal dead
1	0	1	0	1	C signal has no data modulation
1	0	1	1	0	L ₁ signal weak
1	0	1	1	1	L ₁ signal dead
1	1	0	0	0	L ₁ signal has no data modulation
1	1	0	0	1	L ₂ signal weak
1	1	0	1	0	L ₂ signal dead
1	1	0	1	1	L ₂ signal has no data modulation
1	1	1	0	0	SV is temporarily out--do not use this SV during current pass
1	1	1	0	1	SV will be temporarily out--do not use this SV during period for which almanac is valid
1	1	1	1	0	Spare
1	1	1	1	1	Spare

3.6.7.5 SV Identification. The satellite ID word occupies Bits 61 through 68 of the fifth subframe. The two most significant bits designate the ICD revision to which that satellite complies.

3.6.7.6 Data Block III Format. Data Block III occupies the third through tenth word (including parity) of the fifth subframe. The number of bits, the

scale factor of the least significant bit (LSB), and the range and the units of the parameters are as specified in Table 15.

3.6.7.7 Message Block. The message block occupies the third through tenth 30-bit word (including parity) of the fourth subframe. The message block provides space for the transmission of 23 eight-bit ASCII characters. The remaining eight bits do not bear information.

3.6.7.8 Parity. The parity links 30-bit words within and across subframes of 10 words. The SV computes parity only for the TLM word and HOW, the first two words of the 10-word subframe, using the Hamming code. The satellite parity computation computes zeros for the last two bits, D29 and D30, of both the TLM word and HOW. The parity of NAV data words 3 through 10 are computed by the control segment in accordance with the (32, 26) Hamming code.

3.6.7.9 User Parity Algorithm. As far as the user is concerned, several options are available for performing data decoding and error detection. Figure 29 presents an example flow chart which defines one way of receiving data (d_n) and checking parity. The parity bit D30 is used for recovering raw data. Parity bits D29 and D30, along with the recovered raw data (d_n), are Modulo-2 added for D25 . . . D30 which provide computed parity to compare with transmitted parity D25 . . . D30. Regardless of the parity encoding scheme used for satellite transmission during Phase I, the user's parity algorithm will be transparent (no change required) to the encoding scheme.

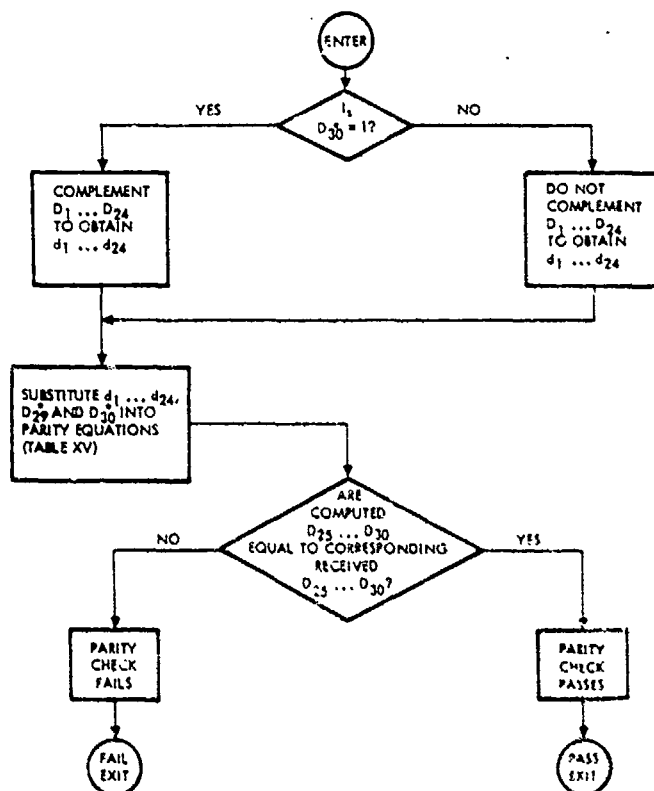


Figure 29. Flow Chart for User Implementation of Parity Algorithm

4. GPS/IGS SUBSYSTEM DESIGN

4.1 REQUIREMENTS AND CONSTRAINTS

The subsystem requirements include full exploitation of the design for all subsystems to minimize cost, risk, and impact on schedule while maximizing performance reliability and legacy. Placement of the IGS on the GPS satellite was constrained by the capability of the GPS vehicle to support the added hardware. Also, a functional constraint imposed on design efforts was that the IGS system in no way compromise the basic mission of the GPS satellite.

4.2 IGS DESIGN

The IGS/GPS overall block diagram is presented in Figure 30 as an introduction to IGS operation. To accomplish accurate three-dimensional location of nuclear events, the IGS user requires burst detection time of arrival information (TOA) from the GPS system. The TOA and signal characteristics are supplied to the L₃ transmitter channel for transmission to the user. Operation of the system can be traced from the X and Y detectors. Analog visible light and X-ray signals are converted into digital information by the sensor processor. The time of a detected arrival and signal characteristics are determined by the BDP, converted to digital information, and passed along via a buffer memory with an enable gate to the L₃ encoder. The L₃ encoder performs block differential, and convolutional encoding of the data from the sensor processor. The resultant signal is reclocked at 10.23 MHz and provides modulation for the transmitted L₃ signal.

The L₃ encoder and the sensor processor use 200- and 400-Hz inputs from the timing interface assembly, which is locked to a 100-Hz signal from the baseband processor. The L₃ transmitter unit multiplies the 10.23-MHz signal from the baseband processor by a factor of 135 to achieve the 1381.05-MHz frequency. The 1381.05-MHz carrier is modulated at 10.23 MHz and then amplified to a worst-case 15-watt RF power level. The output RF (1381.05 MHz) is fed to the L-band triplexer, where it is combined with the L₁ and L₂ frequencies and applied to the L-band antennas. The IGS system also uses the GPS TT&C subsystem to receive commands and transmit state-of-health data.

The IGS components consist of the following:

- Burst detector processor (BDP) and sensors
- Baseband/processor (BBP)
- L₃ encoder
- L₃ transmitter and switch box
- Frequency synthesizer

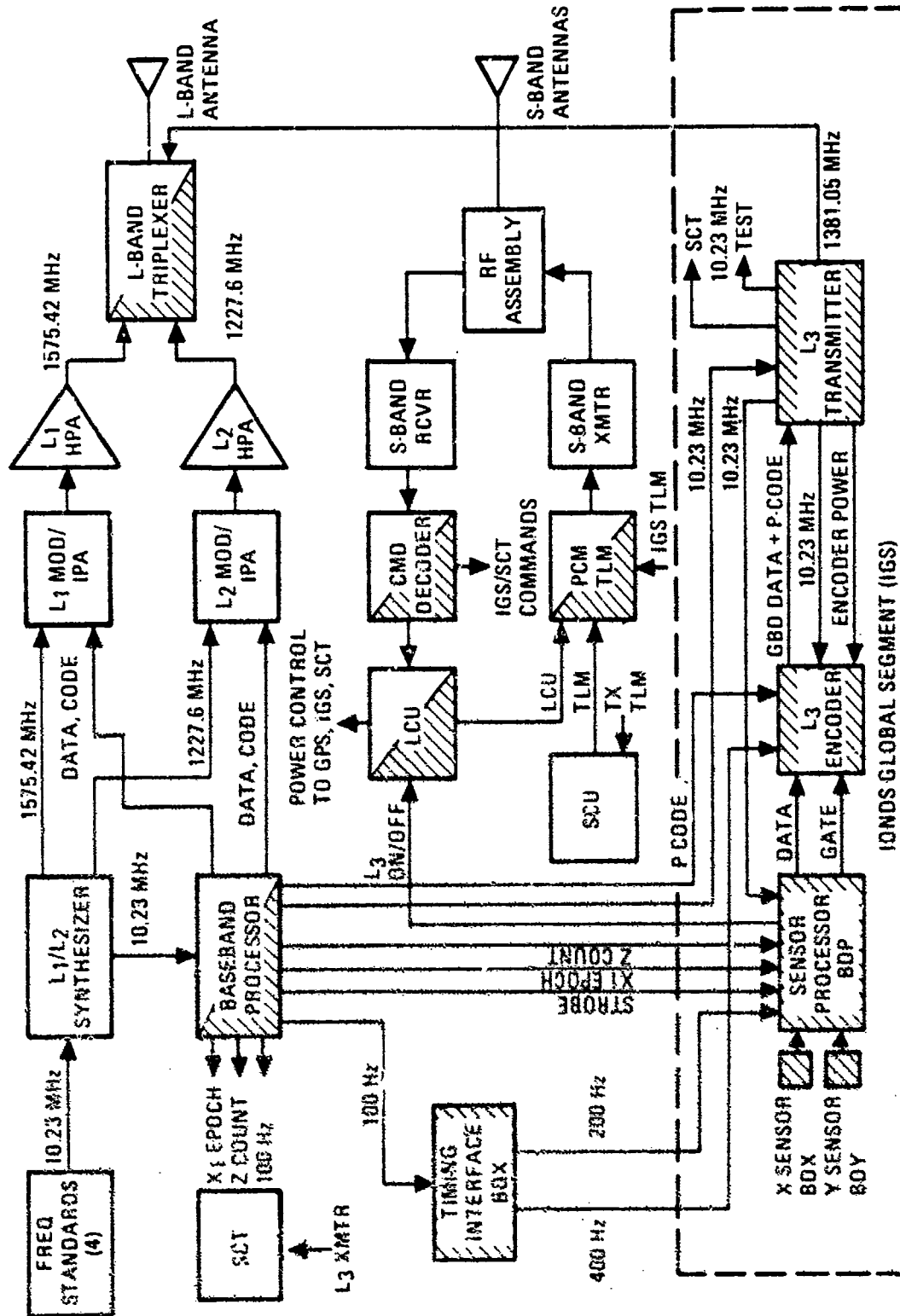


Figure 30. IONDS/GPS Overall Block Diagram



- Multiplier/filter assembly
- Automatic gain control (AGC) amplifier
- QPSK modulator
- Intermediate-power amplifier (IPA)/high-power amplifier (HPA)
- Power monitor
- RF switch box
- L₃ transmitter power supply
- L-band triplexer
- L-band antenna
- Timing interface box

4.2.1 Burst Detector Processor (BDP) and Sensors

Both the sensors and the BDP are GFE manufactured by Sandia Corporation. Much of the information pertaining to the performance of these components is classified and has been omitted from this report. The basic IONDS sensor/processor spacecraft requirements are listed in Table 16. A functional

Table 16. Burst Detection Sensor Spacecraft Requirements

Pointing accuracy:	± 0.5 deg
Maximum pointing drift rate:	0.01 deg/sec
Optical/point axes align:	± 0.1 deg
Field of View:	
A.	Unvignetted: 29 deg
B. BDY	Fully vignetted: 22.5 deg (half angle)
Sensor inputs from GPS:	Power: on/off control
	Timing: Z-count and clock
	Commands: 8 discrete
	14-bit serial
	Control signals for: Commands
	SOH
	Timing
Sensor outputs to GPS:	Payload data: 200 bits
	SOH: 2000 bits/day
	8-bit parallel words
	Interrupt control

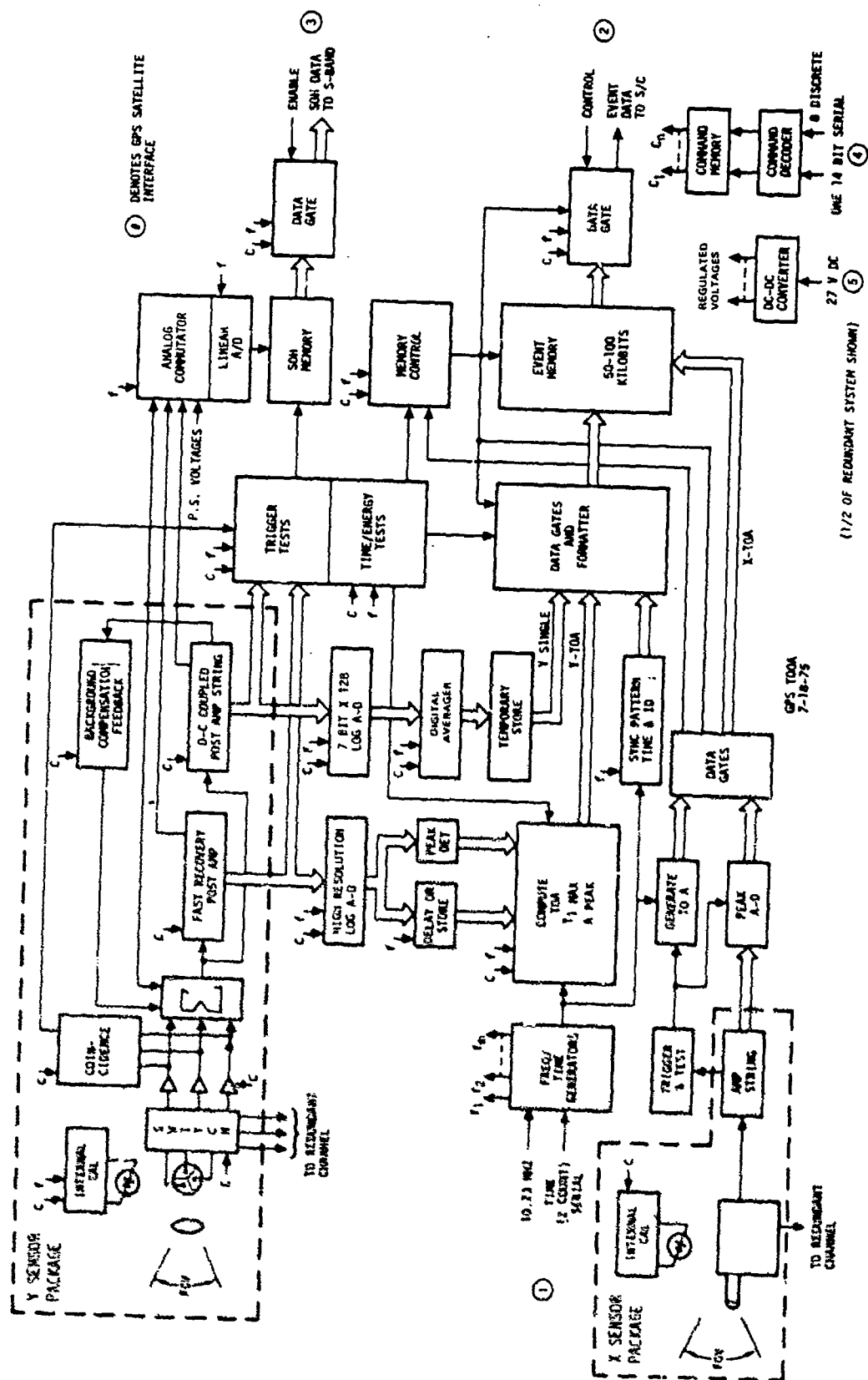


Figure 31. GBD Block Diagram

block diagram of the sensors and the GBD is shown in Figure 31. Required satellite interfaces are denoted by the circled numbers.

4.2.2 Baseband/Processor (BBP)

The BBP is a basic component of the GPS NAV subsystem. This unit has been modified to support IGS operations in several ways:

1. Supplies 10.23-MHz clock for synthesizers and fine grain timing purposes
2. Supplies P code for both NAV and IGS data for identification and spectrum spreading
3. Supplies Z-count, clock, and X1 epoch signals for IGS data annotations

The 10.23-MHz clock signal is derived from an atomic standard and permits precision synchronization of data and events occurring at the SV. The P code signal is unique to each vehicle. The 50- and 200-bus NAV and IGS data streams are Modulo-2 added to the P code, which primarily provides the SV identification and secondarily allows code tracking of interrupted IGS transmission in the absence of a signal.

The Z-count is used for coarse timing of events. The Z-count, together with correction coefficients derived from the 50-bps data stream, is employed by the user to correlate events with GPS time, which, in turn, coordinates all SV events to a single time reference.

The X1 epoch is used as a "fiducial" to provide a precise 1.5-second time base to establish time between Z-counts. The 10.23-MHz signal is up-counted with the X1 epoch used to establish the count period. The sum of the Z-count and the counter contents are used to time events to an accuracy within a few tens of nanoseconds.

A simplified functional block diagram of the BBP is presented in Figure 32.

During the IGS development phase, an IGS engineering model BBP was created by eliminating the baseband board 2 section of the unit and replacing it with an IONDS interface board. The board provided buffered, redundant output signals to both the IGS and SCT payloads. These signals consisted of the 10.23-MHz clock, Z-count, X1 epoch, and 100-Hz clock signals described earlier. This unit was employed in all of the systems tests discussed later. The unit is shown in Figure 33.

The extent of these BBP modifications required that the BBP's volume be increased by 1/3, which would have nullified the unit qualification status. Initially, the BBP was to be radiation hardened, requiring extensive modifications that also would have invalidated its qualification status. Subsequent decisions which precluded hardening of the BBP until Phase III resulted in a minimum baseband modification concept that preserved the BBP packaging by adding functions to the encoder discussed below. The functional growth of the encoder resulted in the timing interface and encoder (TIE) assembly.

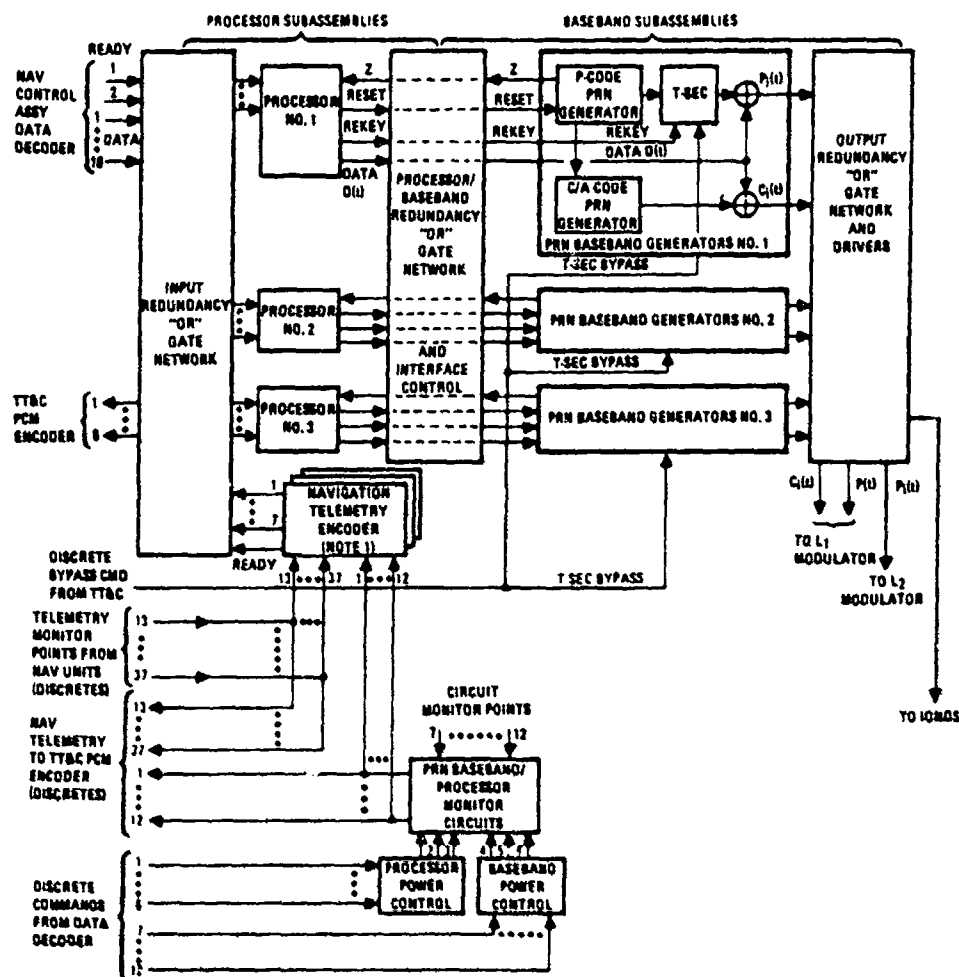


Figure 32. Baseband/Processor Functional Block Diagram

The minimum baseband modification consists of modifying baseband board 2 and rewiring the back plane and the harness to connector J10. This harness provides signals to the TIE assembly for distribution by TIE to other subsystems. J10 (BBP test) has been increased from 37 to 55 pins. Board 2 has been redesigned to accommodate four additional integrated circuits (IC's) to provide isolation and drive to the TIE for 10.23-MHz, P code, Z-count, and 200-Hz clock signals. The modified board is shown in Figure 34.

The board design has been subjected to thermal analysis and is presently being readied for qualification and EMC testing to establish its design by similarity to existing units.

The modification increased power demand 0.6 watt and increased the weight of the BBP a modest 0.2 of a pound. The board and assembly are totally compatible and interchangeable with the existing GPS hardware. The ICS EDM BBP has been converted to the "minimum modification" configuration for ETV use.

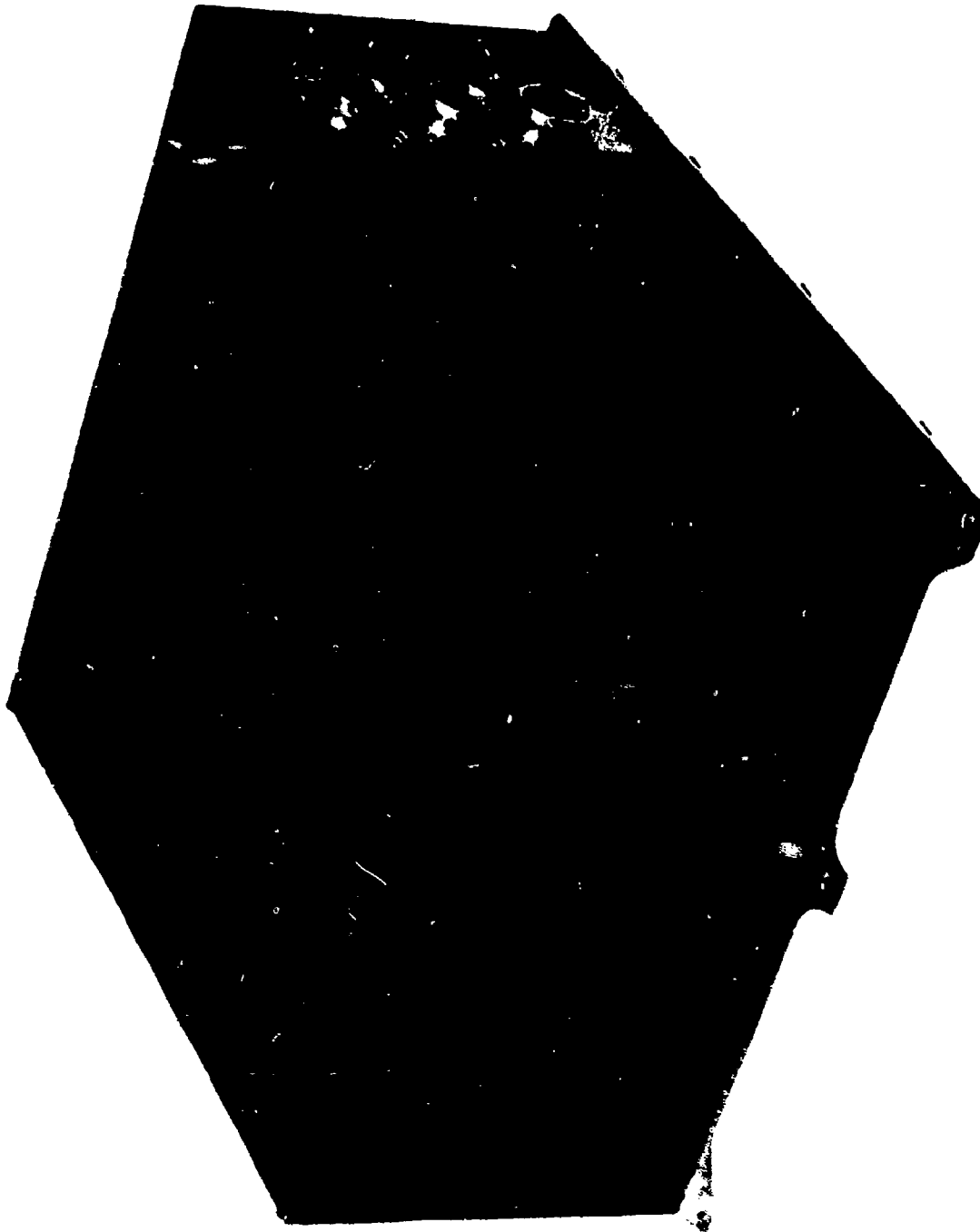


Figure 33. IONDS Modified Baseband

4.2.3 L₃ Encoder

The purpose of the L₃ encoder, shown in Figure 35, is to improve the bit rate (5 dB) by encoding data from the BDP. Logic circuits are basically low-power Schottky TTL and were initially designed to perform block differential, and convolutional encoding. The final operational version will probably use a block/convolutional/interleave/differential sequence. A signal for use by the TT&C subsystem is also provided upon recognition of a 24-bit synchronization word at the beginning of each data block. Finally, convolutionally encoded data are Modulo-2 added with a 10.23-MHz PN sequence supplied by the baseband subsystem. The resultant signal is reclocked at 10.23 MHz and is the modulation signal for the transmitter.

The block encoder section (see Figure 36) consists of a 22-bit shift register and an array of exclusive OR gates to perform division of the incoming message data, $m(x)$, by the polynomial divisor $p(x)$ where

$$p(x) = x^{22} + x^{20} + x^{14} + x^{13} + x^{12} + x^{11} + x^8 + x^7 + x^5 + x^3 + x + 1$$

The first 24 bits of data at the beginning of each data block describe the synchronization word. Therefore, two extra shift register stages are added at the end of the 22-bit register to assist detection of the 24-bit sync word. Upon detection of the word (via a series of gates), a pulse is generated which toggles a flip-flop. The TT&C subsystem periodically samples the state of this flip-flop.

The actual division process uses 22-shift register stages and begins when the enable signal from the BDP is true. Division continues until the enable signal toggles false. Then, the current remainder, $r(x)$, 22 bits in the shift register is immediately shifted out. The remainder (or parity tail) is gated contiguously following the input data stream that was sent directly to the differential encoder when the enable signal was true.

After the 22-bit parity tail is shifted on to the differential encoder, two more zero (or false level) bits are added to complete the tail. The zero bits are provided as error status bit locations.

The resultant signal (serial stream) sent to the differential encoder section then consists of the original message bits followed by the parity tail and 2 zero bits.

The differential encoder, shown in Figure 37, continuously stores each output data bit in a delay flip-flop, whereupon the stored bit inverts the following input data bit only if the stored bit is true (or 1). If the stored bit is false, the following input bit is transmitted unchanged and becomes the next stored bit. This technique then encodes data ones and zeros into data transitions and eliminates ambiguity when the data are later decoded since the RF carrier has a 180-degree phase ambiguity if it is tracked using only the modulated received signal. The penalty for differential encoding-decoding is approximately 0.1 dB in performance.

The output of the differential encoder is sent to the convolutional encoder (see Figure 38). This logic consists of a 7-bit shift register and

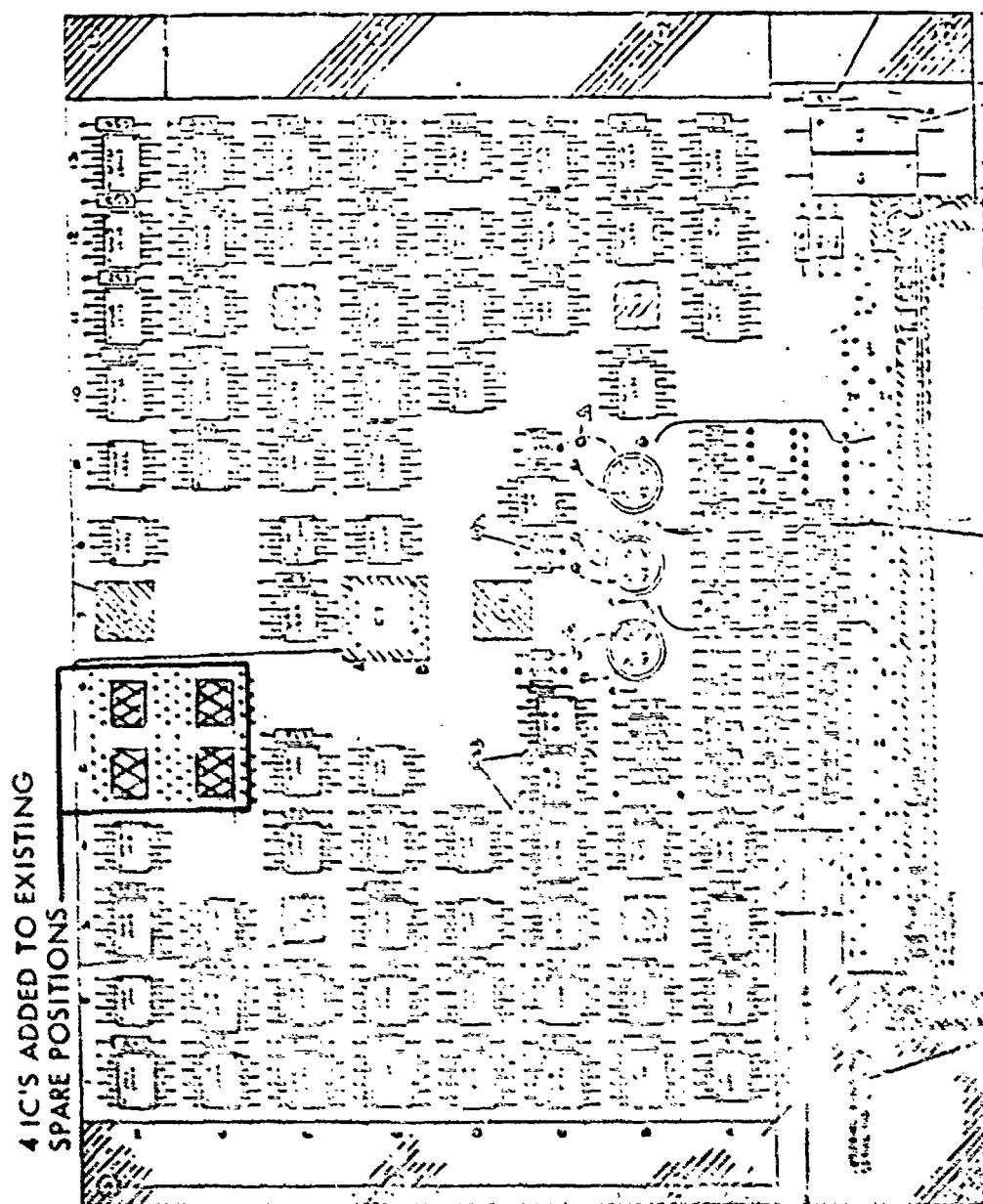


Figure 34. Baseband Board 2 With SPL Components Added

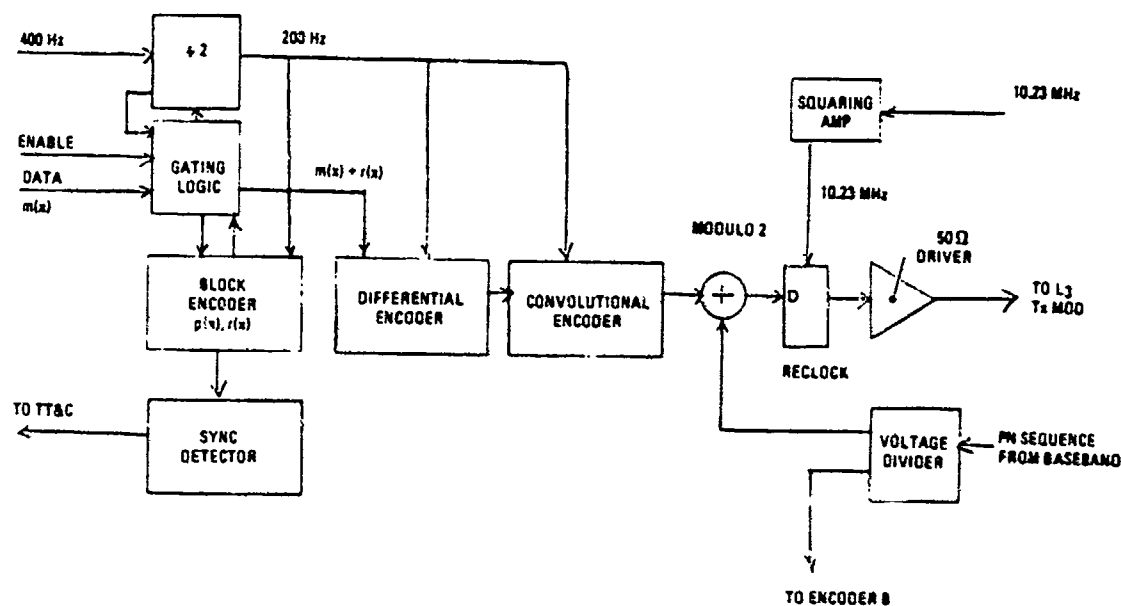


Figure 35. L3 Encoder Block Diagram

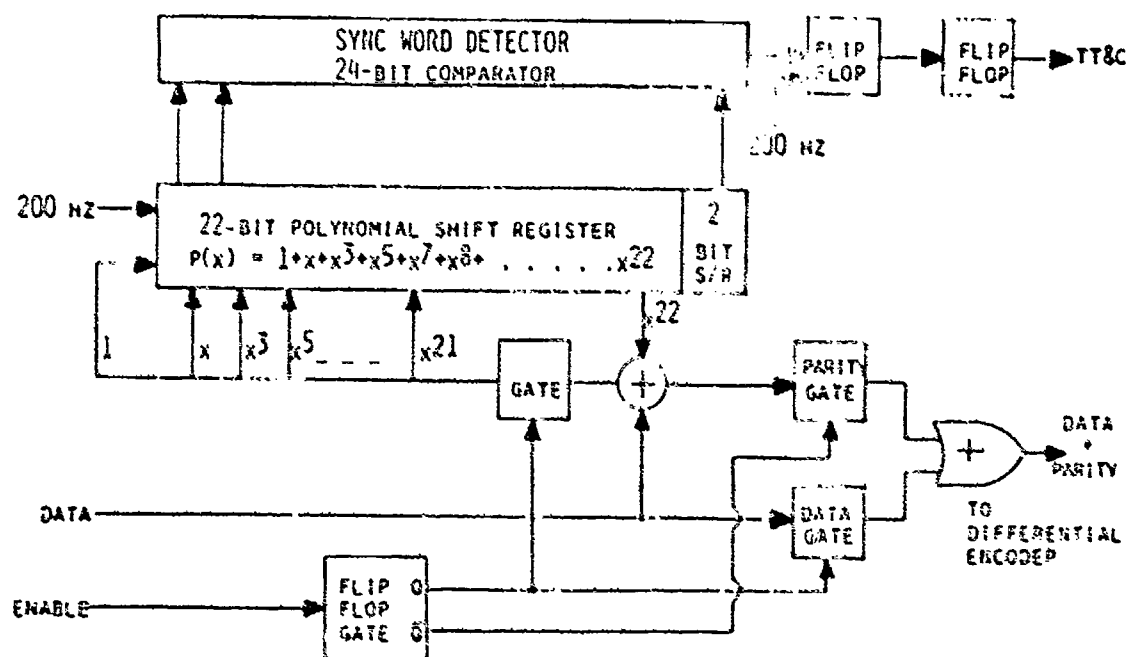
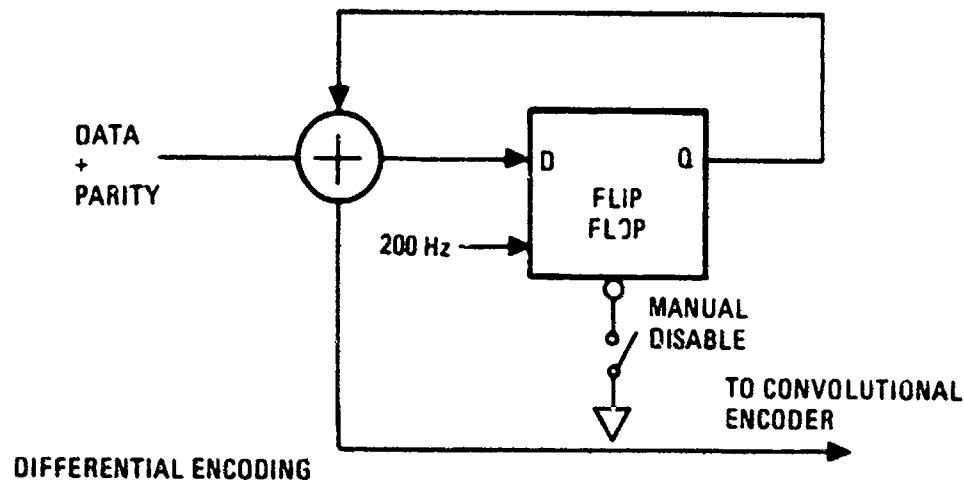


Figure 36. Block Encoder/Sync Detector Block Diagram



DIFFERENTIAL ENCODING

- TRANSPARENT TO 180° CARRIER PHASE AMBIGUITIES.
- DATA ONES AND ZEROS CHANGE OR NO CHANGE, RESPECTIVELY, THE NEXT INPUT BIT IN THE CONVOLUTIONAL ENCODER INPUT STREAM SO THAT INFORMATION IS CONTAINED IN DATA TRANSITIONS.
- TESTED WITH LINKABIT MODEL LV7015 FOR COMPATIBILITY.

Figure 37. Differential Encoder Block Diagram

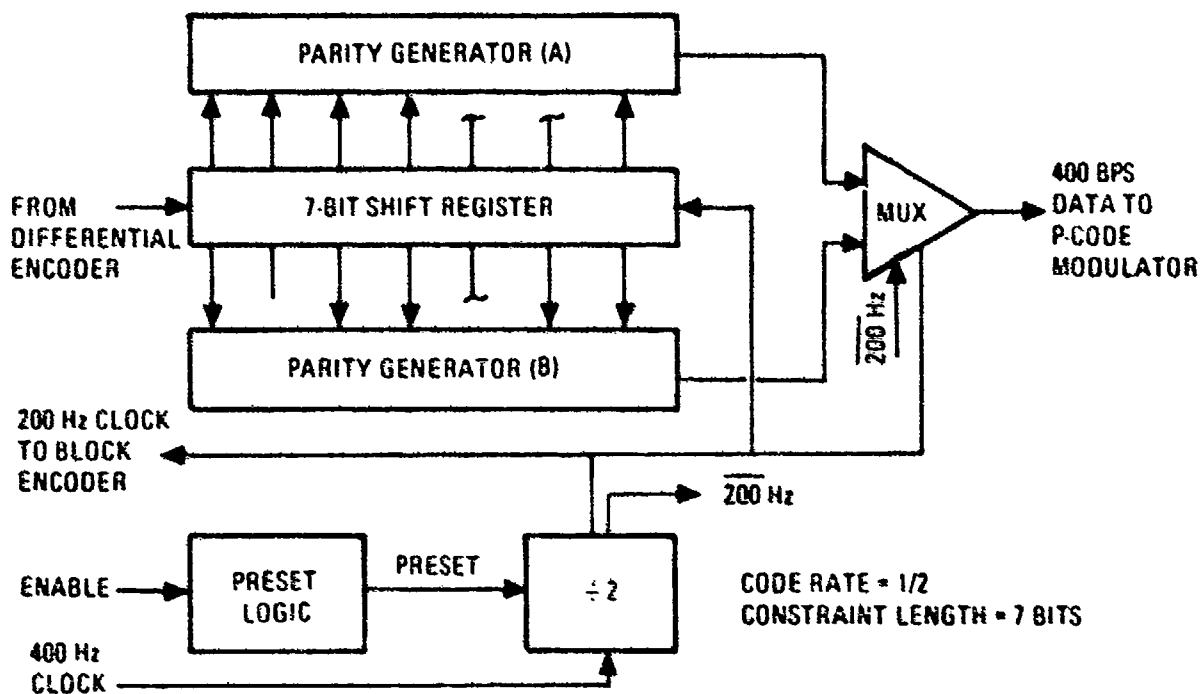


Figure 38. Convolutional Encoder Block Diagram

"exclusive-OR" gates to generate parity values on the shift register contents compatible with the Linkabit Model LV7015 convolutional encoder/decoder algorithm. The outputs of the two parity arrays are selected alternately by a select gate driven by both phases of the 200-Hz clock. The alternately selected output is exclusive ORed with the PN sequence and reclocked at 10.23 MHz. The reclocked signal drives the modulator via a transistor switch.

The clocking signal for the final synchronizing flip-flop is obtained by amplification and squaring of the incoming 10.23-MHz sine wave. The squaring is accomplished by overdriving the amplified sine wave coupled with a Schmitt trigger-type circuit.

The 200-Hz timing clock derived from the 400-Hz clock, is provided to preset the flip-flop in the state that will allow the positive going edge of the 200-Hz clock to sample incoming data near the center of each bit duration. The encoder is totally redundant and is controlled by switching on the appropriate 5-volt power supply. To achieve this design, 24 low-power Schottky IC's, 2 transistors, and an assortment of resistors and capacitors were used. Maximum power dissipation is approximately 1.6 watts for any one unit.

4.2.4 L₃ Transmitter and Switch Box

The IGS transmitter subsystem consists of two transmitters, A and B, a switch/power divider assembly, and a redundant encoder assembly, as shown in the overall operational block diagram in Figure 39. The switch power divider is mounted on transmitter B and is considered a part of transmitter B.¹ The encoders are independently mounted to the GPS bulkhead and are wired to the data input of transmitters A and B via shielded coaxial cable. Figures 40, 41, and 42 define the operational characteristics of the L₃ transmitter, the L₃ switch/power divider, and the L₃ encoder assemblies, respectively.

A block diagram of the transmitter assembly is shown in Figure 43. The 1381.05-MHz output frequency is derived from the GPS 10.23-MHz rubidium standard and is modulated and amplified as described below.

The transmitter assembly consists of five major elements: (1) the frequency synthesizer, (2) the multiplier/filter assembly, (3) the AGC amplifier, (4) the BPSK/QPSK modulator, and (5) the power amplifier assembly. The EDN design details follow; minor changes have been made for producibility into flight hardware.

4.2.5 Frequency Synthesizer

The synthesizer consists of a Colpitts VCO operating at 153.45 MHz and phase-locked to the rubidium standard. (Synthesizer characteristics are summarized in Table 17.) The mechanization uses emitter-coupled logic to provide the frequency division (divide by 30), which is phase-compared at 5.115 MHz (rubidium standard divided by 2), as illustrated in Figure 44. The VCO is buffered at the output to ensure minimum pulling and adequate drive to the subsequent circuitry. The VCO and loop filter are packaged independent of the loop logic circuitry using hybrid technology, resulting in two multipin

¹The switch is considered part of transmitter B in the Phase II development.

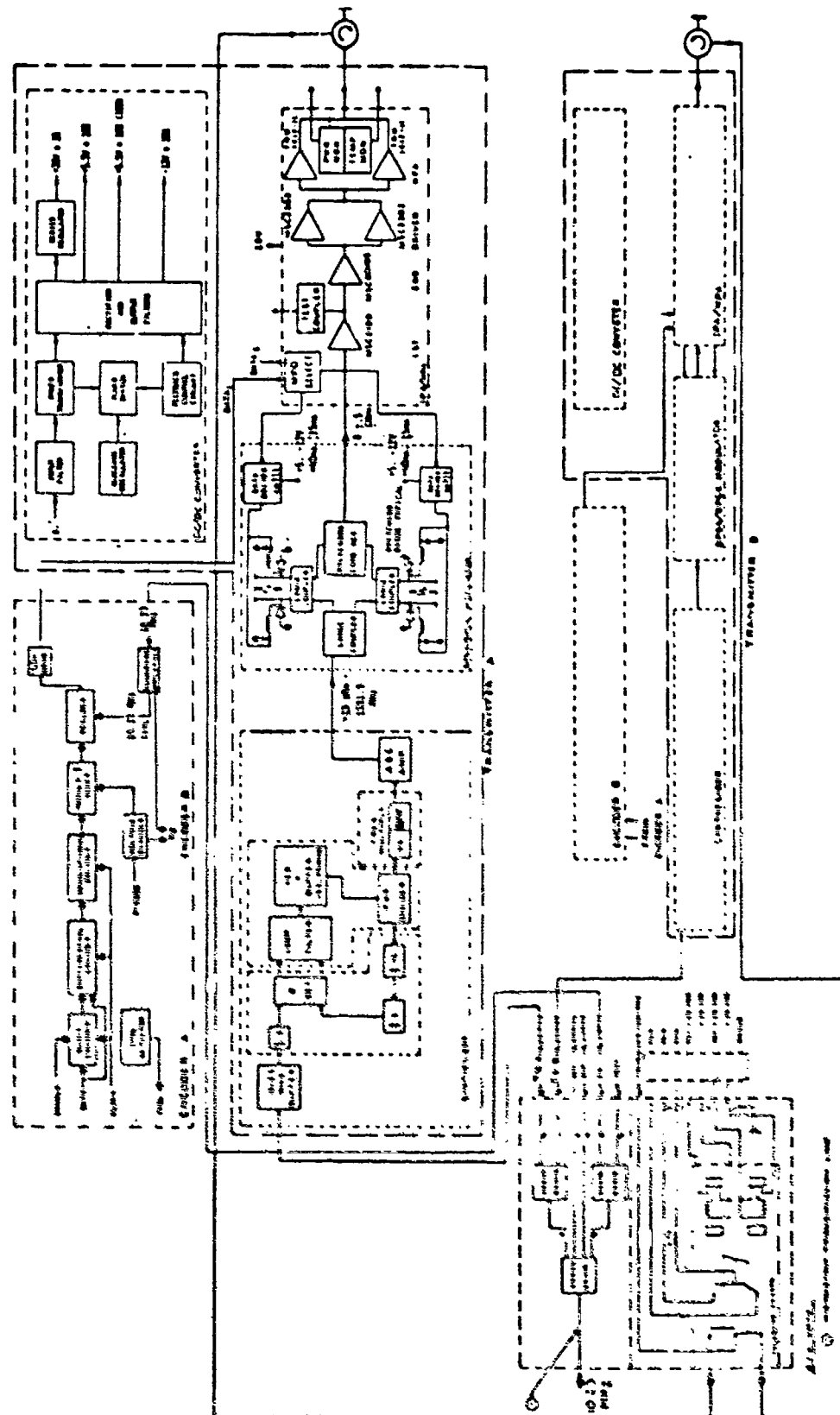


Figure 19. L3 Transmitter and Encoder Schematic

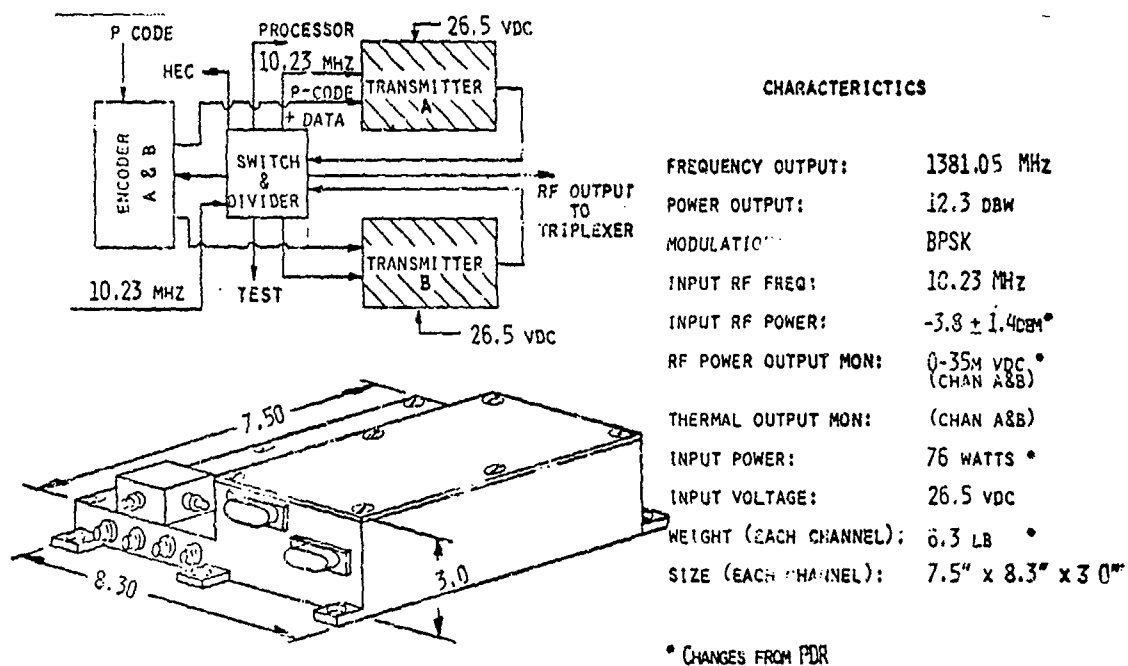


Figure 40. L₃ Transmitter Characteristics (EDM)

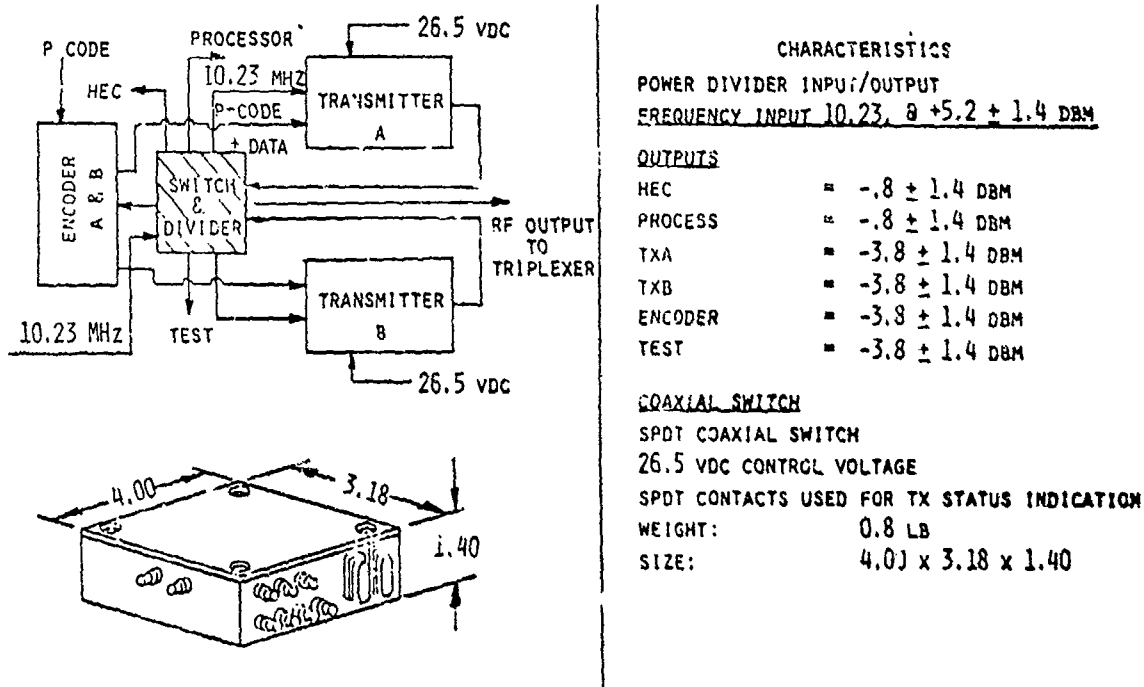


Figure 41. L₃ Switch and Power Divider (EDM)

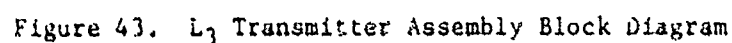


Table 17. L₃ Frequency Synthesizer Characteristics

VCO used as basic frequency source at 153.45 MHz

Phase-locked to 10.23 MHz GPS clock

Low phase noise - long-term drift determined by GPS

High-frequency stability

Active output leveling

Active frequency multiplication to 1381.05 MHz

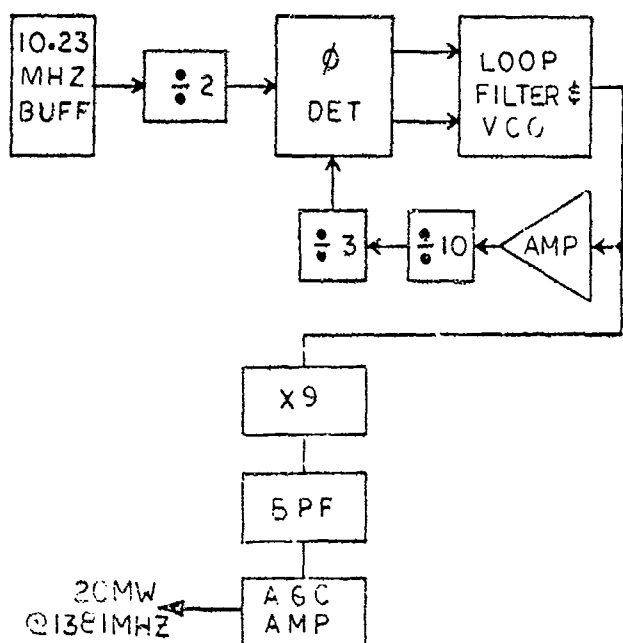
RF power output 16 mW

Spurious levels

In-band greater than 56 dB below signal

Out-of-band greater than 66 dB below signal

Turn-on speed < 100 msec



CHARACTERISTICS

NOISE:

IN BAND SPURII 56 DB
OUT OF BAND SPURII 66 DB
φ: 100 MR IN 10 HZ BAND LOOP
EXTENDING FROM 2-12 HZ

RF POWER:

INPUT -3.8 ± 1.4 DBM
INPUT FREQ. 10.23 MHz
OUTPUT $13.6 \pm .5$ DBM
OUTPUT FREQ. 1381.05 MHz

DC POWER:

VCO LOOP FILTER	+20 VDC	60 MA
LOOP LOGIC	+5 VDC	80 MA
x3	+20 VDC	7 MA
x3	+20 VDC	20 MA
AGC	+20 VDC	30 MA
	-12 VDC	10 MA

TEMP-QUALIFICATION
-340C TO +71°C

Figure 44. L₃ Synthesizer Mechanization

flat-pack hermetic enclosures connected by standard printed circuit board techniques. The loop logic and loop filter/VCO schematics are shown in Figures 45 and 46. Loop filter/VCO performance data is listed in Table 18.

4.2.6 Multiplier/Filter Assembly

The times nine (X9) multiplier consists of 2 times three (X3) multipliers in series, followed by a four-pole, 0.1-dB ripple microstripline filter. Multiplier characteristics are listed in Table 19. The X9 schematic is shown in Figure 47.

The first X3 multiplier uses a 2N2857 transistor whose input is matched at 153.45 MHz and idled at the second harmonic to ensure high-efficiency tripling action. The output is matched and padded slightly (3 dB) to minimize tripler interaction due to temperature and aging effects. The multiplier design uses lumped element and microstripline techniques on an alumina substrate.

The second tripler uses an HP21 transistor to provide adequate gain and power output at 1381.05 MHz. This tripler also uses lumped and distributed elements to accomplish good input/output matching. Idling is again absorbed into the input matching circuitry to optimize multiplier efficiency. This circuit is also built on an alumina substrate.

The filter assembly ensures adequate out-of-band (± 50 MHz) spurious rejection resulting from the X9 multiplier. The filter is an edge-coupled microstripline type, built on 25-mil-thick alumina substrate. The filter is designed for 6-percent bandwidth and provides a Chebyshev response.

4.2.7 AGC Amplifier

After filtering, the output is amplitude-leveled by an AGC circuit. The AGC amplifier is operated Class A and uses a circuit layout similar to the output stage of the frequency multiplier (see Figure 48). The output is sampled by a 10-dB coupler and the amplitude detected by a diode detector. The filtered output drives the inverting input of the operational amplifier. Included in the operational amplifier's feedback loop is a PIN diode. This PIN diode is located in the RF input path of the RF amplifier and effectively functions as a voltage-controlled attenuator. A stable voltage reference is provided for the operational amplifier's noninverting input to compare the detected and filtered RF input signal.

4.2.8 QPSK Modulator

The quadriphase modulator (Figure 49) is designed for high data rate (10 MHz) digital input. It can be used either in the BPSK or QPSK mode. For BPSK operation, the input carrier is modulated by identical data inputs at the modulation input ports (data 1 and data 2) or by connecting the ports together. The output carrier phase, relative to the input carrier, is phase-shifted by 0 or 180 degrees, depending on the data input.

For QPSK operation, the input carrier is modulated by two independent data channels at data 1 and data 2 input ports. Each data channel consists of a two-

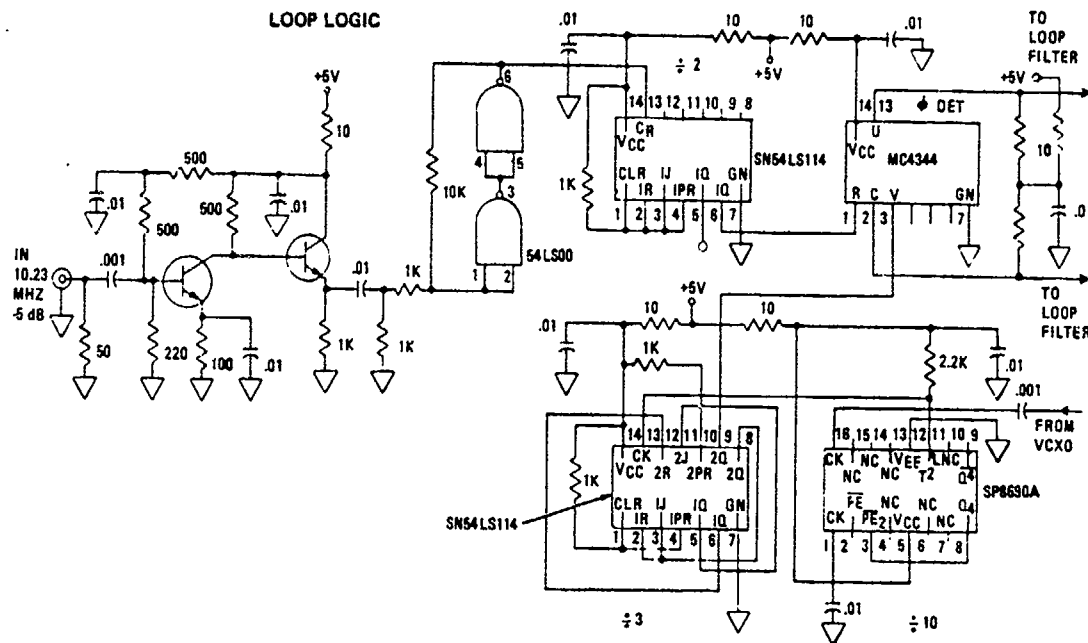


Figure 45. Loop Logic Schematic

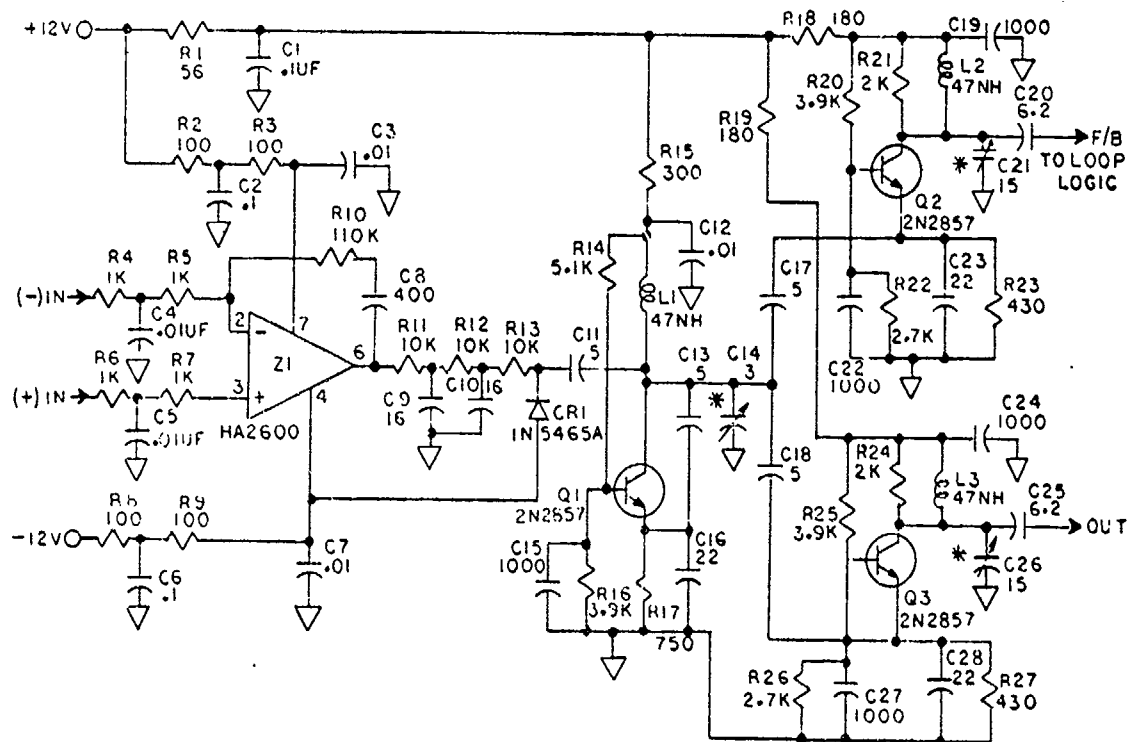


Figure 46. Loop Filter and VCO Schematic

Table 18. Loop Filter/VCO Performance Data

Loop natural frequency	30 kHz
T	150 sec
Open-loop gain	800
Damping factor	0.8
VCO tuning rate	0.5 MHz/volt
VCO output frequency	153.45 MHz

Table 19. X9 Frequency Multiplier

First Tripler:

Input frequency 153.45 MHz
Output frequency 460.35 MHz

Dc power +20V at 6 mA, 0.12 W

RF Input power 0 dBm at 153.45 MHz
RF output power +3.0 dBm (2 mW) at 460.35 MHz

Second Tripler:

Input frequency 460.35 MHz
Output frequency 1381.05 MHz

Dc power +20V at 11 mA, 0.22 W

RF input power +3.0 dBm at 460.35 MHz
RF output power +13.0 dBm (20 mW) at 1381.05 MHz

level biphasic pulse code. The output carrier phase, relative to the input carrier, is phase-shifted 0, 90, 180, or 270 degrees, depending on the properties of the data inputs. Power is split equally between the phases (i.e., 3 dB down from BPSK mode).

Figure 50 shows a simplified vector operation and block diagram of the quadriphase modulator. The heart of the circuit is the phase shift section, used as a biphasic modulator. The unmodulated carrier signal is split in quadrature (90 degrees) and fed to each phase shifter. One data input is used to modulate the 0- to 180-degree phases of the carrier (data 1 input); the other data input modulates the 90- to 270-degree phases of the carrier (data 2 input).

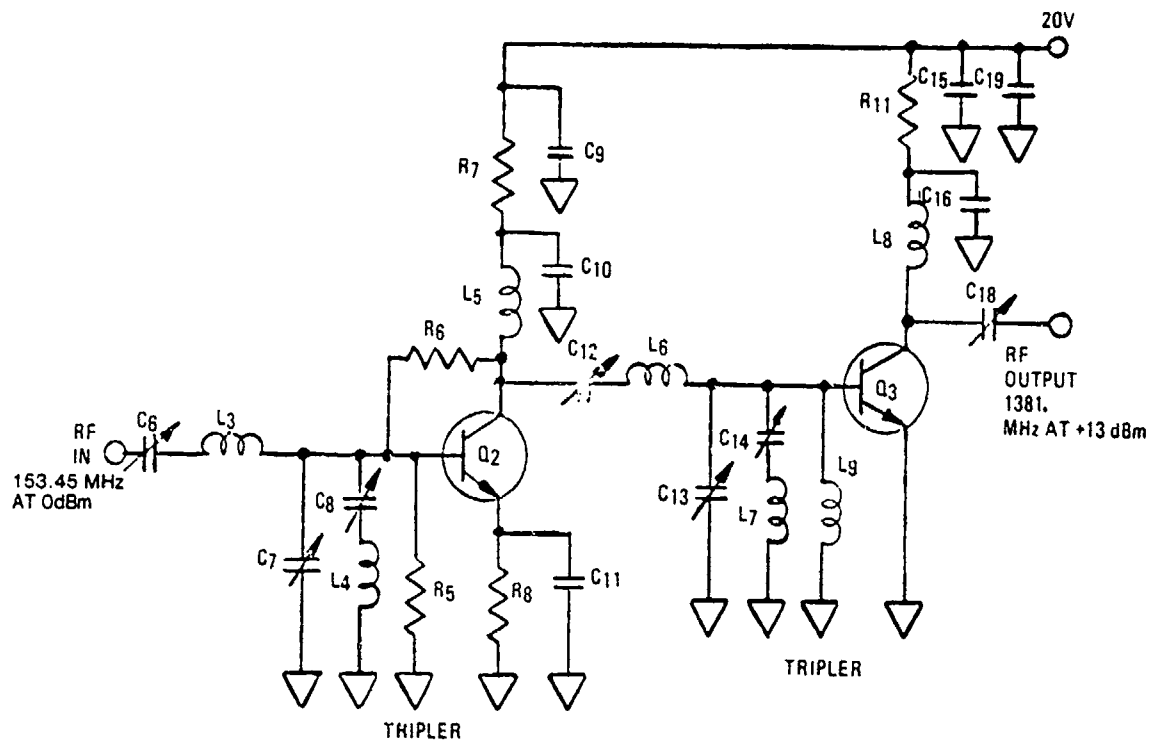


Figure 47. X9 Frequency Multiplier Schematic

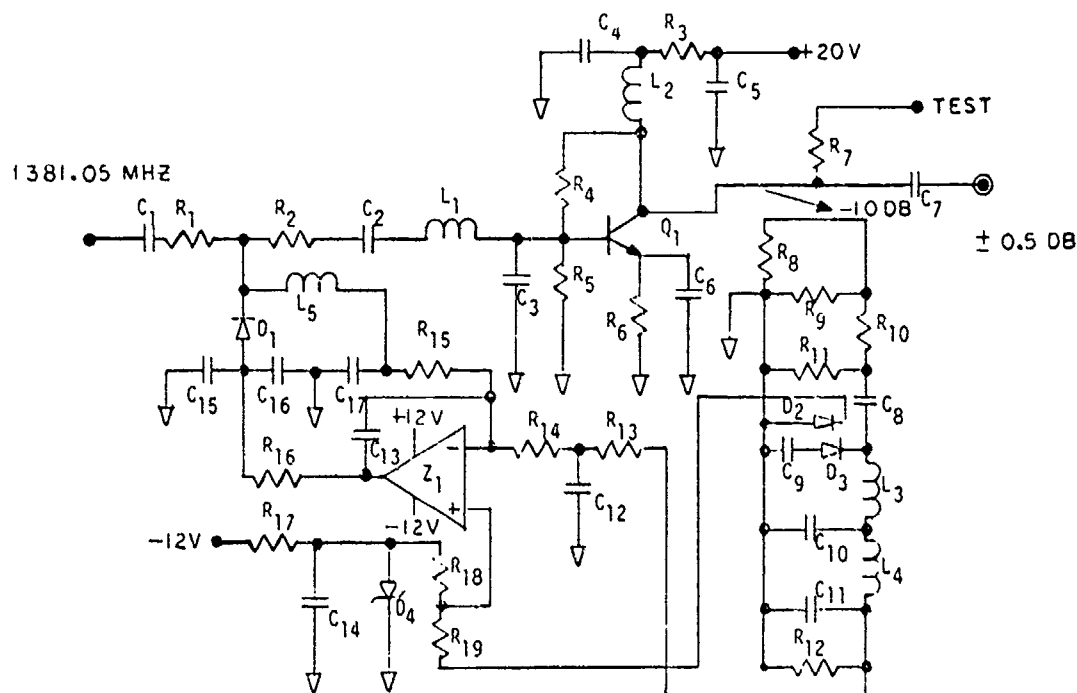


Figure 48. AGC Amplifier Schematic

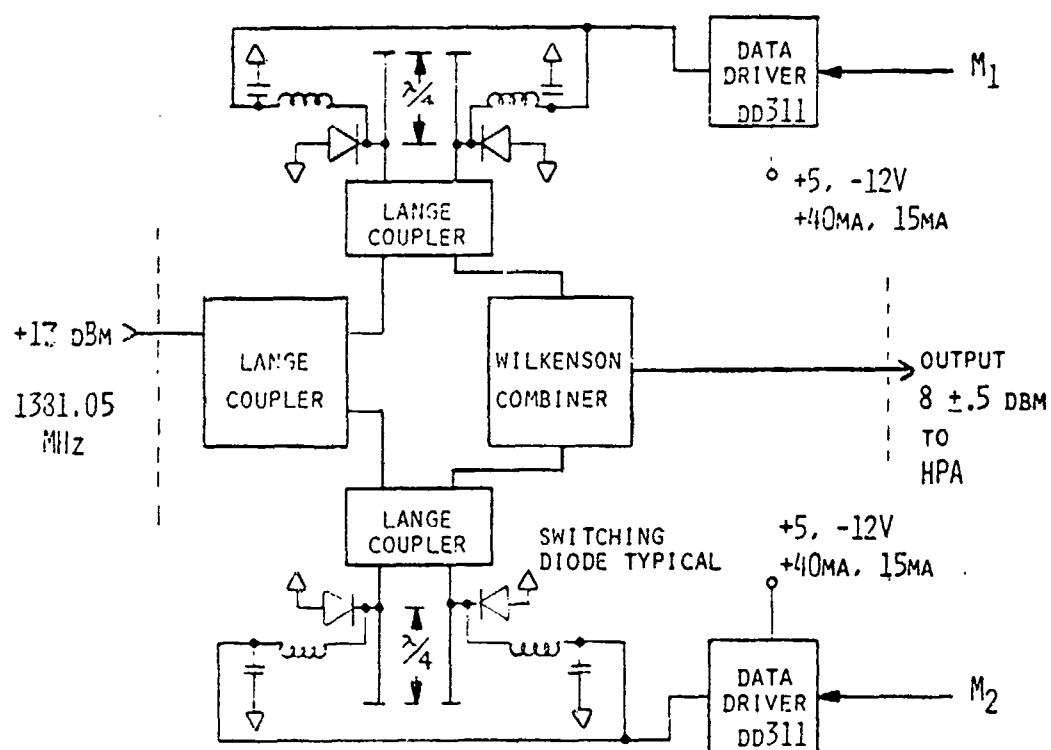


Figure 49. BPSK/QPSK Modulator Diagram

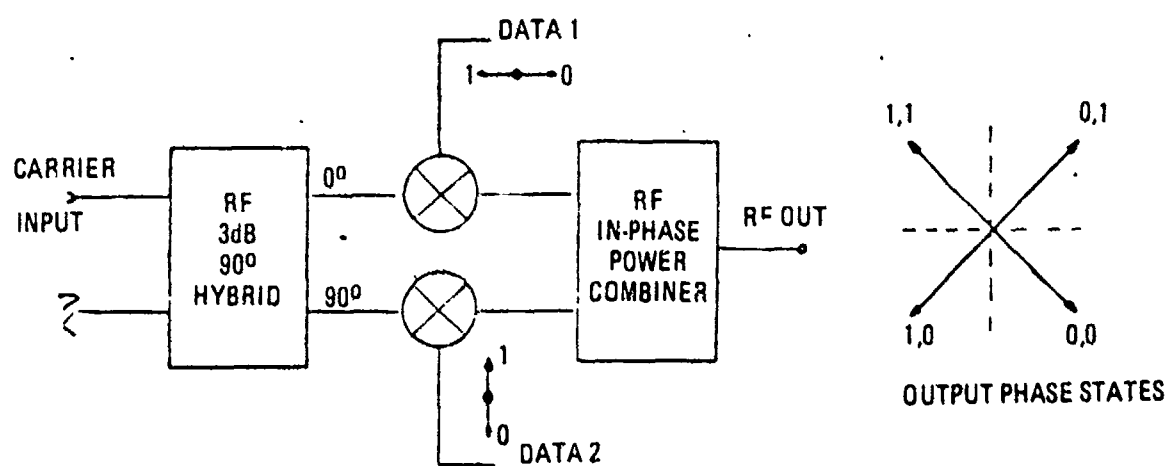


Figure 50. Quadriphase Modulator Diagram



The modulator outputs are then combined by an in-phase power combiner to produce the four phases, 0, 90, 180, or 270 degrees.

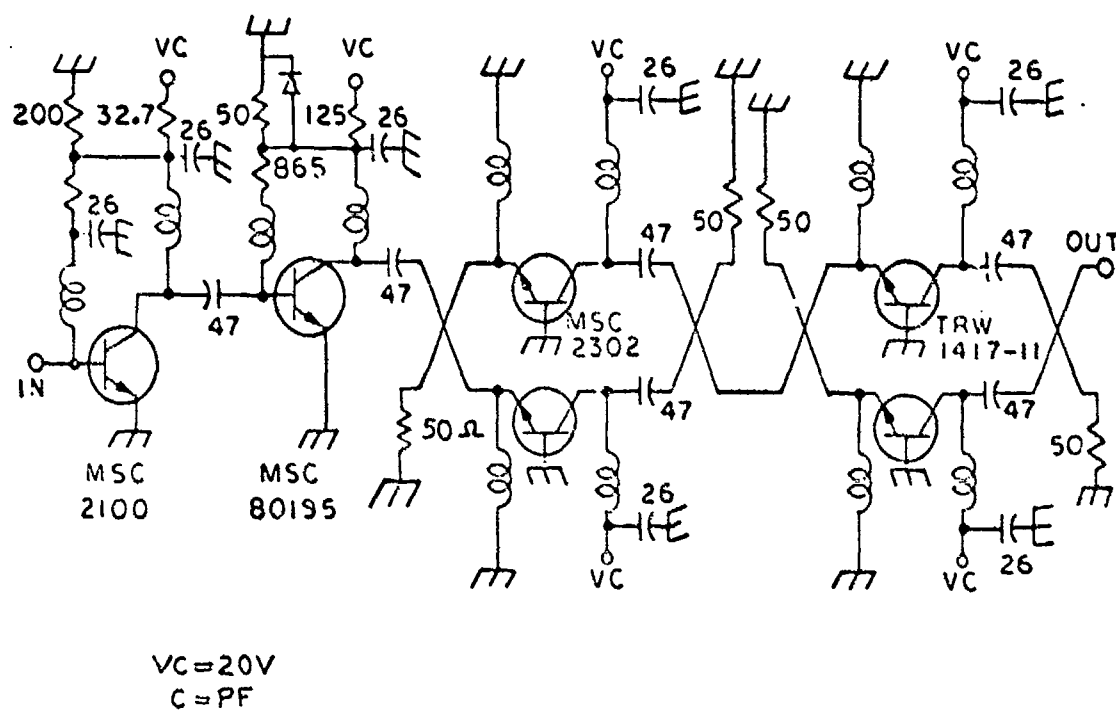
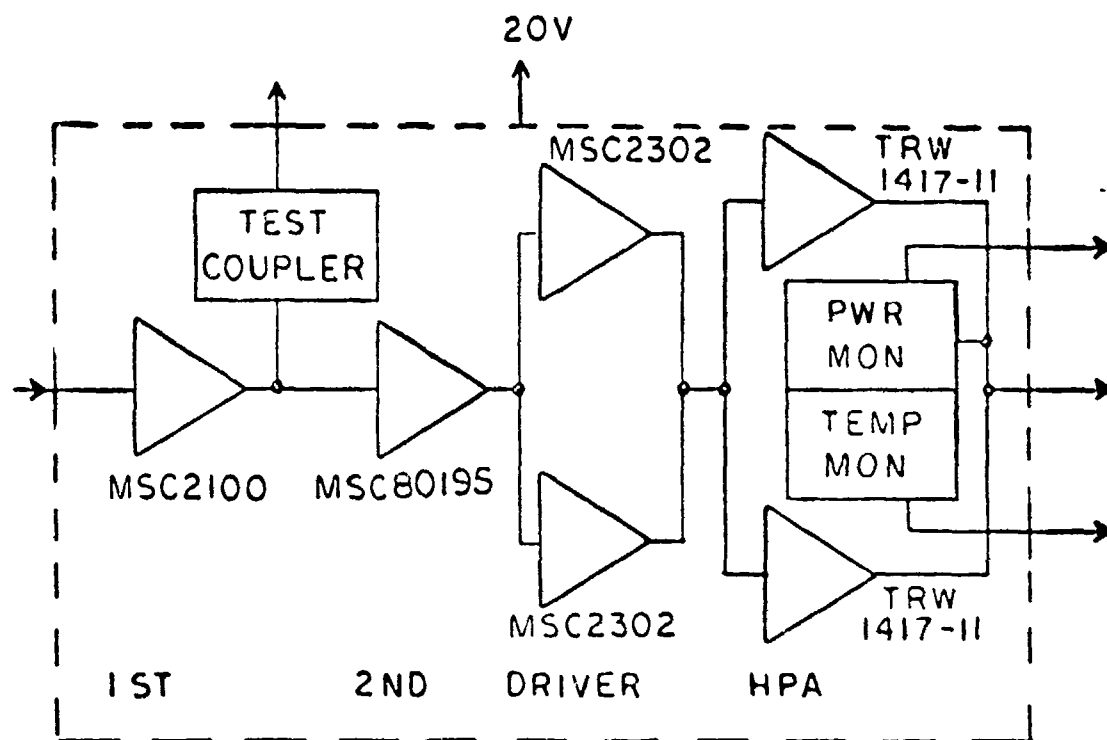
For IONDS operation, data 2 will not be used. The RF input power is kept to a minimum (+13 dBm maximum) to ensure minimal spurious response. The insertion loss of this circuit is 5 dB maximum.

The QPSK modulator uses a 2-inch by 2-inch, 25-mil-thick alumina substrate. The design is based on distributed circuit techniques using microstripline technology. Each phase shifter section consists of a PIN diode driver (EMI DD311) which drives two PIN diodes (HP 5082-0001) in shunt parallel. The 90-degree, 3-dB hybrids are interdigital Lange couplers wired so that planar topology is facilitated for this design. The combiner network is a Wilkenson-type quarter-wavelength line structure in microstrip.

4.2.9 Intermediate-Power Amplifier (IPA)/High-Power Amplifier (HPA)

Advanced transistor and microwave circuit techniques have been used in the development of the power amplifier. To achieve maximum efficiency, lowest junction temperatures (125°C), and at least a 10-percent bandwidth over the temperature range of -21°C to +61°C, transistors capable of 3.0 GHz operation have been selected. To ensure reliability, hermetically sealed transistors are used in conjunction with microstripline technology. To achieve 15.1 watts minimum transistor output power over the temperature range, transistors are efficiently paralleled within the predriver and output stages of the HPA. Combining power stages within the high-power amplifier allows for lower collector temperatures, less interstage interaction, and reasonable impedance match. The collector voltage applied to the transistors has been reduced to the region of 20 volts so that transistor efficiency is optimized.

The IPA/HPA circuit block diagram is shown in Figure 51; the schematic is shown in Figure 52. An intermediate power amplifier is included in this design and acts as a high-gain buffer stage between the QPSK modulator and the high-power Class C amplifier stages. The IPA provides 19 dB of linear gain and delivers 520 mW to a quadrature hybrid to drive a pair of MSC 2302's (predriver). Note that additional buffering (stage isolation) is accomplished via the quadrature hybrid (approximately 20 dB). Advantages of this type of combining are apparent if the multiplicity effects of VSWR in interstage matching of medium- and high-power Class C amplifier design are considered (i.e., any change in input impedance to the pair of predrivers due to temperature or device degradation is selected back to the 90-degree hybrid load and not to the collector of the previous stage). Under worst conditions (base emitter short circuit at one of the predriver transistors), the isolation to the previous stage is 6 dB. This corresponds to a VSWR of less than 3:1 as opposed to infinity. Under normal conditions, the pair of predriver transistors will track in VSWR over temperature and aging, thus yielding at least 20 dB of least 20 dB of isolation between stages (1.2:1 VSWR). Another advantage of hybrid combining is the "graceful degradation" property of this type of design. Note that if for some reason any one device fails during operation, at least one-fourth the power is available to drive the subsequent power stage, resulting in reduced power level at the output port but not total RF power loss.



The predriver stage supplies another 10 dB of Class C gain at 4.19 watts to drive a pair of output power stage transistors. Stage isolation is again accomplished via two low-loss hybrid combiner/splitters. Each power stage transistor yields 10 watts of RF power for a combined output of 19.1 watts (combined loss of 0.2 dB).

4.2.10 Power Monitor

The HPA output is fed to a power monitor assembly consisting of a foreshortened 30-dB coupler (phase = 20 degrees), a 30-dB pad, a shunt-mounted zero-bias Schottky detector diode, and an operational amplifier.¹ Figures 53 and 54 show the block diagram and schematic of this circuit. The insertion loss is 0.1 dB. The RF power level incident upon the diode does not exceed -10 dBm, therefore ensuring square law (linear) operation.

4.2.11 RF Switch Box

An RF switch is provided to connect L₃ transmitter A or B to the L-band triplexer. Considering transmitter B as the redundant transmitter, IONDS operation of the switch would occur after failure of transmitter A. Since the L₃ transmitter is only up after an event or ground command, failure of an L₃ transmitter will not be automatically detected. After an event, any of the GPS satellites in view of an IONDS user and not transmitting on L₃ will be interrogated for status via TT&C. If an event has been noted on one of the satellites and L₃ is not transmitting, ground control will command the RF switch to operate and bring up the redundant channel.

Electrical characteristics of the coaxial RF switch are listed in Table 20. The switch assembly is illustrated in Figure 55.

4.2.12 L₃ Transmitter Power Supply

The L₃ transmitter requires 73 watts of power from the GPS 27-volt power supply. A dc-to-dc conversion is performed in the L₃ transmitter which provides the voltages listed in Table 21. A block diagram of the transmitter power supply is shown in Figure 56. Schematics of the dc/dc converter and the +20 volt regulator are shown in Figures 57 and 58.

4.2.13 L-Band Triplexer

The GPS system diplexer is designed with two three-pole (Chebyshev) bandpass filters and matching networks for the common antenna connection as shown in Figure 59. With the addition of a third signal (L₃) to the antenna feed, a third bandpass filter is necessary for adequate isolation between the three input ports (see Figure 60). In this configuration, the L₃ frequency of 1381.05 MHz has attenuation at L₁ and L₂ equal to or better than either L₁ at L₂ or L₂ at L₁, as indicated in Figure 61. This allows L₃ operation with no appreciable degradation to either L₁ or L₂. The triplexer modification, as noted in Figures 62 and 63, adds 0.4 lb and 7.3 in.³ to the diplexer configuration.

¹The power monitor output at a nominal 14 mV dc is supplied to the SUT where it is amplified to a 2 volt level before being fed to the PCM (Figure 54).

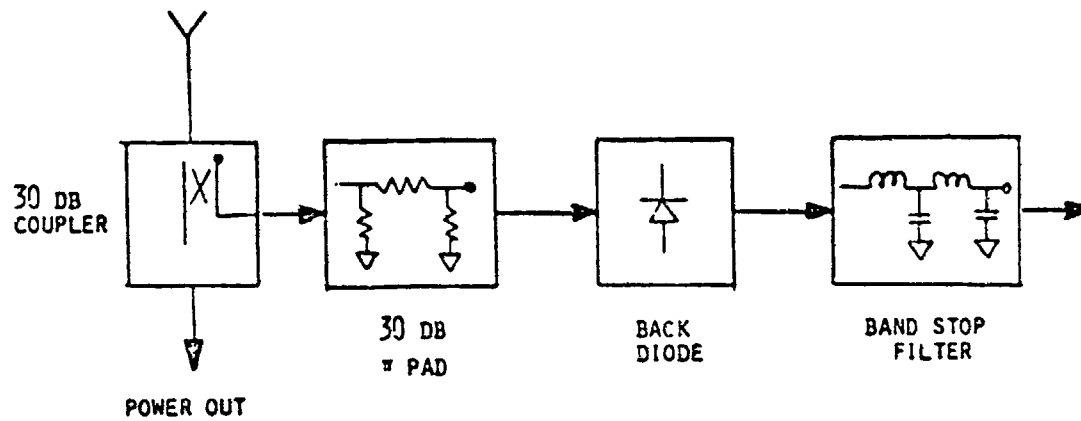


Figure 53. Power Monitor Block Diagram

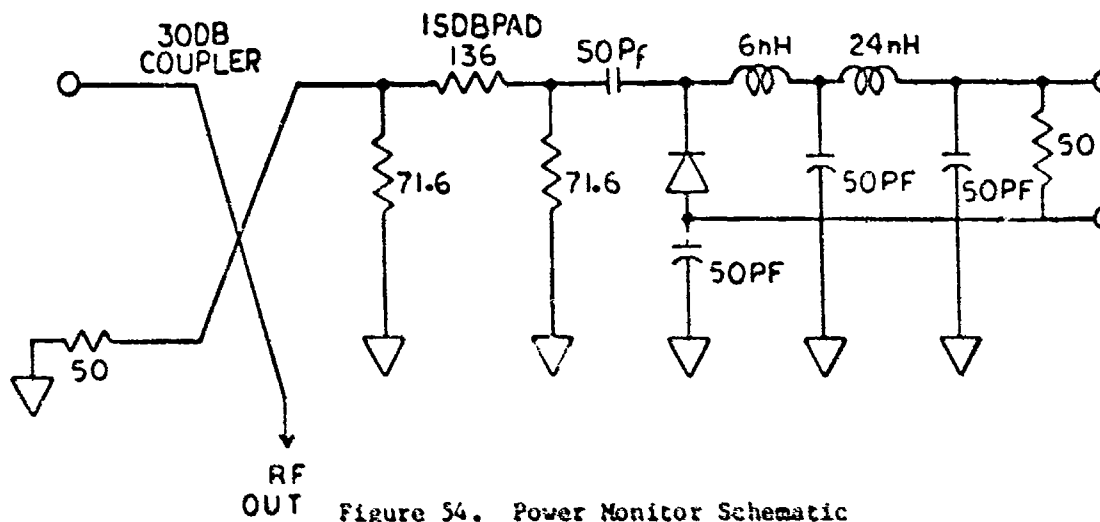


Figure 54. Power Monitor Schematic

Table 20. Teledyne CS33S6-C-Coaxial Switch

Type of switch	SPDT
VSWR	1.25:1 dc to 6 GHz
Maximum insertion loss	0.15 dB
Operating voltage	20 - 27 Vdc
RF power-handling capacity	25 watts
Operating current	90 mA max
Switch action	Break before make
Indicator contacts	100 mA, 28 Vdc
Switching time	30 ms max at 20 Vdc

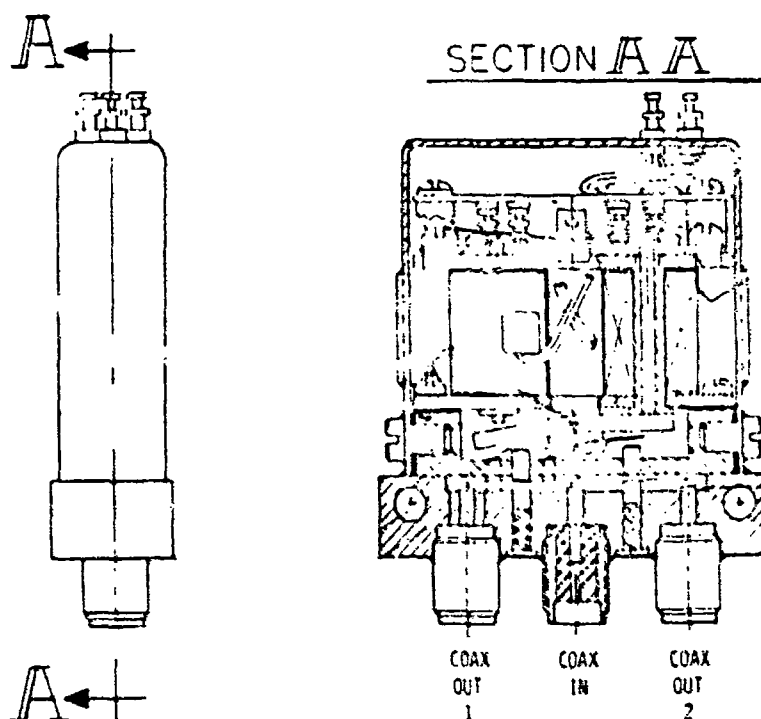


Figure 55. Coaxial Switch Latching Drive Assembly

Table 21. Power Supply Output Requirements

Output Voltage (Vdc)	Maximum Load (amp)	Nominal Load (amp)	Maximum Power (watts)	Maximum AC Ripple (mV p-p)
$20 \pm 1\%$	2.55	2.22	51	150
$5.5 \pm 10\%$	0.105	0.084	0.578	100
$5.5 \pm 10\%$	0.33	0.3	1.815	100
$-12 \pm 10\%$	0.05	0.035	0.6	50
Total output power (max) = 53.99 watts				

4.2.14 L-Band Antenna

The IGS L₃ transmission uses the GPS navigation helix array antenna (Figure 64) in conjunction with the L₁ and L₂ signals. No modifications of the antenna were required due to the addition of the L₃ frequency. However, a detailed antenna compatibility test program was conducted to ensure there was no degradation of L₁ and L₂ antenna performance from the addition of the secondary payload. A typical L₃ principal plane radiation pattern is shown in Figure 65.

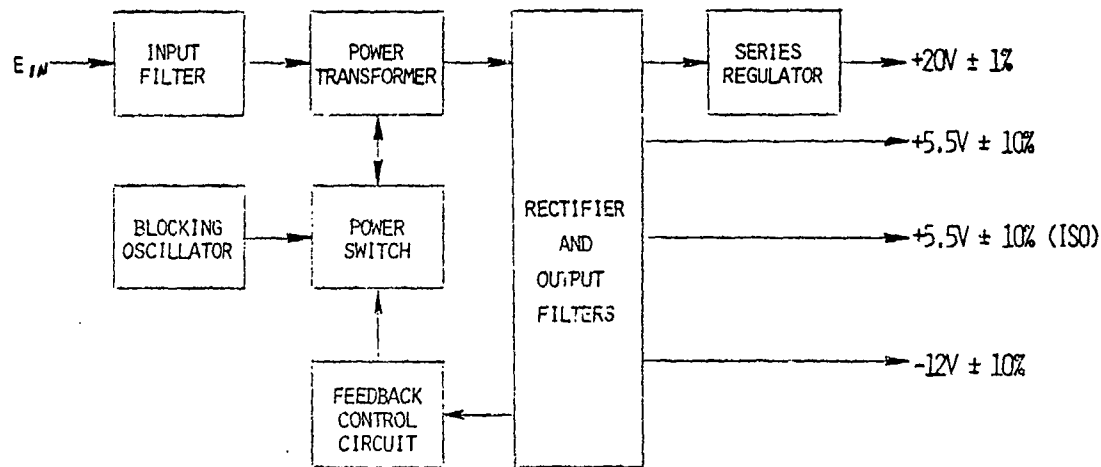


Figure 56. Power Supply Block Diagram

4.2.15 Timing Interface Box

The timing interface box was required to convert the 100-Hz signal from the BBP to 400-Hz for input to the L₃ encoder and to 200 Hz for use in the BDP. The functions of the timing interface box will be incorporated with the L₃ encoder with the TIE box for NDS 6 and NDS 9 through 12. The function will return to the navigation subsystem as part of the new frequency distribution network in NDS 13 (Phase III). A simplified block diagram of the timing interface box is shown in Figure 66.

The circuit consists of a blocking oscillator connected to operate as a VCO, a divider chain to divide the oscillator output down to the reference frequency, a phase detector, and a low-pass filter used as an integrator. The total configuration is that of a phase-locked loop (PLL).

The VCO is a transformer-coupled blocking oscillator, whose output frequency is primarily controlled by a resistor capacitor (RC) time constant in the base biasing circuit. Small variations in the voltage applied to the bias circuit vary the VCO's output over the range required to keep it exactly N times the reference frequency. The locked operating frequency of 8 kHz was chosen to minimize component size, yet not require exact materials for the VCO transformer.

The division by N is mechanized with standard T²L logic and divides by a fixed value of N equals 80. The counter is tapped at the proper point to provide the required output frequencies of 400 and 200 Hz. Some improvement in phase stability could be realized if the SN5474 D-type flip-flops were replaced with an SN54163 four-bit binary counter. The digital-type phase detector provides a quadrature lock. The output voltage from the phase detector is low-pass filtered and used to lock the VCO to the reference frequency.

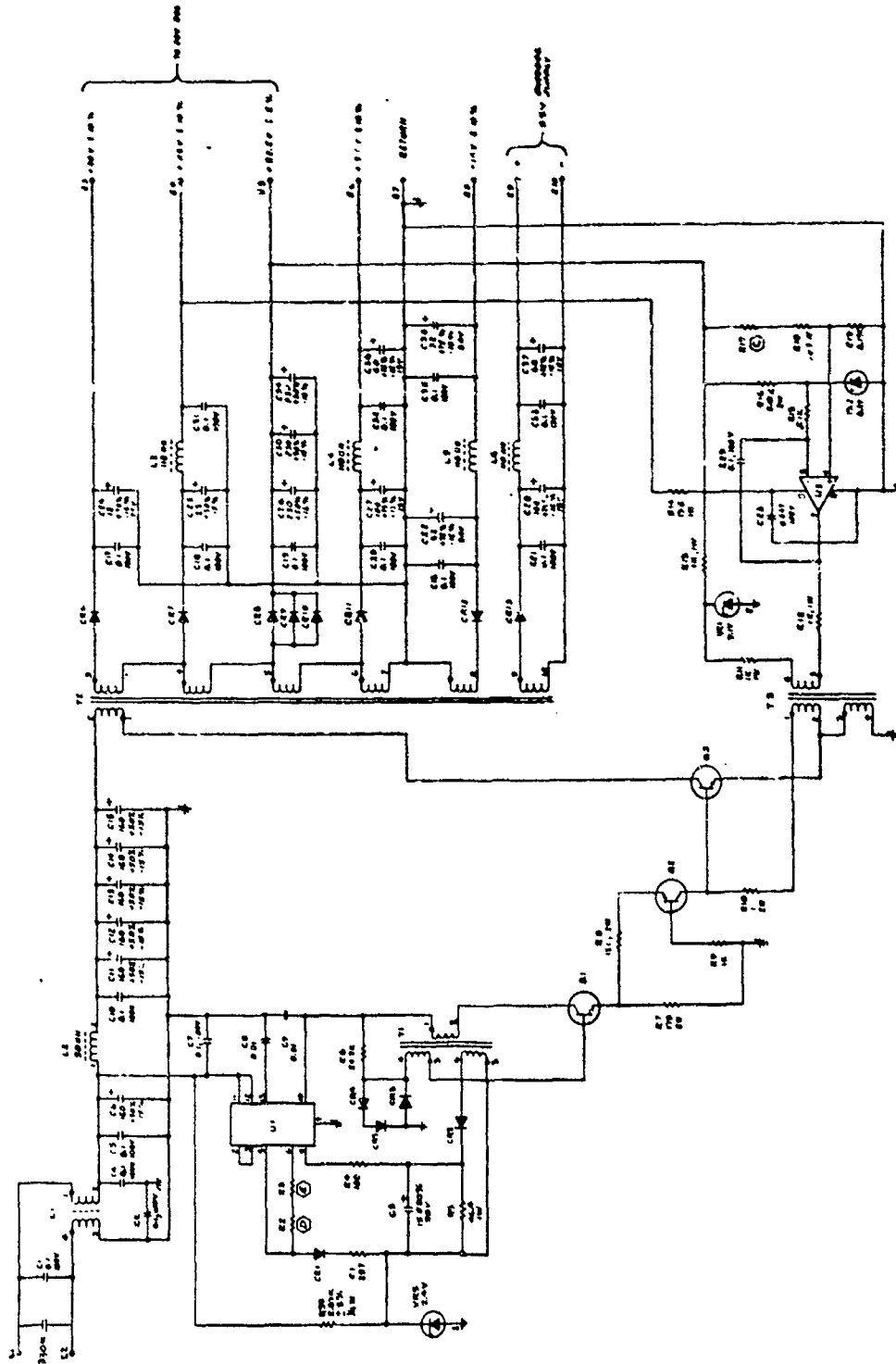


Figure 57. Dc/dc Converter Schematic

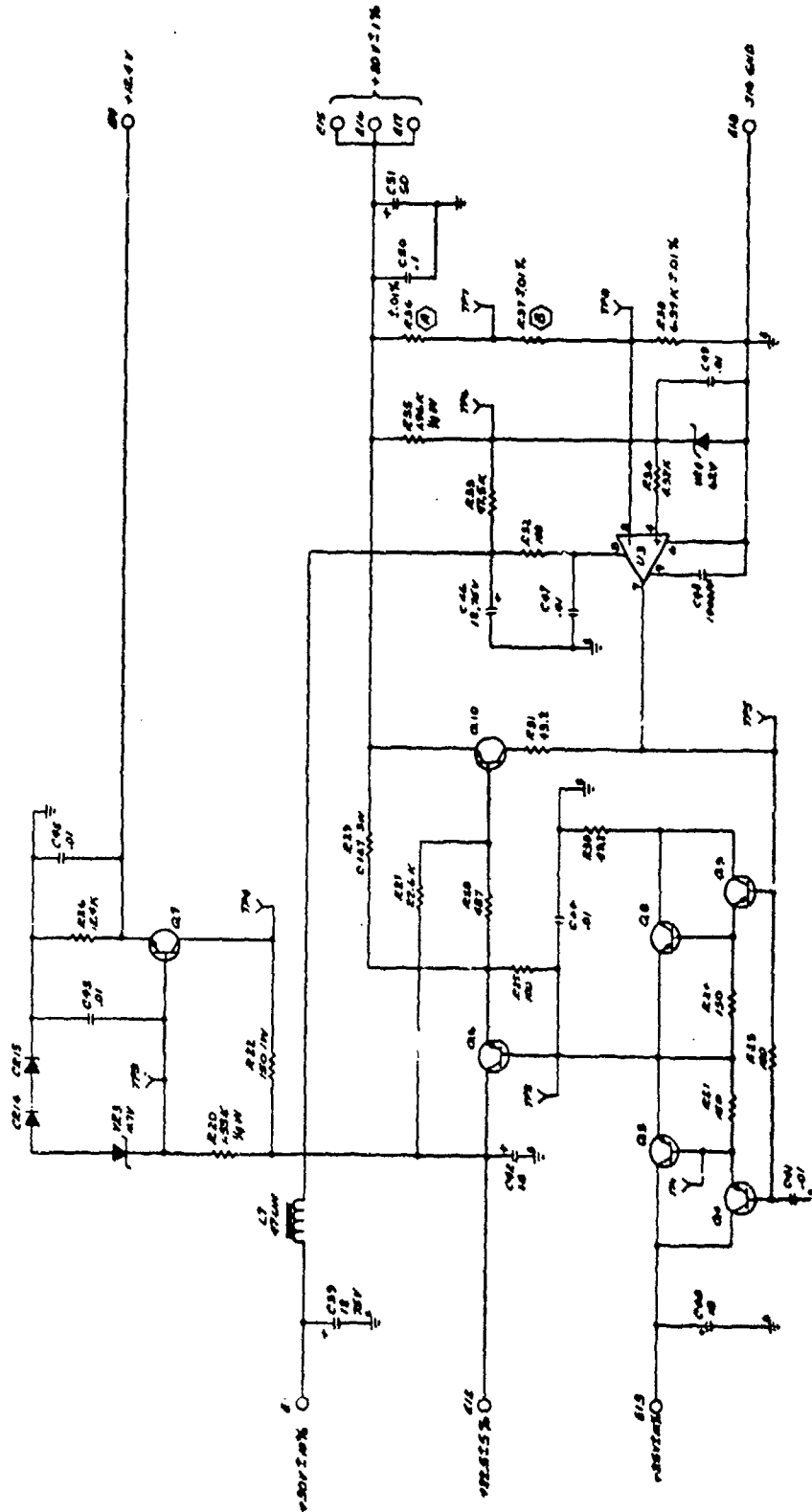


Figure 58. +20 Volt Series Regulator Schematic

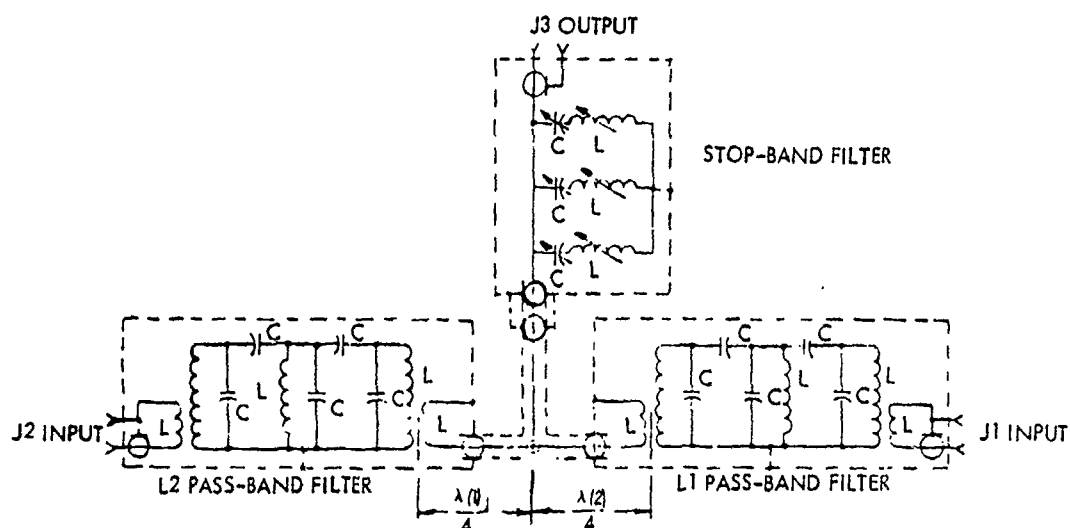


Figure 59. Diplexer Schematic Diagram

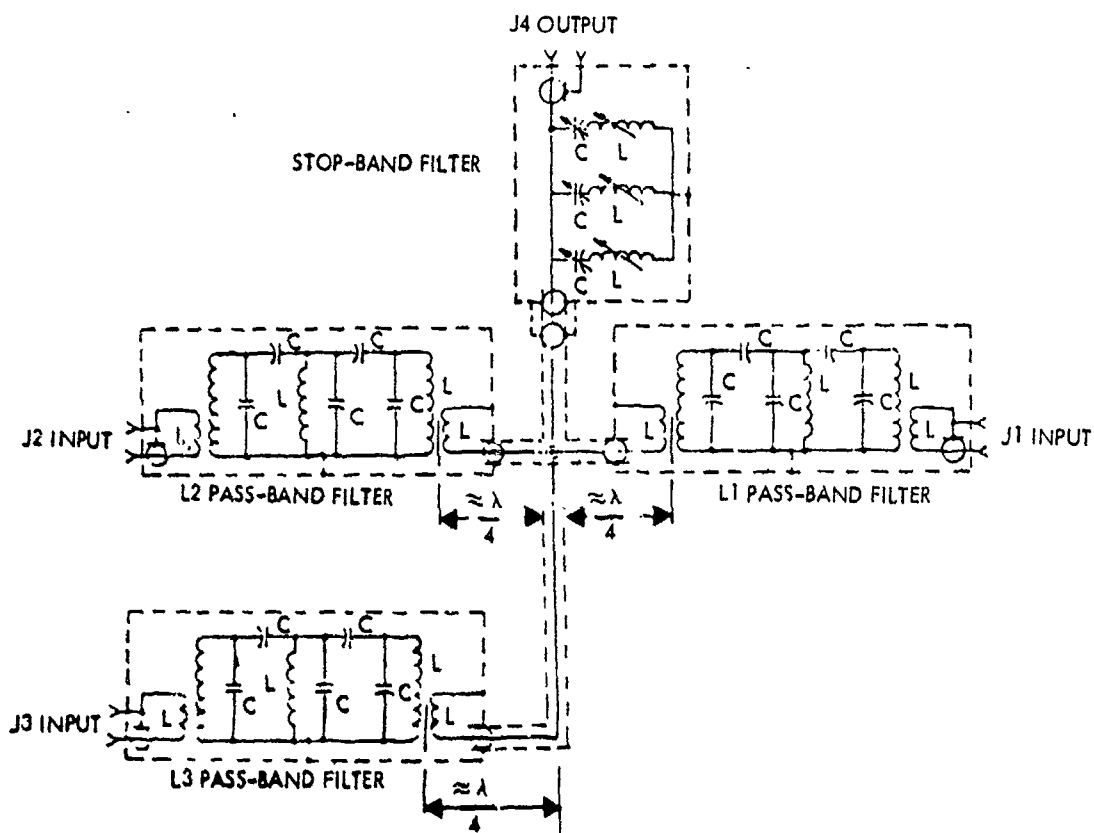


Figure 60. Triplexer Schematic Diagram

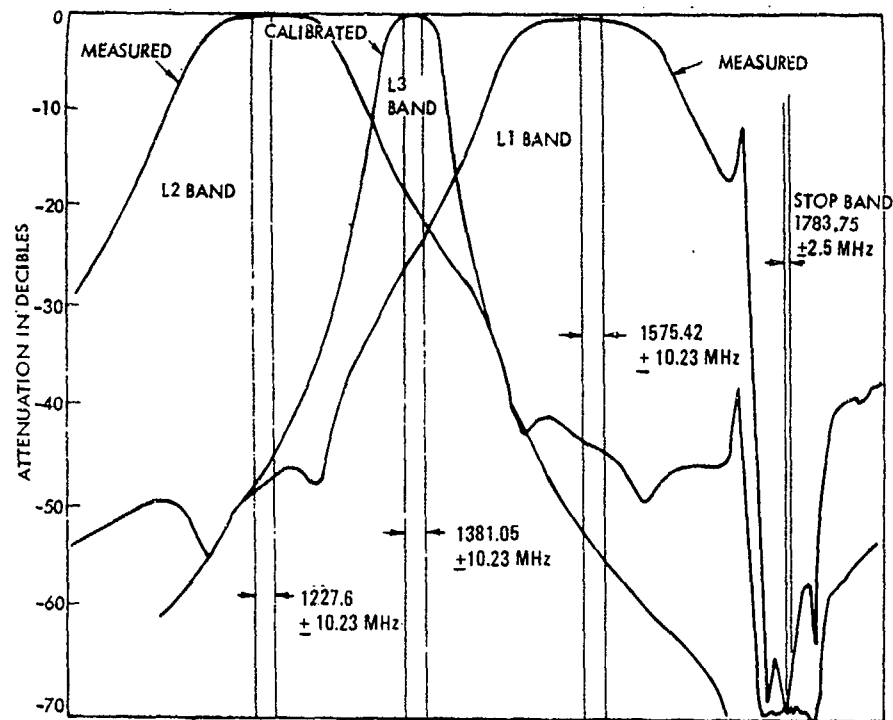


Figure 61. Triplexer Frequency Response Characteristics

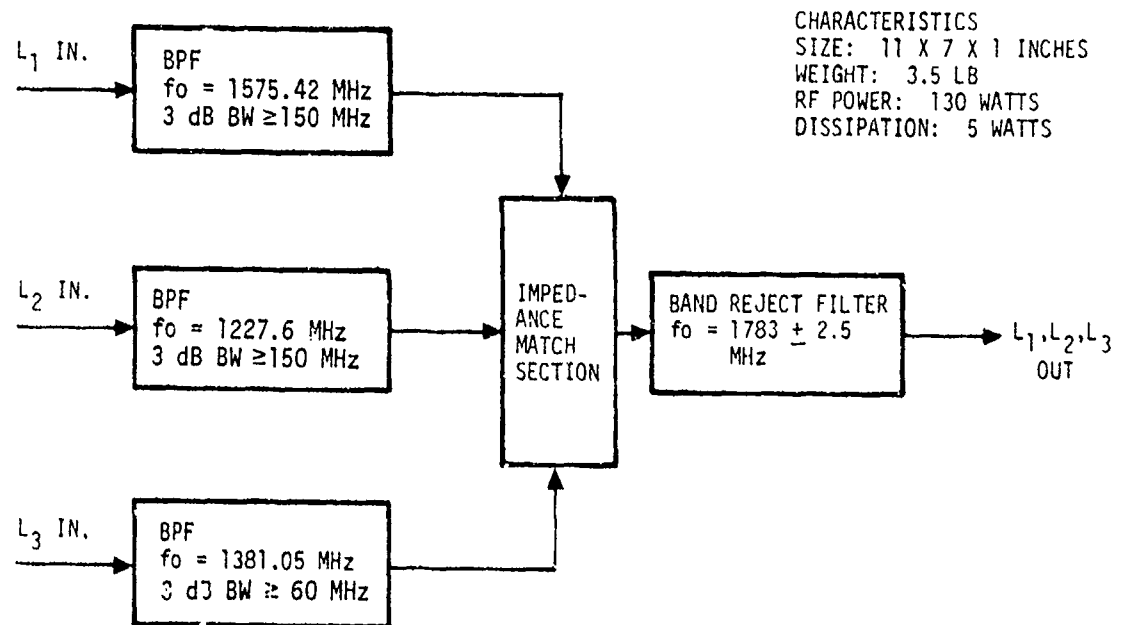


Figure 62. Triplexer Block Diagram

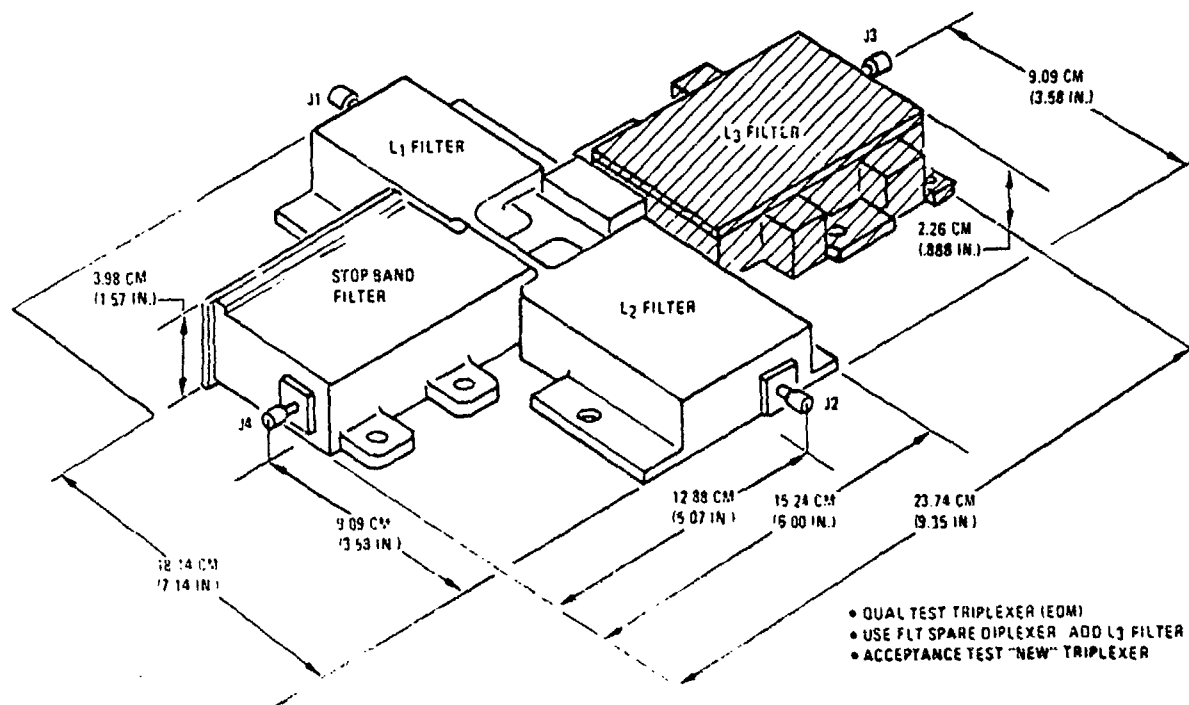


Figure 63. IGS Diplexer/Triplexer Modification

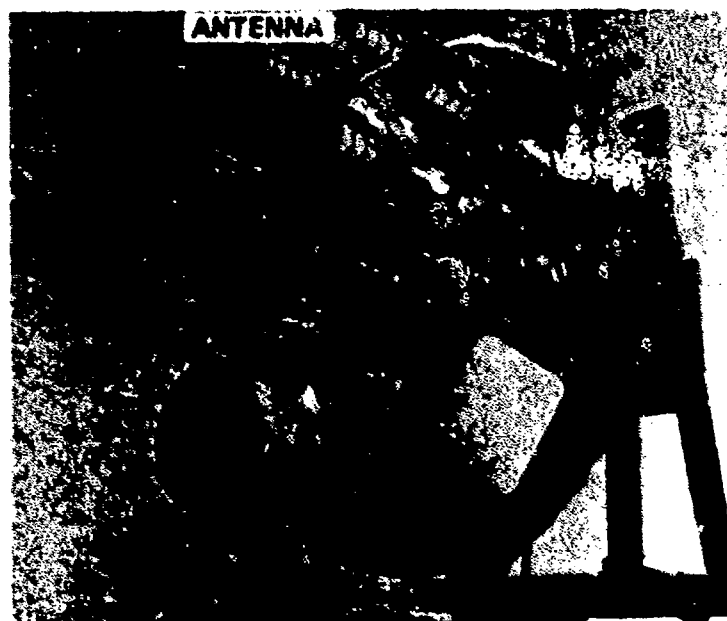


Figure 64. GPS/SPL Antenna

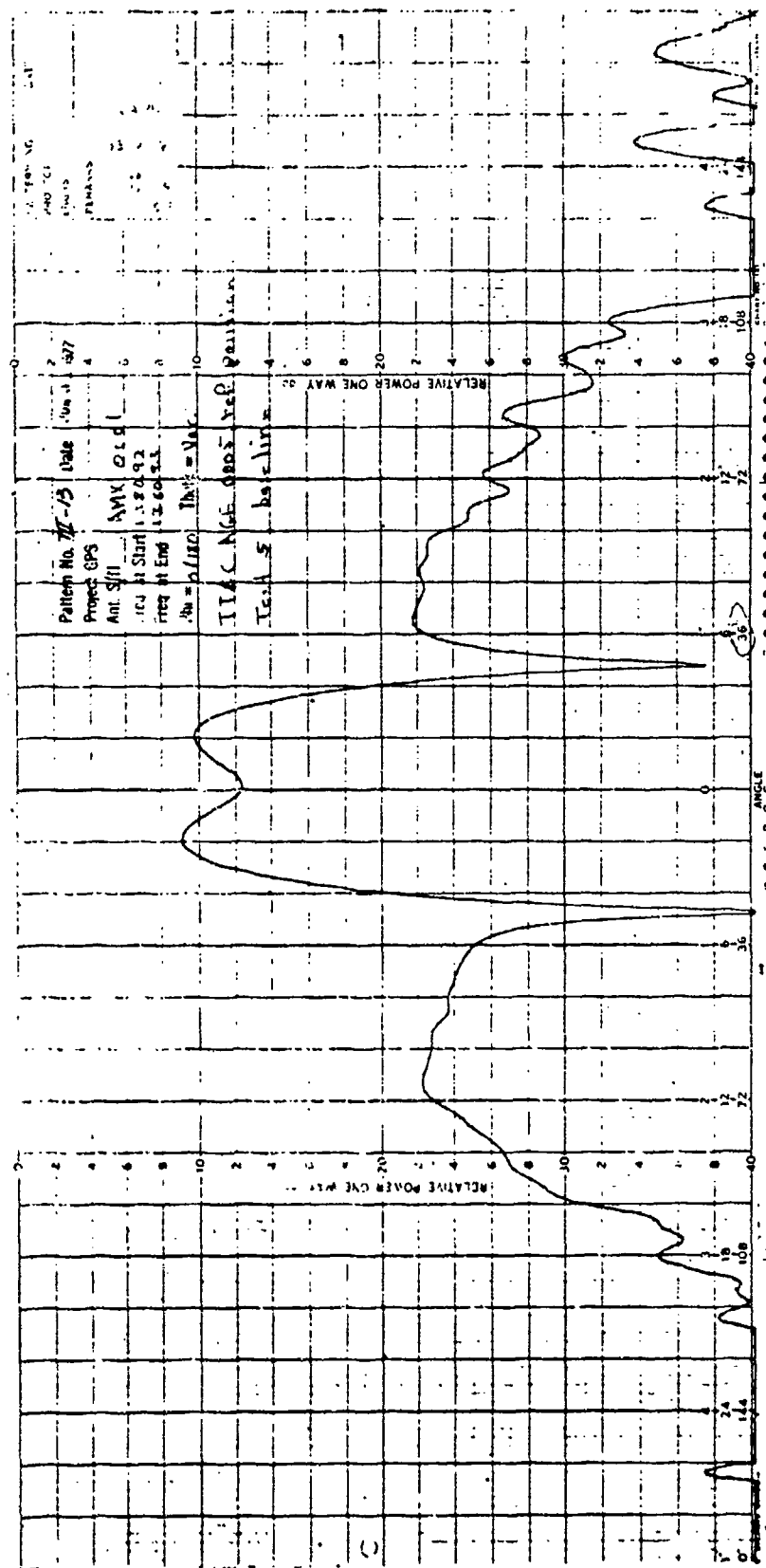


Figure 65. Principal Plane Radiation Pattern

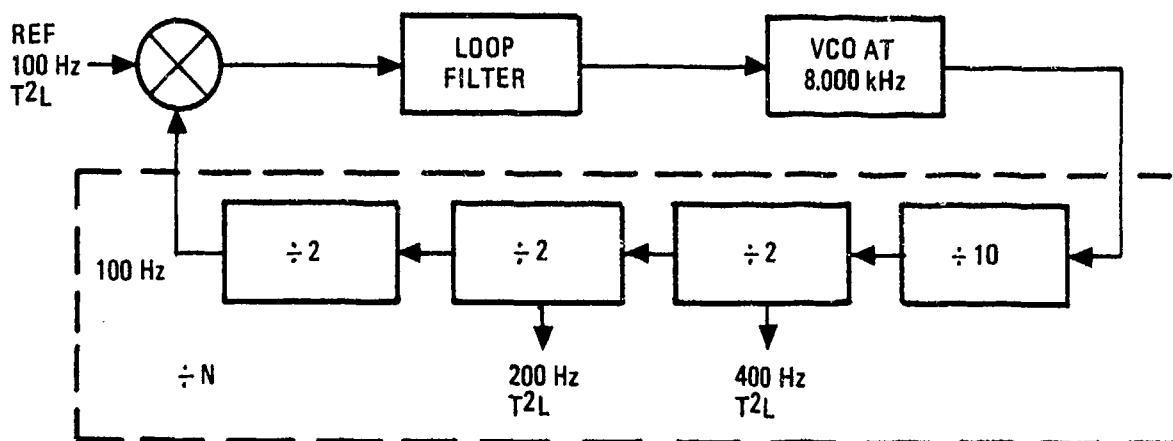


Figure 66. Timing Interface Box

4.3 IGS/GPS DESIGN INTEGRATION

Integration of the IGS with the GPS spacecraft has only minor impact on the spacecraft and an insignificant effect on GPS performance.

The IONDS/GPS overall block diagram was shown in Figure 30. The solid hatched boxes enclosed in the lower part of the figure are 100-percent IONDS components. The half-hatched boxes are original GPS components that are also used for IONDS functions. The current issue of the ICD must be referred to to determine actual requirements.

4.3.1 Navigation Timing Signals

The GPS navigation subsystem provides the sensor processor with dual redundant Z-count, X1 epoch, Z-count strobe signals, and a nonredundant 200-Hz clock signal. The nonredundant 200-Hz clock signal is derived in the timing interface box to support integration tests. The L3 transmitter supplies the sensor processor with a nonredundant 10.23-MHz clock. The purpose of these signals is to provide the sensor processor with satellite system time for determining the time of arrival of the sensor signals. The Z-count is a time-of-week count which is advanced one step every 1.5 seconds by an X1 epoch signal. The 200-Hz clock, which is synchronized to the X1 epoch signal, is used for BDP data transfer. The Z-count strobe is used for Z-count transfer. The X1 epoch is used by the BDP to update the Z-count. The signal and circuit characteristics are as follows:

Z-Count

Signal type: 20-bit serial, NRZ

Data rate: 100 Hz

True Level 1: $+4.5 \pm 0.5$ Vdc

False Level 0: 0.0 to -1.0 Vdc

Rise/fall times (between 10% and 90% points): 5 ms maximum

Source impedance: 10 kilohms maximum

Load: 1 kilohm \pm 10% in series with low-power Schottky T²L in parallel
with less than 50 pF

Cable and connector: Multiconductor

X1 Epoch

Signal type: Pulse

True level: +4.5 \pm 0.5 Vdc

False level: 0.0 to -1.0 Vdc

Rise time between 10% and 90% points: 100 ns maximum

Fall time between 10% and 90% points: 5 μ s maximum

Frequency: 1 per 1.5 sec

Duration: 10 \pm 0.005 ms

Source impedance: 10 kilohms maximum

Load: 1 kilohm in series with low-power Schottky T²L in parallel with less
than 50 pF

Cable and connector: Multiconductor

Z-Count Strobe and 200-Hz Clock

Signal type: Clock

Waveshape: Square wave

True level: +4.5 \pm 0.5 Vdc

False level: 0.0 to -1.0 Vdc (0.0 \pm 0.5 Vdc from TI box only)

Rise/fall times (between 10% and 90% points): 5 μ s maximum

Frequency: 100 Hz (Z-count strobe, derived from the frequency standard)

200 Hz (clock, synchronized with the X1 epoch and derived from
the 10.23-MHz frequency standard)

Source impedance: 10 kilohms maximum (100 Hz); 50 ohms nominal (200 Hz)

Load: 1 kilohm \pm 10% in series with low-power Schottky T²L in parallel
with less than 50 pF

Cable and connector: Multiconnector

10.23-MHz Clock

Signal type: Frequency reference

Waveshape: Sine wave

Power level: $-0.8 \text{ dBm} \pm 1.4 \text{ dB}$ for a 50-ohm load with a VSWR less than 1.3:1

Frequency: 10.2299999545 MHz (prior to launch)

Frequency tolerance: ± 1 in 10^{11} (system)

Drift: 1×10^{-12} per day (rubidium) maximum

Drift: 1×10^{-11} per 5 years (cesium) maximum

Cable and connector: Coax

4.3.2 TT&C Commands

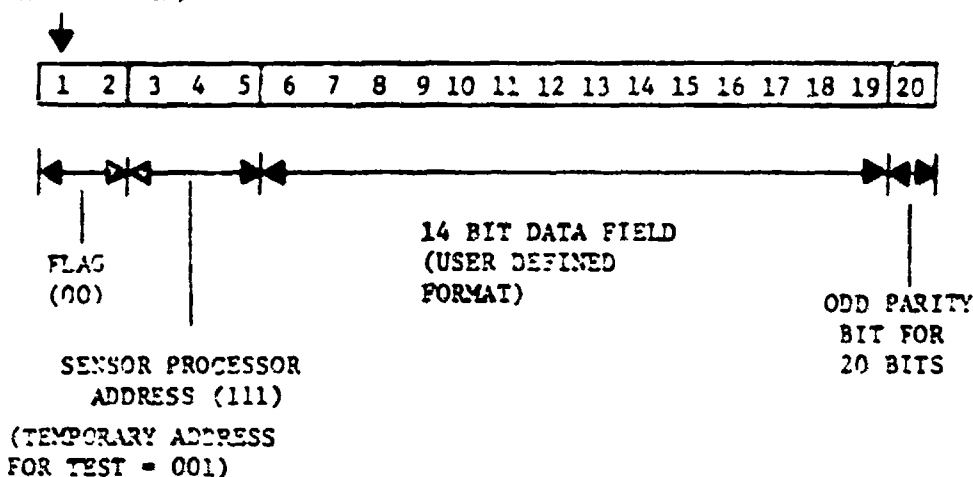
The dual command decoder (DCD) provides the sensor processor (BDP) with one dual-redundant magnitude (serial command) and four nonredundant discrete commands.

4.3.2.1 Magnitude Commands. The command decoder produces dual outputs for the magnitude command, both of which are active and driven by either side of the command decoder (internal cross strap). Each output comprises three lines - data, enable, clock. The 20-bit command format (for input to the AFSCF RTS or equivalent) is as shown in Figure 67. The output from the command decoder is the 14-bit data field. The format of the data field is determined by the processor internal requirements. The data, clock, and enable characteristics are as follows:

Data

Rate:	200 bps $\pm 10\%$
Signal type:	NBZ
True level:	$4.0 \pm 1.0 \text{ Vdc}$
False level:	$0.0 \pm 0.5 \text{ Vdc}$
Rise/fall times (between 10% and 90% points)	5 ns maximum
Load impedance:	90 kilohms to signal ground, minimum

LEADING
BIT
(FIRST BIT
TRANSMITTED)



EXAMPLES: FOR A DATA FIELD OF 00000000000001, THE MAGNITUDE COMMAND BIT STRUCTURE IS 00,111,000,000,000,000,011 OR THE OCTAL EQUIVALENT IS 0700003. FOR A DATA FIELD OF 00000000000011, THE MAGNITUDE COMMAND IS 00,111,000,000,000,000,111 OR THE OCTAL EQUIVALENT IS 0700006.

Figure 67. Magnitude Command Format

Clock

Rate:	200 Hz \pm 10%
Signal type:	RZ
True level:	4.0 \pm 1.0 Vdc
False level:	0.0 \pm 0.5 Vdc
Pulse width (50% amplitude)	1.8 to 2.78 ns
Rise/fall times (between 10% and 90% points)	5 ns maximum
Load impedance:	90 kilohms to signal ground, minimum

Enable

Duration:	14 bits plus overlap
Overlap (leading edge)	0.75 to 1.25 ns

Overlap (trailing edge)	0.0 to 1.25 ms
True level:	4.0 ± 1.0 Vdc
Rise/fall times (between 10% and 90% points)	5 μ s maximum
Load impedance:	90 kilohms to signal ground, minimum

The data, clock, and enable phase relationships are as shown in Figure 68.

4.3.2.2 Telemetry. The addition of the IONDS equipment to the GPS spacecraft does not compromise design or hardware items within the TT&C subsystem. The GPS TT&C command and telemetry functions were purposely oversized in each system to permit growth. The support requirements of IONDS has been accommodated within this spare capacity for the magnitude command detector.

The IONDS has been provided eight discrete commands and 14-bit serial magnitude commands. The IONDS SOH data have been accommodated within the 4,000-bps format.

4.3.2.3 Discrete Commands. The command decoder provides the following discrete commands to the sensor processor:

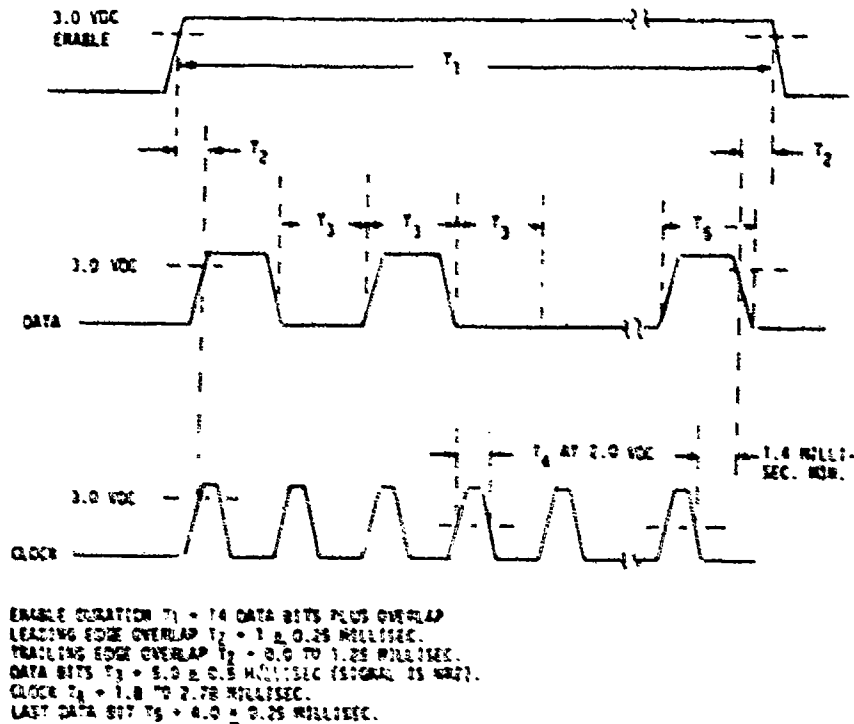


Figure 68. Magnitude Command Data, Clock, and Enable Signal Phase Relationships

- BDP discrete Command 1
- BDP discrete Command 2
- BDP discrete Command 3
- BDP discrete Command 4

The commands are provided on four lines with two (redundant) return lines. Command return lines are isolated from the sensor processor circuit ground in the processor. The discrete command characteristics are as follows:

Amplitude: 20 to 27 Vdc

Pulse duration: 105 ± 5 ms

Rise/fall times (between 10% and 90% points) 50 μ s to 10 ms

Load impedance: 150 to 2,500 ohms resistive. Limit transient, or inrush current to 300 mA, maximum

Return isolation: 1 megohm minimum

4.3.3 TT&C Telemetry

The sensor processor inputs to the pulse code modulator (PCM) are listed in Table 22. The PCM supplies two enable signals to the sensor processor.

Table 22. Sensor Processor Telemetry Outputs

Name	Type	Sampling Rate	Function	No. Bits
Analog 1	Analog	1/sec	Analog Monitor 1	N/A
Analog 2	Analog	1/sec	Analog Monitor 2	N/A
Analog 3	Analog	1/sec	Analog Monitor 3	N/A
Analog 4	Analog	1/sec	Analog Monitor 4	N/A
Analog 5	Analog	1/sec	Analog Monitor 5	N/A
SOH	Digital	2/sec	State of health	8
Discrete 1	Discrete	1/sec	Discrete monitor	1
Discrete 2	Discrete	1/sec	Discrete monitor	1
Discrete 3	Discrete	1/sec	Discrete monitor	1
Discrete 4	Discrete	1/sec	Discrete monitor	1

4.3.3.1 Discrete Telemetry Characteristics. Discrete telemetry inputs to the PCM are differential inputs as shown in Figure 69. The required signal and circuit characteristics are:

Binary 1:	+3 to +32 Vdc
Binary 0:	-1 to +1 Vdc
Load impedance:	0.3 megohm minimum during sampling, nonsampling, and off conditions
Source impedance:	Binary 1: 10 kilohms maximum Binary 0: 0 to infinity with 0.005 μ F or less in parallel
Return isolation (at load)	1 megohm minimum to chassis

4.3.3.2 Analog Telemetry Characteristics. The required signal and circuit characteristics are:

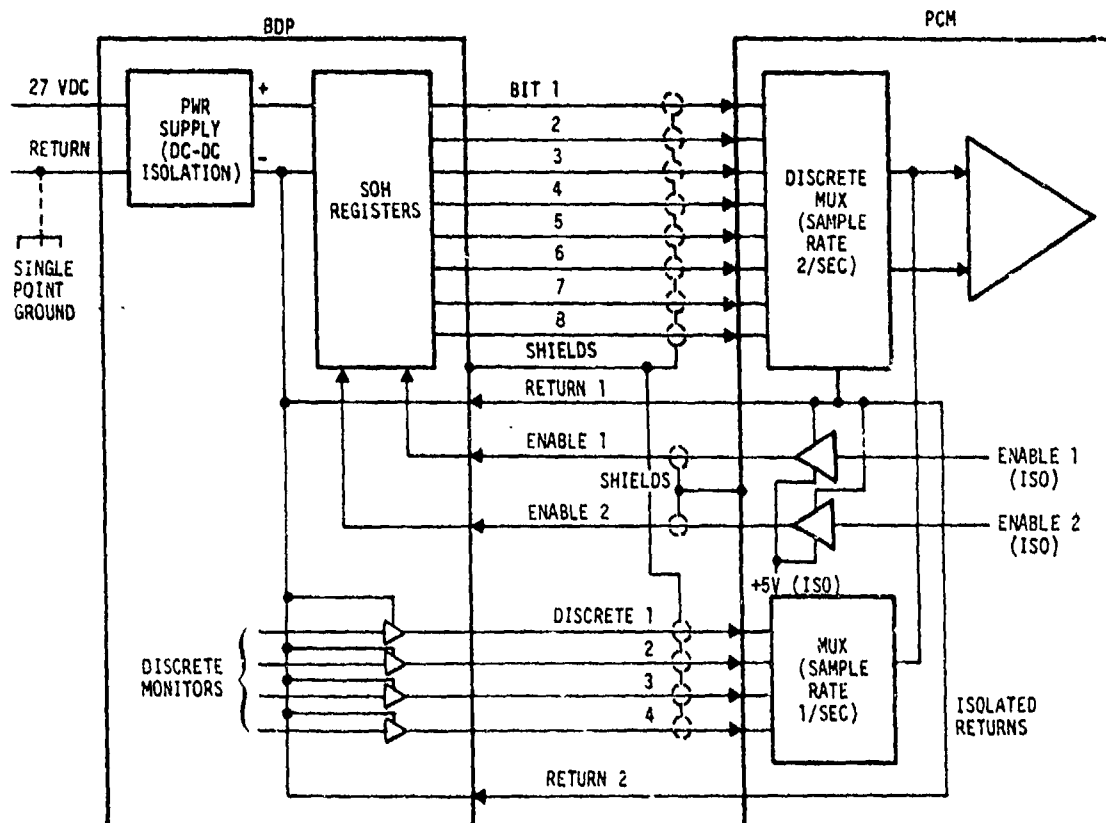


Figure 69. Discrete and SOH Telemetry Interface Schematic (Reference)

Voltage range:	0.0 to 5.12 Vdc
Input frequency range for variable signals:	Dc to 16 Hz
Load impedance:	10 megohms minimum during sampling, and 100 megohms minimum during nonsampling and off conditions
Source impedance:	Less than 5,000 ohms in parallel with less than 0.001 μ F
Return isolation: (at load)	1 megohm minimum to chassis

4.3.3.3 SOH Telemetry. The SOH data are contained in two 8-bit words spaced four subframes apart in the SGLS telemetry (PCM) format. The SOH data are available for transfer from the sensor processor to the PCM unit when the enable gate is high. Updating of the SOH data is inhibited during the transfer period.

Data Read Rate. The enable gates are high for one bit either side of each PCM word (i.e., each enable is 10 bits long). The enable gates are present when the PCM is turned on. When the turn-on period is terminated, the PCM remains on until the end of the current master frame. The expected turn-on period is five minutes per day for each vehicle. The PCM sampling rate is 4,000 or 500 bps (the same as the selected transmission rate). The 16 data bits are transmitted to the ground stations once each second or once each 8 seconds (there are 4,096 bits in a master frame).

PCM Input. The SOH data is supplied to the PCM as eight differential inputs (sampled twice a master frame). The required signal and circuit characteristics are the same as those for discrete telemetry inputs.

Enable Gates. The PCM provides two enable gates per master frame. The required characteristics are:

Wave form:	Positive rectangular pulse
On level:	+4.5 \pm 1.0 Vdc
Off level:	0.0 \pm 0.5 Vdc
Output impedance:	500 ohms maximum
Load impedance:	Greater than 10 kilohms in parallel with 0.005 μ F or less
Rise/fall times: (between 10% and 90% points)	5 μ s maximum

4.3.3.4 GBD Sensor Data. The sensor processor supplies the encoder with dual redundant sensor and sync data and a data gate with the following characteristics. The dual outputs are cross-strapped in the sensor processor.

Sensor Data

Signal type:	Serial digital data, NRZ
Wave form:	Square wave
True level 1:	2.4 to 5.0 Vdc
False level 0:	0.5 ± 0.5 Vdc
Data rate:	200 bps (synchronized with the X1 epoch)
Rise/fall times (between 10% and 90% points)	5 μ s maximum
Load impedance:	One low-power Schottky T ² L unit in parallel with less than 100 pF
Cable and connector:	Multiconductor

The timing relationships between the sensor data and gate are defined in Figure 70.

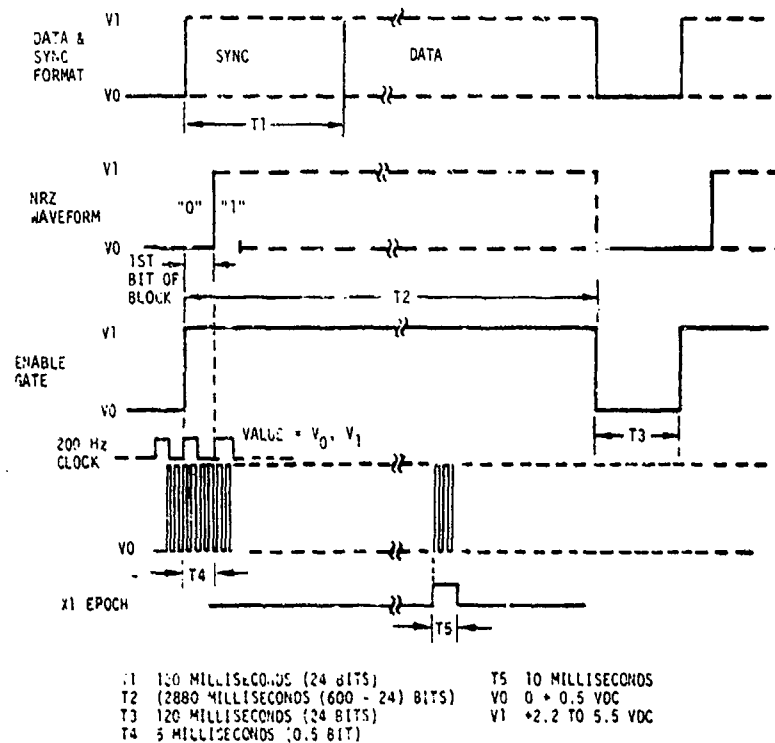


Figure 70. Encoder Interface Timing Relationship

Data Gate

Signal type:	Gate
Wave form:	Square
True Level 1:	2.4 to 5.0 Vdc
False Level 0:	0.0 \pm 0.5 Vdc
Duration:	2,880 ms
Load impedance:	One low-power Schottky T ² L unit in parallel with less than 100 pF
Cable and connector:	Multiconductor

4.3.4 L₃ On/Off Signals

The sensor processor provides the LCU with dual redundancy L₃ on signals and L₃ off signals on four lines isolated from the GBD circuit ground, as shown in Figure 71. The L₃ off signal is delayed at least 120 milliseconds after the

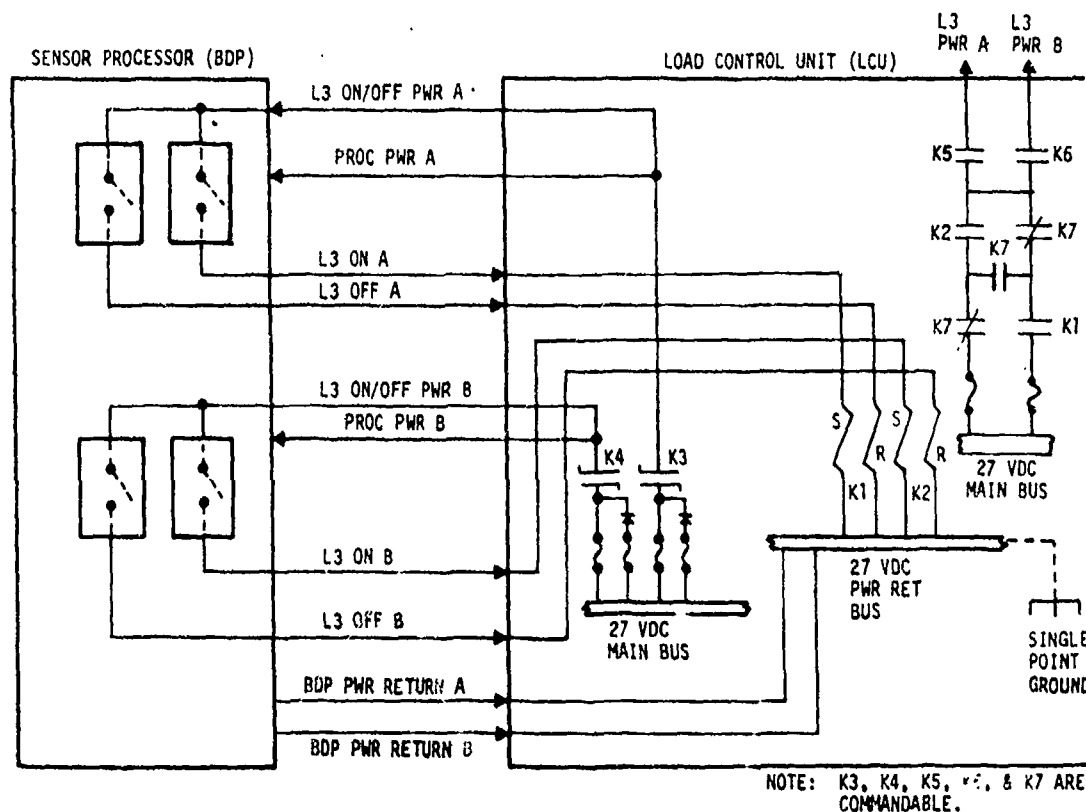


Figure 71. Sensor Processor/Load Control Unit Interface Simplified Schematic (Reference)

last data block that requires processing. The signal characteristics are as follows:

Amplitude:	20 to 28.0 Vdc (27 Vdc bus voltage less driver circuit voltage drop)
Duration:	30 to 120 ms
Rise/fall times: (between 10% and 90% points)	No requirement
Load impedance:	$600 \pm 10\%$ ohms/signal with less than 0.005 μ F in parallel
Cable and connector:	Multiconductor

4.3.5 Design and Construction

4.3.5.1 Electrical Power. Electrical power for all vehicle loads is supplied from the main bus at 27 volts plus or minus 1 volt direct current (Vdc). The voltage at the load interfaces will be within the range of 25.5 to 28.0 Vdc. The power is provided by a two-wire system (power and return). The equipment performs within specified limits when supplied with power within the specified voltage range. GBD secondary power is generated by dc-to-dc conversion. The primary chopping frequency assigned to the GBD is 48 ± 1.0 kHz. Transient voltages are constrained by the source and the loads within the following limits:

	Time Durations	Voltage
Spikes	Less than 50 μ s	± 33 volts line-to-line and ± 27 volts line-to-case
Surges*	Between 50 μ s and 10 ms	36 Vdc maximum 20 Vdc minimum

*Limit voltages are absolute values

4.3.5.2 Dc Electrical Power. Dual redundant primary electrical power for the GBD is supplied by the load control unit (LCU). Power supply redundancy switching is controlled by discrete commands addressed to the LCU. The primary power voltage at the interfaces is 27 plus 1, minus 1.5, Vdc.

The LCU supplies 2-amp relays for switching the GBD primary power and power for the L₃ on/off driver circuits. Relay noise suppression diodes are included in the LCU. The GBD steady-state primary power maximum load does not exceed 15.0 watts. The L₃ on/off driver power load is nominally 45 milliamps (1.215 watts) for 105 msec.

All inductive interrupts such as relay coil circuits are provided with suppression circuits to prevent excessive transients and associated EMC noise.

All vehicle loads are capable of withstanding (without damage) continuous operation of the main bus in a 10-percent over or under voltage condition (24.3 to 29.7 Vdc) and returning to specified performance parameters upon returning to the specified main bus limits. After interruption of power, all equipment will be capable of returning to normal operation upon restoration of power to within normal limits.

4.3.6 Grounding and Isolation

All loads are designed in concert with a single-point ground (SPG) system. Dc-dc isolation is provided in the BDP power supply. The grounding and return system is shown in Figure 72. Multiple-point shield grounding is used on high-frequency circuits (above 100 kHz), on digital circuits with rise or fall times of less than 5 microseconds, and on all electro-explosive device firing circuits. Single and shield grounding is maintained on all other circuits, with the ground at the signal source end. All shielding is insulated to prevent uncontrolled grounding. The shield grounds are carried directly to the vehicle structure by the shortest feasible route and are not returned to the single system ground pilot through conductors in the wiring harness.

4.3.7 X-Sensor and Y-Sensor

The field-of-view of the X-sensor is defined in Figure 73. The field-of-view of the Y-sensor, out to a 22.5-degree half angle, is entirely unobstructed.

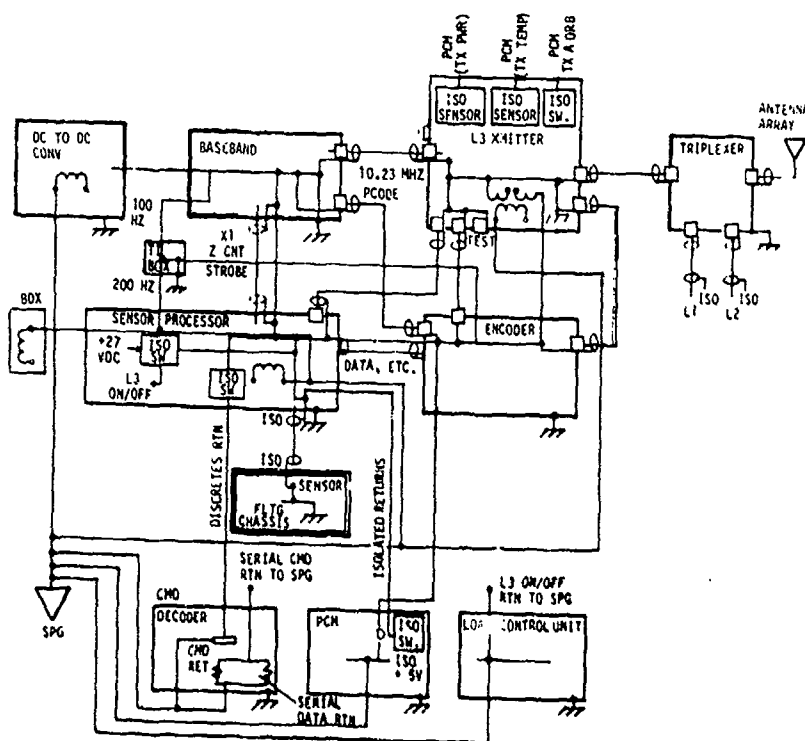


Figure 72. IGS Grounding Schematic

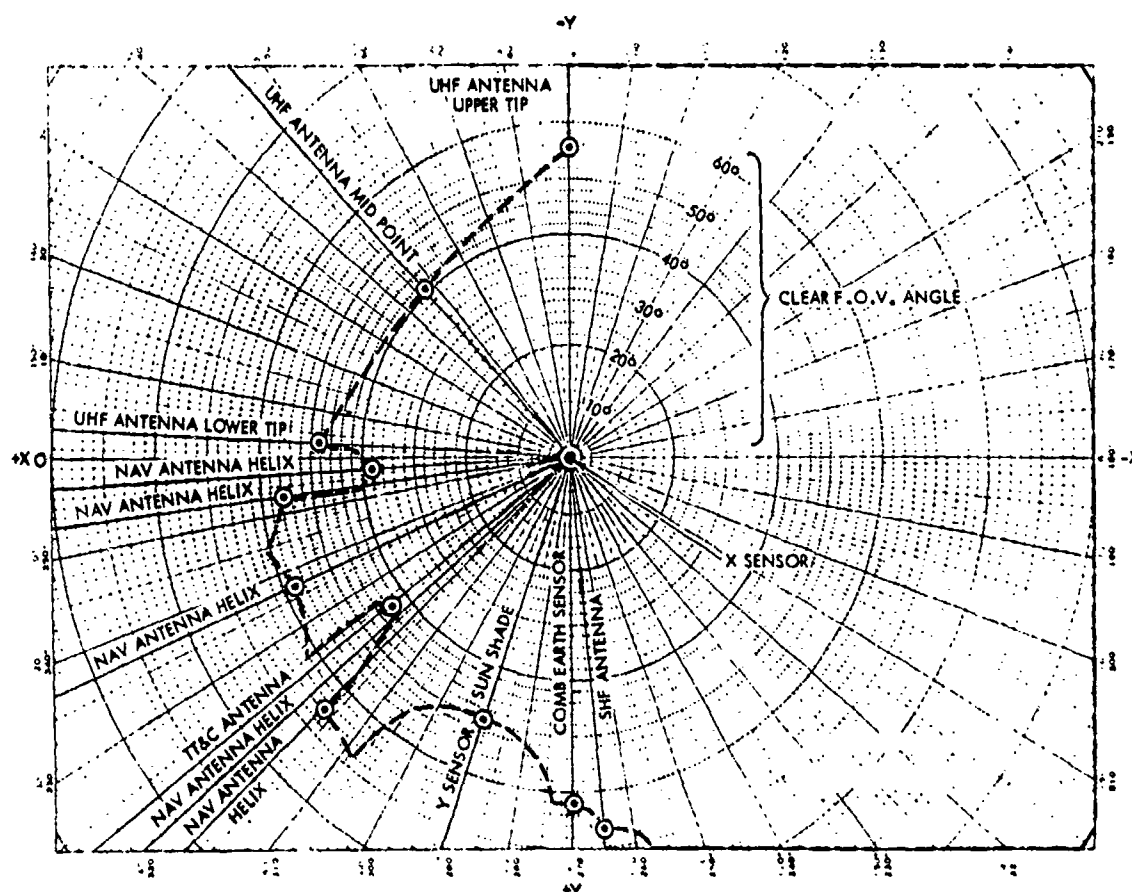


Figure 73. X-Sensor (BDX) Field of View

4.3.8 Structural Data

The weight, center of gravity, and moment of inertia data for the X-sensor (BDX), the Y-sensor (BDY), the Y-sensor sunshade, and the sensor processor (BDP) are compatible with GPS implementation.

4.3.9 Thermal Interface

The GBD maximum thermal dissipation allowances are within the GPS thermal budget. The mounting base is adequate to transfer component heat dissipation. All external GBD box/structure surfaces (excepting mounting surfaces) are coated with passive thermal control surfaces.

4.3.10 IONDS Peculiar Support Equipment

This section describes the special support equipment developed to test and integrate IONDS equipment with the GPS space vehicle. The peculiar support equipment includes the IGS monitor and control system, the telecom test set, the data acquisition and control processor (DACP), and the Sandia GBD test set (CANOE). The integrated space vehicle and peculiar support equipment configuration is illustrated in Figure 74. The space vehicle equipment is above

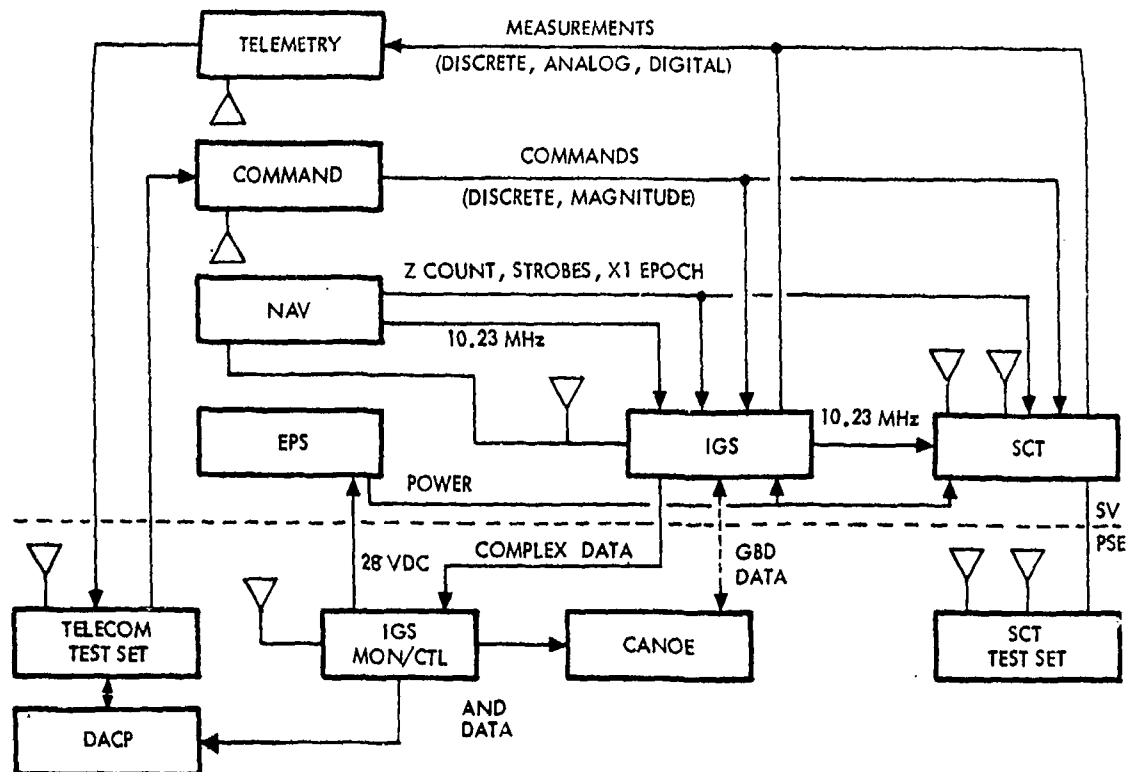


Figure 74. Integrated SV/PSE Configuration

the dashed line with the support below the line. In addition to the IGS support equipment, the SCT test set (not described) has been included for completeness of integration test definition.

4.3.10.1 IGS Control and Monitor Unit. This unit provides the space vehicle's primary power, monitors L₁, L₂, and L₃ RF links, provides the capability to evaluate navigation and IGS system performance, provides L₁, L₂, and L₃ test signals, and provides a decoded data interface to the GBD test set.

4.3.10.2 IGS Telecom Test Set. The telecom test set provides a vehicle/DACP interface for both data and commands for testing purposes. It also provides an S-band uplink signal for commanding IONDS and the space vehicle. The test set receives the S-band downlink signal for data processing and provides timing for the DACP. The telecom test set simulates a remote tracking station of the SCF.

4.3.10.3 Data Acquisition and Control Processor (DACP). The DACP formats the uplink command structure for the telecom test set, continuously monitors PCM data, displays data changes on a printer or teletype, and flags errors detected by comparison with the preprogrammed test routine. The DACP simulates the satellite tracking center of the SCF.

4.3.10.4 Global Burst Detector Test Set (CANOE). The CANOE provides an independent capability to functionally test the GBD equipment. When operated in this capacity, the CANOE simulates all space vehicle interfaces and provides

data storage and display of GBD output, L₃, and PCM data. The CANOE operates with other IGS test sets where it accepts decoded L₃ data from IGS and provides an interim L₃ display capability for DACP. The CANOE provides the following space vehicle functions: (1) 27 volts power, (2) 10.23-MHz sine wave, (3) Z-count, (4) X1 epoch, (5) outputs four discrete commands, (6) outputs one 14-bit serial command, (7) provides four discrete PCM data monitors, 2 eight-bit words per main frame, and five analog monitors, (8) generates the 200 Hz signal, (9) receives BDP L₃ data, and (10) provides display functions for L₃ event data. Figure 75 illustrates the CANOE interface with the IGS system.

4.3.11 L₃ Hardware Compliance Summary

Table 23 summarizes the compliance of the IGS hardware to MIL-STD-1540 and MIL-STD-1541. The tests performed on the L₃ encoder, L₃ transmitter, baseband, sensor, and processor were conducted during the prequalification phase of the program, whereas the tests on the triplexer were conducted during the qualification phase and were completed in August 1978. Although not specified by GPS, the radiated emissions (RE02) from the triplexer were characterized at Rockwell Autonetics during the IGS test program. This helped to estimate the existing radiated emission levels within the GPS satellite. All MIL-STD-1540 and MIL-STD-1541 requirements will be qualified by test, except humidity, which is covered by design practices.

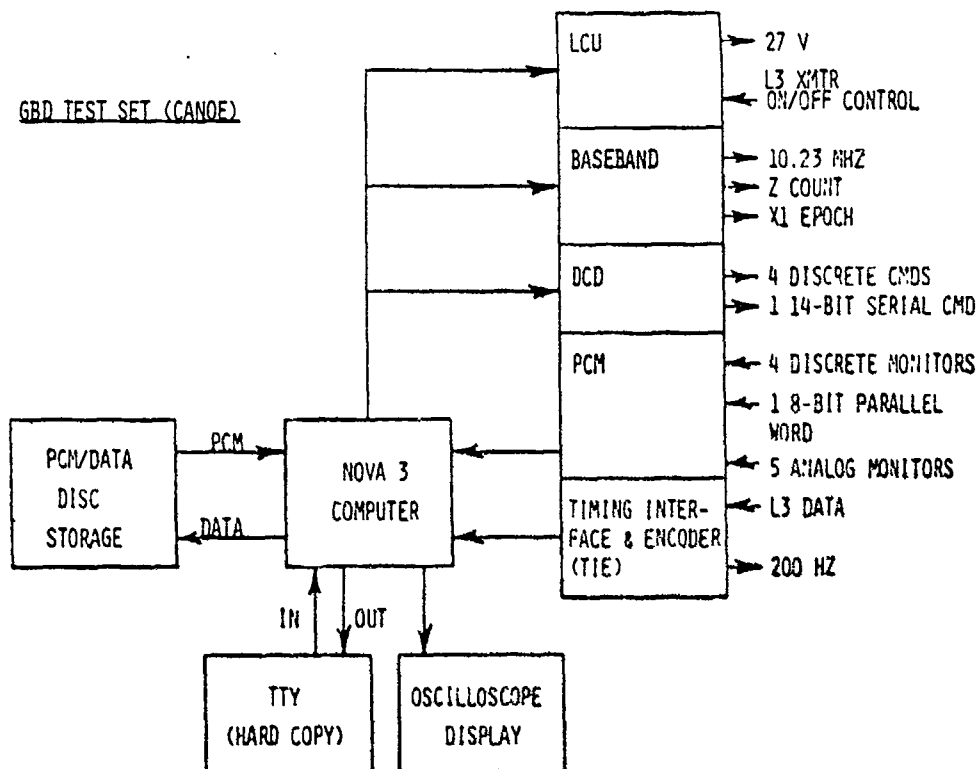


Figure 75. GBD Test Set Interface

Table 23. L₃ Hardware MIL-STD Compliance Summary

Requirement Component	MIL-STD-1540							MIL-STD-1541									
	Functional	Thermal-Vacuum	Thermal Cycle	Random Vibration	Pyro Shock	Acceleration	Humidity	Static Discharge	CE01	CE02	CE03	CE04	CS01	CS02	RE01	RS02	RS03
L ₃ encoder	T	T	T	D	D	D	D	A	A	A	A	A	A	A	A	A	A
L ₃ transmitter	T	T	T	T	D	D	D	A	A	A	A	A	A	A	A	A	A
Sensor processor	Q	Q	Q	Q	Q	Q	D	A	A	A	A	A	A	A	A	A	A
Triplexer	Q	Q	Q	Q	Q	Q	D	N/A	N/A	N/A	N/A	N/A	N/A	N/A	C*	N/A	N/A
Baseband	T	O	O	D	D	D	D	N/A	C	C	C	C	N/A	N/A	C	N/A	N/A
D = Design									A = Tested to MIL-STD-1540 acceptance limits								
T = Tested to MIL-STD-1540 acceptance and limited qualification									C = Characterized								
Q = Qualification tested to GPS levels									N/A = Not applicable								
O = Tested to operational limits									*AT A/N								

The key emphasis from the beginning of the IGS effort was to develop an initial set of hardware virtually identical to a flight unit with the exception of the use of nonscreened parts. This permitted the L₃ hardware to be subjected to a limited qualification test covering the areas of greatest concern. The comprehensive testing already accomplished and the nearly identical design of the prequalification and qualification hardware provided a high degree of confidence in the successful and timely qualification of the L₃ hardware in the current qualification program.

The sensors and processor built by Sandia are GFE provided by the DOE and are tested in accordance with DOE standards to the detailed MIL-STD-1540 and MIL-STD-1541 test limits specified in the Sandia/Rockwell/SANSO Interface Control Drawing. This is the same approach successfully used to provide flight-quality GFE for the VELA satellites. The MIL-STD-1541 (ENC) testing on the hardware was done under a Sandia contract with Rockwell Autonetics by the same group that tested the L₃ hardware.

4.3.12 IGS Weight Summary

Table 24 presents a weight breakdown at the component level. The Sandia sensors and processor along with the Autonetics TIE and L₃ transmitter are the

Table 24. IGS Weight Summary

Component	Baseline* Weight in Pounds	Present Weight in Pounds			Remarks
		Mass	Analysis	Total	
IGS					
Y-sensor electrical	9.4	10.7	6	16.7	
IGS sensor sunshade and wrackery	6.0	4.5	0	4.5	
X-sensor	2.7	3.1	0	3.1	
Data processor	9.5	19.3	1.5	20.8	Shielding added; 1.5-lb growth allocation
TIE box encoder and timing	1.8	1.8	3.7	5.5	Timing and power supply circuits added
IGS transmitter and switch	9.5	6.6	0	6.6	Transmitter A and switch
		5.9	0	5.9	Transmitter B
IGS total	38.9	51.9	5.2	57.1	
Integration units					
FCM		0.4		0.4	Minor wiring and FROM change
Triplexer	1.0				Not required
DW			0.2	0.2	
Baseband			0.7	0.7	
LCU					
Integration total	1.0	0.4	0.9	1.3	
Equipment subtotal	39.9	52.3	6.1	58.4	90% measured
Cabling	TBD	6.3	1.3	7.6	Includes 2.5 lb of Scandia cable
Integration hardware	TBD		8.3	8.3	Includes 0.7-lb doubler and 5.6-lb ballast
Integration total	39.9	58.6	15.7	74.3	79% measured
Growth and uncertainty	8.0			8.2	72% of analysis
Subsystem on orbit	47.9			82.5	
Lift-off equivalent (current AXM)	79.7			139.1	Includes 0.66481 lb of AXM and 0.02545 of RCS propellant per pound of system
*August 1976 Design Review					

IGS subsystem. The integration units are basic GPS units modified to support IGS requirements. Integration hardware, cabling, and hardware such as brackets, thermal doublers, etc., are included to show the total additional weight necessary for the IGS secondary payload. An August 1976 baseline is carried to show the original weight estimates. The weight growth of the IGS hardware as of Sept. 15, 1978, is due to the following:

1. Ten pounds of additional weight for shielding were budgeted to Sandia for the data processor to handle the updated GPS radiation environment. The new environment was established after IONDS (SAMSO and DOE) discussions with Aerospace, NASA/GSFC, and AFWL indicated that designing to the existing GPS environment would probably be marginal at best. Subsequent NTS II measurements in the GPS orbit in conjunction with DMSP measurements have confirmed the new values.
2. Timing distribution circuitry which was to be available in the new GPS Phase II baseband was included in the IONDS encoder when GPS dropped plans for a new baseband before Phase III. The new weight includes a power supply to provide previously unrequired standby power for the TIE box.

3. The independent power supplies were incorporated when the transmitter was changed from a set of internally redundant synthesizers and amplifiers (like GPS) to two individual units. The new design was chosen to help meet MIL-STD-1541 and to simplify integration of the system into GPS.

The IGS weight summary presents the actual measured weights of each unit and weight derived by analyses whenever the total weight was not measurable. For example, in the TIE box/encoder, 3.7 pounds were analytically derived due to the addition of a power supply.

The IGS on-orbit weight budget is 82.5 pounds. Ninety percent of the IGS equipment weight estimate of 58.4 pounds was obtained by actual measurement, providing a high degree of confidence in its validity. The integration equipment total weight allows 8.2 pounds for growth and uncertainty without exceeding the 82.5-pound budget. This should be adequate, as shown on the next tables. The total lift-off weight for the IGS equipment is 139.1 pounds, including 0.66485 pound of AKM and 0.02545 pound of RCS propellant per pound of payload.

4.3.13 IGS Prime Power Summary

Table 25 presents the total IGS subsystem load demand, including increases in GPS equipment required to support IGS. Both standby and operating modes are presented. In standby, IGS is sensing and processing data but not transmitting. In the operating mode IGS is sensing, processing, and transmitting data. This summary tabulates the load demand by component with an equipment subtotal,

Table 25. IGS Prime Power Summary

Component	Max. Standby				Max. Operating				Remarks
	Baseline ^a Power in Watts	Present Power in Watts			Baseline Power in Watts	Present Power in Watts			
		Mean	Analysis	Total		Mean	Analysis	Total	
IGS									
Y-processor	1.3	9.9		9.9	1.3	9.9	9.9	Encoder 50 W dissipated	
X-processor	1.0				1.0				
Processor	9.0				9.0				
TIE box/encoder					3.0				3.0
L ₂ transmitter			68.0	73.0	73.0				
IGS total		9.9		9.9		83.9	83.9		
Integration hardware									
Triplexer	NA	-	-	-	-	-	-		
Baseband		1.0	3.3	1.0		1.0	1.0		
TIE box/timing			3.3			3.3		Timing and power supply	
Integration hardware subtotal		1.0	3.3	4.3		1.0	3.3	4.3	
Equipment subtotal	11.3	10.9	3.3	14.2	84.3	86.9	3.3	97.2	
Typical GPS distribution loss	0.3		0.6	0.6	3.4		3.7	3.7	42 of total equipment subtotal
Integration total	12.0		3.9	14.8	87.9		9.0	99.9	
Growth	3.0			0.5	10.0			1.1	Standby: 142 of analysis Operating: 122 of analysis
Subsystem total	15.0			17.6	97.9			97.0	
*August 1974 Design Review									

distribution loss, and growth allocation. The distribution loss accounts for line loss between the power source and IGS subsystem. A small growth factor has been allocated for power demand uncertainties such as variations from unit to unit.

Growth in power demand has occurred due to moving the timing interface function from the baseband unit to the TIE unit and adding a low-voltage power supply in the TIE unit to provide standby power rather than parallel loading the GPS dc-to-dc converter. This approach is slightly less efficient but was chosen in accordance with SPL ground rules to avoid potential noise interference with GPS subsystems.

5. RELIABILITY

The reliability objectives of the IGS/GPS interfaces would preclude IGS-induced navigation mission failures and GPS failures which would cause IGS mission failure without an accompanying navigation mission failure.

The IGS reliability program included a failure effects analysis used to identify single-point failure and critical items. Part specification reviews also were performed to assure compliance with good reliability engineering and contract requirements. This review verified that the selection of most piece parts were in compliance with the program preferred parts list (PPPL). Where PPPL parts were not obtainable, screening, burn-in, and other tests were imposed on those parts to assure selecting parts of equivalent quality. The reliability of IGS was evaluated by comparing IGS predicted values with IGS and GPS apportioned values, providing a uniform approach for attaining a predicted five-year mission life.

5.1 RELIABILITY/COMPATIBILITY ANALYSIS

A reliability/compatibility analysis was conducted on the IGS system hardware to determine the possible effects of IGS hardware failures in the GPS. The analysis was conducted utilizing a combination of failure simulation by computerized logic and circuit analysis. In addition to establishing the compatibility of the IONDS and GPS systems, a failure mode effects analysis (FMEA) was performed.

The computer simulation used during the analysis was identical to the simulation successfully pioneered for the GPS Program. Inspection of simulation data indicated single-point failures, command sequences for failure work-arounds, and failure definitions. The results of this IGS reliability analysis are contained in Rockwell report SD 77-GP-0035.

The reliability/compatibility analysis defined 31 interfaces between the GPS vehicle and IONDS. There are 16 interfaces with the load control unit; these include the coils and contacts of the eight power transfer relays. All contacts are redundantly fused. The analysis determined that a relay coil short presents a possibility of negating the GPS load shed capability. This failure mode is a second-order failure since the load shed function is only initiated when one failure has occurred and therefore is not considered a single-point failure. Further, the load shed function is made available by the DCD sequenced commands. In addition, relay coil shorting has a low probability of occurrence.

The DCD has six interfaces with IGS. Eight of these commands have individual driver amplifiers and thus isolate the GPS from the IGS. The two redundant commands (enable command) share the same output amplifier as the GPS. An IGS short could force the GPS commands into its redundant mode which is not considered a single-point failure.

The baseband/processor has seven interfaces with the IGS. The X1 epoch, Z-count, and Z-strobe each have an isolation inverter amplifier as a source, thus protecting the GPS system. The P code is derived from the Q side of the P code flip flop, providing the GPS P code, thus isolating the GPS system. Finally, the 10.23-MHz clock signal is routed through a series of cascaded hybrid frequency power dividers. An IGS short or open in the clock signal circuit will not unbalance the source sufficiently to cause system degradation.

The triplexer has one interface with the IGS - the L₃ transmitter. The high isolation of about 50 dB from port 1 to port 3 and from port 2 to port 3 will result in a negligible effect on the operation of L₁ and L₂ in case the cable between the L₃ transmitter and the triplexer is shorted or opened.

From the above reliability analysis, it was determined that single IGS failures, opens, or shorts in the IGS system which could reflect through the interface and cause a failure in the GPS vehicle do not exist.

5.2 RELIABILITY PREDICTIONS AND FAILURE MODE EFFECTS ANALYSIS

The reliability predictions and FMEA of the baseband/processor were reviewed. The logic diagrams and predictions for the transmitter and L₃ encoder are presented in Figure 76. The calculated numbers are $R_T = 0.988178$ for the transmitter and $R_E = 0.99419$ for the encoder.

The logic diagram and results for the baseband and triplexer are presented in Figures 77 and 78. The calculated numbers are $R_B = 0.990494$ for the baseband and $R_T = 0.996502$ for the triplexer.

An analysis was performed to assure that the IGS L₃ channel reliability predictions were comparable to predictions derived from the GPS L₁ and L₂ channels. The calculated numbers were $R_{L1} = 0.9687$, $R_{L2} = 0.9694$, and $R_{L3} = 0.9705$. The logic diagrams and results of this analysis are presented in Figures 79 and 80.

The FMEA emphasized high-power transistor junction temperatures. For the L₃ encoder and transmitter, the transistors in the high-power amplifier are rated at 200°C and derated not to exceed a junction temperature of 125°. One junction's temperature is 106.6°C, two are 102°C, and the remainder are below 85°C. The remaining transistors, hybrids, and diodes are rated at 125°C, and the highest temperature reached is less than 85°C. All components are stress derated at least 50 percent of rated value.

For the baseband assembly, the maximum semiconductor junction temperature is 94°C for four transistors. The next highest junction temperature is 89°C for three components, and all the remaining are below this number.

The FMEA's thus demonstrate that semiconductor junction temperature does not rise above 125°C in normal operation and that no other components are operating at more than 50 percent of their rated capacity.

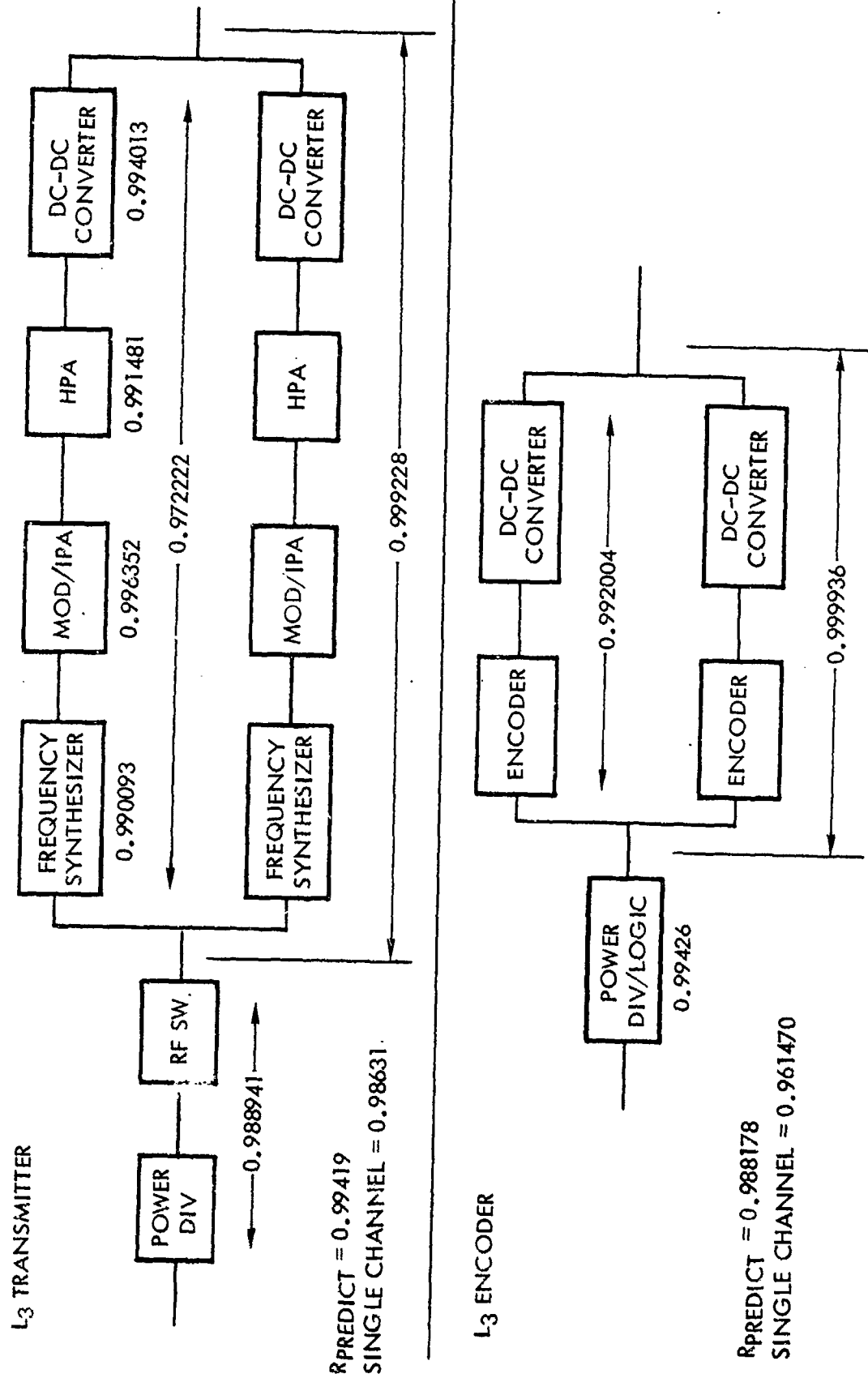


Figure 76. L₃ Transmitter and Encoder Logic Diagrams

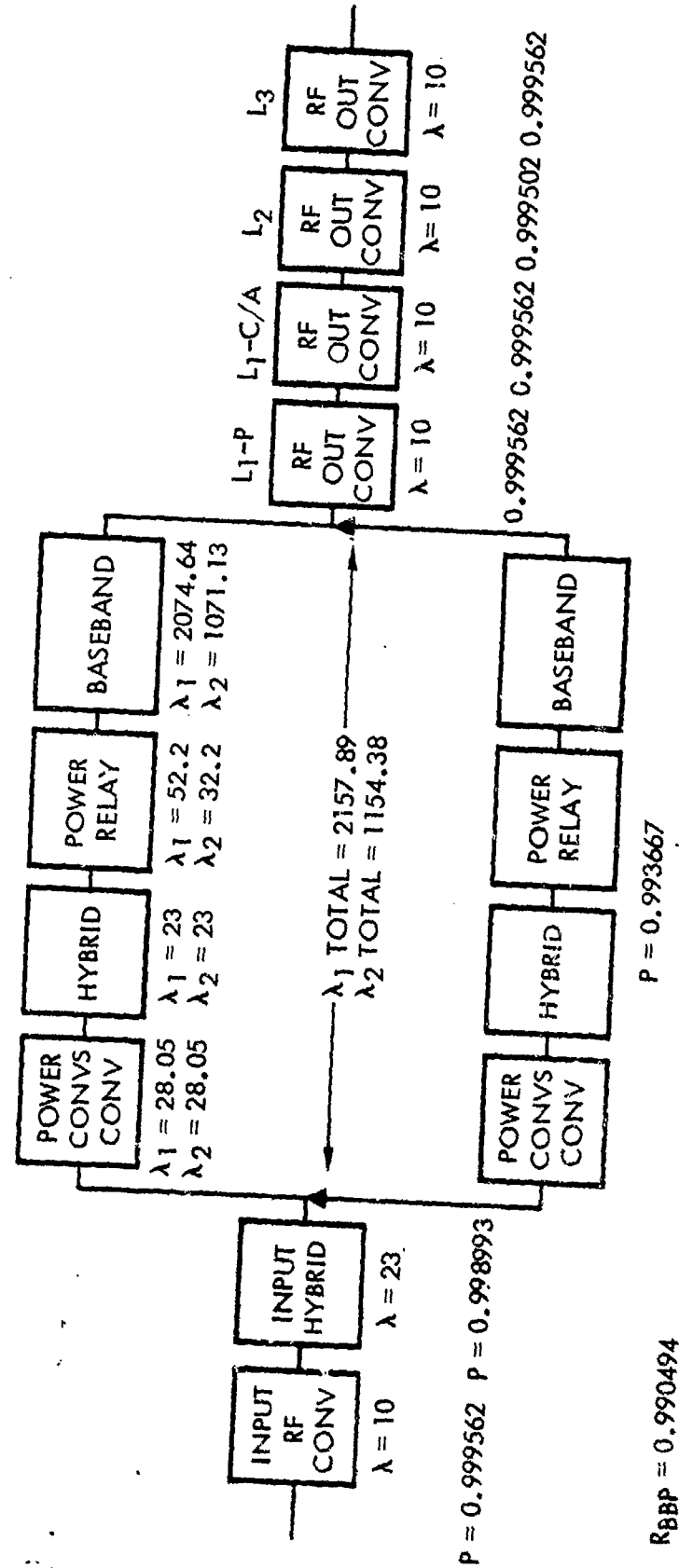


Figure 77. Baseband Processor Reliability Logic Diagram

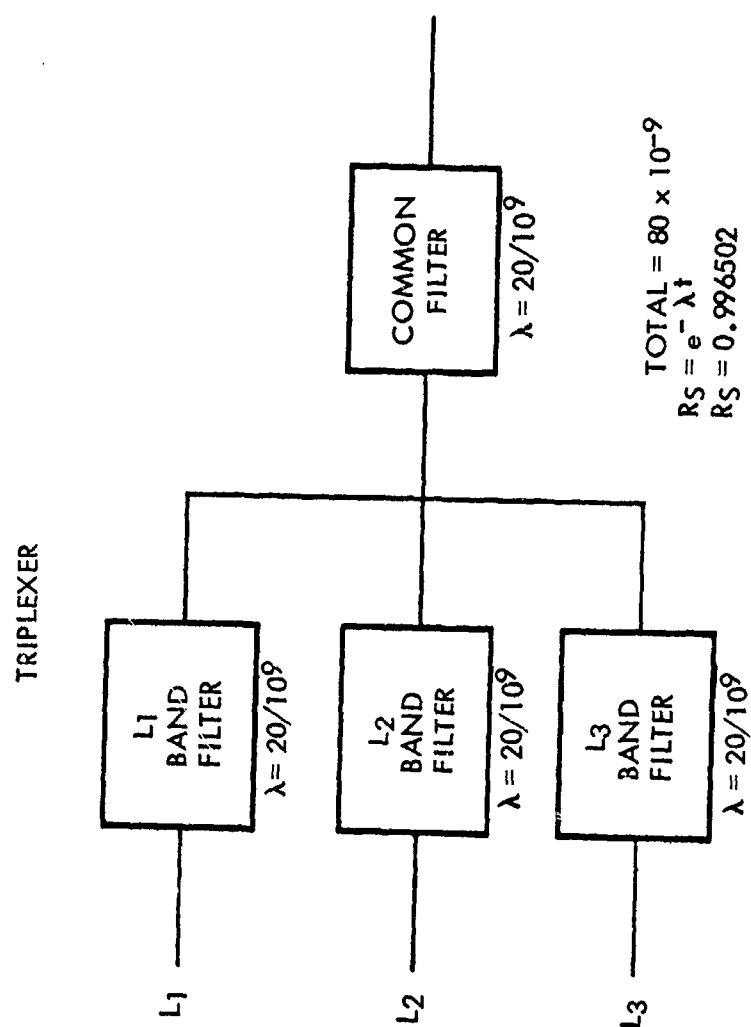


Figure 78. Triplexer Reliability Logic Diagram

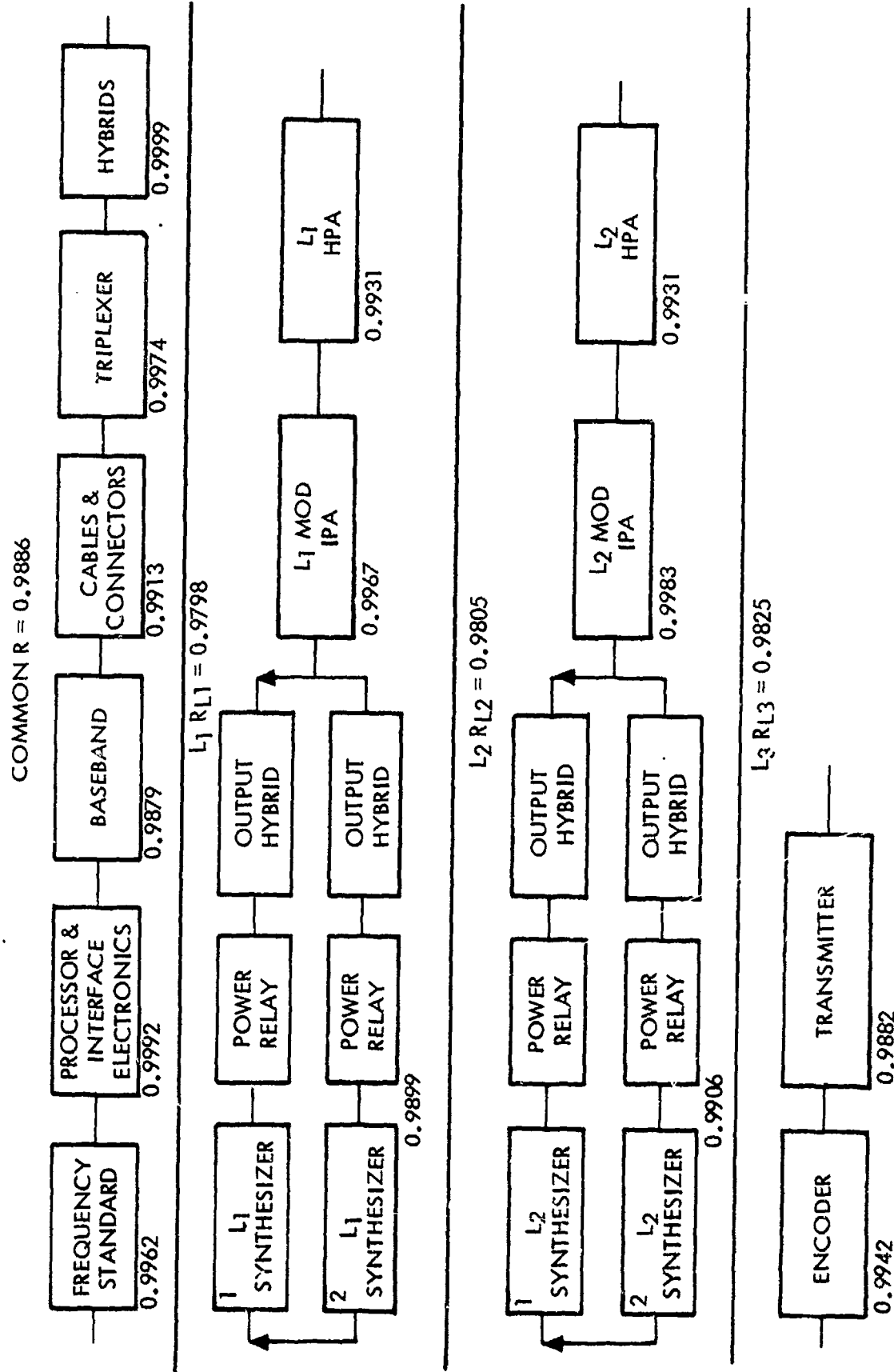
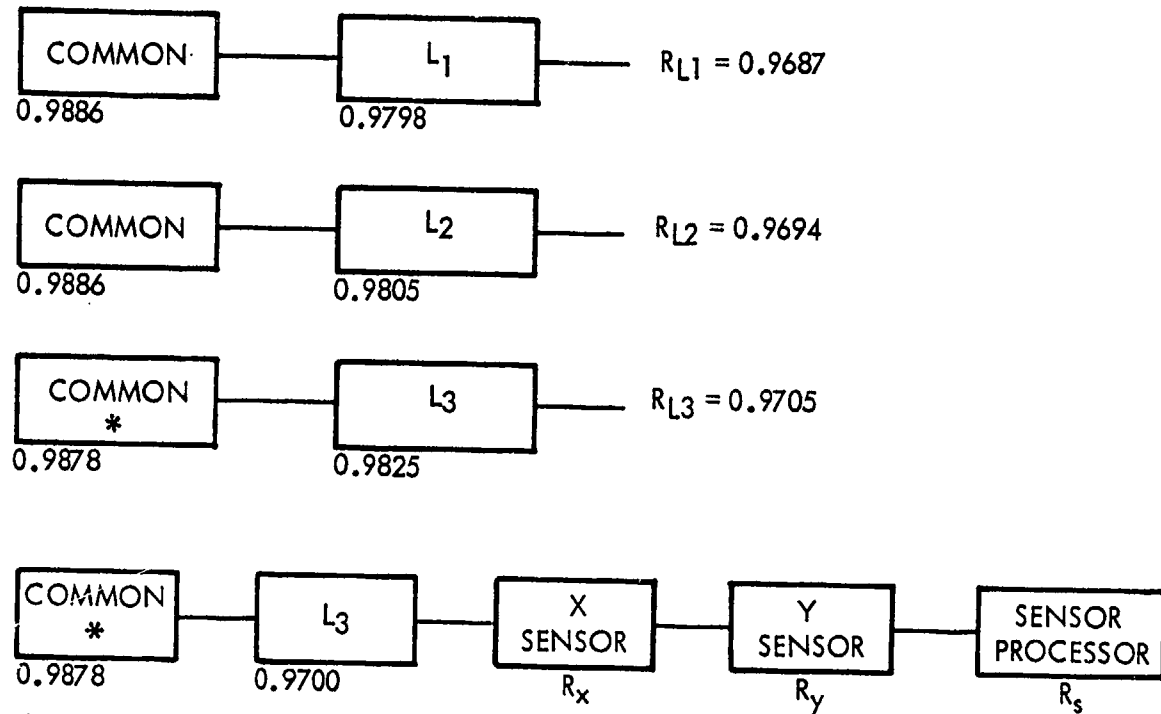


Figure 79. L₁, L₂, L₃ Reliability Logic Diagrams



*Triplexer reliability number

Figure 80. L₁, L₂, and L₃ Reliability Comparison

5.3. CRITICAL ITEM LIST

In applying the GPS-developed computerized logic failure simulation program, the following eight single-point failures were identified in the IONDS critical item list.

1. L₂ synthesizer - Frequency distribution module (no output)
2. Baseband/processor - Power divider (no output)
3. IONDS ANZAC DS310 - Four-way power divider (no output)
4. IONDS ANZAC DS109A - Two-way power divider (no output)
5. IONDS ANZAC DS109B - Two-way power divider (no output)
6. IONDS L₃ encoder - Input power divider (no output)
7. IONDS radio frequency switch (contacts failing to close or stay closed)
8. ITT IONDS triplexer (no output)

5.4 PARTS, MATERIALS, AND PROCESSES

The IGS parts program has the same ground rules and requirements as the GPS Program. The GPS Parts, Materials, and Processes Control Board (PMPCB) was delegated the responsibility of reviewing and approving all IGS parts, processes, and materials and thus provide a common control base. The IGS parts selection process is illustrated in Figure 81. As the subcontractor submits specification control drawings (SCD's) for the procurement of parts for the transmitter and encoder, they are reviewed by Reliability engineers, and if approved, they are submitted to PMPCB for concurrence.

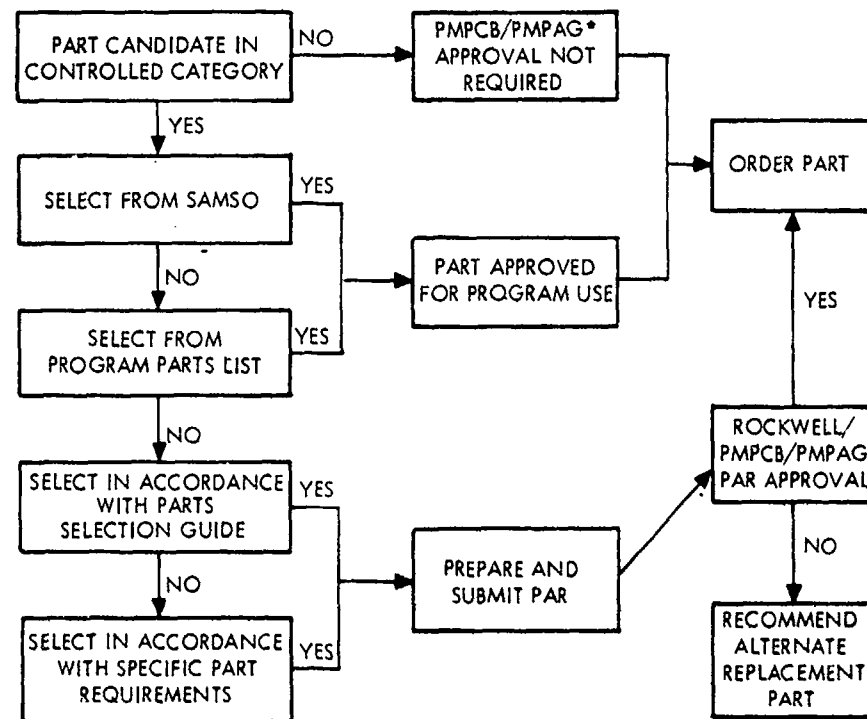


Figure 81. IGS Parts Selection Process

6. TEST PROGRAM

The IONDS test program began in 1976 with component testing and will culminate with an in-orbit demonstration of system capabilities in mid-1980. The objectives of the overall test program are (1) verification that the L3 components satisfy design requirements, (2) verification that the L3 subsystem performance will meet operational requirements, (3) verification that the L3 subsystem will interface with the NUDET sensor subsystem, and (4) verification that the IGS subsystem will interface with the GPS system on a noninterfering basis.

6.1 TEST PLAN

An overview of the IONDS test schedule is illustrated in Figure 7. Both the component and L3 subsystem testing have been completed in addition to integration and compatibility tests. Completion of this series of tests verified the IGS system operational characteristics and compatibility with the GPS vehicle and system. In-orbit verification of IGS operational capability will begin after the launch of the QTV spacecraft tentatively scheduled in 1980. The IONDS and GPS systems will undergo performance verification, integration, and acceptance testing before launch of the QTV spacecraft.

6.2 COMPONENT TESTS

6.2.1 Antenna Tests

The objective of these tests was to demonstrate the compatibility of the GPS antenna system to support IONDS L-band transmissions on a noninterfering basis. Antenna testing is summarized in this section and is documented in detail in Rockwell report SD 77-GP-0011.

6.2.1.1 Configuration. The test configurations included all of the antennas and sensors mounted on the GPS antenna bulkhead and a baseline configuration containing no pending payload components. The flight version of the L-band antenna, the TT&C antenna, and the secondary payloads were installed as shown in Figure 82. Each configuration used a forward bulkhead simulator designed for the secondary payloads program. The front surface of the bulkhead was located 1 inch above the spider surface, as specified by the GPS requirements. Mounting supports for the test fixture and secondary payload elements were the special priorities included in the bulkhead design.

6.2.1.2 Test Results. L₁ Degradation. The test data indicated that the secondary payloads do not degrade the L₁ antenna pattern. The degradation to L₁ was determined by analyzing the gain, ellipticity, and net gain on its 14.3-degree conical cut pattern. This is the critical performance angle for the navigation antenna and is the basis for link margin analysis.

Figure 83 displays the impact of the composite secondary payloads on the L₁ gain pattern. The baseline is derived by averaging L₁ over nine measurements.

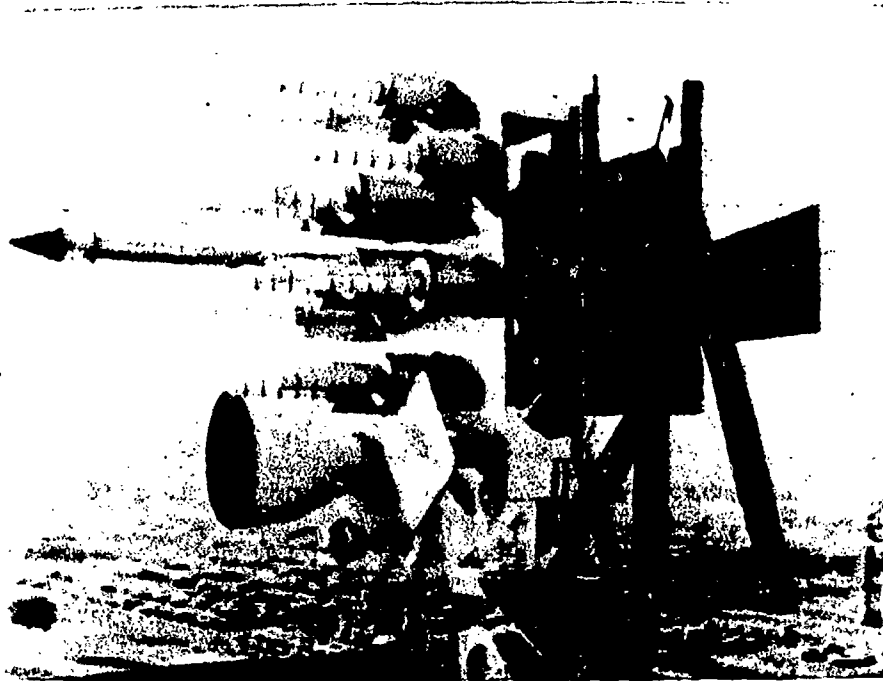


Figure 82. GPS Full-Up Antenna Configuration

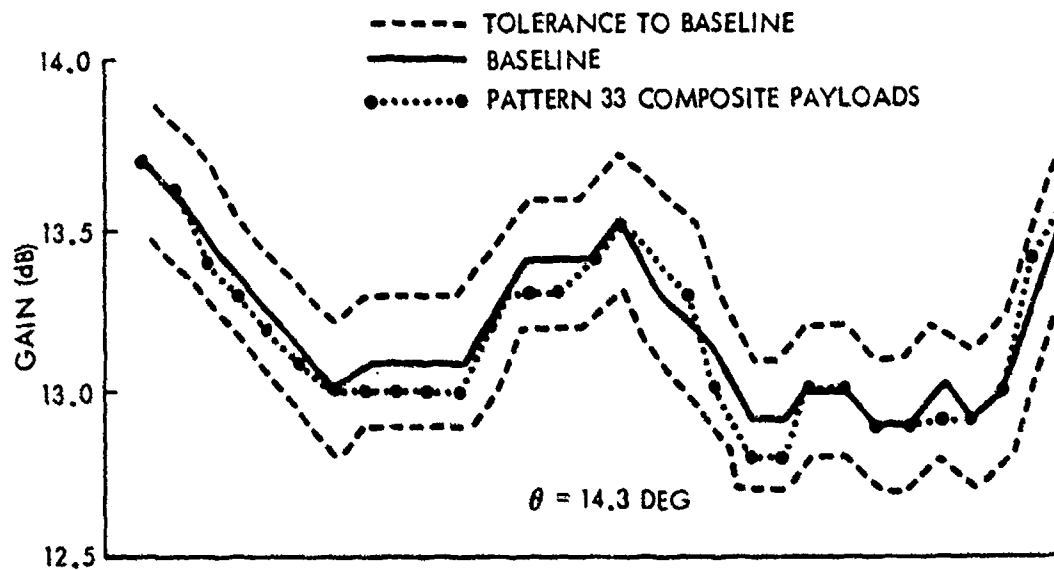


Figure 83. L_1 Gain Impact

The allowable 0.2-dB measurement precision bound for the range is displayed about this average curve. The secondary payload data were within the precision bounds, indicating that the conic was unaffected by the presence of the secondary payload devices. Figure 84 shows that the ellipticity is within limits except for one angle. This anomaly resulted from inaccuracies in the comparative measurement technique.

L₂ Impact. The L₂ patterns generated during this testing indicate that the secondary payloads may have some impact on L₂ gain (0.2 dB) for the $\theta = 14.3$ -degree conic (see Figure 85). However, the 14.3-degree conic gain at L₂ was found to be significantly altered when the thermal blanket was removed (gain was reduced by more than 1.0 dB over part of the conic angle). The antenna failed to meet the acceptance criteria when tested in this condition. The baseline L₂ ellipticity (Figure 86) characteristic also was degraded beyond acceptance, but the secondary payloads do not impact this characteristic.

L₃ Operation. The 14.3-degree conic gain taken at L₃ indicates that 11.4-dB gain is the minimum at 1381 MHz. The coated and uncoated sunshade tests produced similar gain. The VSWR and gain measurements versus frequency indicate that an antenna anomaly that exists at about 1372 MHz affects gain. Antenna performance improves significantly (2.0 dB) by moving more than 25 MHz from this frequency.

Isolation. TT&C isolation was measured at 55.0 dB for both baseline and integrated payload configurations.

VSWR. The VSWR's in the information bandwidths of L₁ and L₂ were less than 1.06:1 and 1.2:1, respectively, in both configurations.

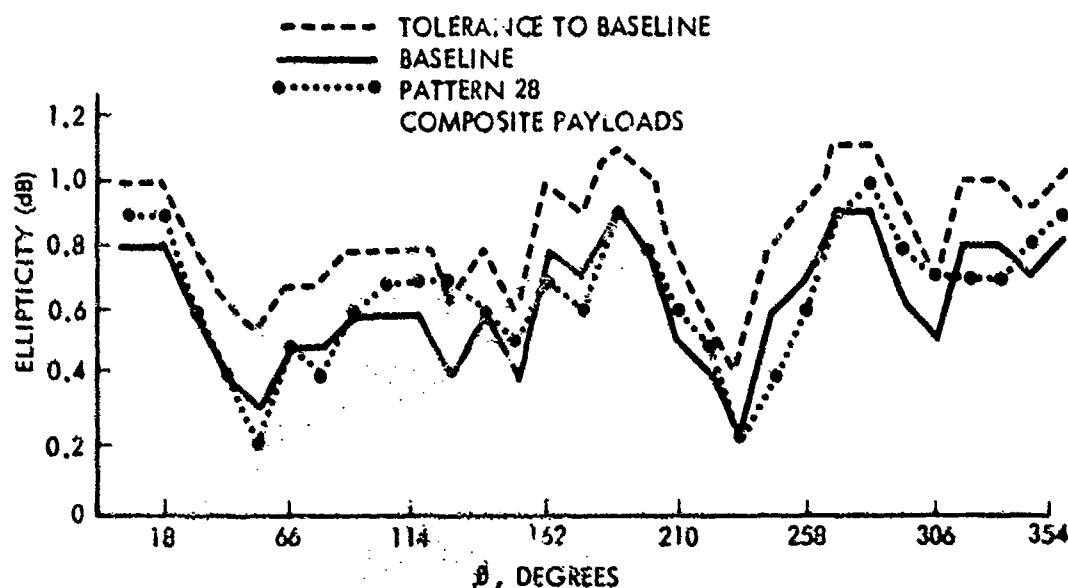


Figure 84. L₁ Ellipticity Impact

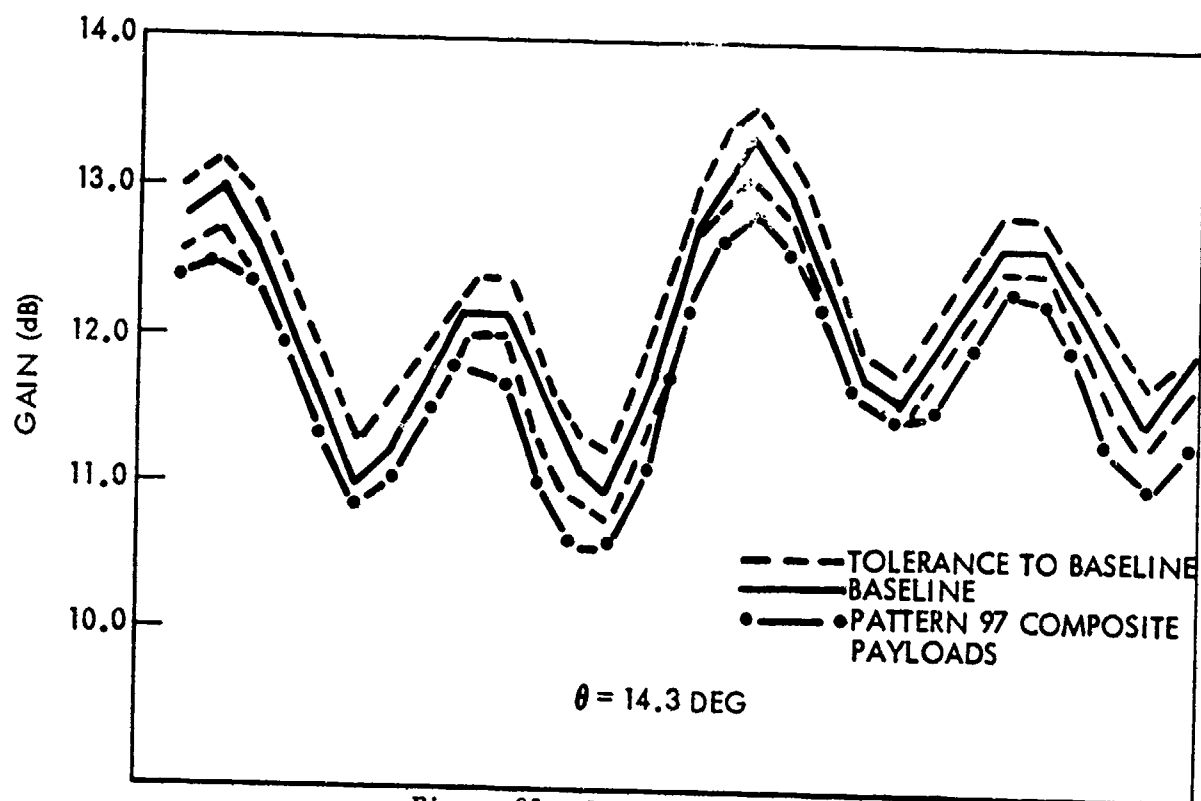


Figure 85. L₂ Gain Impact

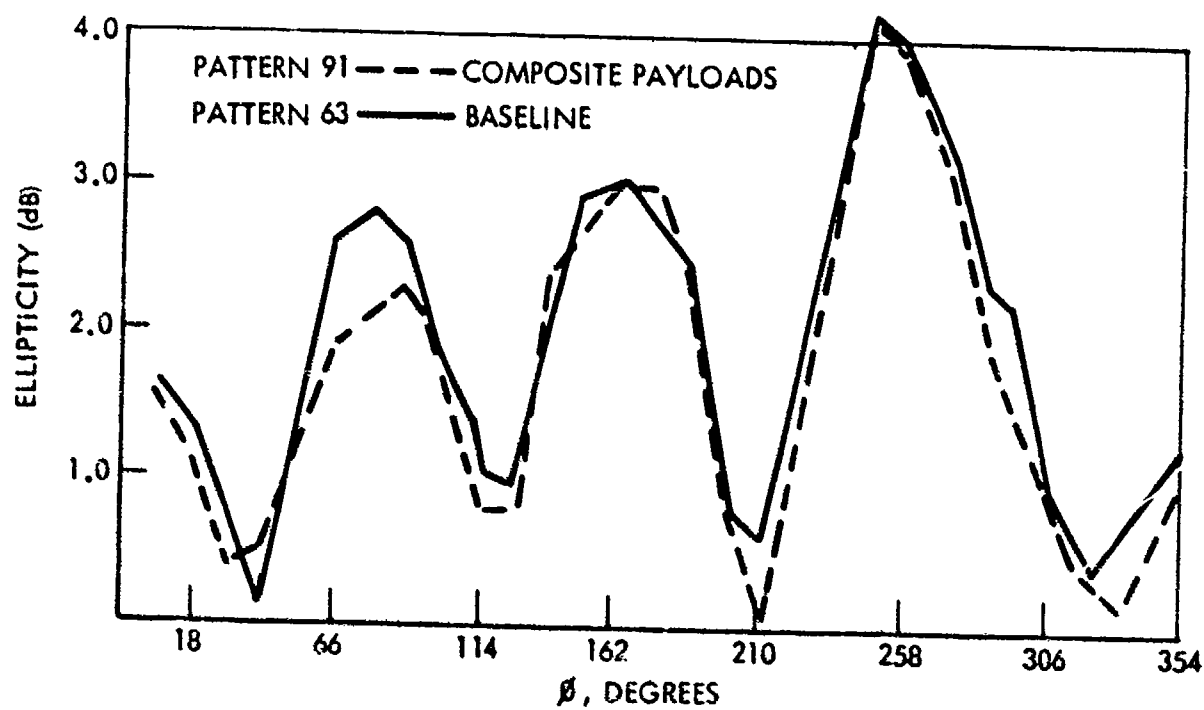


Figure 86. L₂ Ellipticity Impact

A second test with a protective thermal blanket performed in March and April 1977 provided L₂ performance within specification. The test used a production L-band antenna, spider, bulkhead, and thermal blanket.

6.2.2 Triplexer Tests

IGS triplexer testing was performed to verify its functional design and to verify triplexer environmental characteristics. Design objectives included L₃ operation on a noninterfering basis with GPS L₁, L₂ operation. Since the IGS triplexer consists of the GPS diplexer with a third input port added, the testing was used to demonstrate that the triplexer L₁ and L₂ channel performance was equivalent to the GPS L₁, L₂ diplexer performance. Triplexer/diplexer testing involved measuring insertion losses and standing wave ratios (VSWR) to assure that performance objectives were accomplished. The IGS EDM triplexer used the latest GPS flight diplexer configuration.

6.2.2.1 Configuration. The test configuration included an L-band signal generator (1 to 2 GHz), power and VSWR meters, a GPS diplexer, and an IGS triplexer. In the test configuration, triplexer input Ports 1, 2, and 3 correspond to L₁, L₂, and L₃ channels. Triplexer Port 4 is the output to the GPS L-band antenna system.

6.2.2.2 Test Results. Examination of the triplexer test data indicates that the triplexer has performance equivalent to that of the GPS diplexer and will also satisfy L₃ operational requirements. Table 26 summarizes measured diplexer and triplexer VSWR's and losses. It can be seen that the triplexer slightly improves L₁ performance over the GPS diplexer. The L₂ measurements indicate an increased loss of about 0.14 dB for triplexer performance. It was later found that the triplexer was slightly detuned and actual performance could be expected to improve. Since the 0.14-dB loss was small, it was decided that the tests would not be rerun.

Triplexer testing was accomplished by varying input frequency at each port from 1 to 2 GHz and measuring the VSWR and losses to each of the other triplexer ports.

Figures 87 through 92 are automatic plots of an IONDS triplexer VSWR and losses as measured from input Ports 1, 2, and 3 to output Port 4. Figures 93 and 94 show Port 3 to Ports 1 and 2 isolation. At the L₁ frequency of 1575.42 MHz, the cross-coupled energy from Port 3 to Port 1 is down about 45 dB.

Table 26. Diplexer/Triplexer Comparison

Unit	L ₁		L ₂		L ₃	
	VSWR	Loss	VSWR	Loss	VSWR	Loss
GPS Phase 1 Diplexer	1.149	0.485	1.038	0.276	NA	NA
IONDS Triplexer	1.15	0.45	1.11	0.42	1.14	0.51

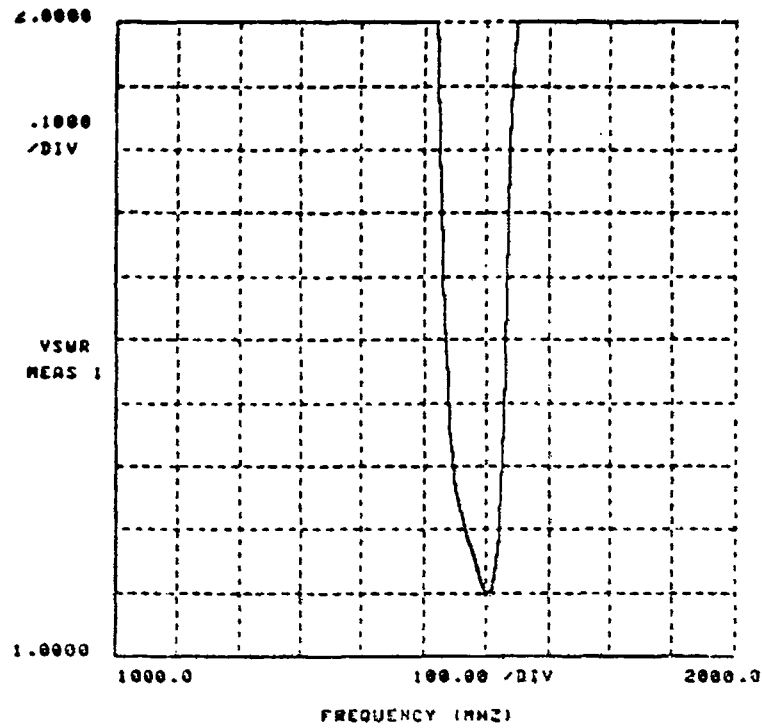


Figure 87. Triplexer VSWR Plot, Port 1 to Port 4

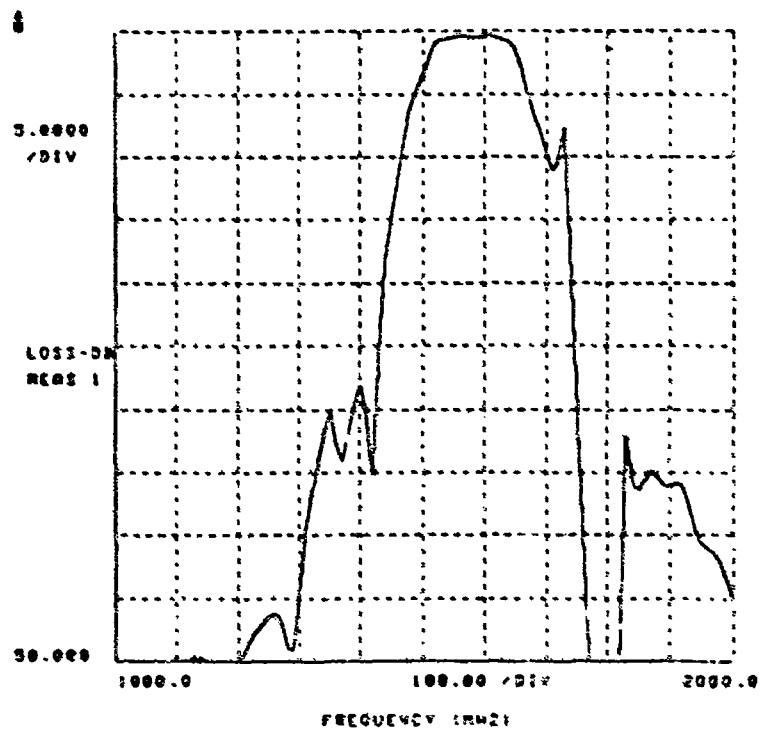


Figure 88. Triplexer Loss Plot, Port 1 to Port 4

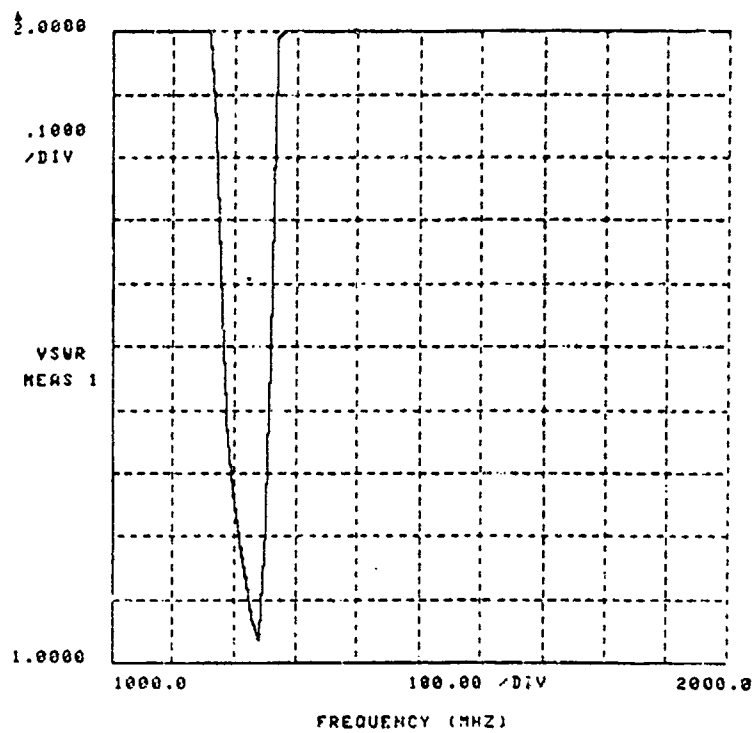


Figure 89. Triplexer VSWR Plot, Port 2 to Port 4

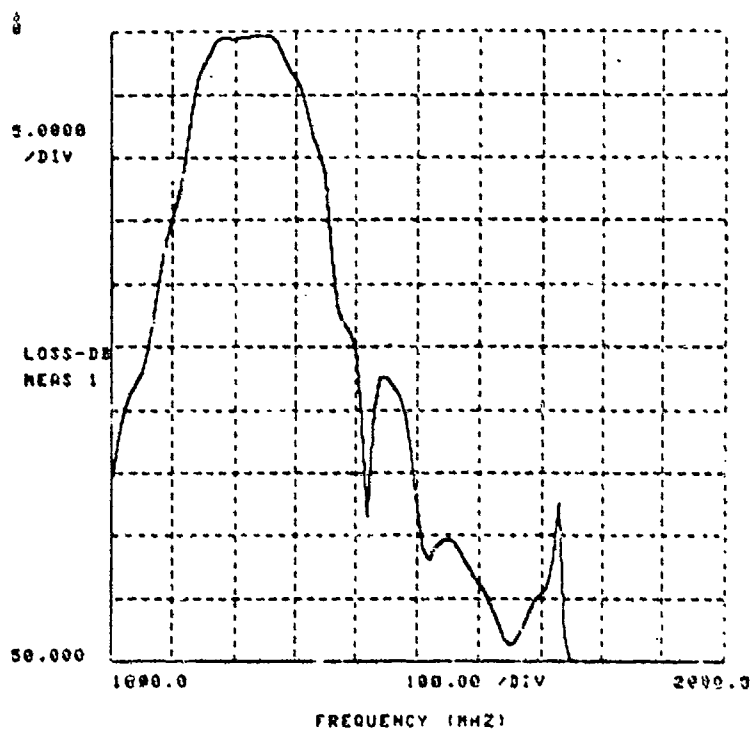


Figure 90. Triplexer Loss Plot, Port 2 to Port 4

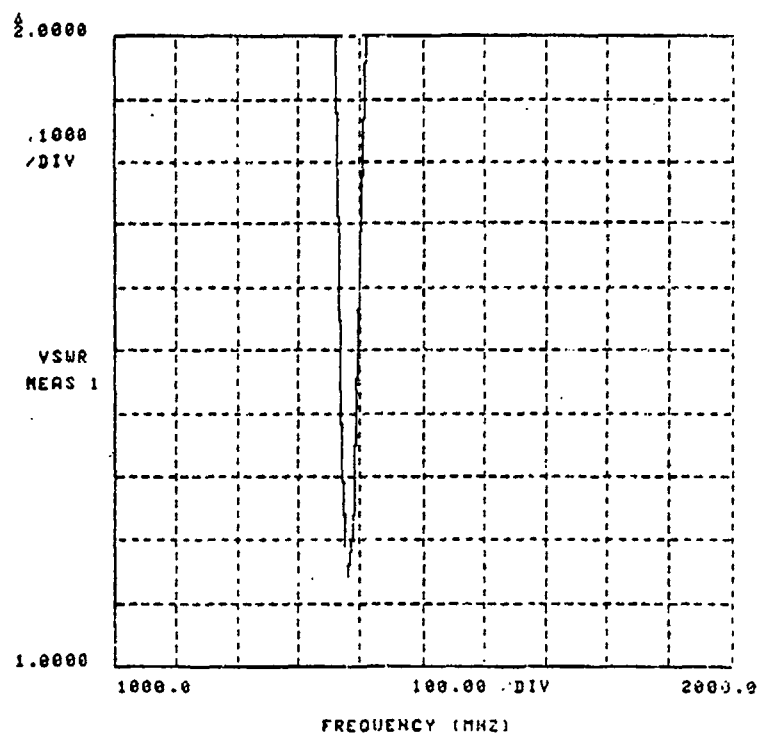


Figure 91. Triplexer VSWR Plot, Port 3 to Port 4

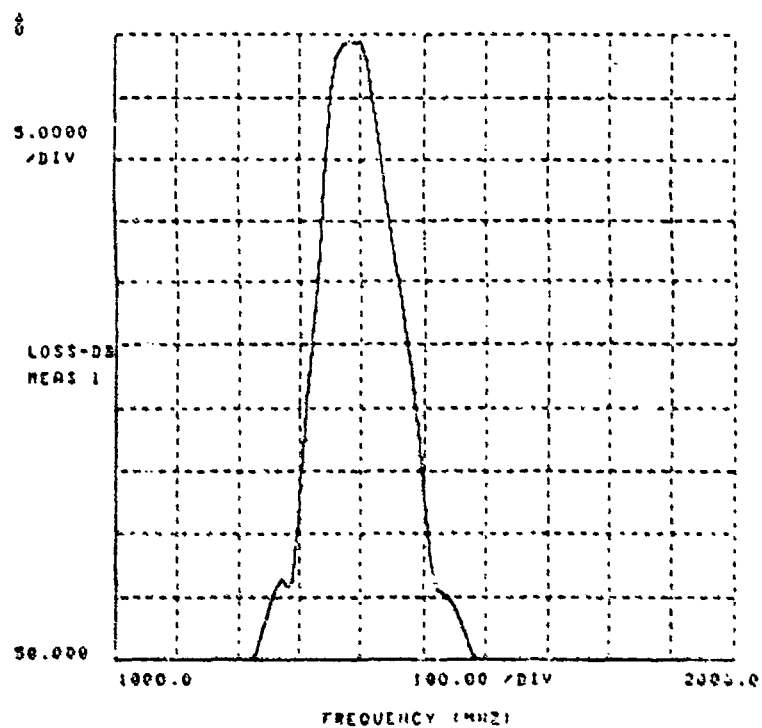


Figure 92. Triplexer Loss Plot, Port 3 to Port 4

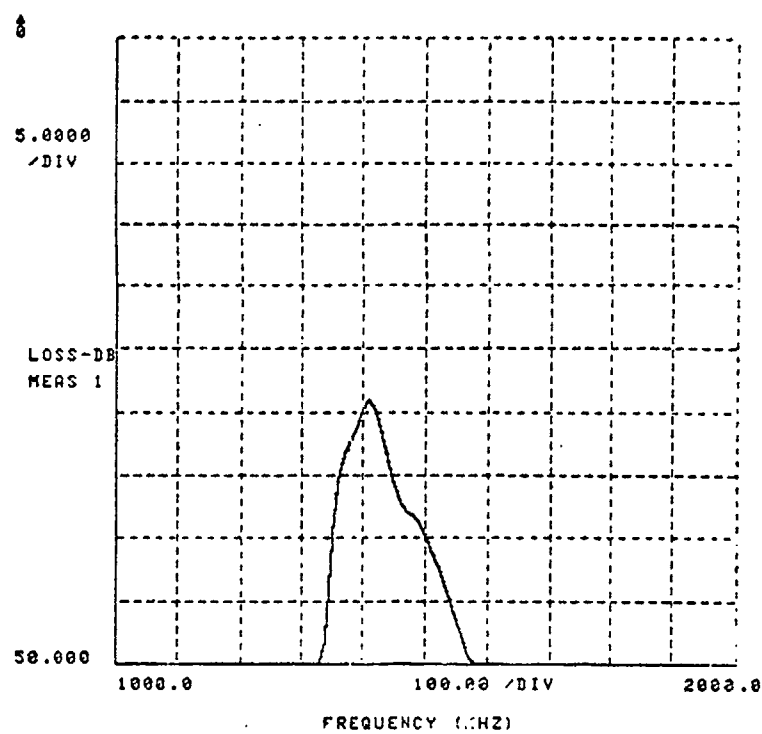


Figure 93. Triplexer Loss Plot, Port 3 to Port 1

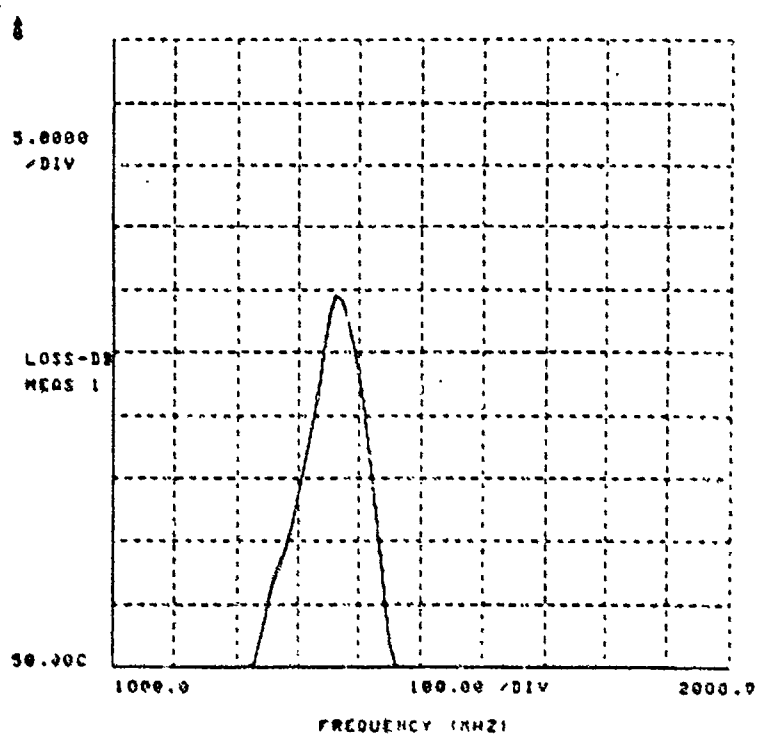


Figure 94. Triplexer Loss Plot, Port 3 to Port 2

At Port 2, the energy from Port 3 at the L₂ frequency of 1227.6 MHz also is down about 45 dB. The peak off-frequency energy is down more than 20 dB. The L₃ frequency of 1381 MHz in Port 1 is down about 35 dB and in Port 2 is down about 25 dB.

The data indicate that the triplexer design will meet all operational requirements and will support the L₃ frequency on a noninterfering basis with operation of the GPS L₁ and L₂ channels.

6.3 L₃ SUBSYSTEM TESTS

The L₃ transmitter and encoder have been subjected to design and development tests, engineering model tests, and functional tests. The design and development test procedures for the L₃ transmitter and encoder are summarized in Figure 95. The tests, which were performed on the L₃ transmitter and encoder engineering models, are listed in sequence in Figure 96. Functional testing of the L₃ transmitter and encoder encompassed the methods summarized in Table 27. The test parameter acceptance levels achieved for the L₃ transmitter are listed in Table 28, and the acceptance levels achieved for the encoder are listed in Table 29. The environmental test conditions for the L₃ transmitter and encoder are summarized in Table 30.

6.3.1 L₃ Transmitter Tests

The L₃ transmitter consists of a frequency synthesizer, modulator, IPA, and HPA. A detailed breakdown of each component's characteristics, including L₁ and L₂ transmitters, is listed in Table 31. The L₁ and L₂ transmitters were included with the L₃ transmitter characteristics because they provide a good comparison in the areas of design and performance. This comparison is of interest because (1) the L₃ output transistor (TRW 1417-11) is the same as the HPA for L₁ and L₂, (2) the basic amplifier design is the same, (3) the transmitters operate in the same frequency range, and (4) L₃ performs the same function as the L₁ or L₂ transmitters. As can be seen, the L₃ transmitters tested meet the design specifications for input power, weight, and volume.

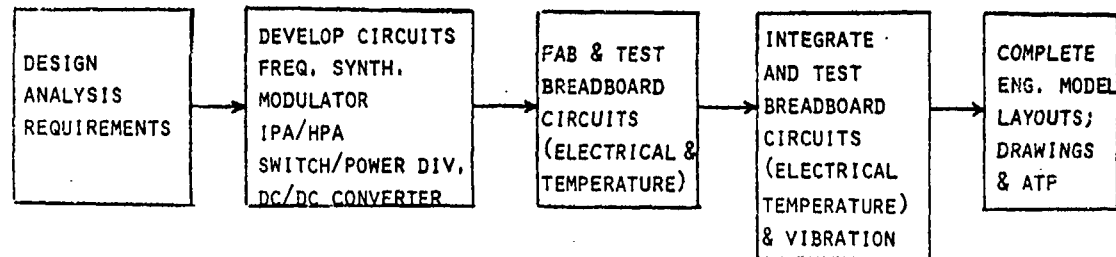
The selection of the TRW 1417-11 output transistor for the L₃ transmitter was based on power consumption tests such as those summarized in Table 32. The L₃ TRW 1417-11 transistor was packed in a more efficient thermal design which resulted in the data listed in Table 33. Transistor junction temperature has an adverse effect on reliability and power output as indicated in Figures 97 and 98. The L₃ transmitter power loss distribution as measured on the prototype unit is illustrated in Figure 99.

The output of the L₃ HPA is fed through a bandpass filter. Characteristics of this filter were measured and are shown in Figure 100.

6.3.2 Encoder Tests

The encoder breadboard test setup and tests are summarized in Figure 101. The encoder squaring amplifier was verified as illustrated in Figure 102.

• L₃ TRANSMITTER



• L₃ ENCODER

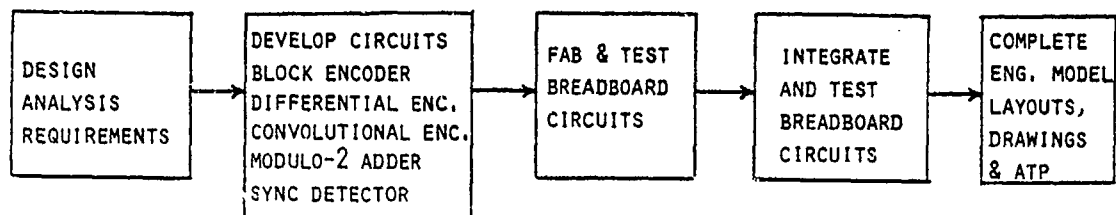
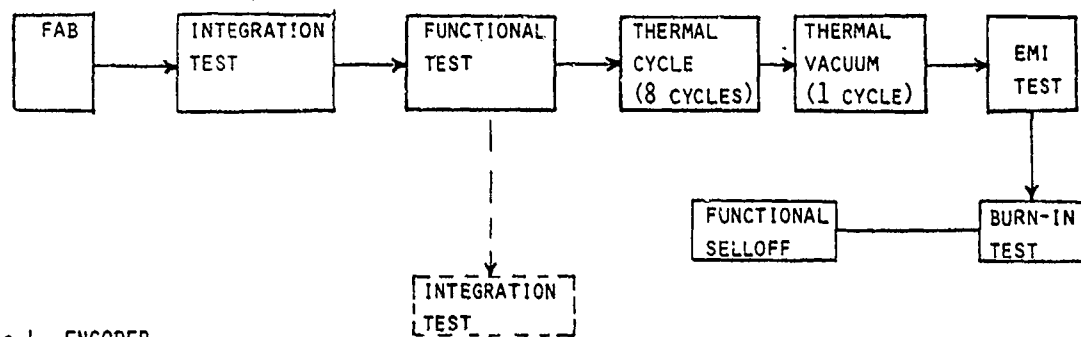


Figure 95. L₃ Transmitter and Encoder Development Procedure

• L₃ TRANSMITTER



• L₃ ENCODER

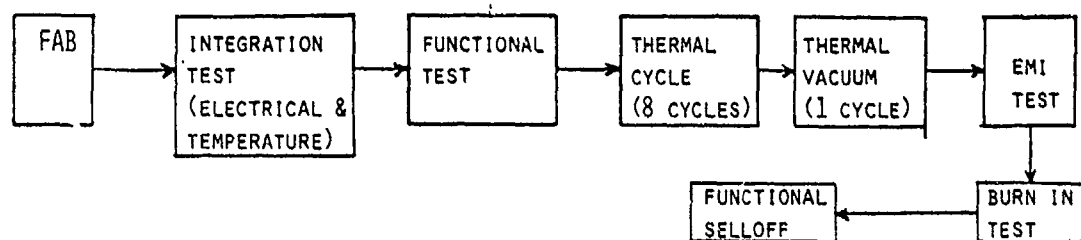


Figure 96. L₃ Transmitter and Encoder Engineering Model Test Summary

Table 27. L₃ Transmitter and Encoder Functional Testing

Test	Method	Assy	Thermal Cycling	Thermal Vacuum
L ₃ Transmitter				
1. Dc input power	Current through resistor	X	X	X
2. RF output power	Thermistor mount and power meter	X	X	X
3. RF output frequency	Counter	X	X	X
4. RF spurious output	Spectrum analyzer	X	X	X
5. VSWR output	Network analyzer	X		
6. Power monitor	Digital voltmeter	X	X	X
7. Modulation output	Receiver	X	X	X
8. Phase noise	Phase-locked loop	X		
L ₃ Encoder				
1. Encoding/decoding	Pattern generator decoder & Linkabit LV 7015	X	X	X

Table 28. L₃ Transmitter Functional Test Parameters

Test	Acceptance Level
Dc input power	76 watts max
RF output power	11.8 dBW min, 13.8 dBW max
RF output frequency	1381.05 MHz
RF spurious output	≥ 50 dBc at $F_0 \pm 50$ MHz ≥ 65 dBc at 1783 MHz
Output VSWR	1.2:1.0 max
Power monitor output	0 to 40 mVdc
Output modulation	
Phase deviation	$\pm 3^\circ$ max
Rise time	≤ 9 ns
Fall time	≤ 9 ns
Mod rate	10.23 mb/s
Phase noise	≤ 100 m radians in a 10 Hz band from 2-12 Hz

Table 29. L₃ Encoder Test Parameters

Test	Acceptance Level
Dc input power	3 watts max
P + data output	
Rise time	≤9 ns
Fall time	≤9 ns
Mod rate	10.23 mb/s
Logic level	TTL at 50 ohms
TT&C monitor	TTL at 300 K ohms

Table 30. Environmental Test Conditions - Transmitter and Encoder

Test	Performance Levels
Thermal cycle (8 cycles) 1 cycle	<ul style="list-style-type: none"> • Start at amb, with component operating monitor critical parameters* • Decrease temp to -24°C, stabilize, functional test, and soak two hours • Increase temp to +61°C on-off cycling unit, stabilize, functional test, and soak two hours • Decrease to ambient on-off cycling unit
Thermal vacuum (1 cycle)	<ul style="list-style-type: none"> • Start at ambient with component operating, monitor critical parameters* • Decrease temperature to -24°C and pressure to 1.38×10^{-3} N/m², monitor for multipacting, soak 30 min off cold start, functional test and soak 12 hours • Increase temp to 61°C, soak 30 min off hot start, functional test and soak 12 hours • Decrease temp and pressure to room ambient
EMI	<ul style="list-style-type: none"> • Test per MIL-STD-1541 for CE01, CE02, RE02 (E&A), CS02, CS06, RS02, RS03, static discharge, CE03, CE04, RE03, and CS01
Burn-in	<ul style="list-style-type: none"> • Operate monitoring critical parameters* for (test hours + thermal vacuum hours + EMI hours + burn-in hours = 300 hours)
*Critical parameters: L ₃ transmitter - prime power, frequency, power output L ₃ encoder - sync detector output	

Table 31. GPS and IGS Transmitter Characteristics

Units	Dc Power (watts)		Weight (lb)		Volume (in. ³)	
	Spec	Measured	Spec	Measured	Spec	Measured
L ₁ HPA	125.00	139.9	23.25	25.7	422.0	726.0
L ₁ MOD/IPA	2.10	2.8	3.34	3.0	85.9	
L ₁ synthesizer	4.80	3.9	3.90	3.9	117.0	
L ₁ HPA filter	.75	(.75)	2.54	2.5	42.8	
Dc/dc converter	3.50	3.9	3.00	3.5	58.3	
Total	137.60	150.50	36.00	38.6	726.0	
L ₂ HPA	25.70	28.40	3.87	3.8	65.0	306.2
L ₂ MOD/IPA	0.90	1.10	1.89	1.9	47.8	
L ₂ synthesizer	4.80	3.90	3.90	3.90	117.0	
L ₂ HPA filter	.56	(.56)	1.50	1.50	33.1	
Dc/dc converter	2.70	2.94	2.40	2.60	43.3	
Total	34.66	36.34	13.56	13.70	306.2	
Incremental HPA		75.5				220.0
L ₃ HPA	73	42.0			32.8	
L ₃ MOD/IPA		4.6				
L ₃ synthesizer		1.2				
Dc/dc converter		21.7			77.2	
Total	73	69.5	12.8	11.6	220.0	

Table 32. HPA Output Transistor Power Consumption

Transistor Type	V _{cc} (volts)	P _o (watts)	P _{dc} (watts)	N _c (%)
MSC 2010	20	9.9	19.6	51
MSC 1315	20	10.5	17.6	59
TRW 1417-11	20	10.5	15.6	66
TRW 2010	18	11.5	18.9	60.8
TRW 2010	16	10.0	16.96	58.9
TRW special	20	11.5	19.4	58.9

P_{in} = 2W, frequency = 1381.05 MHz

6.3.3 BPSK Modulator

The BPSK prototype modulator was tested to verify compliance to specified parameter characteristics. The summary of these test data is presented in Table 34.

6.4 IGS SYSTEM TESTS

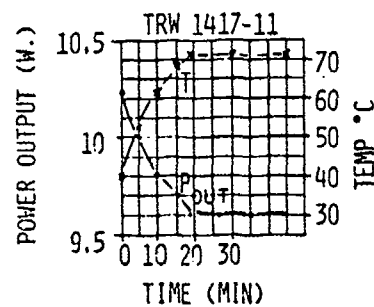
6.4.1 Engineering Data Compatibility (EDC) Tests

The objective of this series of tests was to demonstrate the functional compatibility between the baseband/processor, the BDP, and the L₃ encoder.

Table 33. Thermal Design Analysis for Transistor TRW-1417-11*

Characteristics	L ₁	L ₂	L ₃
Dc power input (Watts)	27.6	21.0	17.3
RF power input (Watts)	2.2	2.0	2.0
RF power output (Watts)	15.15	11.6	10.8
Dissipate power (Watts)	14.65	11.4	9.5
Junction temperature (°C)			
(Due to thermal resistance)	65.92	51.3	42.66
(Due to device case to chassis base)	7.3	5.7	4.74
Local heating (°C)	7.0	7.0	7.0
Junction temperature (°C)			
(At base plate 52°C)	132.2	116.0	106.4
*Output stage for L ₁ , L ₂ , L ₃ (L ₃ uses non-hermetic package) Thermal resistance 4.5°C/W			

TRANSISTOR TEMPERATURE TEST



TURNED ON FAN TO KEEP TEMPERATURE
AT 71°C

SMALL FAN WAS APPROXIMATELY 3 FT
AWAY FROM TRANSISTOR. P_{OUT} AND T
REMAINED CONSTANT WITH FAN ON.

FAN OFF

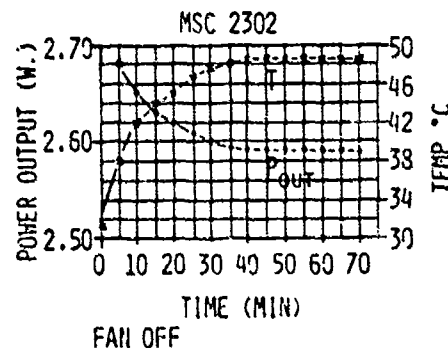


Figure 97. Prototype Circuit Data

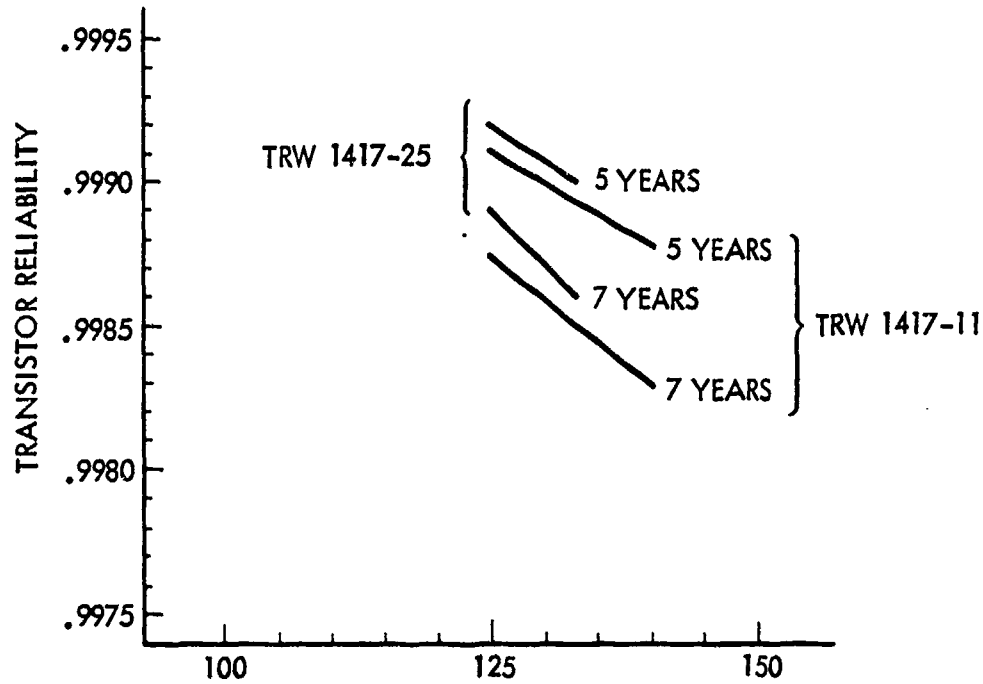


Figure 98. Junction Temperature

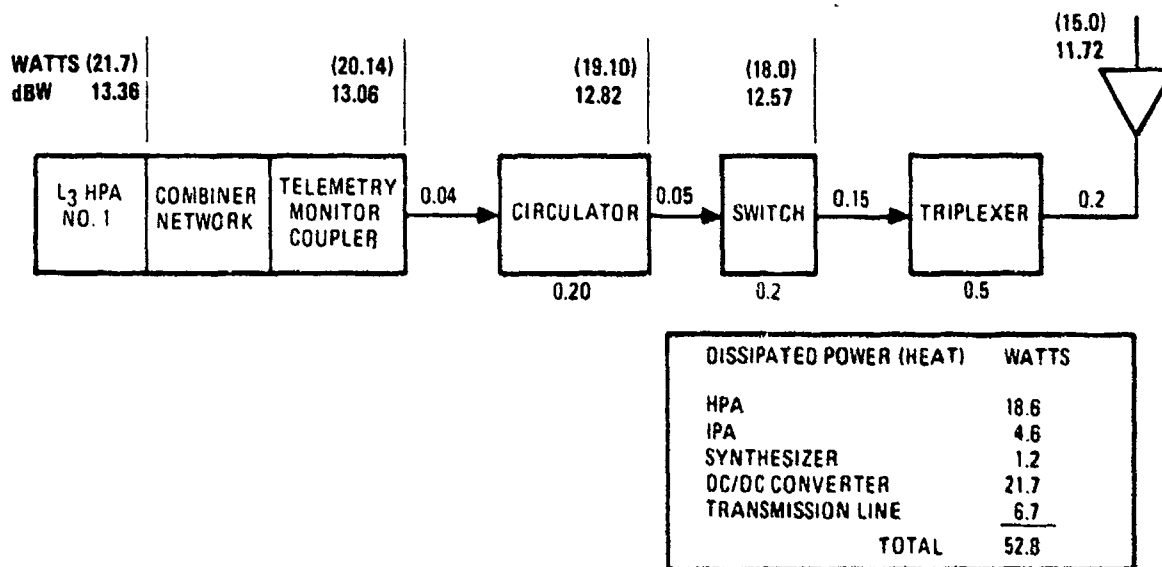


Figure 99. L3 Transmitter Power Loss Distribution

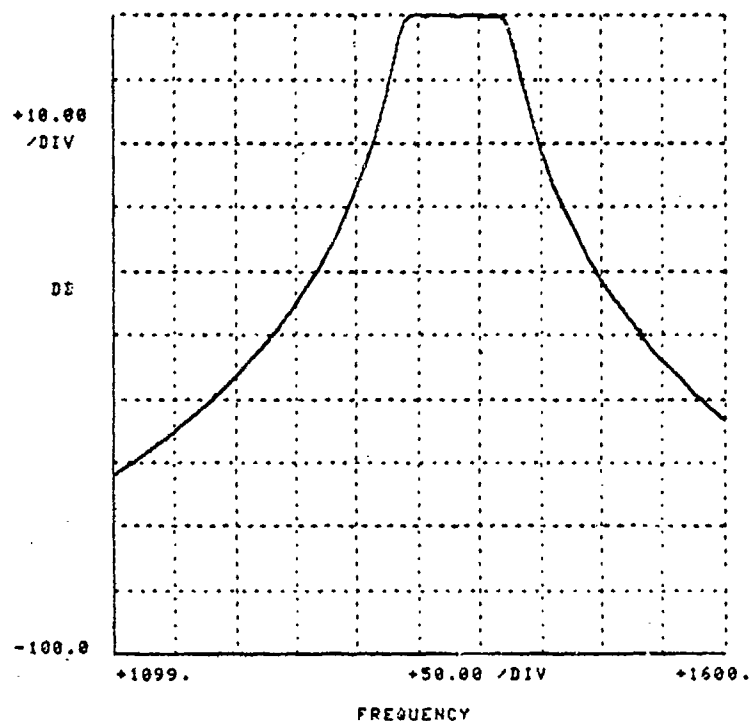


Figure 100. 1381-MHz Filter Response

Testing is summarized in this section and documented in detail in Rockwell report SD 78-GP-0012-1.

6.4.1.1 Configuration. The test configuration consisted of the major IGS components combined in a bench test setup. The components included the baseband/processor, the global burst detector processor, the L3 encoder, and the timing interface (TI) box. Before the components were assembled for the engineering data compatibility (EDC) testing, each of the components was individually checked for signal compatibility. Figures 103, 104, 105, and 106 illustrate these readiness tests. Figure 107 shows the complete EDC test configuration.

6.4.1.2 Test Results. This testing included compatibility of all engineering data. All test objectives were met by demonstrating that the data components of the IGS were electrically compatible.

6.4.2 IGS Component Integration (ICI) Tests

The ICI test was conducted on components developed for IGS in a subsystem configuration to achieve the following objectives:

- Demonstrate compatibility between IGS components when operated in a total subsystem configuration. (Refer to SD 78-GP-0010)
- Measure subsystem turn-on and turn-off characteristics.

1. SQUARING AMPLIFIER TESTED FOR OPERATION BETWEEN -20°C TO $+65^{\circ}\text{C}$ ENVIRONMENT WITH A -3.8 ± 1.4 dBm INPUT.
2. POWER DIVIDER MAY BE SHORTED OR +5 VDC APPLIED AT EITHER INPUT WITHOUT AFFECTING OPERATION OF OPPOSITE OUTPUT PORT (25 DB ISOLATION)

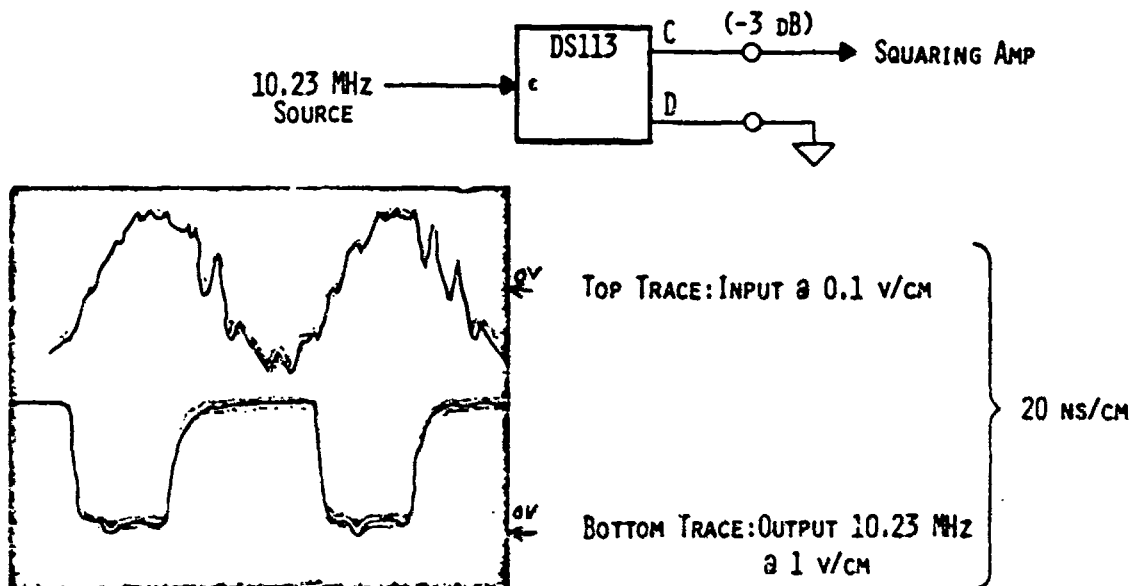


Figure 102. Breadboard Tests - Squaring Amplifier

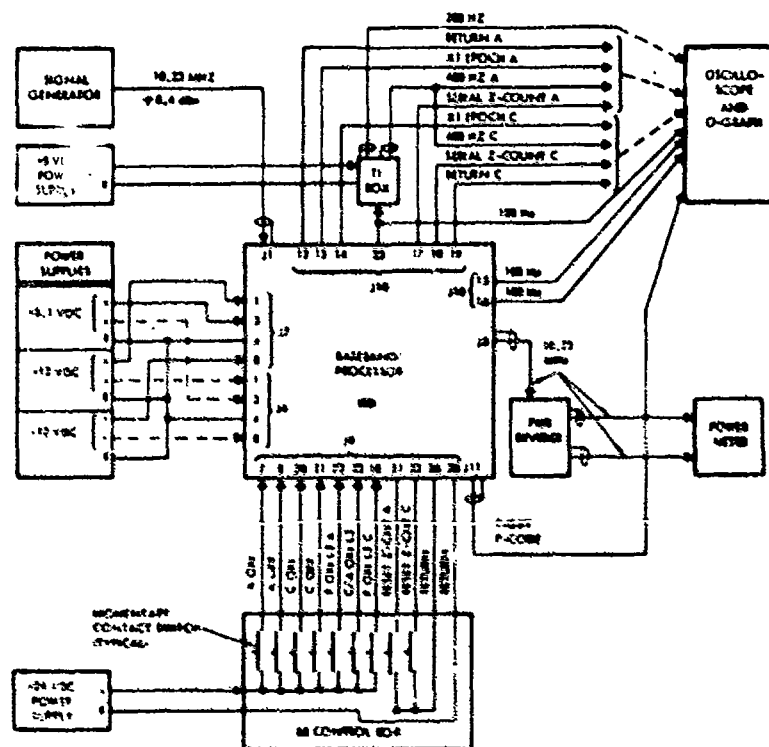


Figure 103. Baseband Processor Readiness Test

Table 34. BPSK Modulator Prototype Test Data

Parameter	Test Data	Specification
VSWR	1.2:1	None
Insertion loss	1.1 dB	None
Phase deviation	$\pm 0.5^\circ$	$\pm 3^\circ$
Rise time	6 ns	≤ 9 ns
Fall time	5 ns	≤ 9 ns
Modulation rate	10.23 MHz	10.23 MHz

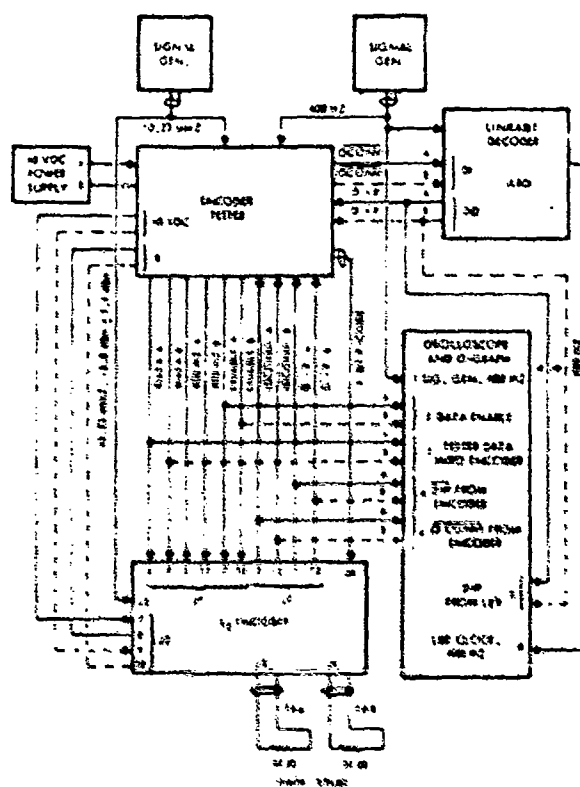


Figure 104. Encoder Readiness Test

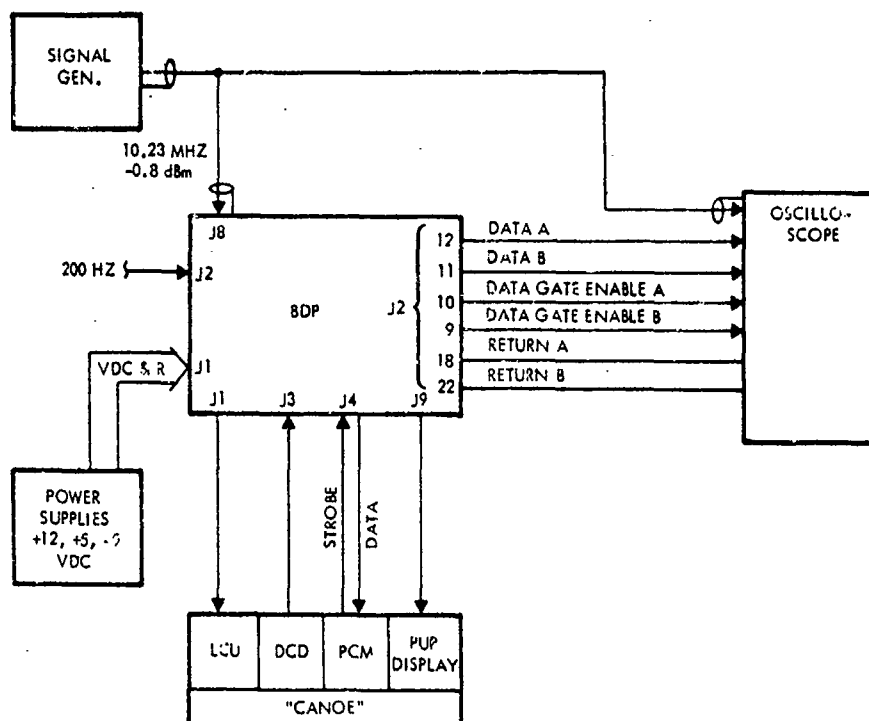


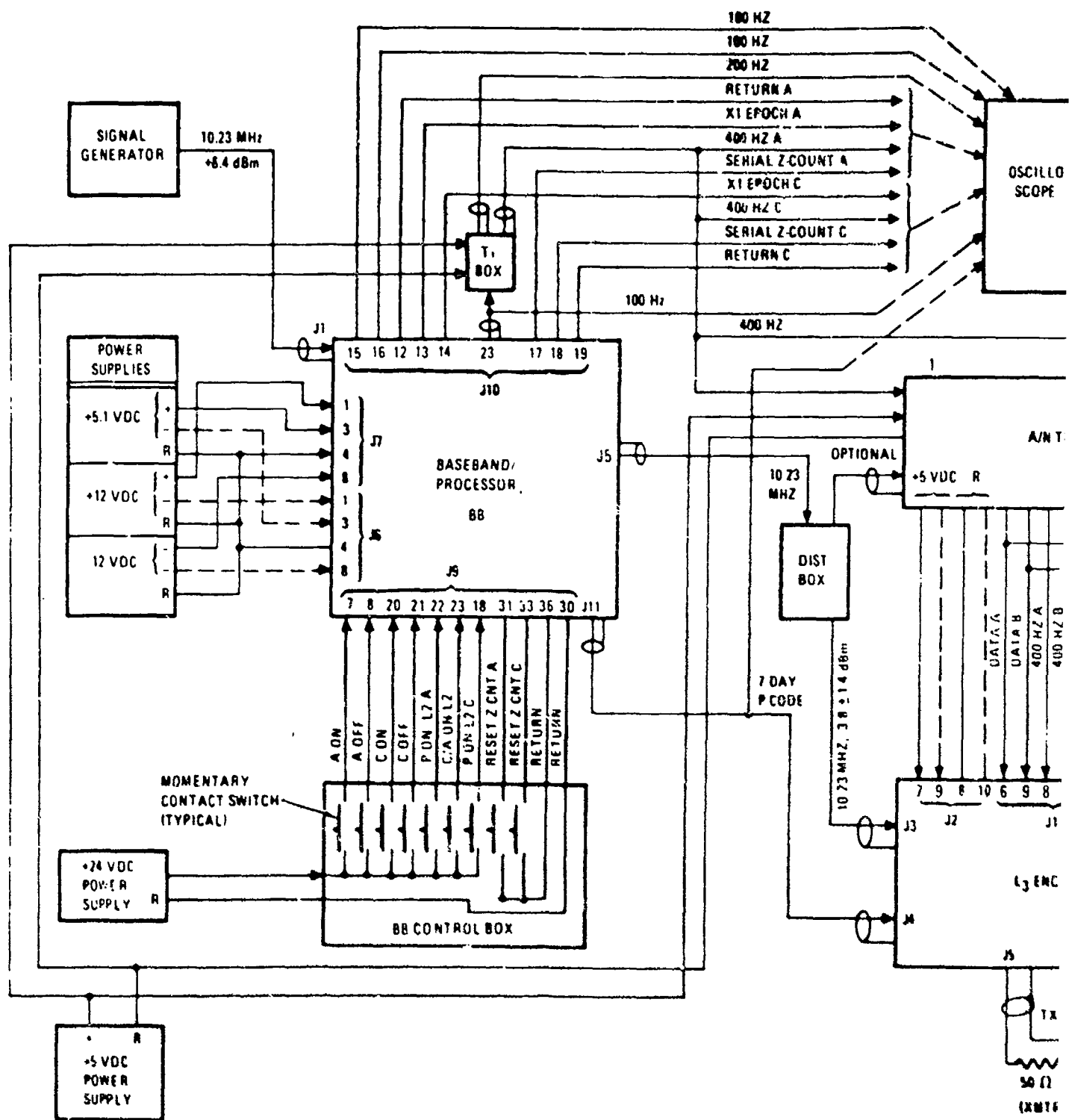
Figure 105. BDP Readiness Test

- Verify subsystem readiness to support GPS/IGS signal compatibility, functional compatibility, and EMC test. (Refer to SD 77-GP-0046)
- Obtain component and subsystem baseline data to support tests to follow in the space vehicle configuration.

6.4.2.1 Test Configuration Description.

Pre-Signal Compatibility. The ICI block diagram configuration is shown in Figure 108. Figures 109 and 110 are photographs of the physical configuration. The 9W2 harness was diverted to the buildup of the ETV for signal compatibility and was unavailable for ICI. The laboratory-type barrier terminal strips, shown in the photographs, were used throughout ICI testing in place of the vehicle terminal blocks because compact blocks would have prevented the insertion of test equipment. With key vehicle wiring not available, test boxes were used to control the L3 components and the baseband/processor. The BDP and sensors were checked out in place by using the Sandia CANOE (test set), Figure 111, but could not be interfaced with the L3 equipment.

Post-Signal Compatibility Test. After the signal compatibility test, the forward bulkhead and antennas were removed from the ETV, and mounting holes were provided for the redundant transmitter and for the BDP. Harnesses and equipment were added. Without the GPS clear/acquisition (C/A) signal on L1, it had been intended to utilize a nonstandard configuration on L3 of both C/A and P codes to allow the test receiver a means of signal acquisition. This acquisition was successfully accomplished in a test just prior to breakdown for signal



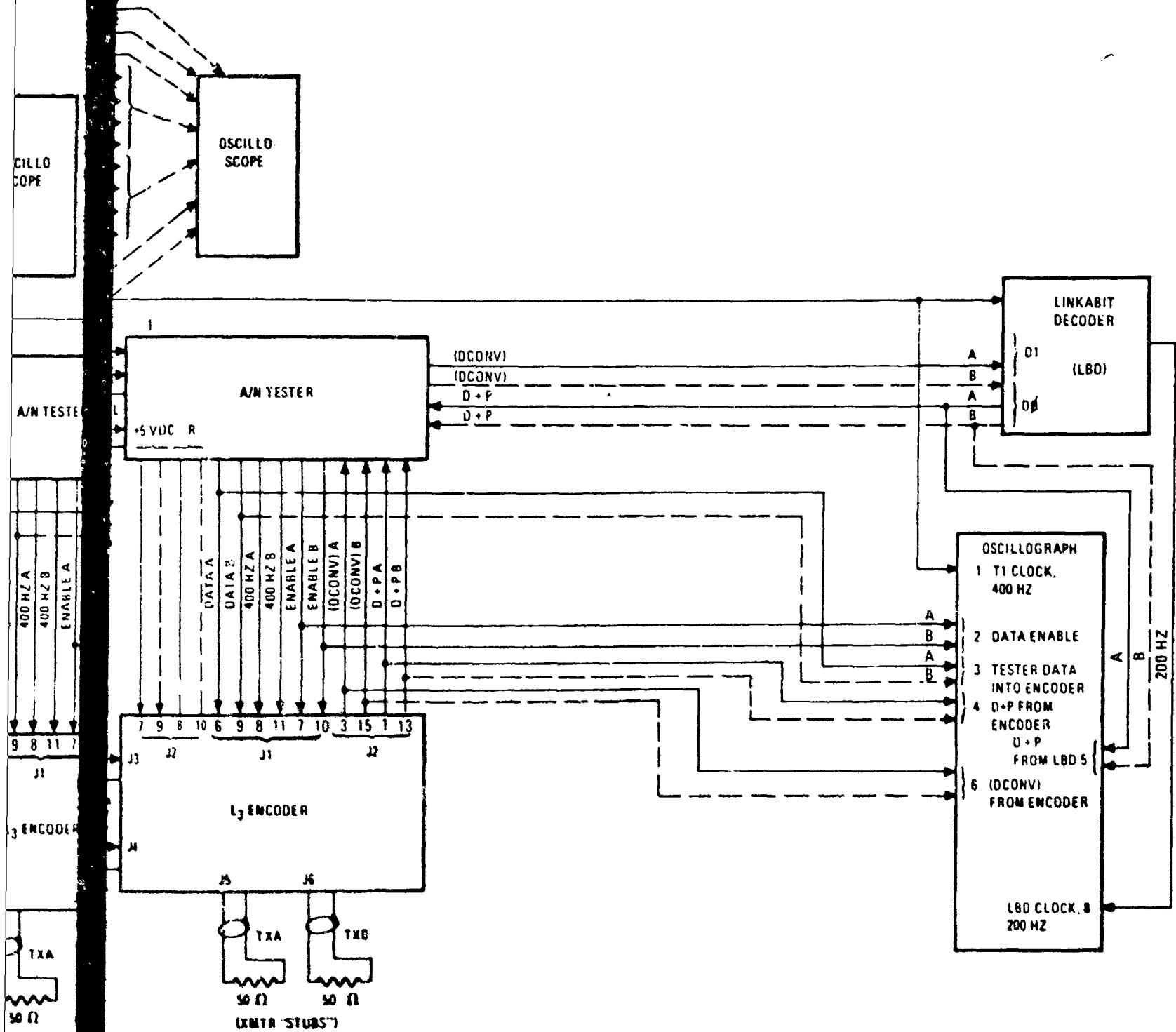
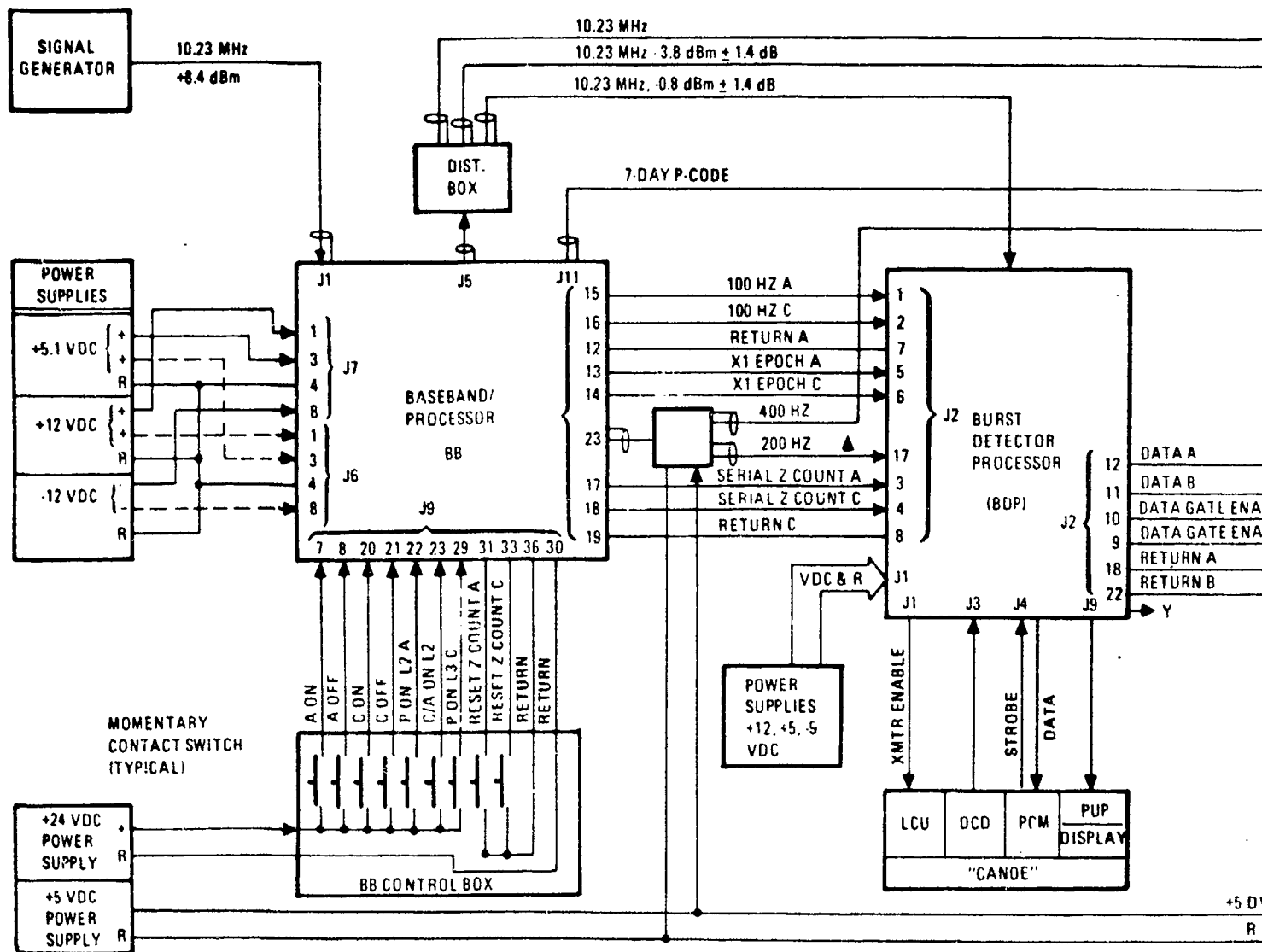


Figure 106. Baseband/Encoder Readiness Test

PRECEDING PAGE BLANK-NOT FILMED



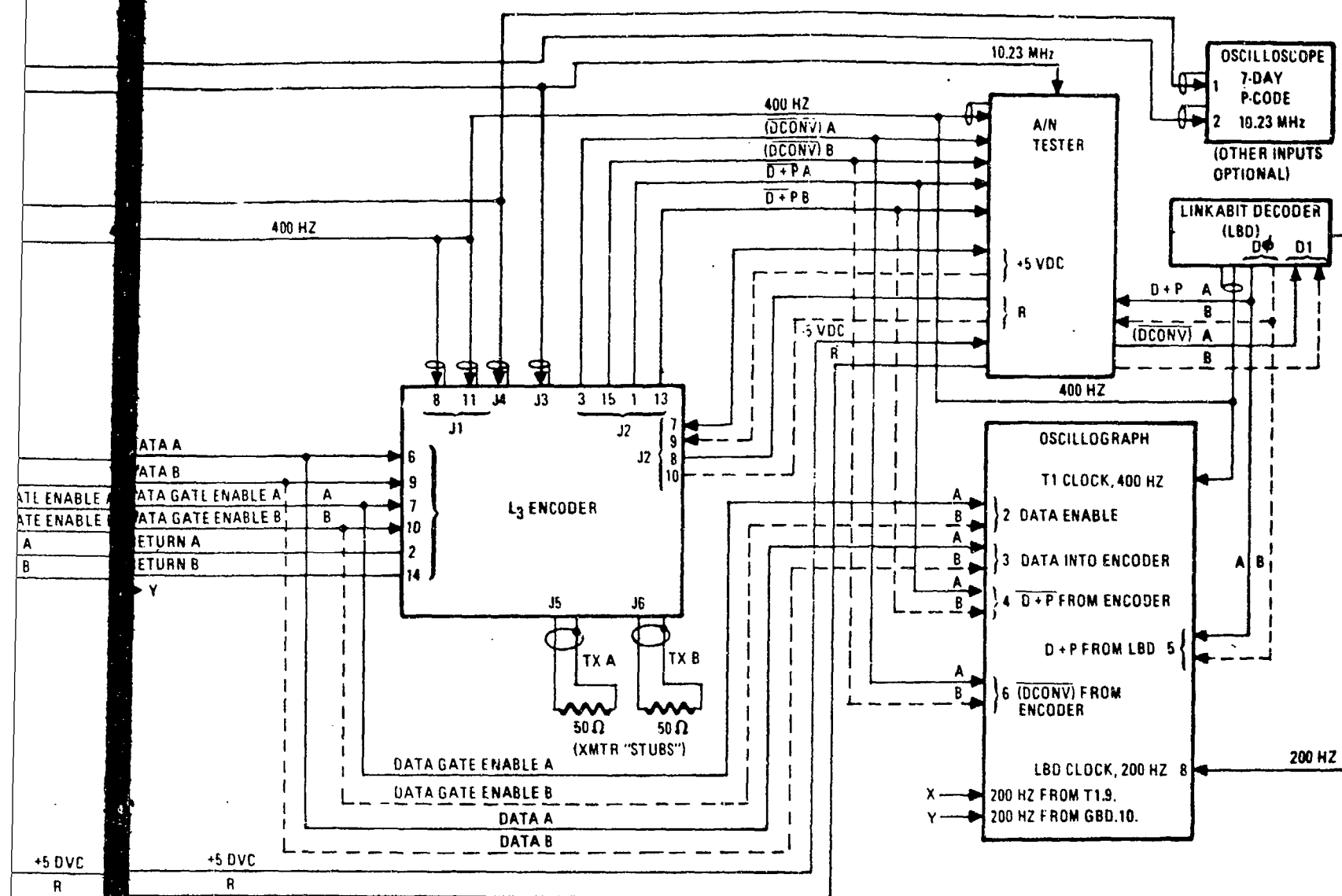


Figure 107. EDC Overall Test Configuration

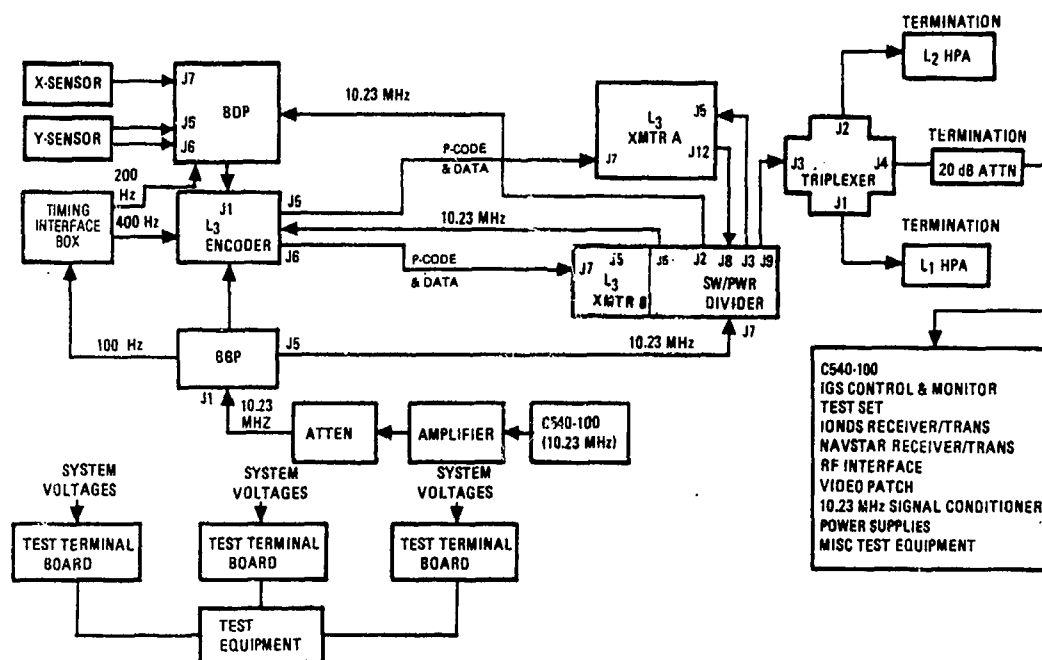


Figure 108. Block Diagram - Final ICI

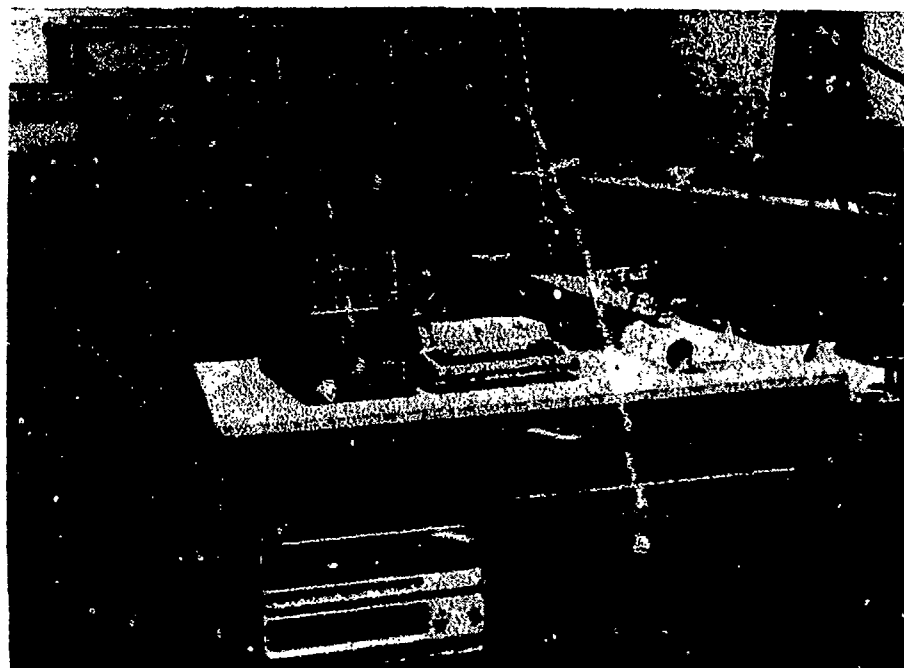


Figure 109. ICI Overall Test Setup



Figure 110. Final ICI ETV Configuration

compatibility and was performed with increasing difficulty during the initial setup in the ETV configuration. A brief trouble-shooting effort, after the difficulty progressed to total failure to lock, pointed out the disadvantage of off-design operation, and the L_1 signal was used from the test receiver system (test transmitter). Mechanical switches provided sufficient contact bounce to guarantee lack of synchronization (and therefore no handover to L_3) when used to reset the basebands. Equipment was added to synchronize the baseband and the test set.

The equipment evaluated in the ICI tests consisted of the following:

- L_3 Transmitter A
- L_3 Transmitter B with RF switch and distribution
- L_3 encoder
- Triplexer
- Baseband/processor
- BDP
- X-sensor
- Y-sensor

All units were IGS engineering models.

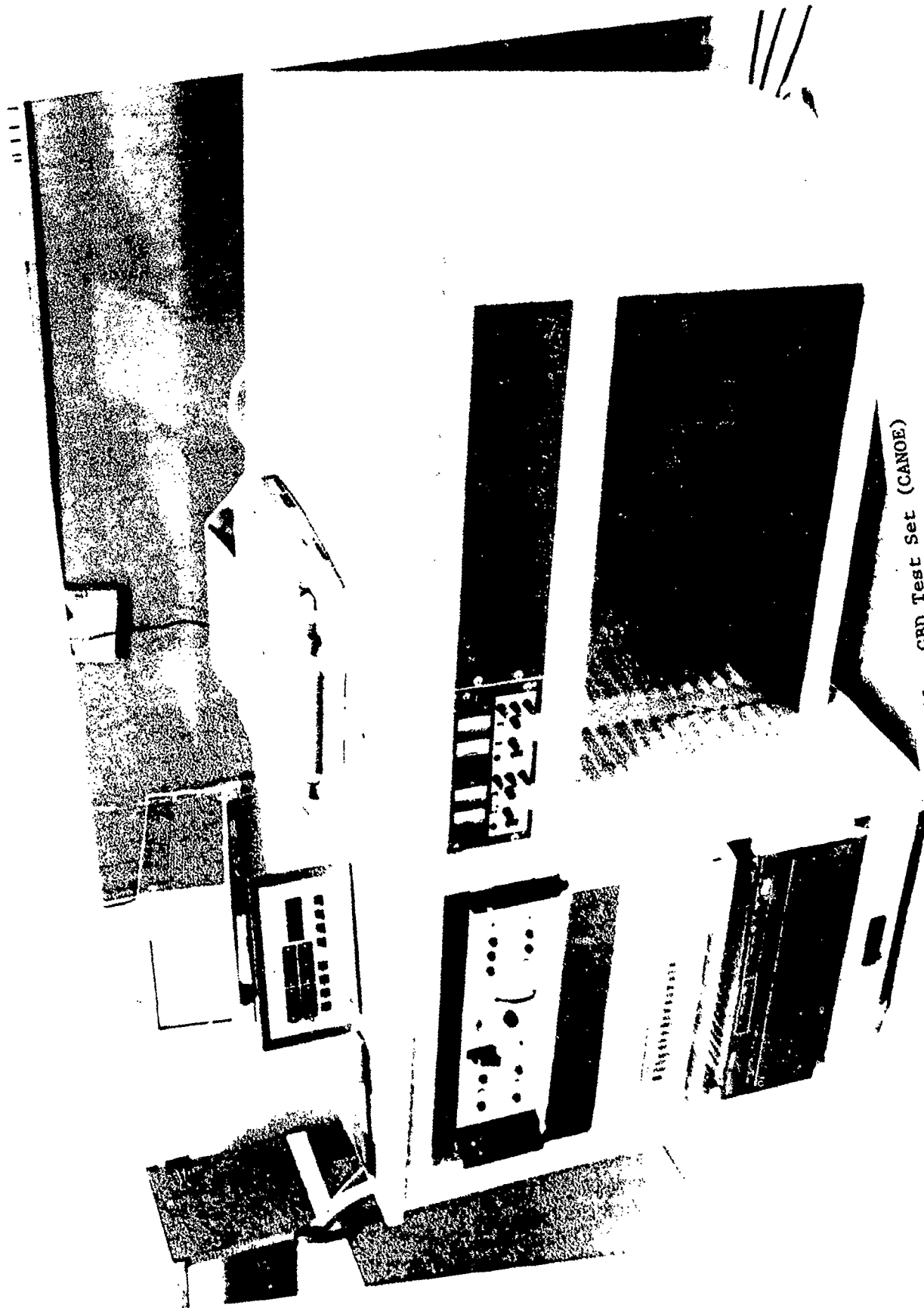


Figure 111. GBD Test Set (CANOE)

The IGS load control unit and vehicle harnesses were also in test, although not identified as primary test items. The test also included the use of the ETV frame as built up for the signal compatibility test, but without side panels, forward bulkhead, and antennas.

Items omitted from the test as originally planned include the breadboard rubidium frequency standard and items of wire harness (primarily harnesses for interfacing terminal strips with PCM, DCD, and signal conditioner equipment).

The B transmitter exhibited slightly higher harmonic output than the A transmitter. In addition, the B transmitter exhibited occasional delay in coming up to normal power output near the end of ICI testing.

Timing Interface (TI) Box. The TI box was found to exhibit overshoot and ringing characteristics when interfaced with the BDP circuit. An external 90-ohm or 50-ohm load reduced the overshoot and ringing effects and provided a usable waveform. The unit is to be deleted in future equipment where the function will be incorporated into a flight design TIE assembly.

Baseband/Processor. The baseband/processor modified for IGS tests includes an internal A string and a C string (B was replaced with IGS circuitry). The 100-Hz IGS A output driver failed between the initial and final ICI setup. Tests were all performed using the C string. A subsequent engineering test utilizing an external 100-Hz did not show differences in signals produced by using the A string.

C540-100, IGS Test Set. The stability of the IONDS test receiver system exhibited considerable variation during testing, due to problems with RF interference from other tests in the facility and apparent high sensitivity to noise on ac power lines. It should be noted that the receiver used was IONDS No. 1, which served in the interim until the full IONDS receiver was delivered. Other known anomalies existing in the Navstar receiver (required to operate IONDS No. 1 receiver) did not affect IONDS operation.

6.4.3 ICI System Testing

Overall IGS component compatibility was demonstrated by successful end-to-end operation. Calibration signals developed in the GBD sensors were processed by the BDP, encoded and transmitted by the L3 equipment operating under control of the BDP, received and demodulated by the test receiver, and the data verified by the GBD test console (CANOE). Redundant channels were verified with the exception of the baseband/processor A string, which contained a failed 100-Hz output driver. The A side was operated using 100-Hz supplied by the BDP, and no difference was noted between A and C baseband output signals (other than the missing 100-Hz output).

A basic discrepancy was found in the interfaces between the inputs to the BDP and the output circuits of the baseband/processor and the timing interface box. The TI box, constructed to supply an interface for test purposes in lieu of circuits not yet incorporated into the IGS hardware, did not provide a suitable output impedance to match the 1000-ohm series resistance required by the ICD on the BDP inputs. The overshoot and ringing on the 200 Hz to the BDP

caused incorrect operation. External loads of 50 to 110 ohms corrected the output to a usable signal. However, the amplitude of the signal was below the ICD value. Approximately 1 microsecond of leading and trailing edge ringing was measured on the X1 epoch line from the baseband to the BDP. No anomalies were noted while operating with the loaded 200 Hz nor were any detected that were due to the X1 epoch ringing, but the flight configuration interfaces, including the cable impedance, must be positively controlled for final hardware designs. The X1 epoch ringing may have been in the test leads and breakout access any may not be inherent in the system; however, the observation still emphasizes the need for tight control of these signal interfaces.

6.4.3.1 Subsystem Turn-on and Turn-off Characteristics. The turn-on and turn-off characteristics were measured by using a Honeywell 1612 Visicorder with 8-kHz response channels. The results show no characteristics which would preclude further system tests. Main bus, L3 transmitter, and BDP currents and voltages were monitored as well as commands and the data enable signal from the BDP test connector and from the IONDS receiver output. Runs were made at 40 inches per second during operational cycles with each string of BDP/L3 chain operating and with the BDP and L3 chains cross-strapped.

Discrete command signals exhibited slight ringing characteristics, which were attributed to the long leads required to the recorder and which would not be detrimental to system operation. The main bus exhibited a drop of about 5 volts approximately 8 milliseconds after the "L3 on" command was initiated by the BDP coincident with application of L3 power on. The drop was accompanied by some ringing and required approximately 25 milliseconds to recover. The bus drop was also reflected as a drop in the command pulse level. This characteristic did not affect ICI subsystem operation but would not be acceptable for a flight bus, since the transient exceeds the bus specification to which equipment is tested.

The bus regulator in this case is dependent on the regulations of the power supply in the C540-100. A flight bus would be regulated by the power control unit (PCU) in the vehicle. The power supply has been returned for calibration and adjustment. It should also be noted that later tests will have additional loads on the supply, which is expected to improve regulation.

The only other unexpected results consisted of activity on the BDP L3 on and off lines during BDP initialization. Sandia advised that these outputs are a function of initialization software only and have no effect on normal operation of the subsystem.

Although detailed EMI tests were performed on L3 components during acceptance and engineering laboratory testing, a survey was performed on the overall ICI configuration. Current probes were used on power lines to check for excessive steady-state signals below 50 MHz. The oscillograph records were checked within their limitations of approximately 6 kHz.

Radio frequency (RF) emission was checked using EMI probes (broadband antennas) with Airborne Instrument Lab (AIL) and Hewlett Packard spectrum analyzers. The ranges observed were from 10 MHz to 10 GHz. Due to the open configuration of the laboratory, numerous RF signals were observed in almost all frequency ranges. The test was performed by observing the spectrum over a given

range of the analyzer with the test setup off, and then operating the IGS through a cycle of the BDP going active, turning the L₃ equipment on, transmitting data, and then turning the L₃ off. The spectrum was monitored for any changes during this cycle. The checks were performed with both A and B strings, as well as with cross-strap operations.

Although several repeat operations were required because of the method of operation, the majority of spectrum changes noted were due to changes in the ambient RF environment. Signals were observed at approximately 150 MHz and at a level of -90 dBm which was determined to be from the CANOE test set when it was operating the BDP. The signals were isolated to the CANOE by observing that they were present when the CANOE was operated with the IGS equipment off. Also, an increase in level was noted when the probe was moved away from the ETV and turned to the CANOE. Signals at the fundamental operating frequency of 1381.05 MHz were noted. However, these were expected under the open operating conditions of the ICI test, with the RF loads and test consoles in the same room with the equipment under test. Second and third harmonic signals were also detectable when using the B transmitter. Again, these were consistent with data from the transmitter tests.

No signals were detected which would preclude proceeding with the vehicle-level EMI testing. Although the environment of the ICI test precludes accurate EMI measurements, any problems which may have been masked by the background and which show up during formal vehicle tests should be at a level which can be controlled by wire routing and/or additional shielding of cable segments. This type of correction could be made at the time of the vehicle-level test without requiring equipment redesign.

6.4.3.2 Component and Subsystem Baseline Data. The data obtained during ICI generally verified the measurements made at the individual equipment level. Additional baseline data consisted of the waveform at the BDP interface and data taken using the IONDS test receiver. The IONDS receiver was difficult to use in that the receiver exhibited stable periods of operation alternating with periods in which noise and/or instability would override attempts to perform measurements. Some of the initial ICI operational problems were traced to EMI from RF testing in the same building. Later problems could not be positively identified. However, considerable noise was observed on the power lines to the test set. In addition, it was noted that connecting or disconnecting test equipment from power lines in the same room (although not the same line with the test set) would generate errors in measurements or cause the recover lock to recycle. Power isolation units were not available during the ICI test, and therefore, measurements were made during stable periods.

The following items summarize the measurements performed with the test receivers.

- **L₁ Variations.** The maximum shift from the value set at ≥ 5.0 volts with the BDP off was 0.1 dB.
- **L₃ Variation.** Correlation was identical at all voltages with the BDP on, and with the BDP off at 25.5 volts. Values measured with the BDP off at 27.0 volts and 28.0 volts were plus and minus 0.3 dB, respectively.

- Carrier Phase Noise. Phase noise was measured on L_1 and on L_3 at ETV bus voltages of 25.5, 27.0, and at 28.0 volts with the BDP on and off. L_1 phase noise varied from 100 to 200 milliradians with the variations apparently time-dependent rather than related to ETV voltage or on/off condition of the BDP. L_3 phase noise was stable at 38 to 40 milliradians.
- Carrier IAM. Carrier incidental amplitude modulation (IAM) was measured on L_1 and L_3 for the three ETV bus voltages and for the BDP on and off. Values obtained ranged from 6.75 to 8.0 milliradians for L_3 and 3.35 to 4.0 milliradians for L_1 . Although values appear to increase with the bus voltage, the range is within the drift of the measurement.

The checkout equipment for the ICI test included the IGS monitor and control test set which housed the ETV 28-volt dc supply, the Navstar receiver, and ancillary test equipment (see Figure 112).



Figure 112. Checkout Equipment for the ICI Test

The Navstar receiver was available for checkout of the simulated navigation subsystem, if required, and for checkout of the L₃ transmission system. This receiver is equivalent in performance to the PSE receiver utilized in the GPS navigation test set.

The general IGS monitor and control set contains transmitters for calibrating the Navstar receiver which can operate L₁, L₂, and L₃ signals and the various special test devices including RF power meters, oscillographs, spectrum analyzer, frequency-time center, digital voltmeter, and the ETV 28-Vdc power supply.

The console was upgraded to include a full sensitivity IONDS receiver for the system/EMC test in March 1978. This receiver was developed specifically for the IGS test program. Panel components are shown in Figure 113. The console functions are listed in Table 35.

6.5 GPS INTEGRATION TESTS

GPS integration tests were undertaken to satisfy two basic requirements: (1) verify that the addition of IGS hardware to the GPS does not impact the primary GPS mission and (2) verify that the GPS is supportive of the IGS payload.

These objectives were satisfied by means of a comprehensive test program which involved the use of the GPS development test vehicle (DTV) and the creation of an ETV together with use of the GPS telecom simulator, GPS user receivers, GPS test sets, a new IGS test set, and GPS software and documentation (including the creation of new software and documentation pertinent to the IGS payload).

The integration program utilized the DTV for tests involving physical characteristics and the ETV for tests involving electrical characteristics for both GPS and IGS. The DTV and IGS configurations varied for each test. Consequently, test configurations were delineated separately for each test.

The GPS integration test program consisted of the following tests:

- RF compatibility test
- Intermodulation noise test
- System test
- EMC test
- IGS threshold sensitivity
- Acoustics

The objectives, locations, key parameters measured, time period, and vehicle are overviewed in Table 36.

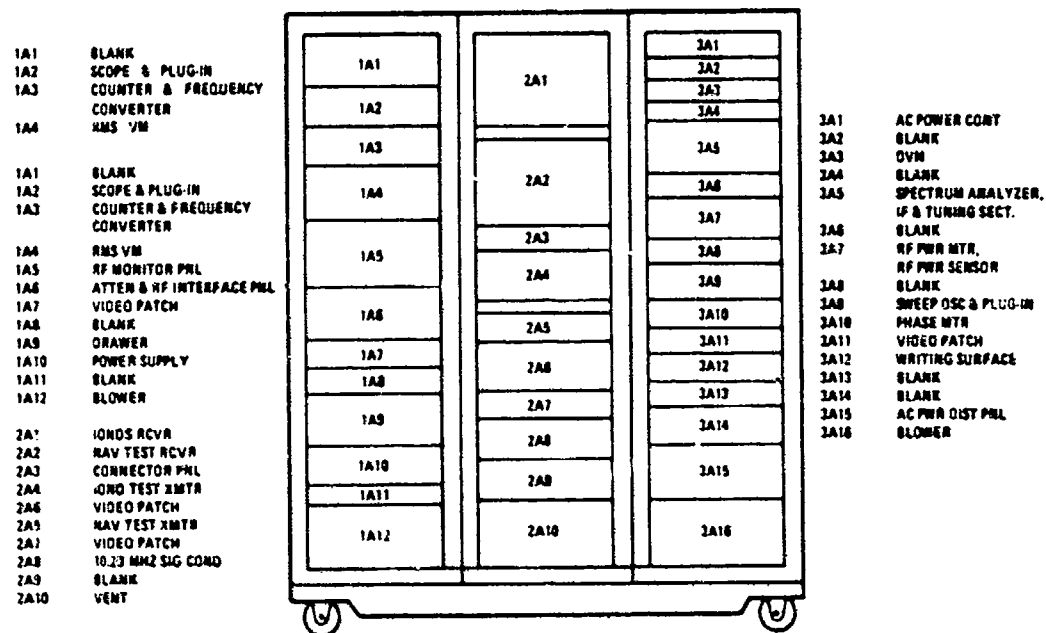


Figure 113. ICS Control and Monitor Test Set Equipment Layout

Table 35. ICI Console Operations

- Detect and output NAV data from L_1 carrier
- Detect and output IONDS data from L_3 carrier
- Acquire C/A-code and handover and track P-code (L₁)
- Correlate and detect L_3 P-code
- High sensitivity spread spectrum receiver
- Compatible with GPS code format
- Provide IF output for signal measurement by NAVSTAR receiver
- Employ noncoherent delay lock loop (DLL) with frequency aiding for code track
- Single DLL is used to position reference code for L_1 - C/A, L_1 - P and L_3 - P signals
- A single carrier reconstruction loop with AFC and PLL modes is used to acquire and track the L_1 or L_3 carrier
- High-resolution digital number controlled oscillators are employed in the code and carrier tracking loops to provide very accurate frequency preset, hold, and handover capability

Table 36. Integration Test Overview

Test	Veh	Date	Objectives	Key Parameters	SD Report
RF signal compatibility	ETV	Aug 13, 1977	Determine impact of IGS transmission on NAV system users	Delta range sigmas on L ₁ and L ₂ (DRS)	SD 77-GP-0046
Intermodulation noise test	ETV	Dec 23, 1977	Determine impact of IGS transmission on NAV system users and TT&C	DRS and TT&C CMD threshold	SD 78-GP-0007
System test	ETV	Mar 21, 1978	Determine impact of IGS interfaces on NAV, EPS, TT&C Develop IGS software and signal interfaces	Interface signals structure D ₁ , D ₂ , D ₃ test software	SD 78-GP-0012
EMC test	ETV	Mar 31, 1978	Determine IGS impact on EPS and other systems	27 Vdc transients	SD 78-GP-TBD
IGS threshold sensitivity	ETV	Mar 21, 1978	Determine IGS system threshold with STI receiver	Receiver threshold BER variation	SD 78-GP-0012-3
Acoustics	DTV	Oct 1976	Determine IGS component impact on GPS levels Determine levels at IGS components	GPS and IGS component GRMS vs frequency	SD 77-GP-0010-1, 2, 3, 4

6.5.1 RF Signal Compatibility Test

The RF signal compatibility testing was performed to confirm that the IGS and SCT secondary payload transmissions do not degrade the GPS L-band navigation signals and to partially confirm the capability of the GPS navigation system to support IGS data transmission. Details of the testing and test data are documented in Rockwell report SD 77-GP-0046.

6.5.1.1 Configuration. The GPS navigation link was simulated using signals generated by the telecommunications simulator. Its outputs were fed to the GPS engineering model L₁ and L₂ high-power amplifiers, which were coupled to a GPS production L-band antenna by means of the GPS engineering model diplexer. Components were mounted in flight locations, together with the secondary payloads RF transmitting hardware (Figure 114). The ETV was installed in the anechoic chamber as illustrated in Figure 115.

The Magnavox X-set receiver, Serial No. 10, was used to verify actual user segment performance on this baseline configuration for subsequent comparisons with operating conditions measured with secondary payloads transmitting. The overall test schematic is shown in Figure 116.

Key X-set parameters that were measured and their specified tolerance limits are tabulated in Table 37. The data acquired during testing included the full scope of the acceptance test analyzer (ATA) program set used to evaluate X-set receiver performance using a calibrated GPS source.

The -163 dBW signal strength is the GPS user average received power level. The -173 dBW signal strength was selected because at lower power levels Costas cycle slips and track losses started to occur.

The test was conducted on a simulated GPS vehicle (ETV) in the Naval Weapons Station anechoic chamber on August 11 and August 12, 1977.

6.5.1.2 Test Results. The data acquired as a baseline (Figures 117 and 118) were favorably compared to data acquired during user receiver acceptance

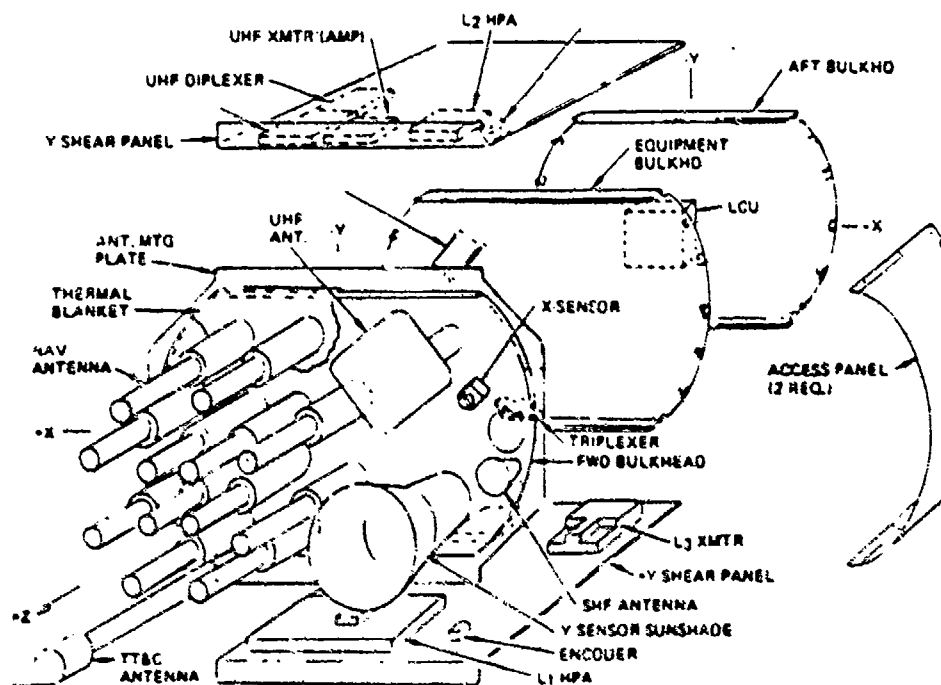


Figure 114. ETV RF Compatibility Test Configuration

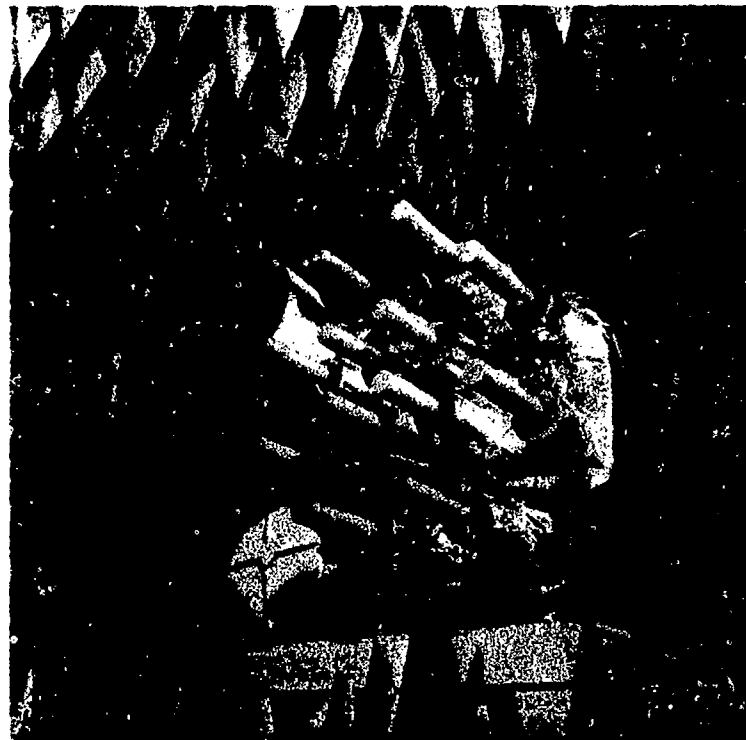


Figure 115. Electrical Test Vehicle Installed
in Anechoic Chamber

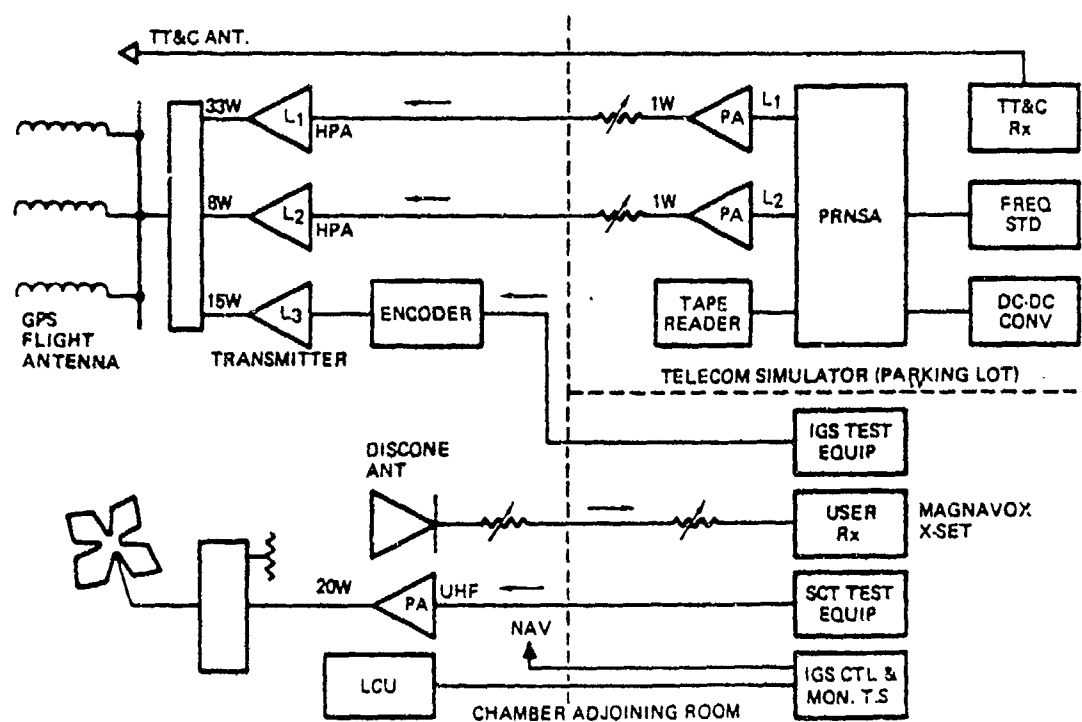


Figure 116. Signal Compatibility Test System

Table 37. GPS/SPL Signal Compatibility Parameters

Key Measurements	Parameter Limits	
Signal strength	-163 dBW	-171 dBW
C/No.	36-38 dB	28-32 dB
Data & parity errors	10^{-5} WER (Six word errors per five subframes)	10^{-5} WER
Pseudo-range	1.5 meters	1.5 meters
Delta range sigmas	0.012 meter	0.02 meter

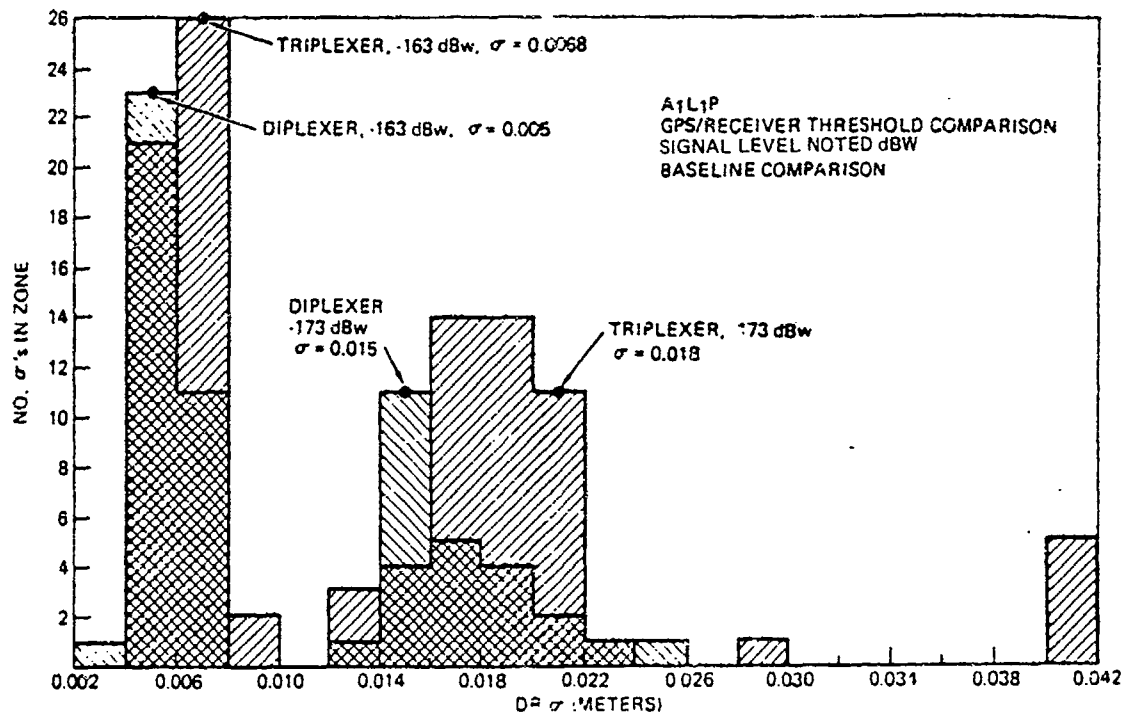
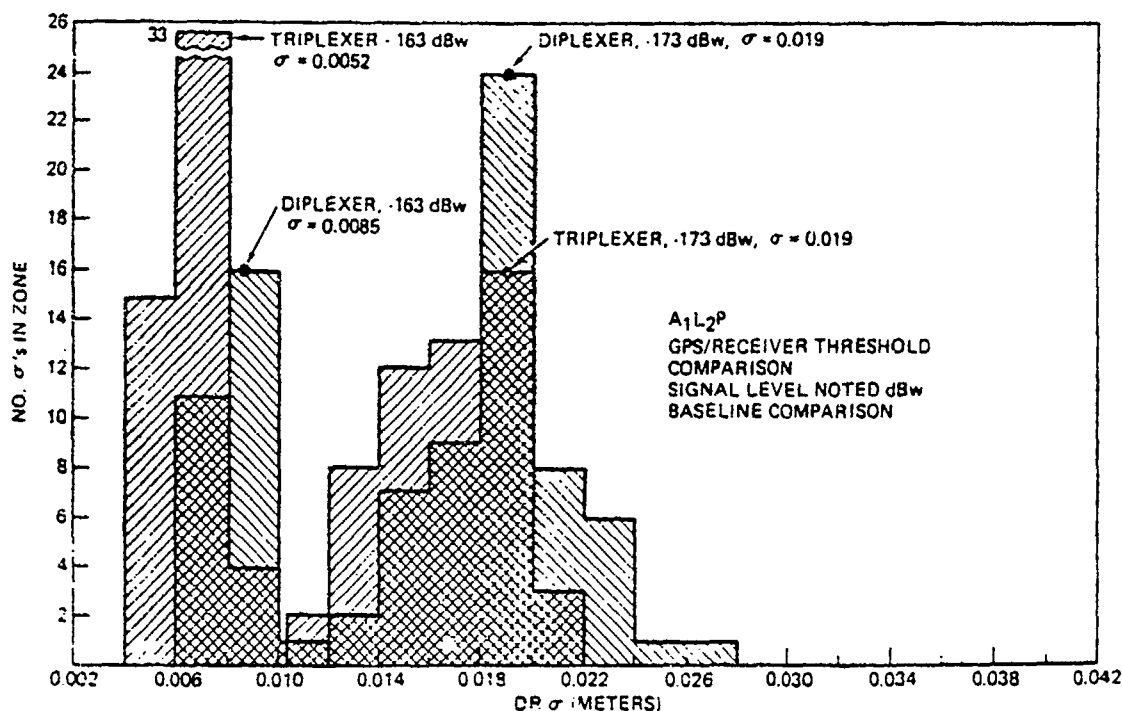


Figure 117. L1 User Impact

tests and NTS 2 tracking. In the figures, the parameter delta range sigma was used for the P code channels. Delta range has been ascertained as the most noise sensitive navigation user parameter.

L1 Channel Impact. Channel degradation was not evident with the normal operating level of -163 dBW. At -173 dBW, a slight shift of 0.003 meter in the value of delta range sigma (DRS) is shown (see Figure 117). This is the only notable test degradation and is caused by a small increase (0.2 dB) in the insertion loss for the L1 channel by the triplexer. This small degradation will be eliminated when a qualified triplexer becomes available.

Figure 118. L₂ User Impact

L₂ Channel Impact. Figure 118 shows that the L₂ channel performance has been improved by the triplexer; this improvement is traceable to a decrease in the triplexer insertion loss for the L₂ channel over the diplexer. The differences in L₁ and L₂ insertion losses between diplexer and triplexer used above were measured in conjunction with the GPS antenna with the appropriate antenna cable. These data were taken at a later date than those shown in Table 26 and under different testing conditions.

Isolation Tests. The IGS transmission impacts also were analyzed at an equivalent signal level of 25 dB greater than specified without impact to L₁ or L₂ users.

6.5.1.3 Intermodulation Noise Test. The intermodulation noise test was designed to determine the extent to which secondary payloads impacted the on-board TT&C receiver. The test also confirmed the results obtained on the RF compatibility test and established that uplink transmissions do not generate deleterious intermodulation noise products.

6.5.1.4 Configuration. The ETV was configured to provide a single-channel TT&C subsystem and a complete navigation subsystem except for the use of a single frequency standard instead of the three used on FSV 1 of the GPS. TT&C and navigation components were flight units derived from the GPS qualification test vehicle (QTV). The IGS system required special interface design, and consequently, the baseband processor and navigation diplexer were modified flight-type units to accommodate the IGS. Again, the components were mounted in flight locations (see Figure 119).

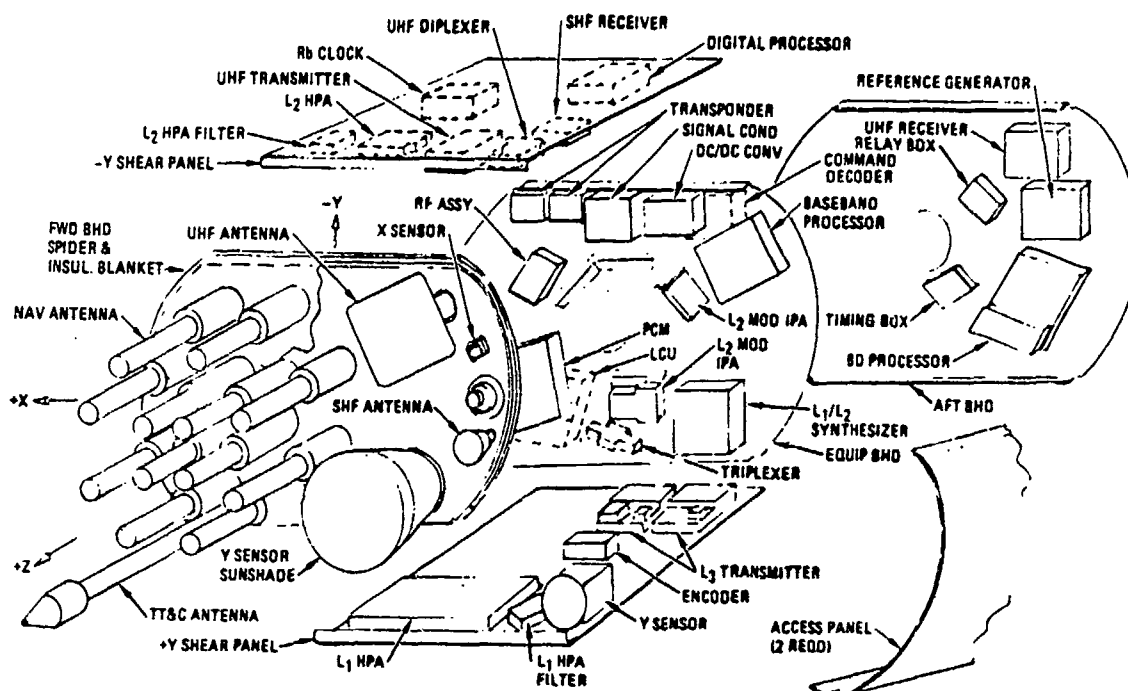


Figure 119. Intermod Test Equipment on ETV

Table 38. TT&C Key Parameters

Key Measurements	Parameter Limits
S-bit error threshold	-105 dBm
Command threshold	-105 dBm
Carrier threshold	-105 dBm

The TT&C key parameters are given in Table 38. These parameters provide a test of the receiver's ability to acquire a carrier, to activate the command decoders, and to satisfactorily decode the commands received. The effect of secondary payloads was delineated as the increase in uplink energy needed to achieve these basic functions.

6.5.1.5 Test Equipment. The addition of the TT&C system to the test configuration required additional GSE. In particular, it was necessary to utilize the telecom test set (Figure 120) and the data acquisition, control, and processing test set (Figures 121 and 122). The telecom test set contained the uplink and downlink signal conditioning hardware necessary to simulate an RTS of the satellite control facility (SCF), while the DACP provided simulation of the satellite test center (STC) (see Table 39). The telecom test set and the DACP were identical to units utilized in the SPS program except for minor changes (memory expansion) in the DACP.

The combined telecom test set and DACP permitted checkout of the TT&C system to the GPS factory test level. Further, when the IGS control and monitor

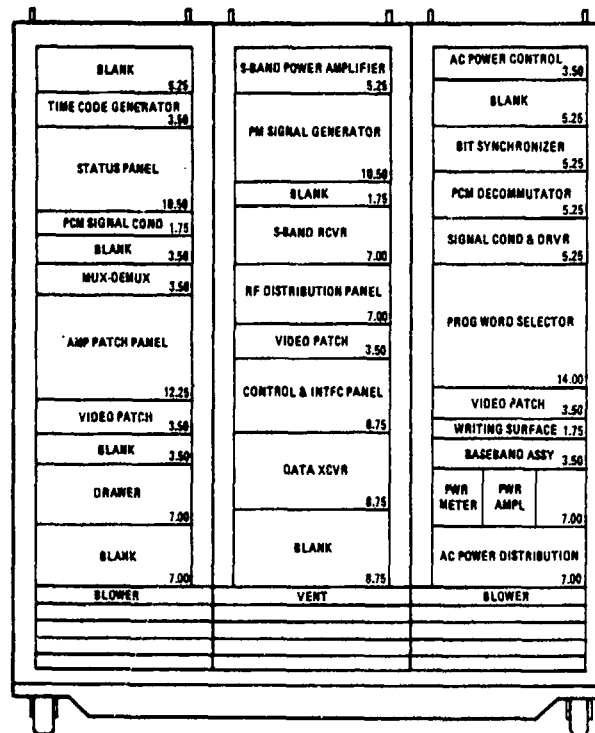


Figure 120. IGS Telecom Test Set

Table 39. IGS Telecom Test Set Functions

- Provides vehicle/DACP interface for data and commands
- Provides S-band up-link signal for commanding
- Receives S-band downlink signal for data processing
- Provides timing for DACP

console was added, checkout of the navigation system to factory levels also was achieved, although the navigation user receiver was maintained as the prime element of navigation system evaluation.

6.5.1.6 Test Results. The data defined for baseline navigation and TT&C system operation were compared to data acquired during the operation of secondary payloads, in the manner described earlier for the RF compatibility tests. Delta range signal was used again as the key test parameter. It was supported by tabulated data of C/N_0 , data errors, signal strength, and absolute values of pseudo-range. The threshold values of TT&C parameters (shown in Figure 123) were used to estimate the impact of the IGS (and SCT) on TT&C performance.

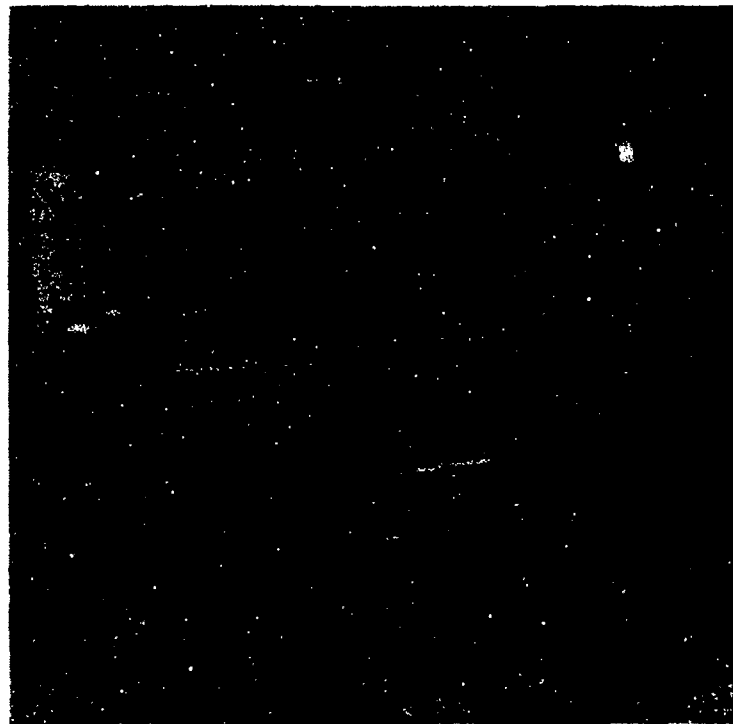
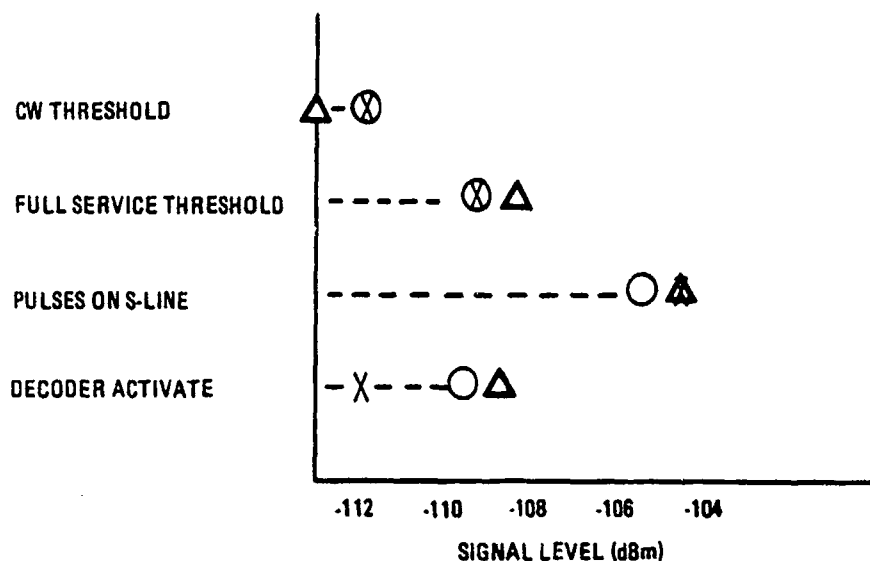


Figure 121. Data Acquisition, Control,
and Processing Test Set .



Figure 122. DACP Peripheral Equipment



○ BASELINE, NAV OFF
 △ BASELINE, NAV ON
 X FULL-UP TEST

Figure 123. TT&C Intermodulation Noise Test Results

L₁ Channel Impact. As in the previous test, degradation was not evident in the L₁ channel. Figures 117 and 118 show no degradation at either -163 dBW or -173 dBW for operation with P-coded data or C/A-coded data.

L₂ Channel Impact. The L₂ channel also was not degraded by secondary payload operations. Figure 118 shows the pseudo-range signal values to be nearly identical for either case with each run displaying the same mean value.

6.5.2 TT&C Impact

Degradation to the TT&C system was not detected during the testing. Figure 123 shows that the four threshold command values have been maintained under both sets of operating conditions.

6.5.3 System Test

The IGS/GPS system test was conducted to determine the capability of the GPS to support IGS operation, as specified, while demonstrating that the IGS does not impact the navigation, EPS, and TT&C subsystems.

The key parameters subjected to test and the source of these parameters are given in Table 40.

In Table 41, it can be seen that the interface signal verification taken during the test certifies the correctness of interface documentation.

Table 40. L₃ Transmission Tests

Test	Parameter	Expected Value	Reference
ETV hardware	RF power output	≥ 15 watts	MH08-00013
	Coding	Diff/block/convol	MH08-00013
	Data rate	200 b/s	MH08-00013
	BPSK spectra	sin x/x wave	MH08-00013
	Carrier phase noise	≤ 100 mrad	MH08-00013
	L ₁ - L ₃ code delay	≤ 15 ns	STI Verbal
	L ₁ -L ₃ code delay variation	≤ 1.5 ns	STI Verbal
	X1 epoch delay	≤ 100 ns	MH08-00012
System	L ₃ data transmission threshold	-133 dBm	Link margin
	Correlation loss	0.6 dB	Link margin
	Character error rate	$\approx \text{BER} = 10^{-5}$	Link margin

Cross-strapping, shown in Figure 124, illustrates the data channel and interface signal interconnection between the IGS and the GPS subsystem. The cross-strapping matrix of Table 42 shows how the various data were routed during the system test.

In Table 43, a readout of prestored BDP memory, the D1 data are "TESTMEM." Table 44 shows D2, which is a readout of the SOH data from the BDP. Table 45 lists D3 data and the X and Y sensor calibration data. D1 and D2 are read out automatically from the DACP. The D3 data were required to be analyzed manually by Sandia.

Figure 125 shows the overall test configuration from ETV through to the DACP. The BDP was uploaded via TT&C, and SOH was read out at the DACP via the telecom test set. D1 and D3 data were read out via the 200-bps data stream emanating from the IGS monitor and control console to the DACP.

Tab Runs A, B, C, and D show typical memory dumps of data acquired at the DACP during the system test. The acquired data correspond precisely to the expected results from D1 and D2. D3 analysis by Sandia verified data transmission accuracy.

During the testing, it was determined that several interface functions were not within specification. Table 46 describes these out-of-specification signals together with the impacts associated with each anomaly, the cause, and the involved interface. Most interface problems were associated with an incorrect specification. The distribution of 10.23-MHz signals by IGS is about 2.8 dB lower than stipulated in the ICD (see Figure 126). Here, losses for cable and power splitters were inadvertently omitted from ICD consideration. The losses encountered were deemed typical for this signal. No adverse impacts to SCT or

Table 41. Interface Verification

Test	Parameter	Value			Reference
		True (V)	False (V)	R/F Time (μs)	
Navigation BBP to BDP (A&B) BBP to BDP (A&B) BBP to BDP (A&B) BBP to TI Box TI Box to BDP TI Box to L3 (A&B) BBP to L3 (A&B) BBP to BDP (A&B) L3A to SCT BBP (ASC) to BDP (A&B)	X1 epoch	+4.5 ± 0.5	0 to -1.0	<0.1/5	MH08-00012
	Z-count	+4.5 ± 0.5	0 to -1.0	5	MH08-00012
	100-Hz strobe	+4.5 ± 0.5	0 to -1.0	5	MH08-00012
	100 Hz clock	+4.5 ± 0.5	0 to -1.0	5	MH08-00013
	200 Hz clock	+4.5 ± 0.5	0 to -1.0	5	MH08-00012
	400 Hz clock	+4.5 ± 0.5	0 to -1.0	5	MH08-00013
	10.23 MHz clock	+3.8 to 6.6 dBm			MH08-00013
	10.23 MHz clock	-0.5 to -3.3 dBm			MH08-00012
	10.23 MHz clock	-3.4 ± 1.4 dBm			MH08-00011
	X1 epoch delay	<100 ns			MH08-00012
Electrical Power LCU - L3 (A&B) LCU - BDP (A&B)	Dc power to transmitter (A&B)	25.5 - 28 Vdc			MH08-00013
	Dc power to BDP (A&B)	25.5 - 28 Vdc			MH08-00012
TT&C DCD (A&B) to BDP (A&B) DCD (A&B) to BDP (A&B) DCD (A&B) to BDP (A&B) SOHS Box to BDP (A&B) SOHS Box to BDP PCM A&B to SOH DCD (A&B) to BDP (A&B) BDP (A&B) to PCM (A&B) BDP (A&B) to PCM (A&B) BDP (A&B) to PCM (A&B)	Magnitude command	4 ± 1.0	0 ± 0.5	5	MH08-00012
	Magnitude command clock	4 ± 1.0	0 ± 0.5	5	MH08-00012
	Magnitude command enable	4 ± 1.0	0 ± 0.5	5	MH08-00012
	PCM enable SF 1	4.5 ± 1.0	0 ± 0.5	5	MH08-00012
	PCM enable SF 5	4.5 ± 1.0	0 ± 0.5	5	MH08-00012
	PCM enable SF 1-8	4.5 ± 1.0	0 ± 0.5	5	MH08-00012
	Discrete commands (1-4)	20 to 27	None	50/10	None
	8-bit SOH	Not specified			MH08-00012
	Analog data (4)	0 to 5.12V			MH08-00012
	Discrete meas	+3 to +32	-1 to +1	Not spec	MH08-00012

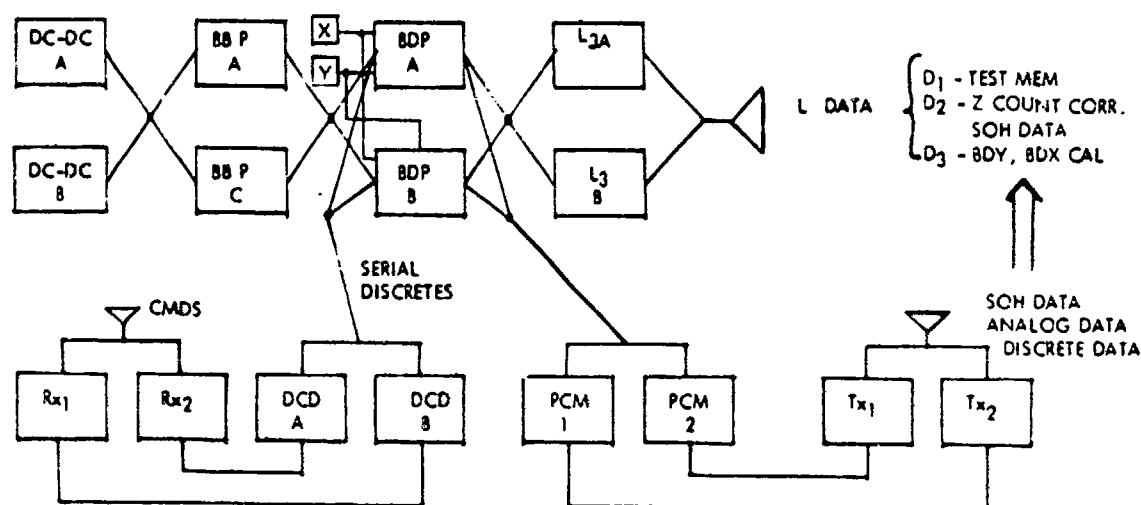


Figure 124. Cross-Strapping

Table 42. Cross-Strapping Matrix

	GPS	IGS			GPS				
	DC-DC	BBP	BDP	L ₃	Rx	DCD	PCM	Tx	Analysis
D ₁	A&B	A&C	A&B	A&B	-	-	-	-	DACP (automatic)
D ₂	A&B	A&C	A&B	A&B	1 & 2	A	1	1 & 2	DACP & visual
D ₃	A&B	A&C	A&B	A&B	1	A	-	1	Sandia

IGS components resulted from the low signal pulse level, indicating that considerable margin is available within the BDP and SCT components. Further, the L₃ system was not impacted by the excessive rise/fall times on data A and B lines.

The X1 epoch delay at the BBP/BDP interface was not measured due to difficulty in achieving measurement with insufficient test points. The PCM 2 SOH signals were not transmitted because some channels were damaged by static electric charges which occurred during QTV thermal-vacuum tests (see Figure 127).

Figure 127 indicates the areas where the cross-strapping tests for powering the BBP were completed. Also, wiring of the ETV for this test (which had a modified BBP) precluded wiring the navigation dc-dc Converter B to the BBP without restructuring the command subsystem. The omission was considered minor with respect to IGS interfaces, and tests were conducted on the dc-dc A side only. The data transmission matrix is listed in Table 47, and the cross-strapping problems are tabulated in Table 48.

Table 43. IGS Checkout Test Run

Reproduced from
best available copy

Table 43. IGS Checkout Test Run (Cont)

FROM CP505-910-0000 TEST: IGSB REDUNDANCY TEST SUP DATE 03/15/78 PAGE 40
TWO LINE AT CDR FILE VALUE UNITS REPAIRS

COMPARE COMPLETE			
07511311211.0 01131111	A= 41 P= 00 A= 42 P= 1C A= 5C P= 70	600 DATA COMPARE, BLOCK 10 EQUUS, DATA NUMBER 73 EQUUS, DATA NUMBER 74 EQUUS, DATA NUMBER 75 COMPARE COMPLETE	
07511311211.0 01131111	A= 60 P= 70 A= 61 P= 6A A= 60 P= 00	600 DATA COMPARE, BLOCK 17 EQUUS, DATA NUMBER 73 EQUUS, DATA NUMBER 74 EQUUS, DATA NUMBER 75 COMPARE COMPLETE	
07511311211.0 01131111	A= 20 P= 00 A= 21 P= 17 A= 24 P= 00	600 DATA COMPARE, BLOCK 16 EQUUS, DATA NUMBER 73 EQUUS, DATA NUMBER 74 EQUUS, DATA NUMBER 75 COMPARE COMPLETE	
07511311211.0 01131111	A= 1C P= 30 A= 2A P= 34 A= 70 P= 70	600 DATA COMPARE, BLOCK 19 EQUUS, DATA NUMBER 73 EQUUS, DATA NUMBER 74 EQUUS, DATA NUMBER 75 COMPARE COMPLETE	
07511311211.0 01131111	A= 77 P= 00 A= 78 P= 34 A= 7C P= 74	600 DATA COMPARE, BLOCK 20 EQUUS, DATA NUMBER 73 EQUUS, DATA NUMBER 74 EQUUS, DATA NUMBER 75 COMPARE COMPLETE	
07511311211.0 01131111	A= 00 P= 00 A= 01 P= 07 A= 0C P= 00	600 DATA COMPARE, BLOCK 21 EQUUS, DATA NUMBER 73 EQUUS, DATA NUMBER 74 EQUUS, DATA NUMBER 75 COMPARE COMPLETE	
07511311211.0 01131111	A= 0F P= 00 A= 00 P= 01 A= 00 P= 00	600 DATA COMPARE, BLOCK 22 EQUUS, DATA NUMBER 73 EQUUS, DATA NUMBER 74 EQUUS, DATA NUMBER 75 COMPARE COMPLETE	
07511311211.0 01131111	A= 00 P= 10 A= 01 P= 1C A= 00 P= 00	600 DATA COMPARE, BLOCK 23 EQUUS, DATA NUMBER 73 EQUUS, DATA NUMBER 74 EQUUS, DATA NUMBER 75 COMPARE COMPLETE	
07511311211.0 01131111	A= 00 P= 30 A= 01 P= 14 A= 00 P= 10	600 DATA COMPARE, BLOCK 24 EQUUS, DATA NUMBER 73 EQUUS, DATA NUMBER 74 EQUUS, DATA NUMBER 75 COMPARE COMPLETE	
FROM CP505-910-0000 TEST: IGSB REDUNDANCY TEST SUP DATE 03/15/78 PAGE 40 TWO LINE AT CDR FILE VALUE UNITS REPAIRS			
07511311211.0 01131111	A= 71 P= 00 A= 70 P= 03 A= 70 P= 00	600 DATA COMPARE, BLOCK 25 EQUUS, DATA NUMBER 73 EQUUS, DATA NUMBER 74 EQUUS, DATA NUMBER 75 COMPARE COMPLETE	
07511311211.0 01131111	A= 53 P= 00 A= 54 P= 00 A= 5C P= 10	600 DATA COMPARE, BLOCK 26 EQUUS, DATA NUMBER 73 EQUUS, DATA NUMBER 74 EQUUS, DATA NUMBER 75 COMPARE COMPLETE	
07511311211.0 01131111	A= 50 P= 00 A= 51 P= 00 A= 50 P= 10	600 DATA COMPARE, BLOCK 27 EQUUS, DATA NUMBER 73 EQUUS, DATA NUMBER 74 EQUUS, DATA NUMBER 75 COMPARE COMPLETE	
07511311211.0 01131111	A= 00 P= 10 A= 01 P= 07 A= 00 P= 00	600 DATA COMPARE, BLOCK 28 EQUUS, DATA NUMBER 73 EQUUS, DATA NUMBER 74 EQUUS, DATA NUMBER 75 COMPARE COMPLETE	
07511311211.0 01131111	A= 00 P= 10 A= 01 P= 07 A= 00 P= 00	600 DATA COMPARE, BLOCK 29 EQUUS, DATA NUMBER 73 EQUUS, DATA NUMBER 74 EQUUS, DATA NUMBER 75 COMPARE COMPLETE	
07511311211.0 01131111	A= 00 P= 00 A= 01 P= 00 A= 00 P= 00	600 DATA COMPARE, BLOCK 30 EQUUS, DATA NUMBER 73 EQUUS, DATA NUMBER 74 EQUUS, DATA NUMBER 75 COMPARE COMPLETE	
07511311211.0 01131111	A= 00 P= 00 A= 01 P= 00 A= 00 P= 00	600 DATA COMPARE, BLOCK 31 EQUUS, DATA NUMBER 73 EQUUS, DATA NUMBER 74 EQUUS, DATA NUMBER 75 COMPARE COMPLETE	
07511311211.0 01131111	A= 00 P= 00 A= 01 P= 00 A= 00 P= 00	600 DATA COMPARE, BLOCK 32 EQUUS, DATA NUMBER 73 EQUUS, DATA NUMBER 74 EQUUS, DATA NUMBER 75 COMPARE COMPLETE	
07511311211.0 01131111	A= 00 P= 00 A= 01 P= 00 A= 00 P= 00	600 DATA COMPARE, BLOCK 33 EQUUS, DATA NUMBER 73 EQUUS, DATA NUMBER 74 EQUUS, DATA NUMBER 75 COMPARE COMPLETE	

Table 43. IGS Checkout Test Run (Cont)

PRG	TIME	ET	CHD	TEST	VALUE	UNIT	REMARKS
07511511147.0	01131124			END DATA COMPARE, BLOCK 34			
				ENRUM, DATA NUMBER 73			
				ENRUM, DATA NUMBER 74			
				ENRUM, DATA NUMBER 75			
				COMPARE COMPLETE			
07511511150.0	01131130			END DATA COMPARE, BLOCK 35			
				ENRUM, DATA NUMBER 73			
				ENRUM, DATA NUMBER 74			
				ENRUM, DATA NUMBER 75			
				COMPARE COMPLETE			
07511511153.0	01131135			END DATA COMPARE, BLOCK 36			
				ENRUM, DATA NUMBER 73			
				ENRUM, DATA NUMBER 74			
				ENRUM, DATA NUMBER 75			
				COMPARE COMPLETE			
07511511156.0	01131140			END DATA COMPARE, BLOCK 37			
				ENRUM, DATA NUMBER 73			
				ENRUM, DATA NUMBER 74			
				ENRUM, DATA NUMBER 75			
				COMPARE COMPLETE			
07511511159.0	01131145			END DATA COMPARE, BLOCK 38			
				ENRUM, DATA NUMBER 73			
				ENRUM, DATA NUMBER 74			
				ENRUM, DATA NUMBER 75			
				COMPARE COMPLETE			
07511511162.0	01131150			END DATA COMPARE, BLOCK 39			
				ENRUM, DATA NUMBER 73			
				ENRUM, DATA NUMBER 74			
				ENRUM, DATA NUMBER 75			
				COMPARE COMPLETE			
07511511165.0	01131155			END DATA COMPARE, BLOCK 40			
				ENRUM, DATA NUMBER 73			
				ENRUM, DATA NUMBER 74			
				ENRUM, DATA NUMBER 75			
				COMPARE COMPLETE			
07511511168.0	01131200			END DATA COMPARE, BLOCK 41			
				ENRUM, DATA NUMBER 73			
				ENRUM, DATA NUMBER 74			
				ENRUM, DATA NUMBER 75			
				COMPARE COMPLETE			
07511511171.0	01131205			END DATA COMPARE, BLOCK 42			
				ENRUM, DATA NUMBER 73			
				ENRUM, DATA NUMBER 74			
				ENRUM, DATA NUMBER 75			
				COMPARE COMPLETE			
07511511174.0	01131210			END DATA COMPARE, BLOCK 43			
				ENRUM, DATA NUMBER 73			
				ENRUM, DATA NUMBER 74			
				ENRUM, DATA NUMBER 75			
				COMPARE COMPLETE			
07511511177.0	01131215			END DATA COMPARE, BLOCK 44			
				ENRUM, DATA NUMBER 73			
				ENRUM, DATA NUMBER 74			
				ENRUM, DATA NUMBER 75			
				COMPARE COMPLETE			
07511511180.0	01131220			END DATA COMPARE, BLOCK 45			
				ENRUM, DATA NUMBER 73			
				ENRUM, DATA NUMBER 74			
				ENRUM, DATA NUMBER 75			
				COMPARE COMPLETE			
07511511183.0	01131225			END DATA COMPARE, BLOCK 46			
				ENRUM, DATA NUMBER 73			
				ENRUM, DATA NUMBER 74			
				ENRUM, DATA NUMBER 75			
				COMPARE COMPLETE			
07511511186.0	01131230			END DATA COMPARE, BLOCK 47			
				ENRUM, DATA NUMBER 73			
				ENRUM, DATA NUMBER 74			
				ENRUM, DATA NUMBER 75			
				COMPARE COMPLETE			
07511511189.0	01131235			END DATA COMPARE, BLOCK 48			
				ENRUM, DATA NUMBER 73			
				ENRUM, DATA NUMBER 74			
				ENRUM, DATA NUMBER 75			
				COMPARE COMPLETE			
07511511192.0	01131240			END INCREMENTING PATTERN			
07511511195.0	01131245			END FOR L3 SYNC LUBS			
07511511198.0	01131250			END L3 SYNC LUBS			
07511511201.0	01131255			START ALL USE'S PATTERN			
07511511204.0	01131300			END L3 SYNC LUBS			
07511511207.0	01131305			END L3 SYNC LUBS			
07511511210.0	01131310			END L3 SYNC LUBS			
07511511213.0	01131315			END L3 SYNC LUBS			
07511511216.0	01131320			END L3 SYNC LUBS			
07511511219.0	01131325			END L3 SYNC LUBS			
07511511222.0	01131330			END L3 SYNC LUBS			
07511511225.0	01131335			END L3 SYNC LUBS			
07511511228.0	01131340			END L3 SYNC LUBS			
07511511231.0	01131345			END L3 SYNC LUBS			
07511511234.0	01131350			END L3 SYNC LUBS			
07511511237.0	01131355			END L3 SYNC LUBS			
07511511240.0	01131400			END L3 SYNC LUBS			
07511511243.0	01131405			END L3 SYNC LUBS			
07511511246.0	01131410			END L3 SYNC LUBS			
07511511249.0	01131415			END L3 SYNC LUBS			
07511511252.0	01131420			END L3 SYNC LUBS			
07511511255.0	01131425			END L3 SYNC LUBS			
07511511258.0	01131430			END L3 SYNC LUBS			
07511511261.0	01131435			END L3 SYNC LUBS			
07511511264.0	01131440			END L3 SYNC LUBS			
07511511267.0	01131445			END L3 SYNC LUBS			
07511511270.0	01131450			END L3 SYNC LUBS			
07511511273.0	01131455			END L3 SYNC LUBS			
07511511276.0	01131500			END L3 SYNC LUBS			
07511511279.0	01131505			END L3 SYNC LUBS			
07511511282.0	01131510			END L3 SYNC LUBS			
07511511285.0	01131515			END L3 SYNC LUBS			
07511511288.0	01131520			END L3 SYNC LUBS			
07511511291.0	01131525			END L3 SYNC LUBS			
07511511294.0	01131530			END L3 SYNC LUBS			
07511511297.0	01131535			END L3 SYNC LUBS			
07511511300.0	01131540			END L3 SYNC LUBS			
07511511303.0	01131545			END L3 SYNC LUBS			
07511511306.0	01131550			END L3 SYNC LUBS			
07511511309.0	01131555			END L3 SYNC LUBS			
07511511312.0	01131600			END L3 SYNC LUBS			
07511511315.0	01131605			END L3 SYNC LUBS			
07511511318.0	01131610			END L3 SYNC LUBS			
07511511321.0	01131615			END L3 SYNC LUBS			
07511511324.0	01131620			END L3 SYNC LUBS			
07511511327.0	01131625			END L3 SYNC LUBS			
07511511330.0	01131630			END L3 SYNC LUBS			
07511511333.0	01131635			END L3 SYNC LUBS			
07511511336.0	01131640			END L3 SYNC LUBS			
07511511339.0	01131645			END L3 SYNC LUBS			
07511511342.0	01131650			END L3 SYNC LUBS			
07511511345.0	01131655			END L3 SYNC LUBS			
07511511348.0	01131700			END L3 SYNC LUBS			
07511511351.0	01131705			END L3 SYNC LUBS			
07511511354.0	01131710			END L3 SYNC LUBS			
07511511357.0	01131715			END L3 SYNC LUBS			
07511511360.0	01131720			END L3 SYNC LUBS			
07511511363.0	01131725			END L3 SYNC LUBS			
07511511366.0	01131730			END L3 SYNC LUBS			
07511511369.0	01131735			END L3 SYNC LUBS			
07511511372.0	01131740			END L3 SYNC LUBS			
07511511375.0	01131745			END L3 SYNC LUBS			
07511511378.0	01131750			END L3 SYNC LUBS			
07511511381.0	01131755			END L3 SYNC LUBS			
07511511384.0	01131800			END L3 SYNC LUBS			
07511511387.0	01131805			END L3 SYNC LUBS			
07511511390.0	01131810			END L3 SYNC LUBS			
07511511393.0	01131815			END L3 SYNC LUBS			
07511511396.0	01131820			END L3 SYNC LUBS			
07511511399.0	01131825			END L3 SYNC LUBS			
07511511402.0	01131830			END L3 SYNC LUBS			
07511511405.0	01131835			END L3 SYNC LUBS			
07511511408.0	01131840			END L3 SYNC LUBS			
07511511411.0	01131845			END L3 SYNC LUBS			
07511511414.0	01131850			END L3 SYNC LUBS			
07511511417.0	01131855			END L3 SYNC LUBS			
07511511420.0	01131900			END L3 SYNC LUBS			
07511511423.0	01131905			END L3 SYNC LUBS			
07511511426.0	01131910			END L3 SYNC LUBS			
07511511429.0	01131915			END L3 SYNC LUBS			
07511511432.0	01131920			END L3 SYNC LUBS			
07511511435.0	01131925			END L3 SYNC LUBS			
07511511438.0	01131930			END L3 SYNC LUBS			
07511511441.0	01131935			END L3 SYNC LUBS			
07511511444.0	01131940			END L3 SYNC LUBS			
07511511447.0	01131945			END L3 SYNC LUBS			
07511511450.0	01131950			END L3 SYNC LUBS			
07511511453.0	01131955			END L3 SYNC LUBS			
07511511456.0	01132000			END L3 SYNC LUBS			
07511511459.0	01132005			END L3 SYNC LUBS			
07511511462.0	01132010			END L3 SYNC LUBS			
07511511465.0	01132015			END L3 SYNC LUBS			
07511511468.0	01132020			END L3 SYNC LUBS			
07511511471.0	01132025			END L3 SYNC LUBS			
07511511474.0	01132030			END L3 SYNC LUBS			
07511511477.0	01132035			END L3 SYNC LUBS			
07511511480.0	01132040			END L3 SYNC LUBS			
07511511483.0	01132045			END L3 SYNC LUBS			
07511511486.0	01132050			END L3 SYNC LUBS			
07511511489.0	01132055			END L3 SYNC LUBS			
07511511492.0	01132100			END L3 SYNC LUBS			
07511511495.0	01132105			END L3 SYNC LUBS			
07511511498.0	01132110			END L3 SYNC LUBS			
07511511501.0	01132115			END L3 SYNC LUBS			
07511511504.0	01132120			END L3 SYNC LUBS			
07511511507.0	01132125			END L3 SYNC LUBS			
07511511510.0	01132130			END L3 SYNC LUBS			
07511511513.0	01132135			END L3 SYNC LUBS			
07511511516.0	01132140			END L3 SYNC LUBS			
07511511519.0	01132145			END L3 SYNC LUBS			
07511511522.0	01132150			END L3 SYNC LUBS			
07511511525.0	01132155			END L3 SYNC LUBS			
07511511528.0	01132200			END L3 SYNC LUBS			
07511511531.0	01132205			END L3 SYNC LUBS			
07511511534.0	01132210			END L3 SYNC LUBS			
07511511537.0	01132215			END L3 SYNC LUBS			
07511511540.0	01132220			END L3 SYNC LUBS			
07511511543.0	01132225			END L3 SYNC LUBS			
07511511546.0	01132230			END L3 SYNC LUBS			
07511511549.0	01132235			END L3 SYNC LUBS			
07511511552.0	01132240			END L3 SYNC LUBS			
07511511555.0	01132245			END L3 SYNC LUBS			
07511511558.0	01132250			END L3 SYNC LUBS			
07511511561.0	01132255			END L3 SYNC LUBS			
07511511564.0	01132300			END L3 SYNC LUBS			
07511511567.0	01132305			END L3 SYNC LUBS			
07511511570.0	01						

Table 43. IGS Checkout Test Run (Cont)

PRGM CP505-510-0000 TEST: IGS REDUNDANCY TEST SUP DATE 03/15/76 PAGE 52					
TD	TIME	CT	CMD	HEAR	VALUE UNIT
			A= 3F	P= 7C	ERROR, DATA NUMBER 73
			A= 40	P= 87	ERROR, DATA NUMBER 74
			A= 08	P= 82	ERROR, DATA NUMBER 75
					COMPARE COMPLETE
07511515101.2	01132143				GOOD DATA COMPARE, BLOCK 6
			A= 24	P= 58	ERROR, DATA NUMBER 73
			A= 0F	P= 1E	ERROR, DATA NUMBER 74
			A= 88	P= 06	ERROR, DATA NUMBER 75
					COMPARE COMPLETE
07511515104.2	01132146				GOOD DATA COMPARE, BLOCK 7
			A= 22	P= 22	ERROR, DATA NUMBER 73
			A= 4D	P= 9A	ERROR, DATA NUMBER 74
			A= 3C	P= 8A	ERROR, DATA NUMBER 75
					COMPARE COMPLETE
07511515107.2	01132149				GOOD DATA COMPARE, BLOCK 8
			A= 25	P= FF	ERROR, DATA NUMBER 73
			A= 0E	P= 7C	ERROR, DATA NUMBER 74
			A= 55	P= AA	ERROR, DATA NUMBER 75
			A= 10	P= 20	ERROR, DATA NUMBER 75
					COMPARE COMPLETE
07511515110.2	01132152				GOOD DATA COMPARE, BLOCK 9
			A= 0A	P= 15	ERROR, DATA NUMBER 73
			A= AC	P= 58	ERROR, DATA NUMBER 74
			A= 58	P= 60	ERROR, DATA NUMBER 75
					COMPARE COMPLETE
07511515113.2	01132155				GOOD DATA COMPARE, BLOCK 10
			A= 0C	P= 79	ERROR, DATA NUMBER 73
			A= 6C	P= 19	ERROR, DATA NUMBER 74
			A= A8	P= 50	ERROR, DATA NUMBER 75
					COMPARE COMPLETE
07511515116.2	01132158				GOOD DATA COMPARE, BLOCK 11
			A= 01	P= C3	ERROR, DATA NUMBER 73
			A= CC	P= 0D	ERROR, DATA NUMBER 74
			A= 4C	P= 3A	ERROR, DATA NUMBER 75
					COMPARE COMPLETE
07511515119.2	01132161				GOOD DATA COMPARE, BLOCK 12
			A= 26	P= FF	ERROR, DATA NUMBER 73
			A= A1	P= 43	ERROR, DATA NUMBER 74
			A= 0D	P= 1A	ERROR, DATA NUMBER 75
			A= CC	P= 58	ERROR, DATA NUMBER 75
					COMPARE COMPLETE
07511515122.2	01132164				GOOD DATA COMPARE, BLOCK 13
			A= 2D	P= 5B	ERROR, DATA NUMBER 73
			A= 0F	P= 1E	ERROR, DATA NUMBER 74
			A= 7C	P= FA	ERROR, DATA NUMBER 75
					COMPARE COMPLETE
PRGM CP505-510-0000 TEST: IGS REDUNDANCY TEST SUP DATE 03/15/76 PAGE 53					
TD	TIME	CT	CMD	HEAR	VALUE UNIT
07511515125.2	01132167				GOOD DATA COMPARE, BLOCK 14
			A= 0A	P= 17	ERROR, DATA NUMBER 73
			A= AF	P= 5F	ERROR, DATA NUMBER 74
			A= 0C	P= 18	ERROR, DATA NUMBER 75
					COMPARE COMPLETE
07511515128.2	01132170				GOOD DATA COMPARE, BLOCK 15
			A= 0A	P= A0	ERROR, DATA NUMBER 73
			A= 4D	P= 0D	ERROR, DATA NUMBER 74
			A= 0A	P= 70	ERROR, DATA NUMBER 75
					COMPARE COMPLETE
07511515131.2	01132173				GOOD DATA COMPARE, BLOCK 16
			A= 27	P= FF	ERROR, DATA NUMBER 73
			A= C3	P= C6	ERROR, DATA NUMBER 74
			A= 77	P= CE	ERROR, DATA NUMBER 75
			A= 29	P= 40	ERROR, DATA NUMBER 75
					COMPARE COMPLETE
07511515134.2	01132176				GOOD DATA COMPARE, BLOCK 17
			A= EA	P= 04	ERROR, DATA NUMBER 73
			A= 4D	P= 9A	ERROR, DATA NUMBER 74
			A= 75	P= E9	ERROR, DATA NUMBER 75
					COMPARE COMPLETE
07511515137.2	01132179				GOOD DATA COMPARE, BLOCK 18
			A= CC	P= 9B	ERROR, DATA NUMBER 73
			A= 4D	P= 0A	ERROR, DATA NUMBER 74
			A= 2A	P= 0A	ERROR, DATA NUMBER 75
					COMPARE COMPLETE
07511515140.2	01132182				GOOD DATA COMPARE, BLOCK 19
			A= 11	P= 22	ERROR, DATA NUMBER 73
			A= 2F	P= 5F	ERROR, DATA NUMBER 74
			A= 89	P= 60	ERROR, DATA NUMBER 75
					COMPARE COMPLETE
07511515143.2	01132185				GOOD DATA COMPARE, BLOCK 20
			A= 29	P= FF	ERROR, DATA NUMBER 73
			A= 41	P= 23	ERROR, DATA NUMBER 74
			A= 02	P= 64	ERROR, DATA NUMBER 75
			A= 6C	P= 08	ERROR, DATA NUMBER 75
					COMPARE COMPLETE
07511515146.2	01132188				GOOD DATA COMPARE, BLOCK 21
			A= 50	P= 0A	ERROR, DATA NUMBER 73
			A= 0E	P= 0C	ERROR, DATA NUMBER 74
			A= 50	P= A0	ERROR, DATA NUMBER 75
					COMPARE COMPLETE
07511515149.2	01132191				GOOD DATA COMPARE, BLOCK 22
			A= 70	P= F0	ERROR, DATA NUMBER 73
			A= 4E	P= 90	ERROR, DATA NUMBER 74
			A= A0	P= 40	ERROR, DATA NUMBER 75
					COMPARE COMPLETE



Table 43. IGS Checkout Test Run (Cont)

PRG#	CP505-510-0000	TEST: IONOS REDUNDANCY TEST SUP	DATE 03/15/76	PAGE 54
TIME	ET	CHD	MEAS VALUE UNITS	REMARKS
07511515152.2	01133134			680 DATA COMPARE, BLOCK 23 ERROR, DATA NUMB 73 ERROR, DATA NUMB 74 ERROR, DATA NUMB 75 COMPARE COMPLETE
07511515155.2	01133137			680 DATA COMPARE, BLOCK 24 ERROR, DATA NUMB 13 ERROR, DATA NUMB 73 ERROR, DATA NUMB 74 ERROR, DATA NUMB 75 COMPARE COMPLETE
07511515158.2	01133140			680 DATA COMPARE, BLOCK 25 ERROR, DATA NUMB 73 ERROR, DATA NUMB 74 ERROR, DATA NUMB 75 COMPARE COMPLETE
075115161791.2	01133143			680 DATA COMPARE, BLOCK 26 ERROR, DATA NUMB 73 ERROR, DATA NUMB 74 ERROR, DATA NUMB 75 COMPARE COMPLETE
07511516174.2	01133146			680 DATA COMPARE, BLOCK 27 ERROR, DATA NUMB 84 ERROR, DATA NUMB 73 ERROR, DATA NUMB 74 ERROR, DATA NUMB 75 COMPARE COMPLETE
07511516177.2	01133149			680 DATA COMPARE, BLOCK 28 ERROR, DATA NUMB 73 ERROR, DATA NUMB 74 ERROR, DATA NUMB 75 COMPARE COMPLETE
07511516110.2	01133152			680 DATA COMPARE, BLOCK 29 ERROR, DATA NUMB 73 ERROR, DATA NUMB 74 ERROR, DATA NUMB 75 COMPARE COMPLETE
07511516113.2	01133155			680 DATA COMPARE, BLOCK 30 ERROR, DATA NUMB 73 ERROR, DATA NUMB 74 ERROR, DATA NUMB 75 COMPARE COMPLETE
07511516116.2	01133158			680 DATA COMPARE, BLOCK 31 ERROR, DATA NUMB 34 ERROR, DATA NUMB 73 ERROR, DATA NUMB 74
07511516119.2	01134101			680 DATA COMPARE, BLOCK 32 ERROR, DATA NUMB 73 ERROR, DATA NUMB 74 ERROR, DATA NUMB 75 COMPARE COMPLETE
07511516122.2	01134104			680 DATA COMPARE, BLOCK 33 ERROR, DATA NUMB 73 ERROR, DATA NUMB 74 ERROR, DATA NUMB 75 COMPARE COMPLETE
07511516125.2	01134107			680 DATA COMPARE, BLOCK 34 ERROR, DATA NUMB 73 ERROR, DATA NUMB 74 ERROR, DATA NUMB 75 COMPARE COMPLETE
07511516128.2	01134110			680 DATA COMPARE, BLOCK 35 ERROR, DATA NUMB 74 ERROR, DATA NUMB 73 ERROR, DATA NUMB 74 ERROR, DATA NUMB 75 COMPARE COMPLETE
07511516131.2	01134113			680 DATA COMPARE, BLOCK 36 ERROR, DATA NUMB 73 ERROR, DATA NUMB 74 ERROR, DATA NUMB 75 COMPARE COMPLETE
07511516134.2	01134116			680 DATA COMPARE, BLOCK 37 ERROR, DATA NUMB 73 ERROR, DATA NUMB 74 ERROR, DATA NUMB 75 COMPARE COMPLETE
07511516137.2	01134119			680 DATA COMPARE, BLOCK 38 ERROR, DATA NUMB 73 ERROR, DATA NUMB 74 ERROR, DATA NUMB 75 COMPARE COMPLETE
07511516140.2	01134122			680 DATA COMPARE, BLOCK 39 ERROR, DATA NUMB 36 ERROR, DATA NUMB 73 ERROR, DATA NUMB 74 ERROR, DATA NUMB 75 COMPARE COMPLETE
07511516143.2	01134125			680 DATA COMPARE, BLOCK 40 ERROR, DATA NUMB 73



Table 43. IGS Checkout Test Run (Cont)

[illegible]

Table 43. IGS Checkout Test Run (Cont)

PHUG SP505-910-0000 TEST: IONOSPHERIC REDUNDANCY TEST SUP DATE 03/15/78 PAGE 58				REMARKS	
TIME	ST	CHD	MEAS. VALUE	UNITS	
COMPARE COMPLETE					
075115117157.5	01135119				GBD DATA COMPARE, BLOCK 12
		A= 32	P= 66		ERRUM, DATA NUMBER 73
		A= 1A	P= 35		ERRUM, DATA NUMBER 74
		A= 00	P= 40		ERRUM, DATA NUMBER 75
					COMPARE COMPLETE
075115118100.5	01135142				GBD DATA COMPARE, BLOCK 13
		A= EF	P= 0E		ERRUM, DATA NUMBER 73
		A= 56	P= 81		ERRUM, DATA NUMBER 74
		A= E4	P= C8		ERRUM, DATA NUMBER 75
					COMPARE COMPLETE
075115118103.5	01135145				GBD DATA COMPARE, BLOCK 14
		A= C9	P= 92		ERRUM, DATA NUMBER 73
		A= 72	P= E0		ERRUM, DATA NUMBER 74
		A= 14	P= 28		ERRUM, DATA NUMBER 75
					COMPARE COMPLETE
075115118106.5	01135148				GBD DATA COMPARE, BLOCK 15
		A= 14	P= 28		ERRUM, DATA NUMBER 73
		A= 3A	P= 74		ERRUM, DATA NUMBER 74
		A= 20	P= 40		ERRUM, DATA NUMBER 75
					COMPARE COMPLETE
075115118109.5	01135151				GBD DATA COMPARE, BLOCK 16
		A= F5	P= E9		ERRUM, DATA NUMBER 73
		A= 05	P= 81		ERRUM, DATA NUMBER 74
		A= 05	P= 40		ERRUM, DATA NUMBER 75
					COMPARE COMPLETE
075115118112.5	01135154				GBD DATA COMPARE, BLOCK 17
		A= 28	P= 51		ERRUM, DATA NUMBER 73
		A= 9A	P= 35		ERRUM, DATA NUMBER 74
		A= EC	P= 08		ERRUM, DATA NUMBER 75
					COMPARE COMPLETE
075115118115.5	01135157				GBD DATA COMPARE, BLOCK 18
		A= 0E	P= 10		ERRUM, DATA NUMBER 73
		A= 0A	P= 74		ERRUM, DATA NUMBER 74
		A= 1C	P= 3A		ERRUM, DATA NUMBER 75
					COMPARE COMPLETE
075115118118.5	01135100				GBD DATA COMPARE, BLOCK 19
		A= 03	P= A7		ERRUM, DATA NUMBER 73
		A= F0	P= F0		ERRUM, DATA NUMBER 74
		A= 28	P= 50		ERRUM, DATA NUMBER 75
					COMPARE COMPLETE
075115118121.5	01135103				GBD DATA COMPARE, BLOCK 20
		A= 42	P= 65		ERRUM, DATA NUMBER 73
		A= E8	P= F7		ERRUM, DATA NUMBER 74
		A= FC	P= F8		ERRUM, DATA NUMBER 75
					COMPARE COMPLETE
PHUG SP505-910-0000 TEST: IONOSPHERIC REDUNDANCY TEST SUP DATE 03/15/78 PAGE 59					
TIME	ST	CHD	MEAS. VALUE	UNITS	
075115118124.5	01135106				GBD DATA COMPARE, BLOCK 21
		A= 0E	P= 3F		ERRUM, DATA NUMBER 73
		A= 09	P= 73		ERRUM, DATA NUMBER 74
		A= C8	P= 90		ERRUM, DATA NUMBER 75
					COMPARE COMPLETE
075115118127.5	01135109				GBD DATA COMPARE, BLOCK 22
		A= 04	P= 73		ERRUM, DATA NUMBER 73
		A= 90	P= 32		ERRUM, DATA NUMBER 74
		A= 36	P= 70		ERRUM, DATA NUMBER 75
					COMPARE COMPLETE
075115118130.5	01135112				GBD DATA COMPARE, BLOCK 23
		A= 04	P= C9		ERRUM, DATA NUMBER 73
		A= 08	P= 06		ERRUM, DATA NUMBER 74
		A= 0C	P= 18		ERRUM, DATA NUMBER 75
					COMPARE COMPLETE
075115118133.5	01135115				GBD DATA COMPARE, BLOCK 24
		A= 0A	P= 04		ERRUM, DATA NUMBER 73
		A= 78	P= F0		ERRUM, DATA NUMBER 74
		A= 3C	P= 78		ERRUM, DATA NUMBER 75
					COMPARE COMPLETE
075115118136.5	01135118				GBD DATA COMPARE, BLOCK 25
		A= 07	P= 0E		ERRUM, DATA NUMBER 73
		A= 3A	P= 74		ERRUM, DATA NUMBER 74
		A= C8	P= 10		ERRUM, DATA NUMBER 75
					COMPARE COMPLETE
075115118139.5	01135121				GBD DATA COMPARE, BLOCK 26
		A= 21	P= 42		ERRUM, DATA NUMBER 73
		A= 1A	P= 35		ERRUM, DATA NUMBER 74
		A= F8	P= F0		ERRUM, DATA NUMBER 75
					COMPARE COMPLETE
075115118142.5	01135124				GBD DATA COMPARE, BLOCK 27
		A= FC	P= F6		ERRUM, DATA NUMBER 73
		A= 0E	P= 81		ERRUM, DATA NUMBER 74
		A= CC	P= 46		ERRUM, DATA NUMBER 75
					COMPARE COMPLETE
075115118145.5	01135127				GBD DATA COMPARE, BLOCK 28
		A= 80	P= 0A		ERRUM, DATA NUMBER 73
		A= 56	P= 06		ERRUM, DATA NUMBER 74
		A= 3A	P= 30		ERRUM, DATA NUMBER 75
					COMPARE COMPLETE
075115118148.5	01135130				GBD DATA COMPARE, BLOCK 29
		A= 04	P= 00		ERRUM, DATA NUMBER 73
		A= 14	P= 32		ERRUM, DATA NUMBER 74
		A= 2C	P= 58		ERRUM, DATA NUMBER 75
					COMPARE COMPLETE

Table 43. IGS Checkout Test Run (Cont)

PRGM	CP300-510-0000	TESTS	IGMS REDUNDANCY TEST	SUP	DATE	03/13/76	PAGE	00
TIME	SI	CMD	NAME	VALUE	UNIT	REMARKS		
0751111111.3	01111111					END DATA COMPARE, BLOCK 30		
		A= 90	P= 20			ERRUM, DATA NUMBER 73		
		A= 10	P= 73			ERRUM, DATA NUMBER 74		
		A= 00	P= 00			ERRUM, DATA NUMBER 75		
						COMPARE COMPLETE		
0751111111.3	01111111					END DATA COMPARE, BLOCK 31		
		A= 40	P= 00			ERRUM, DATA NUMBER 73		
		A= 70	P= 73			ERRUM, DATA NUMBER 74		
		A= 00	P= 00			ERRUM, DATA NUMBER 75		
						COMPARE COMPLETE		
0751111111.3	01111111					END DATA COMPARE, BLOCK 32		
		A= 11	P= 20			ERRUM, DATA NUMBER 73		
		A= 1A	P= 73			ERRUM, DATA NUMBER 74		
		A= 00	P= 00			ERRUM, DATA NUMBER 75		
						COMPARE COMPLETE		
0751111111.3	01111111					END DATA COMPARE, BLOCK 33		
		A= 09	P= 92			ERRUM, DATA NUMBER 73		
		A= 30	P= 81			ERRUM, DATA NUMBER 74		
		A= 00	P= 00			ERRUM, DATA NUMBER 75		
						COMPARE COMPLETE		
0751111111.3	01111111					END DATA COMPARE, BLOCK 34		
		A= 07	P= 00			ERRUM, DATA NUMBER 73		
		A= 20	P= 70			ERRUM, DATA NUMBER 74		
		A= 00	P= 00			ERRUM, DATA NUMBER 75		
						COMPARE COMPLETE		
0751111111.3	01111111					END DATA COMPARE, BLOCK 35		
		A= 34	P= 00			ERRUM, DATA NUMBER 73		
		A= 3A	P= 70			ERRUM, DATA NUMBER 74		
		A= 70	P= 00			ERRUM, DATA NUMBER 75		
						COMPARE COMPLETE		
0751111111.3	01111111					END DATA COMPARE, BLOCK 36		
		A= 43	P= 00			ERRUM, DATA NUMBER 73		
		A= 30	P= 73			ERRUM, DATA NUMBER 74		
		A= 00	P= 00			ERRUM, DATA NUMBER 75		
						COMPARE COMPLETE		
0751111111.3	01111111					END DATA COMPARE, BLOCK 37		
		A= 70	P= 70			ERRUM, DATA NUMBER 73		
		A= 70	P= 77			ERRUM, DATA NUMBER 74		
		A= 00	P= 00			ERRUM, DATA NUMBER 75		
						COMPARE COMPLETE		
0751111111.3	01111111					END DATA COMPARE, BLOCK 38		
		A= 00	P= 00			ERRUM, DATA NUMBER 73		
		A= 00	P= 00			ERRUM, DATA NUMBER 74		
		A= 00	P= 00			ERRUM, DATA NUMBER 75		
						COMPARE COMPLETE		
0751111111.3	01111111					END DATA COMPARE, BLOCK 39		
		A= 00	P= 00			ERRUM, DATA NUMBER 73		
		A= 00	P= 00			ERRUM, DATA NUMBER 74		
		A= 00	P= 00			ERRUM, DATA NUMBER 75		
						COMPARE COMPLETE		
0751111111.3	01111111					END DATA COMPARE, BLOCK 40		
		A= 00	P= 00			ERRUM, DATA NUMBER 73		
		A= 00	P= 00			ERRUM, DATA NUMBER 74		
		A= 00	P= 00			ERRUM, DATA NUMBER 75		
						COMPARE COMPLETE		
0751111111.3	01111111					END DATA COMPARE, BLOCK 41		
		A= 00	P= 00			ERRUM, DATA NUMBER 73		
		A= 00	P= 00			ERRUM, DATA NUMBER 74		
		A= 00	P= 00			ERRUM, DATA NUMBER 75		
						COMPARE COMPLETE		
0751111111.3	01111111					END DATA COMPARE, BLOCK 42		
		A= 00	P= 00			ERRUM, DATA NUMBER 73		
		A= 00	P= 00			ERRUM, DATA NUMBER 74		
		A= 00	P= 00			ERRUM, DATA NUMBER 75		
						COMPARE COMPLETE		
0751111111.3	01111111					END DATA COMPARE, BLOCK 43		
		A= 00	P= 00			ERRUM, DATA NUMBER 73		
		A= 00	P= 00			ERRUM, DATA NUMBER 74		
		A= 00	P= 00			ERRUM, DATA NUMBER 75		
						COMPARE COMPLETE		
0751111111.3	01111111					END DATA COMPARE, BLOCK 44		
		A= 00	P= 00			ERRUM, DATA NUMBER 73		
		A= 00	P= 00			ERRUM, DATA NUMBER 74		
		A= 00	P= 00			ERRUM, DATA NUMBER 75		
						COMPARE COMPLETE		
0751111111.3	01111111					END DATA COMPARE, BLOCK 45		
		A= 00	P= 00			ERRUM, DATA NUMBER 73		
		A= 00	P= 00			ERRUM, DATA NUMBER 74		
		A= 00	P= 00			ERRUM, DATA NUMBER 75		
						COMPARE COMPLETE		
0751111111.3	01111111					END DATA COMPARE, BLOCK 46		
		A= 00	P= 00			ERRUM, DATA NUMBER 73		
		A= 00	P= 00			ERRUM, DATA NUMBER 74		
		A= 00	P= 00			ERRUM, DATA NUMBER 75		
						COMPARE COMPLETE		
0751111111.3	01111111					END DATA COMPARE, BLOCK 47		
		A= 00	P= 00			ERRUM, DATA NUMBER 73		
		A= 00	P= 00			ERRUM, DATA NUMBER 74		
		A= 00	P= 00			ERRUM, DATA NUMBER 75		
						COMPARE COMPLETE		
0751111111.3	01111111					END DATA COMPARE, BLOCK 48		
		A= 00	P= 00			ERRUM, DATA NUMBER 73		
		A= 00	P= 00			ERRUM, DATA NUMBER 74		
		A= 00	P= 00			ERRUM, DATA NUMBER 75		
						COMPARE COMPLETE		
0751111111.3	01111111					END DATA COMPARE, BLOCK 49		
		A= 00	P= 00			ERRUM, DATA NUMBER 73		
		A= 00	P= 00			ERRUM, DATA NUMBER 74		
		A= 00	P= 00			ERRUM, DATA NUMBER 75		
						COMPARE COMPLETE		
0751111111.3	01111111					END DATA COMPARE, BLOCK 50		
		A= 00	P= 00			ERRUM, DATA NUMBER 73		
		A= 00	P= 00			ERRUM, DATA NUMBER 74		
		A= 00	P= 00			ERRUM, DATA NUMBER 75		
						COMPARE COMPLETE		

END
D1 DATA ROUTINE



Table 43. IGS Checkout Test Run (Cont)

CP505-019-0000 LS DATA JUMP, PROCESSING DATE: 03/21/70 PAGE 25
LS LINK DATA REQ'D FOR TEST. CIV. INTEGRATED SYSTEM. ICD DATE 03/21/70 REEL 1
PROCESSING MODE: CONTINUOUS

IGS DATA ROUTINE D1
(INCREMENTING PATTERN)

FRAME TIME 001118146130.5
1F 90 CA 12 AR 07 08 09 BA AC AG AV AE AF IV
71 72 73 74 75 76 77 78 79 8A AB AC AD AE AF VE
AA AB AC AD AE AF 07 08 09 0A 0B 0C 0D 0E 0F
AF 91 92 93 94 95 96 97 98 99 AA AB AC AD AE AF
9E 9F AA AB AC AD AE AF 07 08 09 0A 0B 0C 0D 0E 0F

FRAME TIME 001118146130.5
1F 90 CA 13 00 AA AB AC AD AE AF BV CV DI E2 B3
EA EB EC ED EE EF 07 08 09 0A 0B 0C 0D 0E 0F
C3 C4 C5 C6 C7 C8 C9 CA CB CC CD CE CF 00 01
02 03 04 05 06 07 08 09 0A 0B 0C 0D 0E 0F EV
E1 E2 E3 E4 E5 E6 E7 E8 E9 EA EB EC ED EA FA

FRAME TIME 001118146130.5
1F 90 CA 15 00 30 31 32 33 34 35 36 37 38 39
3A 3B 3C 3D 3E 3F 40 41 42 43 44 45 46 47 48
49 4A 4B 4C 4D 4E 4F 50 51 52 53 54 55 56 57
58 59 5A 5B 5C 5D 5E 5F 60 61 62 63 64 65 66
67 68 69 6A 6B 6C 6D 6E 6F 70 71 72 73 74 75

FRAME TIME 001118146130.5
1F 90 CA 16 00 73 74 75 76 77 78 79 7A 7B 7C
7D 7E 7F 80 81 82 83 84 85 86 87 88 89 8A 8B
8C 8D 8E 8F 90 91 92 93 94 95 96 97 98 99 9A
9B 9C 9D 9E 9F A0 A1 A2 A3 A4 A5 A6 A7 A8 A9
AA AB AC AD AE AF 80 81 82 83 84 85 86 87 88 89

FRAME TIME 001118146131.5
1F 90 CA 17 00 8B 8C 8D 8E 8F 9A 9B 9C 9D 9E 9F
CA CB CC CD CE CF 00 01 02 03 04 05 06 07 08 09
0A 0B 0C 0D 0E 0F 00 01 02 03 04 05 06 07 08 09
0A 0B 0C 0D 0E 0F 00 01 02 03 04 05 06 07 08 09
0A 0B 0C 0D 0E 0F 00 01 02 03 04 05 06 07 08 09

FRAME TIME 001118146132.5
1F 90 CA 18 00 F9 FA FB FC FD FE FF 00 01 02
03 04 05 06 07 08 09 0A 0B 0C 0D CE UF 10 11
12 13 14 15 16 17 18 19 1A 1B 1C 1D 1E 1F 20
21 22 23 24 25 26 27 28 29 2A 2B 2C 2D 2E 2F
30 31 32 33 34 35 36 37 38 39 3A 3B 3C 3D 3E 3F

FRAME TIME 001118146137.5
1F 90 CA 19 00 3C 3D 3E 3F 40 41 42 43 44 45
46 47 48 49 4A 4B 4C 4D 4E 4F 50 51 52 53 54
55 56 57 58 59 5A 5B 5C 5D 5E 5F 60 61 62 63
64 65 66 67 68 69 6A 6B 6C 6D 6E 6F 70 71 72
73 74 75 76 77 78 79 7A 7B 7C 7D 7E 7F 29 2A

63 SYNC WORD
FRAME COUNT
EVENT PRINT



Table 43. IGS Checkout Test Run (Cont)

CP505-619-0000 L3 DATA DUMP, PROCESSING DATE: 03/21/76 PAGE 32
L3 LINK DATA DECOM FOR TEST: ETV INTEGRATED SYSTEM TEST DATE 03/21/76 REEL 1
PROCESSING MODE: CONTINUOUS

FRAME TIME 08110149107.0
IF 90 CA 10 00 FF FF FF FF FF FF FF FF FF
FF FF FF FF FF FF FF FF FF FF FF FF FF
FF FF FF FF FF FF FF FF FF FF FF FF FF
FF FF FF FF FF FF FF FF FF FF FF FF FF

IGS DATA ROUTINE D1
(ALL ONE'S PATTERN)

FRAME TIME 08110149130.0
IF 90 CA 10 00 FF FF FF FF FF FF FF FF FF
FF FF FF FF FF FF FF FF FF FF FF FF FF
FF FF FF FF FF FF FF FF FF FF FF FF FF
FF FF FF FF FF FF FF FF FF FF FF FF FF

RAW DATA FROM TAPE (TYPICAL)

FRAME TIME 08110149153.0
IF 90 CA 10 00 FF FF FF FF FF FF FF FF FF
FF FF FF FF FF FF FF FF FF FF FF FF FF
FF FF FF FF FF FF FF FF FF FF FF FF FF
FF FF FF FF FF FF FF FF FF FF FF FF FF

FRAME TIME 08110149159.0
IF 90 CA 21 00 FF FF FF FF FF FF FF FF FF
FF FF FF FF FF FF FF FF FF FF FF FF FF
FF FF FF FF FF FF FF FF FF FF FF FF FF
FF FF FF FF FF FF FF FF FF FF FF FF FF

FRAME TIME 08110150102.0
IF 90 CA 22 00 FF FF FF FF FF FF FF FF FF
FF FF FF FF FF FF FF FF FF FF FF FF FF
FF FF FF FF FF FF FF FF FF FF FF FF FF
FF FF FF FF FF FF FF FF FF FF FF FF FF

FRAME TIME 08110150125.0
IF 90 CA 23 00 FF FF FF FF FF FF FF FF FF
FF FF FF FF FF FF FF FF FF FF FF FF FF
FF FF FF FF FF FF FF FF FF FF FF FF FF
FF FF FF FF FF FF FF FF FF FF FF FF FF

FRAME TIME 08110150100.0
IF 90 CA 24 00 FF FF FF FF FF FF FF FF FF
FF FF FF FF FF FF FF FF FF FF FF FF FF
FF FF FF FF FF FF FF FF FF FF FF FF FF
FF FF FF FF FF FF FF FF FF FF FF FF FF

CP505-619-0000 L3 DATA DUMP, PROCESSING DATE: 03/21/76 PAGE 33
L3 LINK DATA DECOM FOR TEST: ETV INTEGRATED SYSTEM TEST DATE 03/21/76 REEL 1
PROCESSING MODE: CONTINUOUS

FRAME TIME 08110152132.5
IF 90 CA 1F 00 00 00 00 00 00 00 00 00 00 00
00 00 00 00 00 00 00 00 00 00 00 00
00 00 00 00 00 00 00 00 00 00 00 00
00 00 00 00 00 00 00 00 00 00 00 00

IGS DATA ROUTINE D1
(ALL ZERO'S PATTERN)

FRAME TIME 08110152138.5
IF 90 CA 21 00 00 00 00 00 00 00 00 00 00 00
00 00 00 00 00 00 00 00 00 00 00 00
00 00 00 00 00 00 00 00 00 00 00 00
00 00 00 00 00 00 00 00 00 00 00 00

RAW DATA FROM TAPE
(TYPICAL)

FRAME TIME 08110152141.5
IF 90 CA 22 00 00 00 00 00 00 00 00 00 00 00
00 00 00 00 00 00 00 00 00 00 00 00
00 00 00 00 00 00 00 00 00 00 00 00
00 00 00 00 00 00 00 00 00 00 00 00

FRAME TIME 08110152144.5
IF 90 CA 23 00 00 00 00 00 00 00 00 00 00 00
00 00 00 00 00 00 00 00 00 00 00 00
00 00 00 00 00 00 00 00 00 00 00 00
00 00 00 00 00 00 00 00 00 00 00 00

FRAME TIME 08110152147.5
IF 90 CA 24 00 00 00 00 00 00 00 00 00 00 00
00 00 00 00 00 00 00 00 00 00 00 00
00 00 00 00 00 00 00 00 00 00 00 00
00 00 00 00 00 00 00 00 00 00 00 00

FRAME TIME 08110152150.5
IF 90 CA 25 00 00 00 00 00 00 00 00 00 00 00
00 00 00 00 00 00 00 00 00 00 00 00
00 00 00 00 00 00 00 00 00 00 00 00
00 00 00 00 00 00 00 00 00 00 00 00

FRAME TIME 08110152153.5
IF 90 CA 27 00 00 00 00 00 00 00 00 00 00 00
00 00 00 00 00 00 00 00 00 00 00 00
00 00 00 00 00 00 00 00 00 00 00 00
00 00 00 00 00 00 00 00 00 00 00 00



Table 44. SOH Readout

[illegible]

Table 44. SOH Readout (Cont)

FROM CRDS 05/15/76	TESTS	STATUS	REUNDANCY	TEST	SUP	DATE 05/15/76	PAGE 120	REMARKS
TYPE	UNIT	CL	Q-0	MEAS	VALUE	UNITS		
1	0	0	20	29	1	0	20	15 00 00
2	0	0	20	29	2	0	1	00 15 00 00
3	0	0	20	29	3	0	0	00 20 00 00
4	0	0	20	29	4	0	0	00 25 00 00
5	0	0	20	29	5	0	0	00 30 00 00
6	0	0	20	29	6	0	0	00 35 00 00
7	0	0	20	29	7	0	0	00 40 00 00
8	0	0	20	29	8	0	0	00 45 00 00
9	0	0	1F	29	9	1	0	00 50 00 00
10	0	0	20	29	10	1	1	00 55 00 00
11	0	0	20	29	11	1	0	00 00 00 00
12	0	0	20	29	12	1	0	00 05 00 00
13	0	0	20	29	13	1	0	00 10 00 00
14	0	0	20	29	14	1	0	00 15 00 00
15	0	0	20	29	15	1	0	00 20 00 00
16	0	0	20	29	16	1	0	00 25 00 00

STORED SOH DATA

075117100123.1	00120155	MONITOR NO 5	4533	+0.000	VOC	MUX 0, MUX 3	PARA	STATE 1
			4534	+0.173	VOC	MUX 0, MUX 3	30PARA	STATE 2
			4535	+0.000	VOC	MUX 0, MUX 3	PARA	STATE 3
			4536	+0.350	VOC	MUX 0, MUX 3	30PARA	STATE 4
			4537	+0.050	VOC	MUX 0, MUX 3	12V A	STATE 5
			4538	+0.050	VOC	MUX 0, MUX 3	12V S	STATE 6
			4539	+0.070	VOC	MUX 0, MUX 3	A1 V	STATE 7
			4540	+0.070	VOC	MUX 0, MUX 3	A2 V	STATE 8

REAL TIME ANALOG MONITORS #5 THRU 8

075117100123.1	00120156	MONITOR NO 6	4541	+0.000	VOC	MUX 0, MUX 3	PARA	STATE 9
			4542	+0.173	VOC	MUX 0, MUX 3	30PARA	STATE 10
			4543	+0.000	VOC	MUX 0, MUX 3	PARA	STATE 11
			4544	+0.350	VOC	MUX 0, MUX 3	30PARA	STATE 12
			4545	+0.050	VOC	MUX 0, MUX 3	12V A	STATE 13
			4546	+0.050	VOC	MUX 0, MUX 3	12V S	STATE 14
			4547	+0.070	VOC	MUX 0, MUX 3	A1 V	STATE 15
			4548	+0.070	VOC	MUX 0, MUX 3	A2 V	STATE 16

TIMED TEST CMD

075117100124.0	00120155	MONITOR NO 7	4549	+0.020	NA	MUX 0, MUX 4	NOISE N	STATE 1
			4550	+0.020	NA	MUX 0, MUX 4	NOISE F	STATE 2
			4551	+0.020	NA	MUX 0, MUX 4	NOISE Y	STATE 3
			4552	+0.020	NA	MUX 0, MUX 4	NOISE R	STATE 4
			4553	+0.011	NA	MUX 0, MUX 4	NOISE C	STATE 5
			4554	+0.011	NA	MUX 0, MUX 4	NOISE G	STATE 6
			4555	+0.000	NA	MUX 0, MUX 4	NOISE B	STATE 7
			4556	+0.000	DESP	MUX 0, MUX 4	SEND T	STATE 8

075117100125.0	00120155	MONITOR NO 8	4557	+0.150	VOC	MUX 0, MUX 4	+15VOC	STATE 9
			4558	+0.150	VOC	MUX 0, MUX 4	+15VOC	STATE 10
			4559	+0.000	DESP	MUX 0, MUX 4	LEND T	STATE 11
			4560	+0.000	VOC	MUX 0, MUX 4	+18VOC	STATE 12
			4561	+0.000	VOC	MUX 0, MUX 4	+18VOC	STATE 13
			4562	+0.000	VOC	MUX 0, MUX 4	+18VOC	STATE 14

FROM CRDS 05/15/76	TESTS	STATUS	REUNDANCY	TEST	SUP	DATE 05/15/76	PAGE 127	REMARKS
TYPE	UNIT	CL	Q-0	MEAS	VALUE	UNITS		
4563	+0.000	VOC	MUX 0, MUX 4	+11VOC	STATE 12			
4564	+0.000	VOC	MUX 0, MUX 4	+10VOC	STATE 10			

TIMED TEST CMD

075117100126.0	00120156	MONITOR NO 9	4565	+0.000	NA	MUX 0, MUX 4	NOISE N	STATE 1
			4566	+0.000	NA	MUX 0, MUX 4	NOISE F	STATE 2
			4567	+0.000	NA	MUX 0, MUX 4	NOISE Y	STATE 3
			4568	+0.000	NA	MUX 0, MUX 4	NOISE R	STATE 4
			4569	+0.000	NA	MUX 0, MUX 4	NOISE C	STATE 5
			4570	+0.000	NA	MUX 0, MUX 4	NOISE G	STATE 6
			4571	+0.000	NA	MUX 0, MUX 4	NOISE B	STATE 7
			4572	+0.000	DESP	MUX 0, MUX 4	SEND T	STATE 8

075117100127.0	00120156	MONITOR NO 10	4573	+0.000	VOC	MUX 0, MUX 4	+15VOC	STATE 9
			4574	+0.000	VOC	MUX 0, MUX 4	+15VOC	STATE 10
			4575	+0.000	DESP	MUX 0, MUX 4	LEND T	STATE 11
			4576	+0.000	VOC	MUX 0, MUX 4	+18VOC	STATE 12
			4577	+0.000	VOC	MUX 0, MUX 4	+18VOC	STATE 13
			4578	+0.000	VOC	MUX 0, MUX 4	+18VOC	STATE 14

075117100128.0	00120156	MONITOR NO 11	4579	+0.000	VOC	MUX 0, MUX 4	+15VOC	STATE 9
			4580	+0.000	VOC	MUX 0, MUX 4	+15VOC	STATE 10
			4581	+0.000	DESP	MUX 0, MUX 4	LEND T	STATE 11
			4582	+0.000	VOC	MUX 0, MUX 4	+18VOC	STATE 12
			4583	+0.000	VOC	MUX 0, MUX 4	+18VOC	STATE 13
			4584	+0.000	VOC	MUX 0, MUX 4	+18VOC	STATE 14

075117100129.0	00120156	MONITOR NO 12	4585	+0.000	VOC	MUX 0, MUX 4	+15VOC	STATE 9
			4586	+0.000	VOC	MUX 0, MUX 4	+15VOC	STATE 10
			4587	+0.000	DESP	MUX 0, MUX 4	LEND T	STATE 11
			4588	+0.000	VOC	MUX 0, MUX 4	+18VOC	STATE 12
			4589	+0.000	VOC	MUX 0, MUX 4	+18VOC	STATE 13
			4590	+0.000	VOC	MUX 0, MUX 4	+18VOC	STATE 14

075117100130.0	00120156	MONITOR NO 13	4591	+0.000	VOC	MUX 0, MUX 4	+15VOC	STATE 9
			4592	+0.000	VOC	MUX 0, MUX 4	+15VOC	STATE 10
			4593	+0.000	DESP	MUX 0, MUX 4	LEND T	STATE 11
			4594	+0.000	VOC	MUX 0, MUX 4	+18VOC	STATE 12
			4595	+0.000	VOC	MUX 0, MUX 4	+18VOC	STATE 13
			4596	+0.000	VOC	MUX 0, MUX 4	+18VOC	STATE 14

075117100131.0	00120156	MONITOR NO 14	4597	+0.000	VOC	MUX 0, MUX 4	+15VOC	STATE 9
			4598	+0.000	VOC	MUX 0, MUX 4	+15VOC	STATE 10
			4599	+0.000	DESP	MUX 0, MUX 4	LEND T	STATE 11
			4600	+0.000	VOC	MUX 0, MUX 4	+18VOC	STATE 12
			4601	+0.000	VOC	MUX 0, MUX 4	+18VOC	STATE 13
			4602	+0.000	VOC	MUX 0, MUX 4	+18VOC	STATE 14

075117100132.0	00120156	MONITOR NO 15	4603	+0.000	VOC	MUX 0, MUX 4	+15VOC	STATE 9
			4604	+0.000	VOC	MUX 0, MUX 4	+15VOC	STATE 10
			4605	+0.000	DESP	MUX 0, MUX 4	LEND T	STATE 11
			4606	+0.000	VOC	MUX 0, MUX 4	+18VOC	STATE 12
			4607	+0.000	VOC	MUX 0, MUX 4	+18VOC	STATE 13
			4608	+0.000	VOC	MUX 0, MUX 4	+18VOC	STATE 14

075117100133.0	00120156	MONITOR NO 16	4609	+0.000	VOC	MUX 0, MUX 4	+15VOC	STATE 9
			4610	+0.000	VOC	MUX 0, MUX 4	+15VOC	STATE 10
			4611	+0.000	DESP	MUX 0, MUX 4	LEND T	STATE 11
			4612	+0.000	VOC	MUX 0, MUX 4	+18VOC	STATE 12
			4613	+0.000	VOC	MUX 0, MUX 4	+18VOC	STATE 13
			4614	+0.000	VOC	MUX 0, MUX 4	+18VOC	STATE 14

075117100134.0	00120156	MONITOR NO 17	4615	+0.000	VOC	MUX 0, MUX 4	+15VOC	STATE 9
			4616	+0.000	VOC	MUX 0, MUX 4	+15VOC	STATE 10
			4617	+0.000	DESP	MUX 0, MUX 4	LEND T	STATE 11
			4618	+0.000	VOC	MUX 0, MUX 4	+18VOC	STATE 12
			4619	+0.000	VOC	MUX 0, MUX 4	+18VOC	STATE 13
			4620	+0.000	VOC	MUX 0, MUX 4	+18VOC	STATE 14

075117100135.0	00120156	MONITOR NO 18	4621	+0.000	VOC	MUX 0, MUX 4	+15VOC	STATE 9
			4622	+0.000	VOC	MUX 0, MUX 4	+15VOC	STATE 10
			4623	+0.000	DESP	MUX 0, MUX 4	LEND T	STATE 11
			4624	+0.000	VOC	MUX 0, MUX 4	+18VOC	STATE 12
			4625	+0.000	VOC	MUX 0, MUX 4	+18VOC	STATE 13
			4626	+0.000	VOC	MUX 0, MUX 4	+18VOC	STATE 14

075117100136.0	00120156	MONITOR NO 19	4627	+0.000	VOC	MUX 0, MUX 4	+15VOC	STATE 9
			4628	+0.000	VOC	MUX 0, MUX 4	+15VOC	STATE 10
			4629	+0.000	DESP	MUX 0, MUX 4	LEND T	STATE 11
			4630	+0.000	VOC	MUX 0, MUX 4	+18VOC	STATE 12
			4631	+0.000	VOC	MUX 0, MUX 4	+18VOC	STATE 13
			4632	+0.000	VOC	MUX 0, MUX 4	+18VOC	STATE 14

075117100137.0	00120156	MONITOR NO 20	4633	+0.000	VOC	MUX 0, MUX 4	+15VOC	STATE 9
			4634	+0.000	VOC	MUX 0, MUX 4	+15VOC	STATE 10
			4635	+0.000	DESP	MUX 0, MUX 4	LEND T	STATE 11
			4636	+0.000	VOC	MUX 0, MUX 4	+18VOC	STATE 12
			4637	+0.000	VOC	MUX 0, MUX 4	+18VOC	STATE 13
			4638	+0.000	VOC	MUX 0, MUX 4	+18VOC	STATE 14

075117100138.0	00120156	MONITOR NO 21	4639	+0.000	VOC	MUX 0, MUX 4	+15VOC	STATE 9
			4640	+0.000	VOC	MUX 0, MUX 4	+15VOC	STATE 10
			4641	+0.000	DESP	MUX 0, MUX 4	LEND T	STATE 11
			4642	+0.000	VOC	MUX 0, MUX 4	+18VOC	STATE 12
			4643	+0.000	VOC	MUX 0, MUX 4	+18VOC	STATE 13
			4644	+0.000	VOC	MUX 0, MUX 4	+18VOC	STATE 14

075117100139.0	00120156	MONITOR NO 22	4645	+0.000	VOC	MUX 0, MUX 4	+15VOC	STATE 9
			4646	+0.000	VOC	MUX 0, MUX 4	+15VOC	STATE 10
			4647	+0.000	DESP	MUX 0, MUX 4	LEND T	STATE 11
			4648	+0.000	VOC	MUX 0, MUX 4	+18VOC	STATE 12
			4649	+0.000	VOC	MUX 0, MUX 4	+18VOC	STATE 13
			4650	+0.000	VOC	MUX 0, MUX 4	+18VOC	STATE 14

075117100140.0	00120156	MONITOR NO 23	4651	+0.000	VOC	MUX 0, MUX 4	+15VOC	STATE 9
			4652	+0.000	VOC	MUX 0, MUX 4	+15VOC	STATE 10
			4653	+0.000	DESP	MUX 0, MUX 4	LEND T	STATE 11
			4654	+0.000	VOC	MUX 0, MUX 4	+18VOC	STATE 12
			4655	+0.000	VOC	MUX 0, MUX 4	+18VOC	STATE 13
			4656	+0.000	VOC	MUX 0, MUX 4	+18VOC	STATE 14

075117100141.0	00120156	MONITOR NO 24	4657	+0.000	VOC	MUX 0, MUX 4	+15VOC	STATE 9
			4658	+0.000	VOC	MUX 0, MUX 4	+15VOC	STATE 10
			4659	+0.000	DESP	MUX 0, MUX 4	LEND T	STATE 11
			4660	+0.000	VOC	MUX 0, MUX 4	+18VOC	STATE 12
			4661	+0.000	VOC	MUX 0, MUX 4	+18VOC	STATE 13
			4662	+0.000	VOC	MUX 0, MUX 4	+18VOC	STATE 14

075117100142.0	00120156	MONITOR NO 25	4663	+0.000	VOC	MUX 0, MUX 4	+15VOC	STATE 9
			4664	+0.000	VOC	MUX 0, MUX 4	+15VOC	STATE 10
			4665	+0.000	DESP	MUX 0, MUX 4	LEND T	STATE 11
			4666	+0.000	VOC	MUX 0, MUX 4	+18VOC	STATE 12
			4667	+0.000	VOC	MUX 0, MUX 4	+18VOC	STATE 13
			4668	+0.000	VOC	MUX 0, MUX 4	+18VOC	STATE 14

075117100143.0	00120156	MONITOR NO 26	4669	+0.000	VOC	MUX 0, MUX 4	+15VOC	STATE 9
			4670	+0.000	VOC	MUX 0, MUX 4	+15VOC	STATE 10
			4671	+0.000	DESP	MUX 0, MUX 4	LEND T	STATE 11
			4672	+0.000	VOC	MUX 0, MUX		

Table 44. SOH Reactant (Cont)

LAST TIMED TEST CND

Table 44. SOH Readout (Cont)

PRG#	CP#	SP#	1000	4000	8000	TEST	DATE	03/15/78	PAGE	138
TRD	FILE	SL	CH	DATA	VALUE	UNIT	ALPHA			
075017400113.2 00127143										
0341	03.101	VDC	MUX 1, MUX 2	CR52	STATE 11					
0340	03.100	VDC	MUX 1, MUX 3	CR5008	STATE 10					
0343	03.103	VDC	MUX 1, MUX 1	12V A	STATE 13					
0340	03.100	VDC	MUX 1, MUX 3	12V B	STATE 10					
0347	03.107	VDC	MUX 1, MUX 3	41 V	STATE 13					
0340	03.100	VDC	MUX 1, MUX 3	12 V	STATE 10					
075017400113.2 00127143										
0342	03.102	HA	MUX 1, MUX 4	NOISE N	STATE 1					
0340	03.100	HA	MUX 1, MUX 4	NOISE P	STATE 2					
0341	03.101	HA	MUX 1, MUX 4	97CUB N	STATE 3					
0342	03.102	HA	MUX 1, MUX 4	97CUB P	STATE 4					
0343	03.103	HA	MUX 1, MUX 4	30 AS C	STATE 5					
0340	03.100	HA	MUX 1, MUX 4	30 B C	STATE 6					
0343	03.103	HA	MUX 1, MUX 4	35 C C	STATE 7					
0340	03.100	HA	MUX 1, MUX 4	30 AS 1	STATE 8					
075017400113.2 00127144										
0347	03.107	VDC	MUX 1, MUX 4	013VDC	STATE 9					
0340	03.100	VDC	MUX 1, MUX 4	013VDC	STATE 10					
0340	03.100	VDC	MUX 1, MUX 4	013VDC	STATE 11					
0340	03.100	VDC	MUX 1, MUX 4	013VDC	STATE 12					
0341	03.101	VDC	MUX 1, MUX 4	013VDC	STATE 13					
0342	03.102	VDC	MUX 1, MUX 4	013VDC	STATE 14					
0343	03.103	VDC	MUX 1, MUX 4	013VDC	STATE 15					
0340	03.100	VDC	MUX 1, MUX 4	013VDC	STATE 16					
075017400113.2 00127150										
SA MP1 UN2 AM2 AM3 AM4 AM5 AM6 AM7 AM8 AM9 AM10 AM11 AM12										
1	0	0	0	0	0	0	0	0	0	0
2	0	0	0	0	0	0	0	0	0	0
3	0	0	0	0	0	0	0	0	0	0
4	0	0	0	0	0	0	0	0	0	0
5	0	0	0	0	0	0	0	0	0	0
6	0	0	0	0	0	0	0	0	0	0
7	0	0	0	0	0	0	0	0	0	0
8	0	0	0	0	0	0	0	0	0	0
9	0	0	0	0	0	0	0	0	0	0
10	0	0	0	0	0	0	0	0	0	0
11	0	0	0	0	0	0	0	0	0	0
12	0	0	0	0	0	0	0	0	0	0
13	0	0	0	0	0	0	0	0	0	0
14	0	0	0	0	0	0	0	0	0	0
15	0	0	0	0	0	0	0	0	0	0
16	0	0	0	0	0	0	0	0	0	0
17	0	0	0	0	0	0	0	0	0	0
18	0	0	0	0	0	0	0	0	0	0
19	0	0	0	0	0	0	0	0	0	0
20	0	0	0	0	0	0	0	0	0	0
075017400113.2 00127151										
0343	03.103	VDC	MUX 1, MUX 5	CR5008	STATE 1					
0342	03.102	VDC	MUX 1, MUX 5	CR5008	STATE 2					
0343	03.103	VDC	MUX 1, MUX 5	CR5008	STATE 3					
0340	03.100	VDC	MUX 1, MUX 5	CR5008	STATE 4					
0347	03.107	VDC	MUX 1, MUX 5	CR5008	STATE 5					
0340	03.100	VDC	MUX 1, MUX 5	CR5008	STATE 6					
075017400113.2 00127152										
0347	03.107	VDC	MUX 1, MUX 5	CR5008	STATE 7					
0340	03.100	VDC	MUX 1, MUX 5	CR5008	STATE 8					
075017400113.2 00127153										
0347	03.107	VDC	MUX 1, MUX 5	CR5008	STATE 9					
0340	03.100	VDC	MUX 1, MUX 5	CR5008	STATE 10					
0343	03.103	VDC	MUX 1, MUX 5	CR5008	STATE 11					
0340	03.100	VDC	MUX 1, MUX 5	CR5008	STATE 12					
0347	03.107	VDC	MUX 1, MUX 5	CR5008	STATE 13					
0340	03.100	VDC	MUX 1, MUX 5	CR5008	STATE 14					
0347	03.107	VDC	MUX 1, MUX 5	CR5008	STATE 15					
0340	03.100	VDC	MUX 1, MUX 5	CR5008	STATE 16					
075017400113.2 00127154										
0347	03.107	VDC	MUX 1, MUX 5	CR5008	STATE 17					
0340	03.100	VDC	MUX 1, MUX 5	CR5008	STATE 18					
0343	03.103	VDC	MUX 1, MUX 5	CR5008	STATE 19					
0340	03.100	VDC	MUX 1, MUX 5	CR5008	STATE 20					
0347	03.107	VDC	MUX 1, MUX 5	CR5008	STATE 21					
0340	03.100	VDC	MUX 1, MUX 5	CR5008	STATE 22					
0343	03.103	VDC	MUX 1, MUX 5	CR5008	STATE 23					
0340	03.100	VDC	MUX 1, MUX 5	CR5008	STATE 24					
0347	03.107	VDC	MUX 1, MUX 5	CR5008	STATE 25					
0340	03.100	VDC	MUX 1, MUX 5	CR5008	STATE 26					
0343	03.103	VDC	MUX 1, MUX 5	CR5008	STATE 27					
0340	03.100	VDC	MUX 1, MUX 5	CR5008	STATE 28					
0347	03.107	VDC	MUX 1, MUX 5	CR5008	STATE 29					
0340	03.100	VDC	MUX 1, MUX 5	CR5008	STATE 30					

4751754734.2 20120100 P87640 100 2070 0000

PROCESSED
STRESS SENS DATA

1961-1962 1963-1964 1965-1966 1967-1968 1969-1970 1971-1972 1973-1974 1975-1976 1977-1978 1979-1980 1981-1982 1983-1984 1985-1986 1987-1988 1989-1990 1991-1992 1993-1994 1995-1996 1997-1998 1999-2000 2001-2002 2003-2004 2005-2006 2007-2008 2009-2010 2011-2012 2013-2014 2015-2016 2017-2018 2019-2020 2021-2022 2023-2024 2025-2026 2027-2028 2029-2030 2031-2032 2033-2034 2035-2036 2037-2038 2039-2040 2041-2042 2043-2044 2045-2046 2047-2048 2049-2050 2051-2052 2053-2054 2055-2056 2057-2058 2059-2060 2061-2062 2063-2064 2065-2066 2067-2068 2069-2070 2071-2072 2073-2074 2075-2076 2077-2078 2079-2080 2081-2082 2083-2084 2085-2086 2087-2088 2089-2090 2091-2092 2093-2094 2095-2096 2097-2098 2099-2100 2101-2102 2103-2104 2105-2106 2107-2108 2109-2110 2111-2112 2113-2114 2115-2116 2117-2118 2119-2120 2121-2122 2123-2124 2125-2126 2127-2128 2129-2130 2131-2132 2133-2134 2135-2136 2137-2138 2139-2140 2141-2142 2143-2144 2145-2146 2147-2148 2149-2150 2151-2152 2153-2154 2155-2156 2157-2158 2159-2160 2161-2162 2163-2164 2165-2166 2167-2168 2169-2170 2171-2172 2173-2174 2175-2176 2177-2178 2179-2180 2181-2182 2183-2184 2185-2186 2187-2188 2189-2190 2191-2192 2193-2194 2195-2196 2197-2198 2199-2200 2201-2202 2203-2204 2205-2206 2207-2208 2209-2210 2211-2212 2213-2214 2215-2216 2217-2218 2219-2220 2221-2222 2223-2224 2225-2226 2227-2228 2229-2230 2231-2232 2233-2234 2235-2236 2237-2238 2239-2240 2241-2242 2243-2244 2245-2246 2247-2248 2249-2250 2251-2252 2253-2254 2255-2256 2257-2258 2259-2260 2261-2262 2263-2264 2265-2266 2267-2268 2269-2270 2271-2272 2273-2274 2275-2276 2277-2278 2279-2280 2281-2282 2283-2284 2285-2286 2287-2288 2289-2290 2291-2292 2293-2294 2295-2296 2297-2298 2299-2300 2301-2302 2303-2304 2305-2306 2307-2308 2309-2310 2311-2312 2313-2314 2315-2316 2317-2318 2319-2320 2321-2322 2323-2324 2325-2326 2327-2328 2329-2330 2331-2332 2333-2334 2335-2336 2337-2338 2339-2340 2341-2342 2343-2344 2345-2346 2347-2348 2349-2350 2351-2352 2353-2354 2355-2356 2357-2358 2359-2360 2361-2362 2363-2364 2365-2366 2367-2368 2369-2370 2371-2372 2373-2374 2375-2376 2377-2378 2379-2380 2381-2382 2383-2384 2385-2386 2387-2388 2389-2390 2391-2392 2393-2394 2395-2396 2397-2398 2399-2400 2401-2402 2403-2404 2405-2406 2407-2408 2409-2410 2411-2412 2413-2414 2415-2416 2417-2418 2419-2420 2421-2422 2423-2424 2425-2426 2427-2428 2429-2430 2431-2432 2433-2434 2435-2436 2437-2438 2439-2440 2441-2442 2443-2444 2445-2446 2447-2448 2449-2450 2451-2452 2453-2454 2455-2456 2457-2458 2459-2460 2461-2462 2463-2464 2465-2466 2467-2468 2469-2470 2471-2472 2473-2474 2475-2476 2477-2478 2479-2480 2481-2482 2483-2484 2485-2486 2487-2488 2489-2490 2491-2492 2493-2494 2495-2496 2497-2498 2499-2500 2501-2502 2503-2504 2505-2506 2507-2508 2509-2510 2511-2512 2513-2514 2515-2516 2517-2518 2519-2520 2521-2522 2523-2524 2525-2526 2527-2528 2529-2530 2531-2532 2533-2534 2535-2536 2537-2538 2539-2540 2541-2542 2543-2544 2545-2546 2547-2548 2549-2550 2551-2552 2553-2554 2555-2556 2557-2558 2559-2560 2561-2562 2563-2564 2565-2566 2567-2568 2569-2570 2571-2572 2573-2574 2575-2576 2577-2578 2579-2580 2581-2582 2583-2584 2585-2586 2587-2588 2589-2590 2591-2592 2593-2594 2595-2596 2597-2598 2599-2600 2601-2602 2603-2604 2605-2606 2607-2608 2609-2610 2611-2612 2613-2614 2615-2616 2617-2618 2619-2620 2621-2622 2623-2624 2625-2626 2627-2628 2629-2630 2631-2632 2633-2634 2635-2636 2637-2638 2639-2640 2641-2642 2643-2644 2645-2646 2647-2648 2649-2650 2651-2652 2653-2654 2655-2656 2657-2658 2659-2660 2661-2662 2663-2664 2665-2666 2667-2668 2669-2670 2671-2672 2673-2674 2675-2676 2677-2678 2679-2680 2681-2682 2683-2684 2685-2686 2687-2688 2689-2690 2691-2692 2693-2694 2695-2696 2697-2698 2699-2700 2701-2702 2703-2704 2705-2706 2707-2708 2709-2710 2711-2712 2713-2714 2715-2716 2717-2718 2719-2720 2721-2722 2723-2724 2725-2726 2727-2728 2729-2730 2731-2732 2733-2734 2735-2736 2737-2738 2739-2740 2741-2742 2743-2744 2745-2746 2747-2748 2749-2750 2751-2752 2753-2754 2755-2756 2757-2758 2759-2760 2761-2762 2763-2764 2765-2766 2767-2768 2769-2770 2771-2772 2773-2774 2775-2776 2777-2778 2779

[illegible]

23 DUMP CMD

[illegible]

STORED L3 DATA
SHOWING B-COUNT
INCREMENTING

079811111111-1	01020110			0100 03 00000000
079811111111-2	01020110			00 03 1100 000 00
079811111111-3	01020110	-		100 03 0000000000

Reproduced from
best available copy.



Table 45. X and Y Calibration Readout

[illegible]

BDY, BDY CALIBRATION
DATA
(SIMULATED EVENTS)

183

```

PAGE 04505-510-0000 TESTS (UNOS REDUNDANCY TEST SUP DATE 03/15/78 PAGE 121
LNO. 11. 12. 13. 14. 15. 16. 17. 18. 19. 20. 21. 22. 23. 24. 25. 26. 27. 28. 29. 30. 31. 32. 33. 34. 35. 36. 37. 38. 39. 40. 41. 42. 43. 44. 45. 46. 47. 48. 49. 50. 51. 52. 53. 54. 55. 56. 57. 58. 59. 60. 61. 62. 63. 64. 65. 66. 67. 68. 69. 70. 71. 72. 73. 74. 75. 76. 77. 78. 79. 80. 81. 82. 83. 84. 85. 86. 87. 88. 89. 90. 91. 92. 93. 94. 95. 96. 97. 98. 99. 100. 101. 102. 103. 104. 105. 106. 107. 108. 109. 110. 111. 112. 113. 114. 115. 116. 117. 118. 119. 120. 121. 122. 123. 124. 125. 126. 127. 128. 129. 130. 131. 132. 133. 134. 135. 136. 137. 138. 139. 140. 141. 142. 143. 144. 145. 146. 147. 148. 149. 150. 151. 152. 153. 154. 155. 156. 157. 158. 159. 160. 161. 162. 163. 164. 165. 166. 167. 168. 169. 170. 171. 172. 173. 174. 175. 176. 177. 178. 179. 180. 181. 182. 183. 184. 185. 186. 187. 188. 189. 190. 191. 192. 193. 194. 195. 196. 197. 198. 199. 200. 201. 202. 203. 204. 205. 206. 207. 208. 209. 210. 211. 212. 213. 214. 215. 216. 217. 218. 219. 220. 221. 222. 223. 224. 225. 226. 227. 228. 229. 230. 231. 232. 233. 234. 235. 236. 237. 238. 239. 240. 241. 242. 243. 244. 245. 246. 247. 248. 249. 250. 251. 252. 253. 254. 255. 256. 257. 258. 259. 260. 261. 262. 263. 264. 265. 266. 267. 268. 269. 270. 271. 272. 273. 274. 275. 276. 277. 278. 279. 280. 281. 282. 283. 284. 285. 286. 287. 288. 289. 290. 291. 292. 293. 294. 295. 296. 297. 298. 299. 300. 301. 302. 303. 304. 305. 306. 307. 308. 309. 310. 311. 312. 313. 314. 315. 316. 317. 318. 319. 320. 321. 322. 323. 324. 325. 326. 327. 328. 329. 330. 331. 332. 333. 334. 335. 336. 337. 338. 339. 340. 341. 342. 343. 344. 345. 346. 347. 348. 349. 350. 351. 352. 353. 354. 355. 356. 357. 358. 359. 360. 361. 362. 363. 364. 365. 366. 367. 368. 369. 370. 371. 372. 373. 374. 375. 376. 377. 378. 379. 380. 381. 382. 383. 384. 385. 386. 387. 388. 389. 390. 391. 392. 393. 394. 395. 396. 397. 398. 399. 400. 401. 402. 403. 404. 405. 406. 407. 408. 409. 410. 411. 412. 413. 414. 415. 416. 417. 418. 419. 420. 421. 422. 423. 424. 425. 426. 427. 428. 429. 430. 431. 432. 433. 434. 435. 436. 437. 438. 439. 440. 441. 442. 443. 444. 445. 446. 447. 448. 449. 450. 451. 452. 453. 454. 455. 456. 457. 458. 459. 460. 461. 462. 463. 464. 465. 466. 467. 468. 469. 470. 471. 472. 473. 474. 475. 476. 477. 478. 479. 480. 481. 482. 483. 484. 485. 486. 487. 488. 489. 490. 491. 492. 493. 494. 495. 496. 497. 498. 499. 500. 501. 502. 503. 504. 505. 506. 507. 508. 509. 510. 511. 512. 513. 514. 515. 516. 517. 518. 519. 520. 521. 522. 523. 524. 525. 526. 527. 528. 529. 530. 531. 532. 533. 534. 535. 536. 537. 538. 539. 540. 541. 542. 543. 544. 545. 546. 547. 548. 549. 550. 551. 552. 553. 554. 555. 556. 557. 558. 559. 560. 561. 562. 563. 564. 565. 566. 567. 568. 569. 570. 571. 572. 573. 574. 575. 576. 577. 578. 579. 580. 581. 582. 583. 584. 585. 586. 587. 588. 589. 590. 591. 592. 593. 594. 595. 596. 597. 598. 599. 600. 601. 602. 603. 604. 605. 606. 607. 608. 609. 610. 611. 612. 613. 614. 615. 616. 617. 618. 619. 620. 621. 622. 623. 624. 625. 626. 627. 628. 629. 630. 631. 632. 633. 634. 635. 636. 637. 638. 639. 640. 641. 642. 643. 644. 645. 646. 647. 648. 649. 650. 651. 652. 653. 654. 655. 656. 657. 658. 659. 660. 661. 662. 663. 664. 665. 666. 667. 668. 669. 670. 671. 672. 673. 674. 675. 676. 677. 678. 679. 680. 681. 682. 683. 684. 685. 686. 687. 688. 689. 690. 691. 692. 693. 694. 695. 696. 697. 698. 699. 700. 701. 702. 703. 704. 705. 706. 707. 708. 709. 710. 711. 712. 713. 714. 715. 716. 717. 718. 719. 720. 721. 722. 723. 724. 725. 726. 727. 728. 729. 730. 731. 732. 733. 734. 735. 736. 737. 738. 739. 740. 741. 742. 743. 744. 745. 746. 747. 748. 749. 750. 751. 752. 753. 754. 755. 756. 757. 758. 759. 760. 761. 762. 763. 764. 765. 766. 767. 768. 769. 770. 771. 772. 773. 774. 775. 776. 777. 778. 779. 780. 781. 782. 783. 784. 785. 786. 787. 788. 789. 790. 791. 792. 793. 794. 795. 796. 797. 798. 799. 800. 801. 802. 803. 804. 805. 806. 807. 808. 809. 810. 811. 812. 813. 814. 815. 816. 817. 818. 819. 820. 821. 822. 823. 824. 825. 826. 827. 828. 829. 830. 831. 832. 833. 834. 835. 836. 837. 
```

Reproduced from
best available copy.

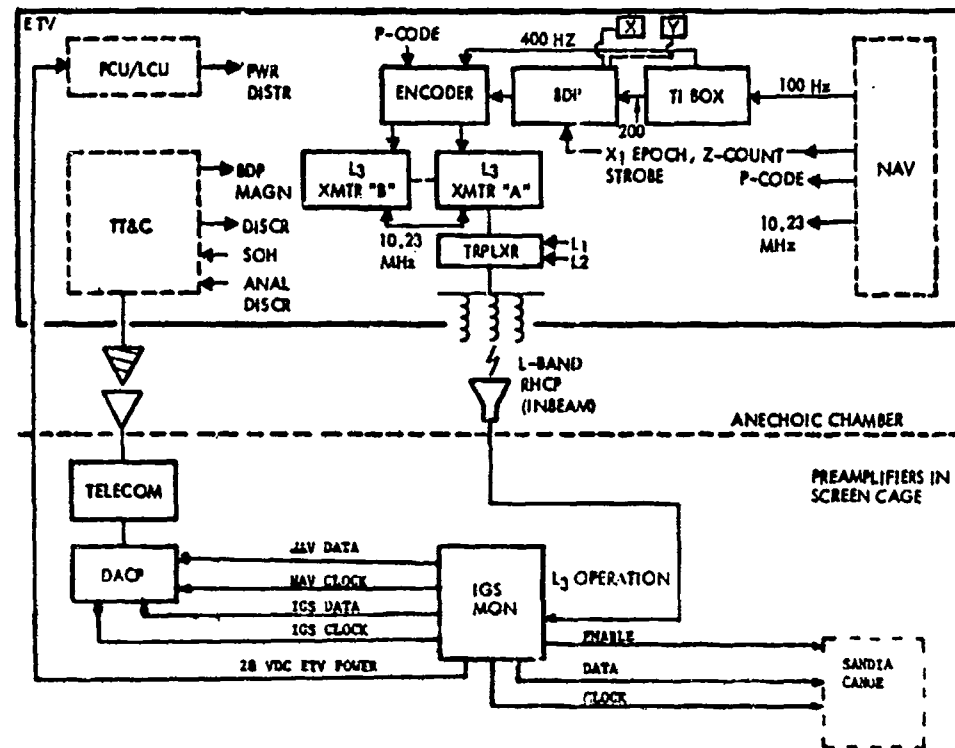


Figure 125. IGS Test Configuration

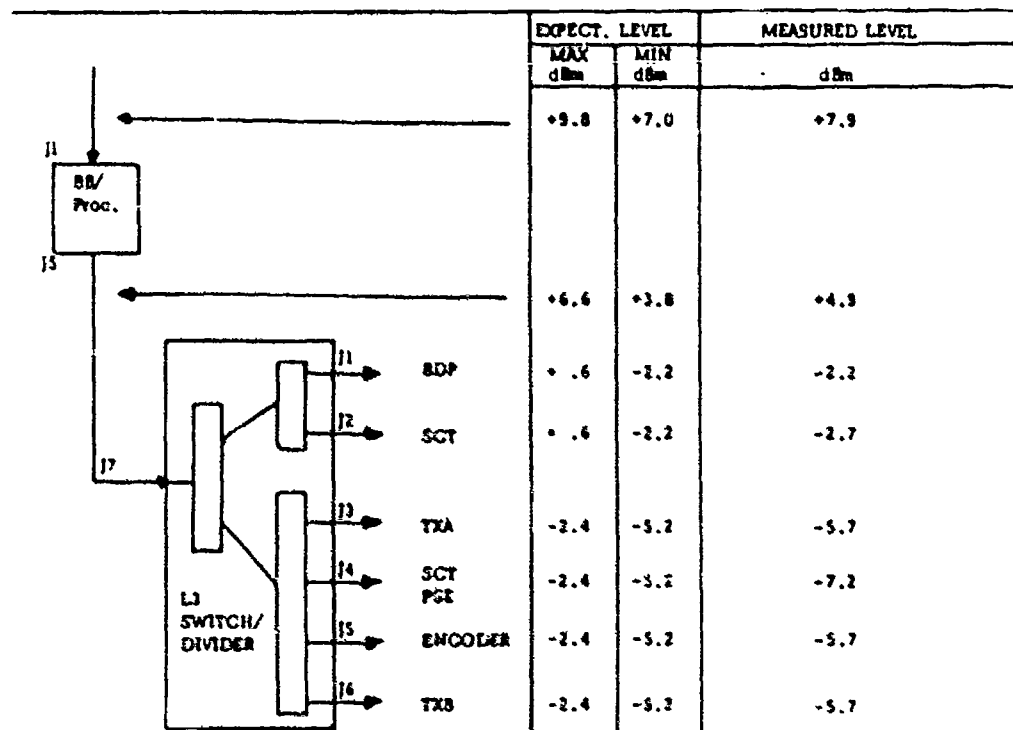


Figure 126. 10.23 MHz Distribution

Table 46. Interface Verification Test Anomalies

Test	Parameter	Remarks	Impact
BB/P-IGS/SCT	10.23 MHz distr	Levels marginal (see chart); inadequate distr losses considered	None; to be corrected in NDS 6 and Phase II hardware
BB/P-BDP	X1 epoch	False Z-count triggering caused by clock spiking into X1 epoch cable	Corrected by replacing shielded wire with coax cable
DCD-BDP	Data A&B	Rise time degradation due to cable capacitance ($S/B \leq 5 \mu s$, $IS \approx 25 \mu s$)	None; respecify T_R at end of cable
DCD-BDP	Data & enable	Some clock noise & spiking on signals	None; investigate for origin
TI-BOX-BDP	200 Hz clock	No ICD compliance with respect to level, overshoot, & crosstalk	None; interim engineering solution; corrected in TIE box design
PCM No. 2-BDP	PCM signals	PCM No. 2 unit not operational	None; testing complete on PCM No. 1
BB/P-BDP	X1 epoch delay	Not completed due to measurement difficulty	None; reschedule test
PCM-BDP/SCT	SOH enables	TTL-levels (engineering solution)	None; Phase II hardware will correct

VERIFIED FUNCTIONALLY

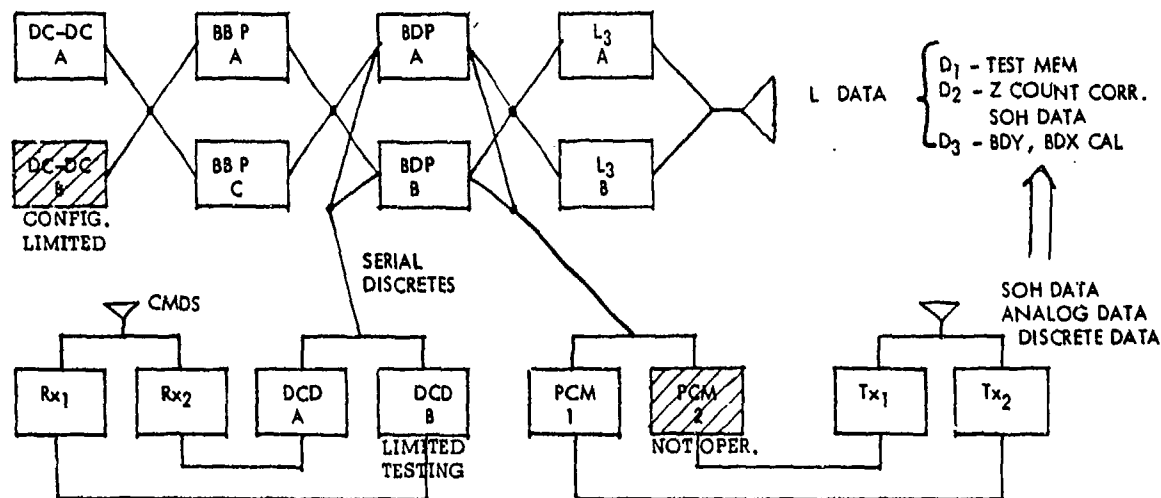


Figure 127. Cross-Strapping Results

Table 47. Data Transmission Matrix

	GPS	IGS			GPS				Analysis
	DC-DC	BBP	BDP	L ₃	Rx	DCD	PCM	Tx	
D ₁	A	A&C	A&B	A&B	-	-	-	-	DCAP (Automatic)
D ₂	A	A&C	A&B	A&B	1&2	A&B	1&2	1&2	DCAP & visual
D ₃	A	A&C	A&B	A&B	1	A&B	1	1	Sandia

Table 48. ETV Cross-Strapping Problems

Unit	Remarks	IGS Impact
DC-dc Converter A only	ETV unable to switch to B side of converter without second clock	None; supplies power to basic GPS units only. Has been proven in GPS tests
PCM No. 1 only	PCM No. 2 not operational (defective TT&C component)	None; GPS proven capability
• Conclusion: IGS data transmission compatible with all signal and power switching functions within IGS. Dc-dc and TT&C switching proven on GPS.		

6.5.4 EMC Test

The space vehicle EMC test was conducted as an adjunct to the integrated system test (IST). It involved hardware, software, and procedures that were identical to those used on IST. The test itself was concerned with the impact of secondary payloads on the GPS power system. The IGS system impact occurred when the BDP commands "power on" to the L₃ transmission system.

Power transients in the BDP were negligible. The space vehicle, equipped with a power conditioning unit having a poor load regulation did, however, display a transient drop of 4 volts in the line for approximately 10 milliseconds. The in-rush current level reached 31 amperes for 1 millisecond. These rather large transients did not, however, impact the space vehicle subsystem operation. The excessive voltage drop did require that the SCT processor power supply be modified to preclude memory dumps during IGS L₃ transmitter turn on.

An analysis coupled with a test program using breadboard transmitters and the EDM models was undertaken to establish transient characteristics of a typical transmitter design. A second test phase was implemented which evolved

techniques for limiting the in-rush current to 10 amperes for 50 microseconds. Appropriate modifications have been made to the flight transmitters.

6.5.5 Threshold Sensitivity Tests

The IGS threshold sensitivity tests were conducted before and after the space vehicle EMC test on the ETV vehicle. Sensor thresholds (both X and Y sensors) were tested by Sandia in the Y-sensor grading test series. The X and Y sensors achieved threshold level settings of 12C4 and 10C4, respectively, without data transmission degradation on the D3 routine. Operation at 12C3 and 10C3 with the Y-sensor confirmed that the sensitivity had exceeded the background noise level.

The Y-sensor ground test was conducted prior to EMC with the EMC instrumentation installed on the ETV. The L3 transmission threshold sensitivity tests were conducted after EMC without instrumentation.

The L3 transmission test involved the IONDS receiver manufactured by Stanford Telecommunications, Inc. The receiver had been partially tested, and some unfinished boards were substituted for items still in assembly. Also, this receiver's L3 channel had not been factory adjusted for optimum L3 operation. (The L1 channel had been utilized extensively during IST/EMC testing periods for tracking the NDS 1 data for GPS support.) Since NDS 1 effective radiated power (ERP) was rated at -121 dBm and data of excellent quality had been acquired on NDS-1, good performance on L1 was a certainty, and good performance on L3 would be achievable on the as-built receiver.

The overall L3 transmission sensitivity test setup is shown in Figure 128.

The L3 and L1 transmitter outputs as received on the chamber antenna were measured separately on the HP 435A power meter. The L1 threshold for C/A, P code, carrier, and sync lock was then determined by increasing attenuator settings (which decreases signal to receiver). Subsequently, the signal was decreased until P-code lock was lost (the most sensitive signal parameter). The attenuator setting corresponded to a signal level of -137 dBm.

Attenuator settings were then adjusted beyond the point where all signals were lost and then decreased to find the point where lock on all functions was regained. The power setting corresponded to a signal level of -136 dBm (a loss of 1 dB). This was determined to be the L1 signal threshold.

It was not possible to cause L1 to handover to L3 at -136 dBm. Handover was accomplished at a setting of -126.5 dBm for all functions (9.5 dB less sensitivity than L1). Several iterations of this procedure produced the same result.

Estimations of group delay loss for group delay greater than 15 nanoseconds between L1 and L3 might reasonably account for more than a 2-dB loss in threshold sensitivity (see Figure 129 for group delay loss impact). The Stanford Telecommunications representative stipulated that, when properly adjusted, the L3 channel sensitivity (assuming no group delay) would perform as well as the L1 channel (-136 dBm). This condition will be shown at IONDS receiver acceptance testing. Note that this is a function of the Stanford

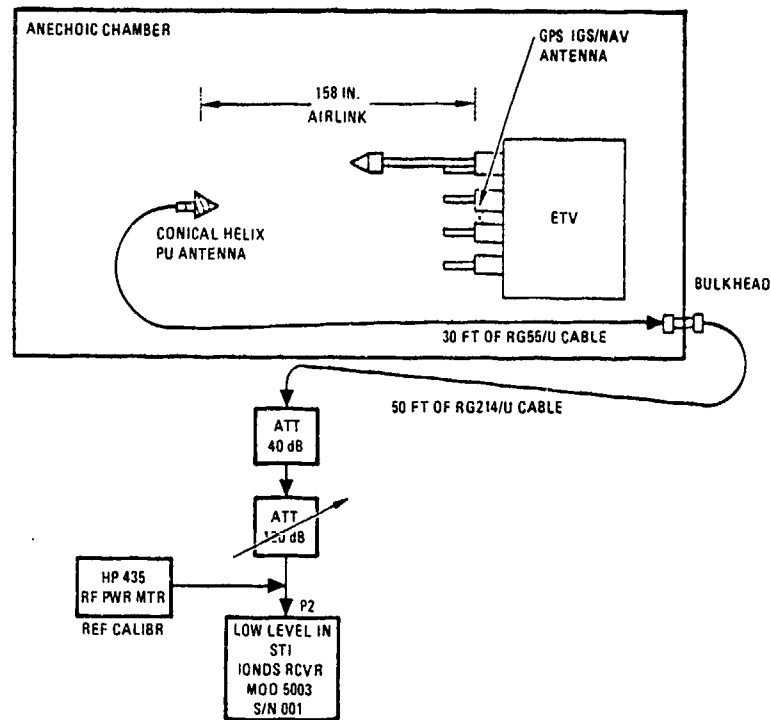


Figure 128. IONDS Receiver Threshold Sensitivity
Test Setup

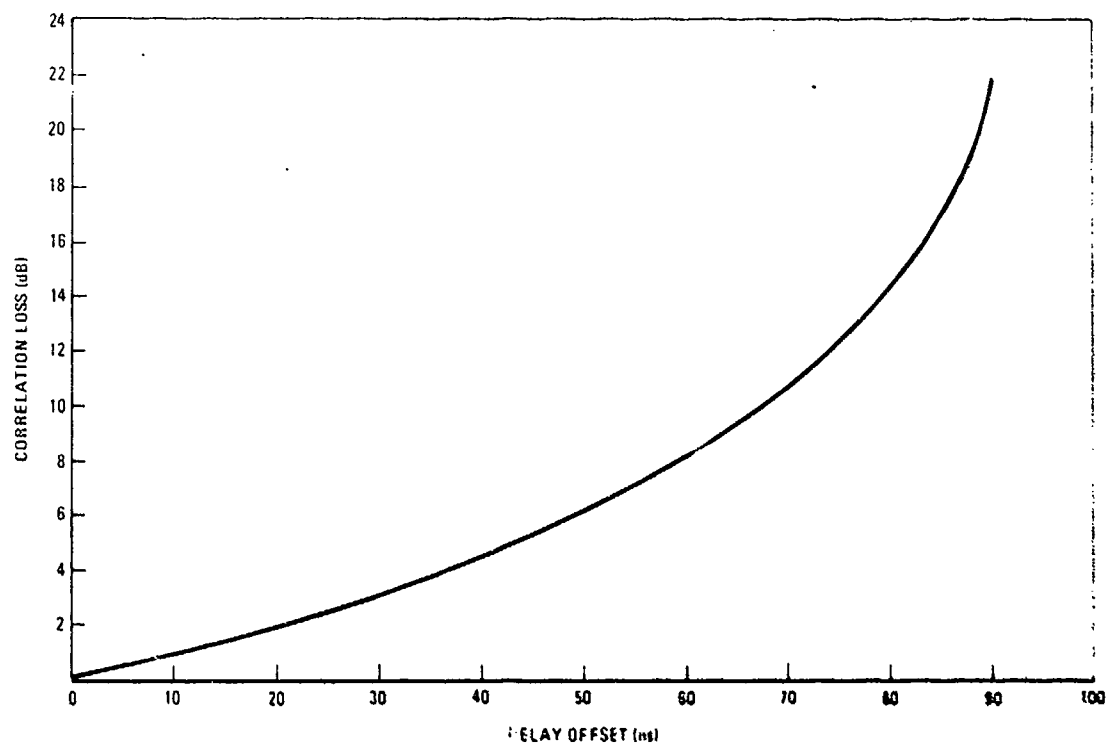


Figure 129. Delay Offset Versus Correlation Loss

Telecommunications design because it uses a single delay lock loop to position the reference code for L_1 -C/A, L_1 -P, and L_3 -P signals. Other sets, such as the Magnavox X-set, are not sensitive to this delay.

The group delay (L_1 to L_3) was not measured due to test hardware limitations which could not be overcome during the IST schedule. The group delay could account for the entire 9.5-dB loss if the actual delay were of the order of 65 nanoseconds (refer to correlation loss versus group delay plotted in Figure 129).

The group delay measurement is scheduled for July 1978 to confirm the sensitivity loss and to establish receiver sensitivity capability in the event that the L_3 receiver performance meets the -133 dBm power level specification during the acceptance test.

The procedure used on threshold sensitivity included sending test routine D1 and adjusting the attenuator until the transmission became errorless on all three routines. This occurred at the same setting, -126.5 dBm, establishing that performance was limited by RF signal amplitude, not bit data content.

The procedure was then altered to add D2 and D3 test routines to establish that all data transmission could be successfully achieved at threshold on both the A/A (transmission and processor systems in A channel) and B/B (transmission and processor set to B channels) configurations.

6.5.6 Y-Sensor Grounding and Threshold Tests

The X- and Y-sensor thresholds were set to 12C8 and 10C8, respectively. (Sandia asserted that these will be the sensor threshold level settings in operation.) Oscilloscope probes were attached to monitor frame-to-circuit common noise at the BDY detector and to monitor sensor signal and noise at the YTOA S6 analog amplifier. The S6 amplifier output had an amplification of 69 dB above the actual silicon diode optical sensor output. Traces on these two oscilloscopes were monitored during various ETV configurations and tests. These configurations included STC on and off, L_1 , L_2 , and L_3 on and off, and D3 GBD operational modes and sensor excitation.

During ETV full-up configuration, the GPS optical trigger sensitivities were lowered to determine the noise and background levels which would pass trigger thresholds. Those signals passing the trigger test conditions generated L_3 event data outputs.

A comparison of previous Sandia bench tests and ETV tests was made to determine if any major degrading occurred on the ETV. No serious degrading, because of system noise, was noticed. These tests were made with the low light background of the anechoic chamber. Future testing may require an artificial light source to simulate the earth albedo.

During some of the ETV configuration changes, the GBD was configured in a sensitive trigger mode (IGS serial commands 10C4 and 12C4). Although these GBD trigger levels were near the level at which noise and background triggers would occur, no false triggers were experienced.

The link margin analysis stipulates that L3 operation be accomplished at a signal level of -133 dBm. While the results of the above test were extremely encouraging from a total system viewpoint, the test will be repeated (on hardline coaxial cables) when the TONDS receiver is completed. A summary of the preliminary threshold test results is listed in Table 49.

6.5.7 Vehicle Acoustic Test

The GPS forward bulkhead design allowed for installation of additional devices for both primary and secondary missions. The spider, which is the vehicle forward load bearing surface, was considered to be stressed by these secondary payloads. At best, the payloads were considered as additional weight whose mass reduced the vibration levels on the panel and, at worst, a load which could impact design integrity. Further, it was necessary to determine the vibration environment for all secondary payload components at the space vehicle locations planned for orbital operation.

The vehicle acoustic test was performed at the B-1 Division of Rockwell International in the same manner as the three previous GPS tests performed on the GPS development test vehicle. Instrumentation, facilities, and test procedures duplicated these of the third test of the DTV series.

The acoustic test consisted of five separate acoustic runs devised to evaluate alternative secondary payload configurations that may exist on the GPS spacecraft. The variation in the resultant spectrums was small for the configurations of the IGS hardware tested. In all cases, the components experienced relatively benign environments, with the exception of a few low energy peaks at structural resonance frequencies.

During the equalization run before the first test run at qualification test levels, a failure of one of the Y-sensor sunshade baffles occurred. The baffle ring had partially separated at its bond inside the sunshade. It was subsequently bolted to the sunshade, and the tests were carried out. In the last run, the bolts were removed to determine whether they caused any deviation to the test results; no noticeable difference in the sunshade spectrum was detected and total separation did not occur. Subsequent failure analysis revealed that the baffle was slightly oversized, preventing the baffle from being fully seated prior to bonding per design. None of the other baffles had this problem, and no problem is anticipated with the flight sunshade. Complete test data and procedures are published in Rockwell report SD 77-GP-0010-1, 2, 3, and 4.

6.5.7.1 Configuration. The test configuration consisted of the GPS development test vehicle with mass simulators of the GPS and secondary payload hardware installed. Figure 130 shows the secondary payload hardware mounted on the forward bulkhead (i.e., the IGS sunshade, the X-sensor, and the AFSAT single-channel transponder antennas).

Five runs made up the total acoustic program. Table 50 describes the test configuration of each run. During the first two runs (Runs A and B), the IGS and SCT payload hardware were installed on the DTV. Two runs were necessary to make all of the accelerometer measurements required. The Y-sensor sunshade configuration differed in Runs A and B. During Run B, the sunshade was attached

Table 49. Threshold Test Summary

Signal	Specification	Predicted Threshold		Measured Threshold		Margin
		C	C/No.	C	C/No.	
Tracking	L ₁ C/A code	-133 dBm	37 dB-Hz	-144.5 dBm	25.5 dB-Hz	-145.7 dBm 12.7 dB
	L ₁ C/A carrier	-133 dBm	37 dB-Hz	-142 dBm	28 dB-Hz	-145.7 dBm 12.7 dB
	L ₁ P code	-133 dBm	37 dB-Hz	-137 dBm	33 dB-Hz	-136.8 dBm 3.6 dB
	L ₁ P carrier	-133 dBm	37 dB-Hz	-142 dBm	28 dB-Hz	-142.8 dBm 9.8 dB
	L ₃ P code	-133 dBm	37 dB-Hz	-137 dBm	33 dB-Hz	-127.5 dBm ⁽¹⁾ (5.5 dB)
	L ₃ carrier	-133 dBm	37 dB-Hz	-142 dBm	28 dB-Hz	-134.5 dBm 1.5 dB
Acquisition	L ₁ C/A carrier	-133 dBm	37 dB-Hz	-146 dBm AFC 24 dB-Hz -142 dBm PLL 28 dB-Hz		-145.7 dBm 12.7 dB
	L ₁ P code	-133 dBm	37 dB-Hz	-137 dBm	33 dB-Hz	-135.9 dBm 2.3 dB
	L ₃ P code	-133 dBm	37 dB-Hz	-137 dBm	33 dB-Hz	-126.5 dBm ⁽¹⁾ (6.5 dB)

(1) Threshold adjustment on L₃ correlator/and L₃ delay with respect to L₁. Receiver noise figure is assumed to be 4.5 dB.

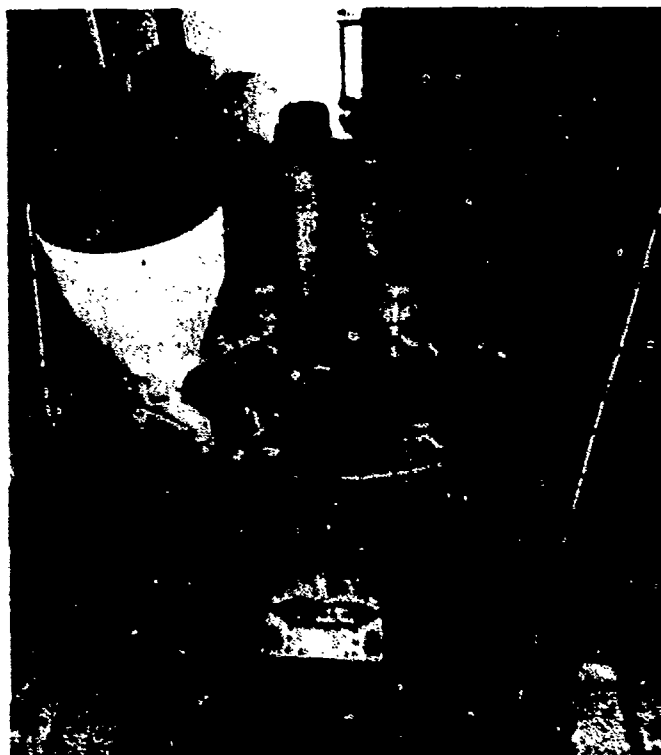


Figure 130. DTV With Secondary Payload
Hardware on Forward Bulkhead

Table 50. Summary of Secondary Payloads Acoustic Testing

Test Task ID	SCT Test Configuration/Conditions
DTV test preparation	<ol style="list-style-type: none"> 1. IGS Y-sensor sunshade configuration 2. ALL IGS, SCT, and GPS mass simulators and 66 accelerometers installed at Seal Beach facility. <ol style="list-style-type: none"> a. All 27 SCT system mass simulator component accelerometers installed b. All 28 IGS mass simulator component accelerometers installed c. 11 of the GPS mass simulator component accelerometers installed
Phase I: (Acoustic test chamber and DTV test preparation)	<ol style="list-style-type: none"> 1. Empty acoustic chamber checkout 2. Pre-test instrumentation setup 3. Qualification-level equalization
Phase II: Run A (SCT + IGS baseline)	All 27 SCT, all 28 IGS, and 11 GPS accelerometers utilized
Phase II: Run B (SCT + IGS baseline)	All SCT accelerometers except the 3 identified as 3XYZ are removed and reinstalled at untested GPS mass simulator locations, and the Y-sensor sunshade is changed to Configuration 2. Accelerometer 48Y installed at +X side of Y-sensor/sunshade interface
Phase III: Run C (IGS baseline)	All SCT mass simulators removed from DTV (including accelerometers 3XYZ), and the preferred Y-sensor sunshade configuration (determined from Runs A and B) utilized. Sunshade Configuration 2 was used.
Phase III: Run D (IGS baseline)	Same as Run C, above, with Y-sensor sunshade mounting bracket on forward bulkhead removed. Accelerometer 127Z was moved and renamed 197Z
Phase III: Run E (IGS baseline)	Same as Run D, above, with Y-sensor sunshade radiation baffle ring holding bolts removed

to the Y-sensor as well as the forward structural member. This configuration is shown in Figure 131 and is referred to as Installation Configuration 2. In the first run, with both payloads installed, Y-sensor Sunshade Configuration 1 was selected. In this configuration, the sunshade was not attached to the Y-sensor. In the third run (Run C), the SCT packages were removed, and only the IGS secondary payload packages remained. The objective of this run was to determine if the environment was different for an IGS-only configuration. The sunshade was removed from the forward structural member and attached to the top of the Y-sensor on the mounting flange in Run D. The objective of this fourth run was to determine if the Y-sensor and the sunshade could be tested as an integral unit with only a single interface to the GPS spacecraft at a Y-sensor shear panel mounting. Again, the SCT packages were not present. The bolts were removed

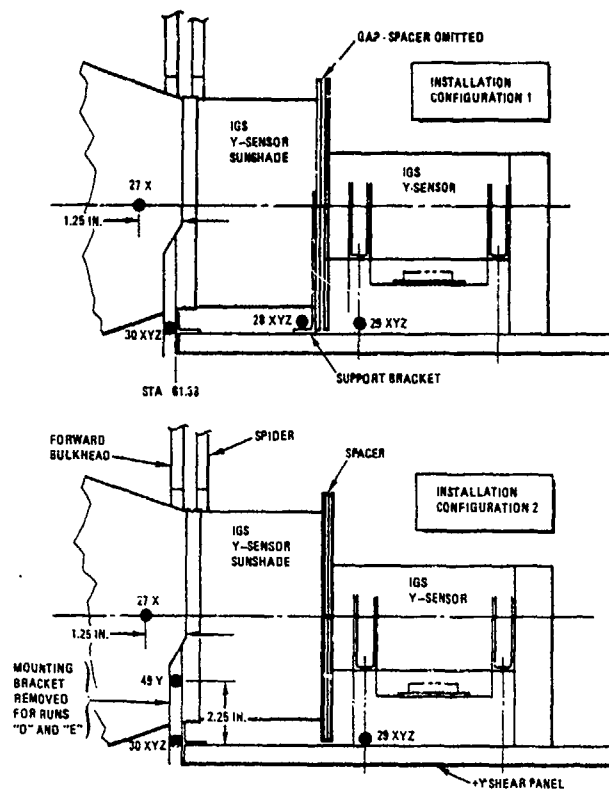


Figure 131. Alternative Sunshade Mountings

from the failed baffle ring, and a final run was made to determine whether further separation would occur when exposed to the severe acoustic environment and whether the bolts affected the recorded spectrums.

6.5.7.2 Test Results. Component qualification environments, Figures 132 through 139, were derived from a composite of the spectrums of the first four test runs. Environments recommended are presented for different types of component testing hardware. Reduction in induced total energy can be obtained by proper spectrum selection and still encompass the spectrums recorded during the test.

It was concluded from the test results that the sunshade only needs to be attached to the Y-sensor. The variation in Y-sensor electronics vibration spectrums between alternative attachment configurations was negligible. This approach eases the complexity of the component vibration test fixture and satellite installation.

In general, the highest excitation occurred in the direction perpendicular to the bulkhead to which the component is mounted. The peak level for Accelerometer 23 mounted on the L3 transmitter, for example, was $2.0 \text{ g}^2/\text{Hz}$ in the Y directions. Appendixes A through D of Rockwell Vibration Test Report, SD 77-GP-0012-2, present the vibration spectrums recorded on the IGS components.

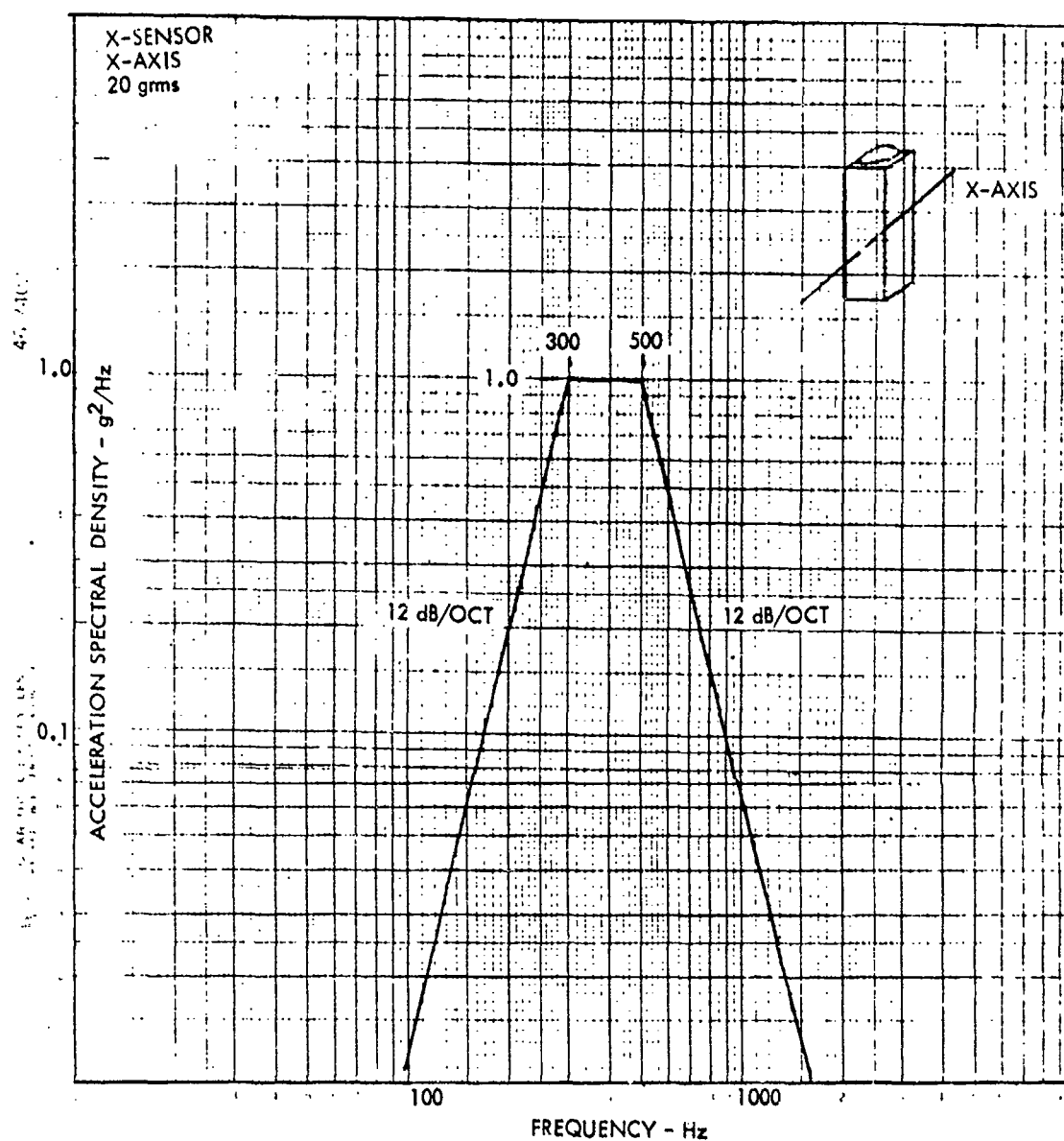


Figure 132. IGS X-Sensor Random Vibration Qualification Levels (X-Axis)

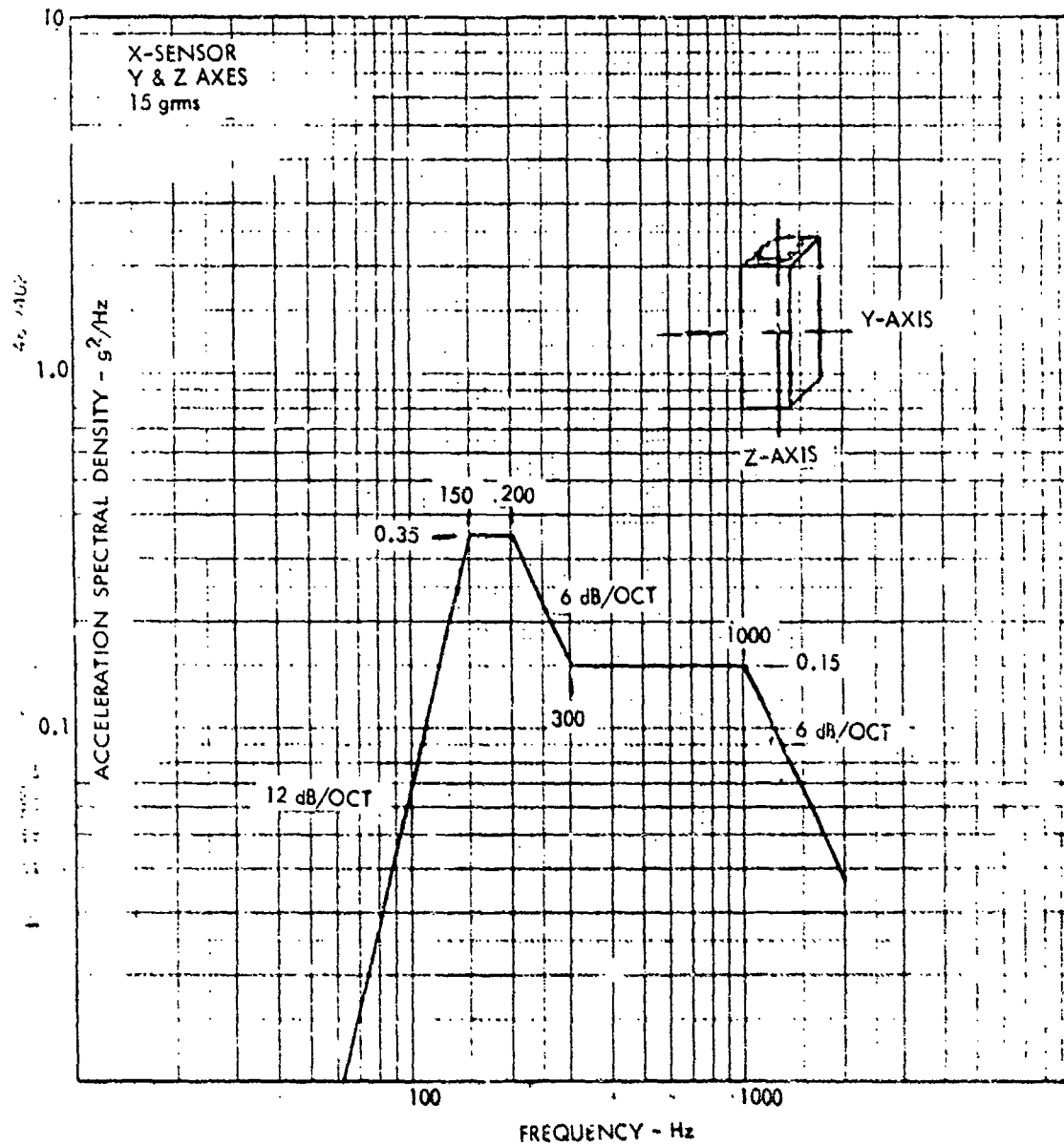


Figure 133. IGS X-Sensor Random Vibration Qualification Levels
(Y- and Z-Axes)

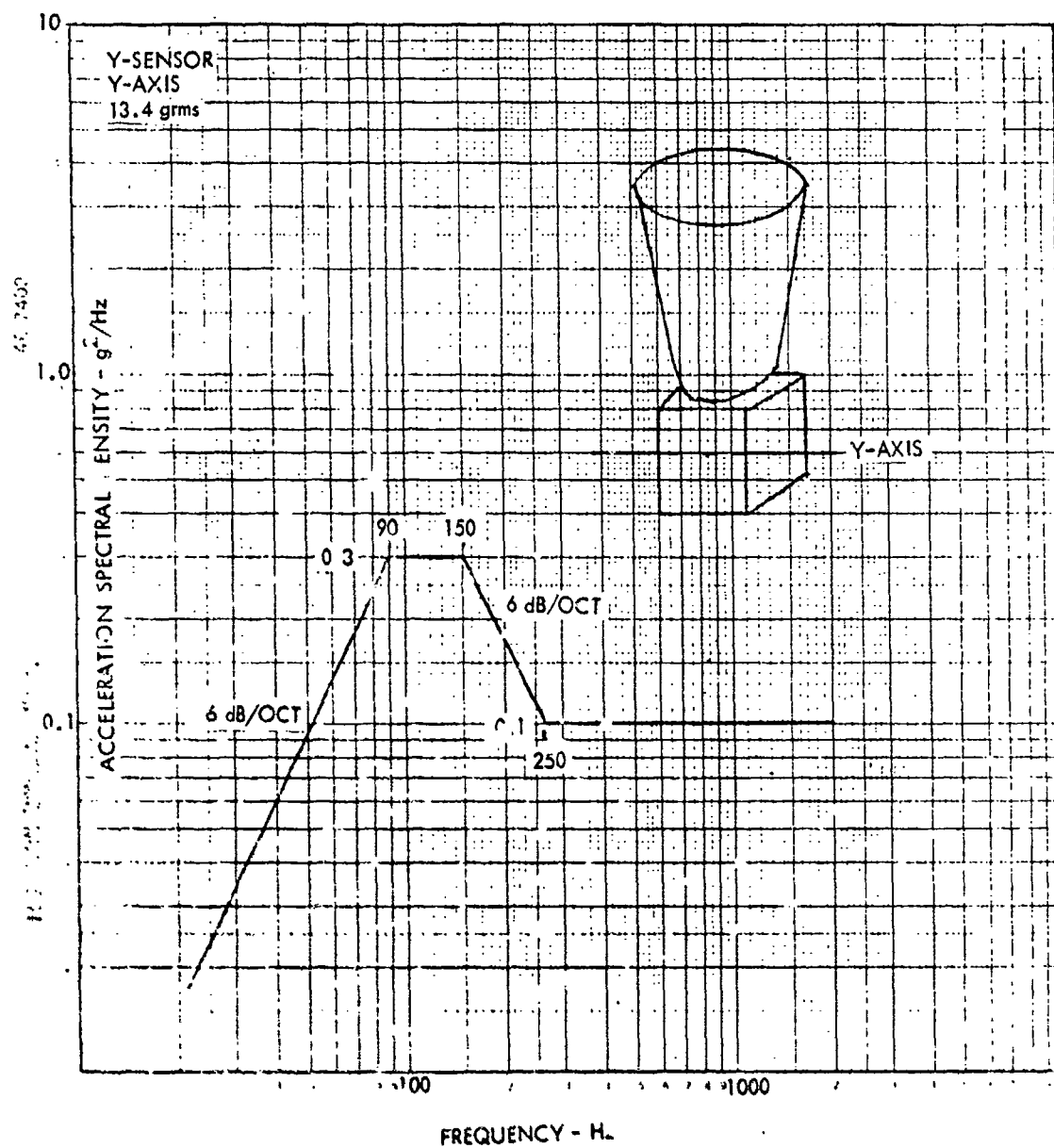


Figure 134. IGS Y-Sensor Random Vibration Qualification Levels
(Y-Axis)

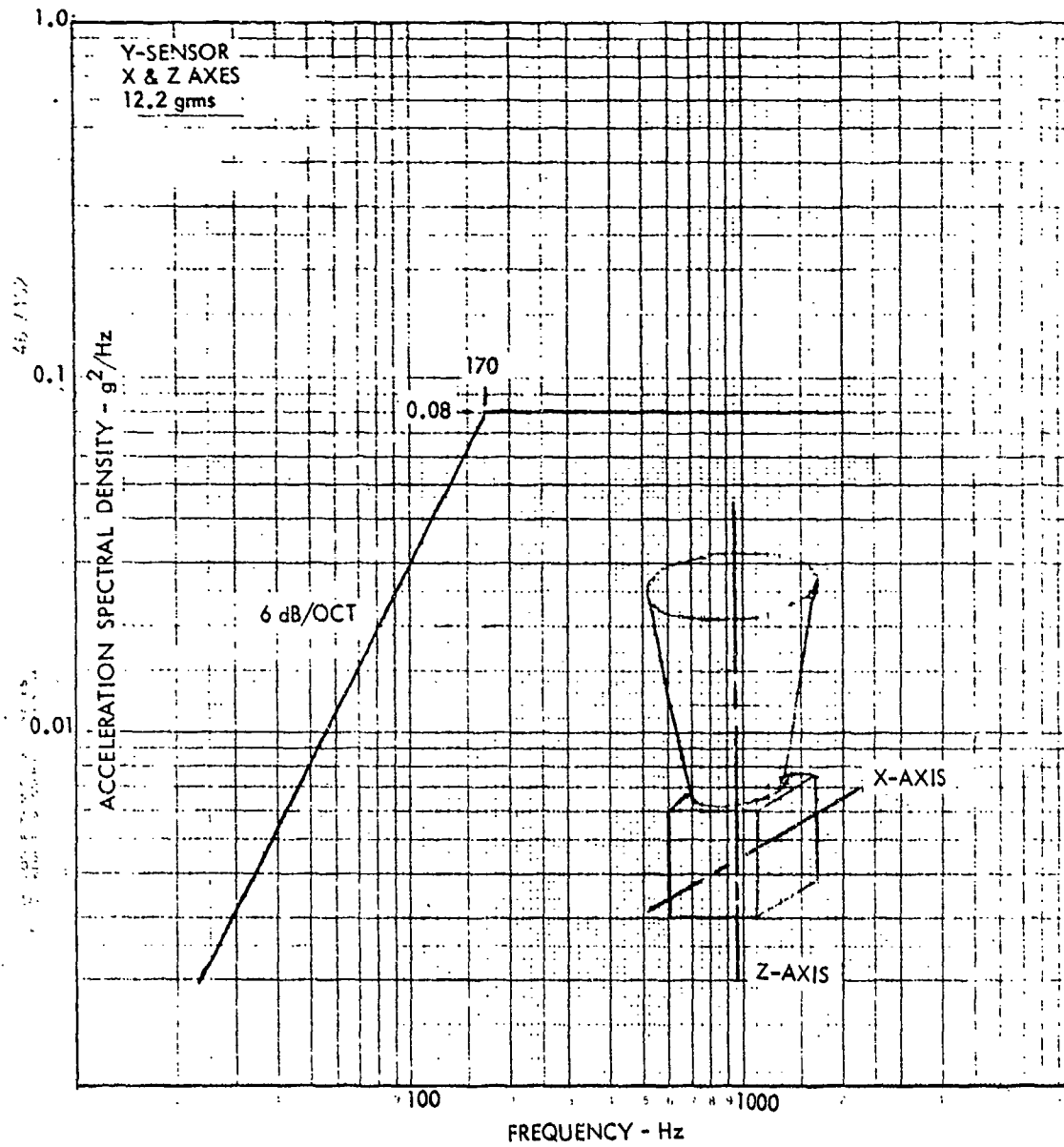


Figure 135. IGS Y-Sensor Random Vibration Qualification Levels
(X and Z-Axes)

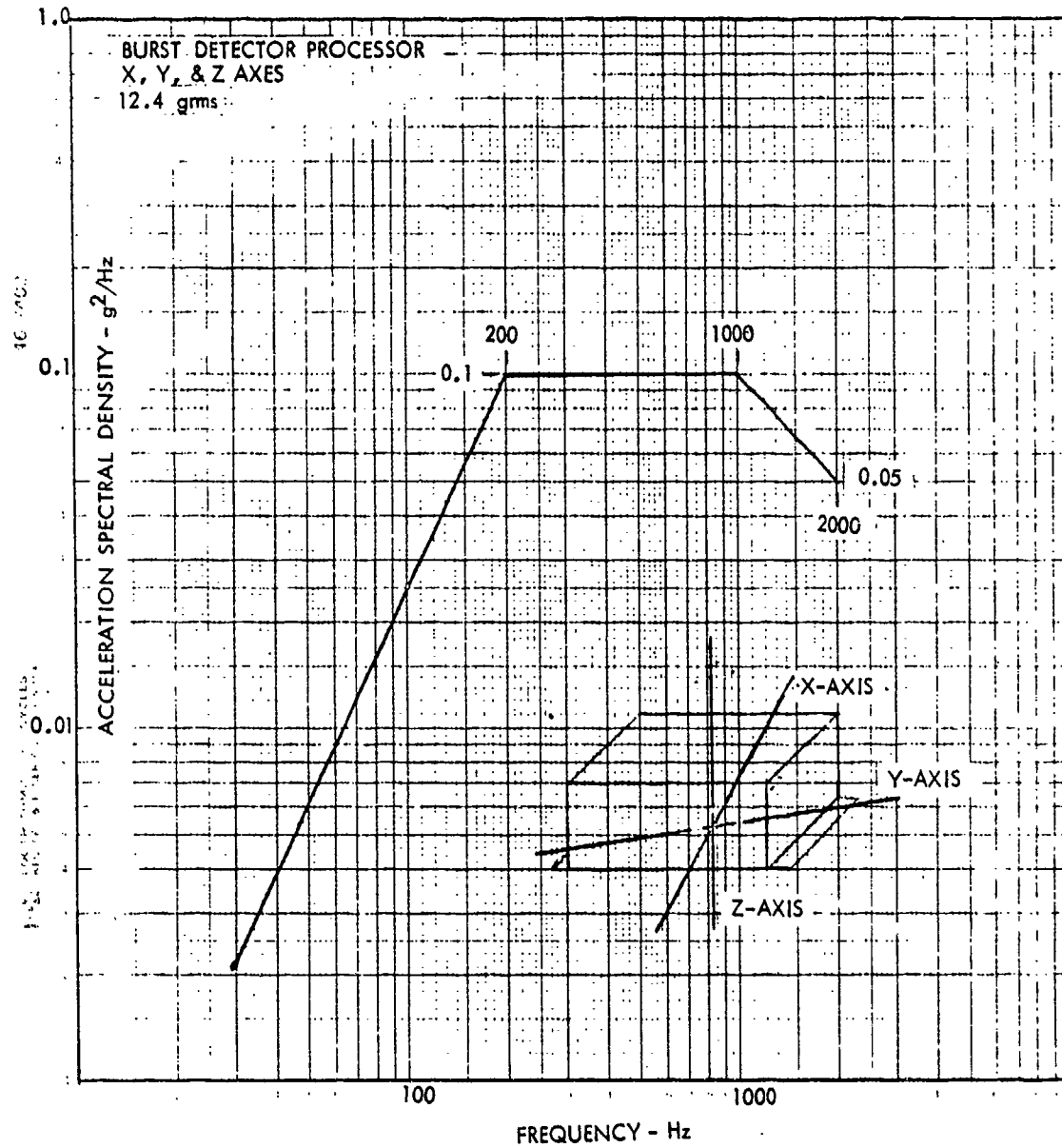


Figure 136. BDP Y-Sensor Random Vibration Qualification Levels
(X-, Y-, and Z-Axes)

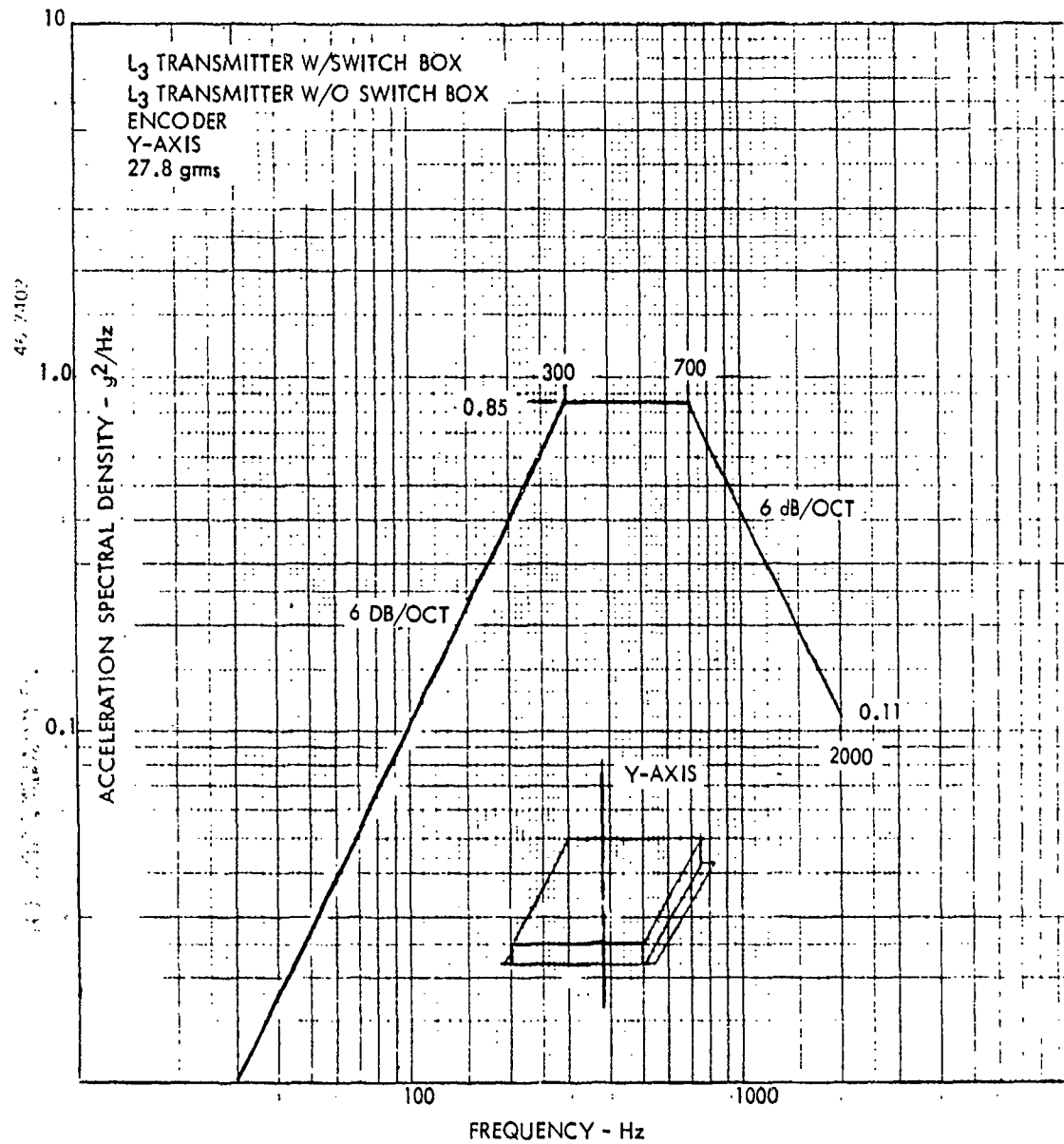


Figure 137. L_3 Transmitter and Encoder Random Vibration Qualification Levels (Y-Axis)

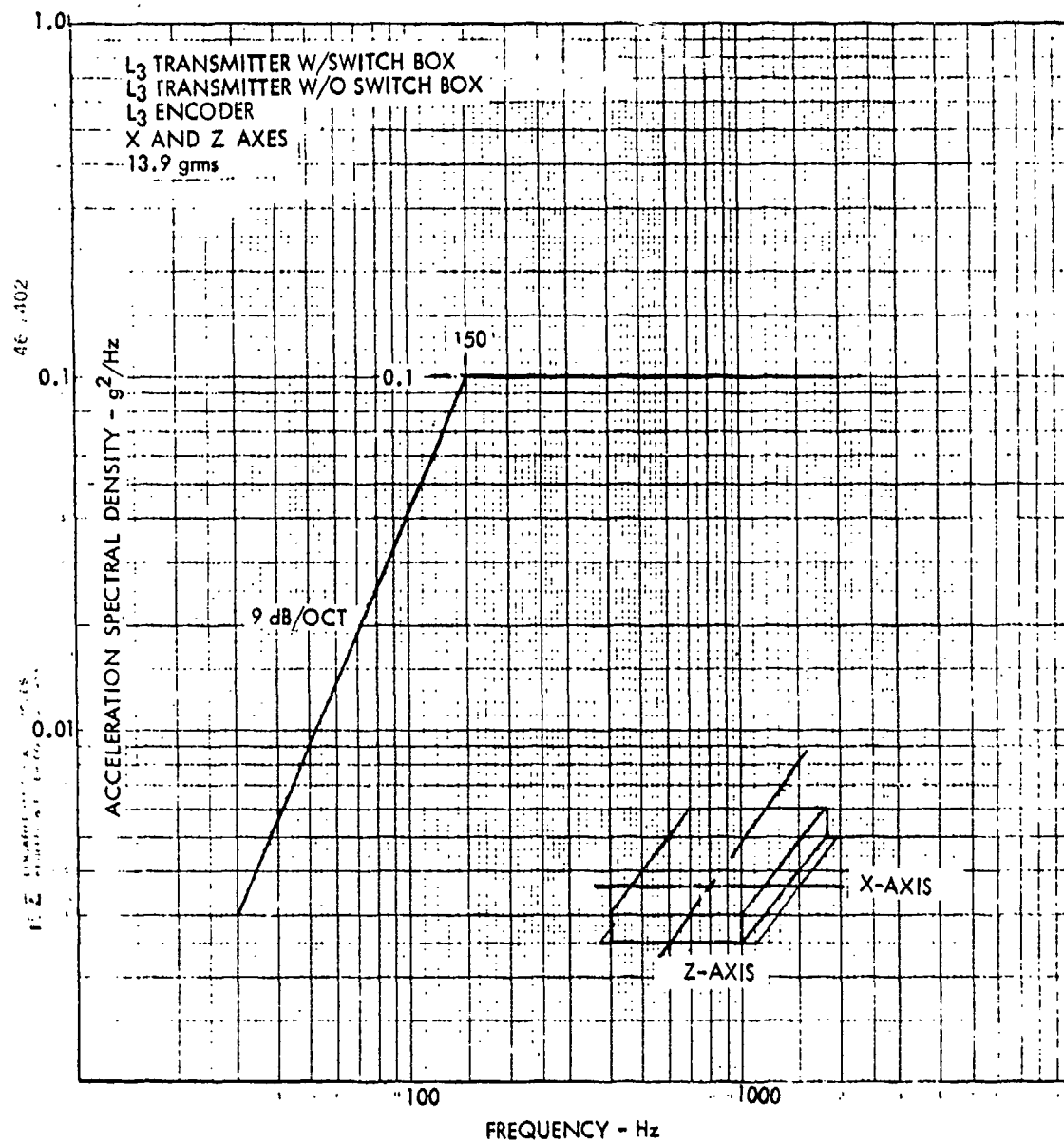


Figure 138. L₃ Transmitter and Encoder Random Vibration Qualification Levels (X-and Z-Axes)

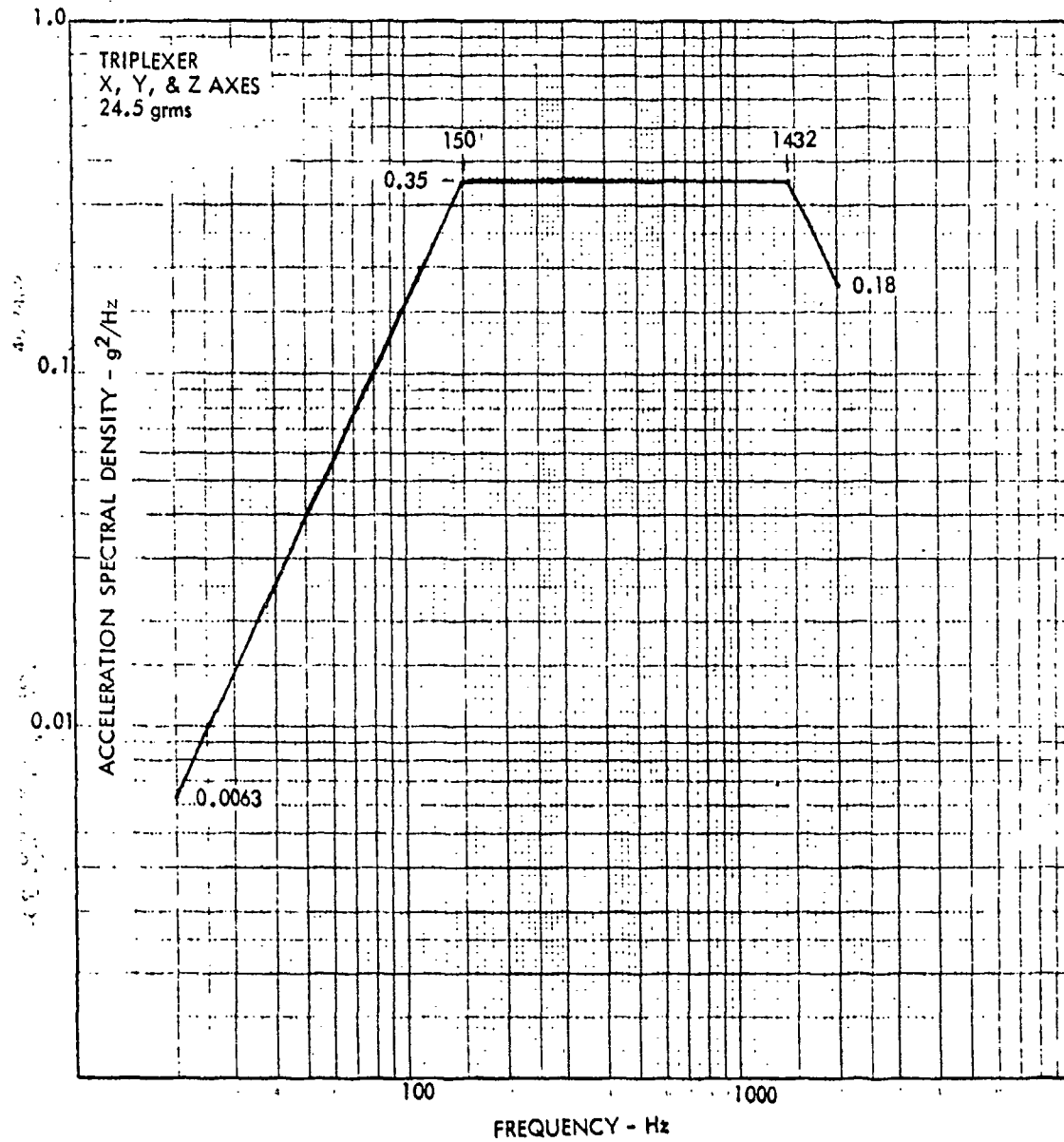


Figure 139. Triplexer Random Vibration Qualification Levels
(X-, Y-, and Z-Axes)

Vibration of the spacecraft was most severe in the 400- to 700-Hz range. A secondary level of vibration was in the 100-Hz to 250-Hz frequency range. As a unit, the spacecraft is expected to respond quite well in the frequency range of its ring frequency, which is approximately 600 Hz. Responses in the 100- to 250-Hz frequency range indicate the frequency range of the natural frequencies of panels and bulkheads.

The data indicate system noise influence in the frequency range from 20 to 150 Hz, with a maximum around 100 Hz. This noise was corrected during the vibration testing by using trial and error methods. Noise could not be eliminated by an exact procedure due to the nature of the noise, which tended to be more pronounced at low-energy levels than at high-energy levels.

Table 51 tabulates the maximum g root mean square (rms) measured by a given accelerometer during the various test runs. The rms value represents the total energy of the entire acoustics spectrum, while the plot itself depicts only the energy from 20 to 2,000 Hz. Integration of the plot will therefore result in lower g rms value than measured.

Table 52 compares the differences between the g rms level obtained during the test and that of the resultant plot defining the environment for the component testing. These values indicate the total energy to be imparted during component qualification testing as compared to that measured during the acoustic test.

Table 51. Summary of IGS Component G rms Test Results

IGS Component Identification	Accelerometer Location ID	Test (grms)	Recommended Qualification Test Level
X-sensor, X-axis	2X	9.0	20.0
X-sensor, Y-axis	2Y	6.9	15.0
X-sensor, Z-axis	2Z	6.7	15.0
IGS-GPS triplexer, X-axis	6X	2.6	24.5
IGS-GPS triplexer, Y-axis	6Y	7.8	24.5
IGS-GPS triplexer, Z-axis	6Z	7.1	24.5
Data processor, X-axis	15X	2.5	12.4
Data processor, Y-axis	15Y	1.9	12.4
Data processor, Z-axis	15Z	2.9	12.4
Blk conv encoder, X-axis	22X	4.8	13.9
Blk conv encoder, Y-axis	22Y	17.5	27.8
Blk conv encoder, Z-axis	22Z	5.0	13.9
L3 HPA Transmitter 1, X-axis	23X	5.5	13.9
L3 HPA Transmitter 1, Y-axis	23Y	14.0	27.8
L3 HPA Transmitter 1, Z-axis	23Z	5.6	13.9
L3 HPA Transmitter 2, X-axis	24X	4.7	13.9
L3 HPA Transmitter 2, Y-axis	24Y	15.6	27.8
L3 HPA Transmitter 2, Z-axis	24Z	9.3	13.9
Y-sensor, X-axis	29X	5.3	12.2
Y-sensor, Y-axis	29Y	12.0	13.4
Y-sensor, Z-axis	29Z	9.0	12.2

Table 52. Comparison of IGS Test G rms Values

IGS Component Mass Simulator Identification	Accelerometer ID	SCT + IGS Baseline*		IGS Baseline*
		Runs A and B (g rms)		Run C (g rms)
X-sensor	2X	8.2	7.9	9.0
X-sensor	2Y	6.5	7.4	6.9
X-sensor	2Z	7.0	7.9	6.7
IGS-GPS triplexer	6X	2.6	2.6	2.6
IGS-GPS triplexer	6Y	8.7	7.3	7.8
IGS-GPS triplexer	6Z	7.9	7.1	7.1
Data processor	15X	2.5	2.7	2.5
Data processor	15Y	2.0	1.9	1.9
Data processor	15Z	2.4	2.5	2.9
Blk conv encoder	22X	4.9	4.6	4.8
Blk conv encoder	22Y	16.5	17.2	17.5
Blk conv encoder	22Z	5.5	5.2	5.0
L ₃ HPA Transmitter 1	23X	5.1	5.0	5.5
L ₃ HPA Transmitter 1	23Y	13.5	13.6	14.0
L ₃ HPA Transmitter 1	23Z	5.9	5.5	5.6
L ₃ HPA Transmitter 2	24X	4.3	4.3	4.7
L ₃ HPA Transmitter 2	24Y	15.0	14.6	15.6
L ₃ HPA Transmitter 2	24Z	9.1	8.2	9.3
Y-sensor	29X	5.7	5.9	6.3
Y-sensor	29Y	8.0	10.6	12.0
Y-sensor	29Z		7.2	9.0
*SCT plus IGS baseline and the IGS baseline DTV configurations				

6.6 GPS/SPL THERMAL CONTROL TESTS

Extensive QTV thermal testing during the GPS development and the detailed thermal math model developed for GPS combined to provide an excellent data base for IGS thermal designs. In addition, the thermal math model for GPS was validated by comprehensive testing performed on the DTV and QTV corroborated by orbital data from NDS 1 and NDS 2. When direction was received to install IGS on NDS 6, it was determined to be most cost-effective and low risk not to conduct thermal control testing until full thermal-vacuum testing is accomplished on the NDS 6 IGS.

The basic objectives of the GPS secondary payloads thermal control program implemented for IGS were (1) to verify the IGS thermal control design, (2) to provide thermal orbital flight prediction, and (3) to establish the temperature impact on GPS equipment from the implementation of the IGS system.

6.6.1 Thermal Control System Objectives

The objective of the GPS thermal control system is to assure the long-life reliability of all components by maintaining their temperature within proper bounds. This is accomplished passively for most equipment by the following:

- Thermal control louvers which regulate the heat rejection to space as a function of space vehicle temperature
- Thermal control coatings and thermal blankets, which establish the temperature level of the space vehicle
- Thermal doublers and the basic structure of the space vehicle to distribute and store thermal energy

The RCS wetted surfaces, the batteries, the RCS motor, and the L₁-MOD/IPA are controlled by thermostatically controlled heaters.

The thermal design was verified at various stages in the program by thermal-vacuum tests on the development test vehicle, the RCS breadboard, and the qualification test vehicle. Flight test data on NDS 1 and NDS 2 have shown that the thermal control system is performing within requirements and as expected.

To incorporate secondary payloads into the GPS vehicle, a thermal analysis was performed to define the SPL thermal control design modification and determine the temperature effects of adding the payloads to the GPS satellite. The analysis indicated that temperature changes for GPS components were minor and all components remain within their specified temperature limits. The minimal temperature impact of secondary payloads on the GPS satellite is due to an optimized thermal control design which requires a minimum of modifications to the satellite and establishes a high level of assurance that the GPS/SPL thermal control design will perform as expected.

6.6.2 Thermal Requirements

The SPL thermal control subsystem (TCS) requirements are to integrate the SPL equipment into the GPS thermal control design and maintain SPL and GPS equipment temperatures within specified limits. To eliminate the need for temperature requalification of GPS equipment, the integration of SPL equipment must not modify the GPS thermal control design or significantly impact the energy balance. The SPL TCS also must provide a reasonable margin in controlling component temperature extremes to account for uncertainties or variations in equipment dissipation, mounting interface conductances, satellite orientation, solar radiation, and degradation of thermal control surface properties during the life of the mission.

The SPL equipment will be qualified according to MIL-STD-1540 component temperature limits of -34°C to +71°C. The GPS equipment qualification limits are more restrictive. In particular, the cesium clock and rubidium frequency standard temperature variation must be controlled to less than 4°C per orbit. This temperature variation requirement must be met during various satellite operational modes in which equipment power dissipation varies considerably.

6.6.3 Thermal Control Configuration

The SPL thermal control design for IGS and IGS/SCT configurations emphasizes the placement of equipment in locations that minimize conduction and

radiation exchange with GPS equipment and thereby minimize impact on GPS component temperatures. The design philosophy is to couple equipment conductively to radiator areas or exterior panels and thereby reduce energy exchange coupling between SPL and GPS equipment. High heat dissipating equipment is located on the shear panels to take advantage of their optimum heat rejection capability due to minimal solar exposure. Mounting equipment on shear panels also reduces thermal doubler requirements and weight impact.

The remaining equipment, mainly the low heat dissipating components, are located on the aft bulkhead and require no heater control. An additional radiator on the aft bulkhead is utilized for the IGS/SCT configuration to maintain SPL equipment (UHF and SHF receivers) within temperature limits. The aft bulkhead radiator utilizes silverized Teflon tape and is sized for degradation of surface properties due to plume impingement and solar exposure. The thermal control design of the IGS and IGS/SCT configurations is identical except for the aft bulkhead radiator required for the UHF and SHF receivers on the IGS/SCT configuration.

6.6.4 Component Mounting

The SPL component mounting requirements are divided into two categories: high and low heat dissipating components. The high heat dissipating equipment is mounted on the shear panels to take advantage of their optimum heat rejection capability. The existing GPS shear panel doubler areas are enlarged to provide mounting areas for the SPL equipment, giving required mounting interface surface flatness and conduction fin efficiency for proper temperature control. The low heat dissipating equipment is mounted on the aft bulkhead and requires no thermal doublers since the structural bulkhead is adequate in conducting the low level of heat dissipation.

6.6.5 Thermal Doublers

The GPS thermal control design relies on doublers to assist in the conduction of equipment heat to the shear panel radiator areas. The design requires only minor enlargements of existing doublers to accommodate the mounting of SPL equipment and provide the required conduction fin efficiencies. The weight of the additional doubler areas required for SPL is 1.55 pounds. The SPL doubler requirements (enlargements of existing GPS doublers) are illustrated in Figure 140.

6.6.6 Thermal Control Coatings

The SPL thermal control design relies solely on the use of GPS-approved thermal coatings and tapes and requires no modifications of the thermal control utilized on the GPS satellite. The exterior surfaces of SPL electronic components are coated with a high-emittance black paint to enhance internal radiation exchange and minimize temperature gradients within the spacecraft. The aft bulkhead radiator is covered with silverized Teflon to aid in component heat rejection and reflection of incident solar radiation. S-13 GLO white paint and multilayer insulation are utilized on the UHF and SHF antenna exteriors as well as on the X-sensor and Y-sensor sunshade to reduce temperature excursions.

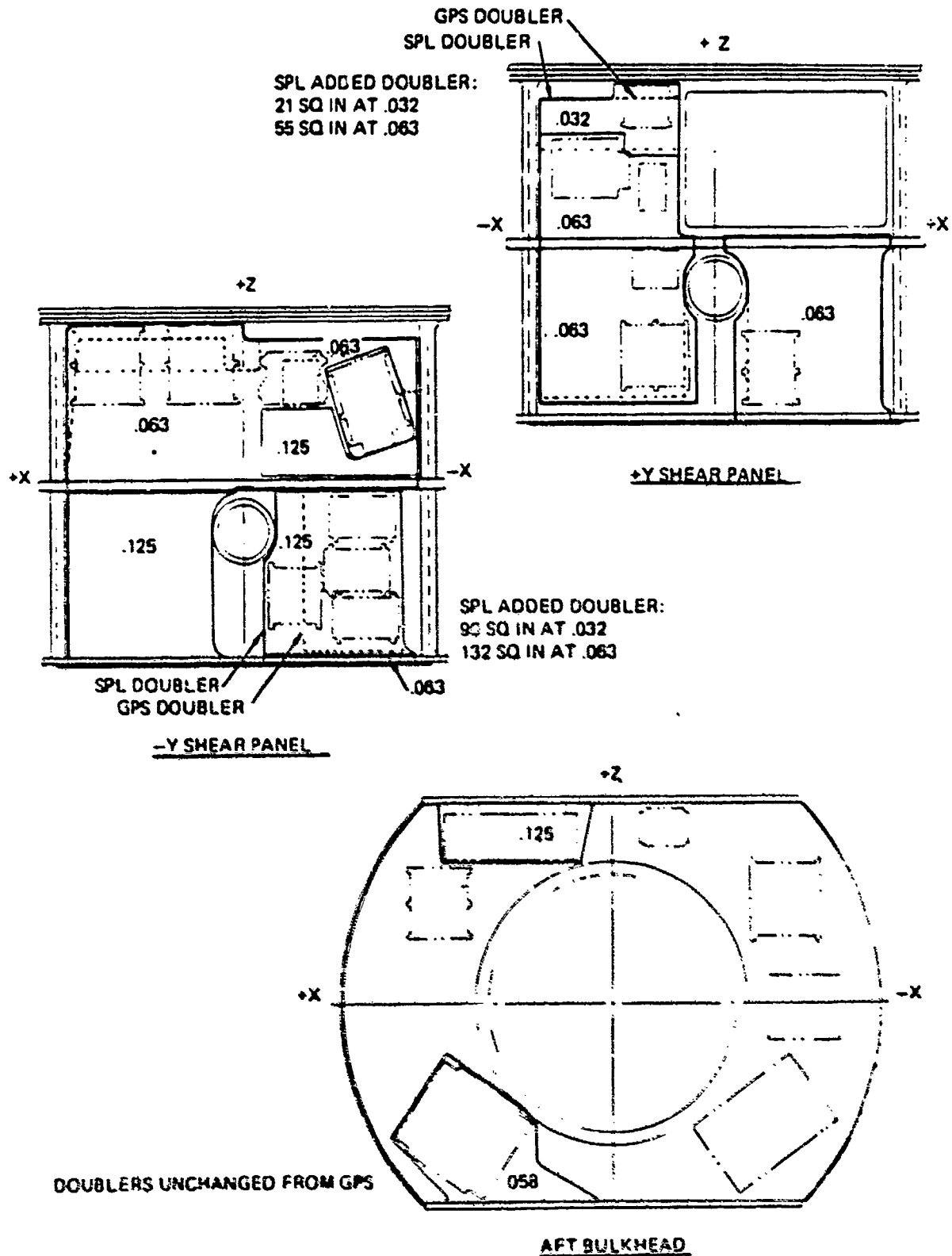


Figure 140. SPL Doubler Requirements

6.6.7 Thermal Math Model

The thermal math model consists of a network of lumped nodal capacitances, conductances, radiation couplings, heat inputs, and boundary conditions representing spacecraft structure, energy transfer paths, mission-related power dissipation timelines, and environmental heat loadings. The GPS math model has been validated by correlation with vehicle qualification test results. The SPL math model is basically the GPS model modified for the incorporation of SPL equipment. The SPL nodal inputs are described in Table 53, while the SPL equipment dissipation is given in Table 54. The SPL equipment nodal locations are shown in Figures 141 through 145.

6.6.3 Thermal Control Subsystem Impacts

An analysis was performed to determine the temperature effects of adding both IGS and IGS/SCT payloads to the GPS spacecraft. Results of the analysis, shown in Tables 55 through 60, indicate only minor temperature changes for GPS components, with all components remaining within their acceptance temperature limits. The minimal temperature impact of IGS and IGS/SCT payloads on the GPS satellite is due to an optimized thermal control design which requires minimum modifications of the GPS satellite.

The temperature effects caused by adding the IGS and IGS/SCT payloads are shown in Tables 57 and 60, respectively. The tables list the maximum acceptance limits, maximum allowable predictions, and vehicle qualification test results for each GPS component. The remaining columns show the impact of IGS or IGS/SCT payload additions to GPS component temperatures. Two conditions were examined

Table 53. SPL Nodal Inputs

Node No.	Component	Weight (lb)	Specific Heat (Btu/lb-°F)
784	Reference generator (SCT)	7.7	0.25
785	Digital processor (SCT)	8.3	
787	UHF receiver (SCT)	10.3	
786	UHF diplexer (SCT)	4.5	
788	UHF transmitter (SCT)	11.6	
789	SHF receiver (SCT)	10.5	
790	Transec (SCT)	5.0	0.25
791	UHF antenna (SCT)	3.1	-
792	SHF antenna (SCT)	1.8	-
793	X-sensor (IGS)	3.1	0.25
794	Y-sensor (IGS)	10.7	
712	Triplexer (IGS)	0.4	
796	Data processor (IGS)	20.8	
797	L3 HPA + switch (IGS)	6.6	
798	L3 HPA (IGS)	5.9	
799	TI encoder (IGS)	1.7	0.25
795,800,801	Y-sensor sunshade (IGS)	4.5	-
802,804	Y-sensor MLI (IGS)	10.7	-
805	UHF antenna MLI (SCT)	-	-
806	SHF antenna MLI (SCT)	-	-
807	X-sensor shade (IGS)	3.1	-

Table 54. SPL Equipment Power Dissipation

Item	Power Dissipation (w)	
	Standby Mode	Transmit Mode
SCT		
Reference Generator	5.3	5.3
Digital processor	12.3	12.3
UHF receiver	8.7	8.7
UHF diplexer	0.0	1.8
UHF transmitter	0.1	49.4
SHF receiver	9.8	9.8
Transec	6.3	6.3
IGS		
X-sensor	1.0	1.0
Y-sensor	1.5	1.5
Triplexer	5.8	7.5
Data processor	9.0	9.0
L3 HPA + switch	0.0	58.0
L3 HPA	0.0	58.0*
TI encoder	3.2	6.2
*Redundant		

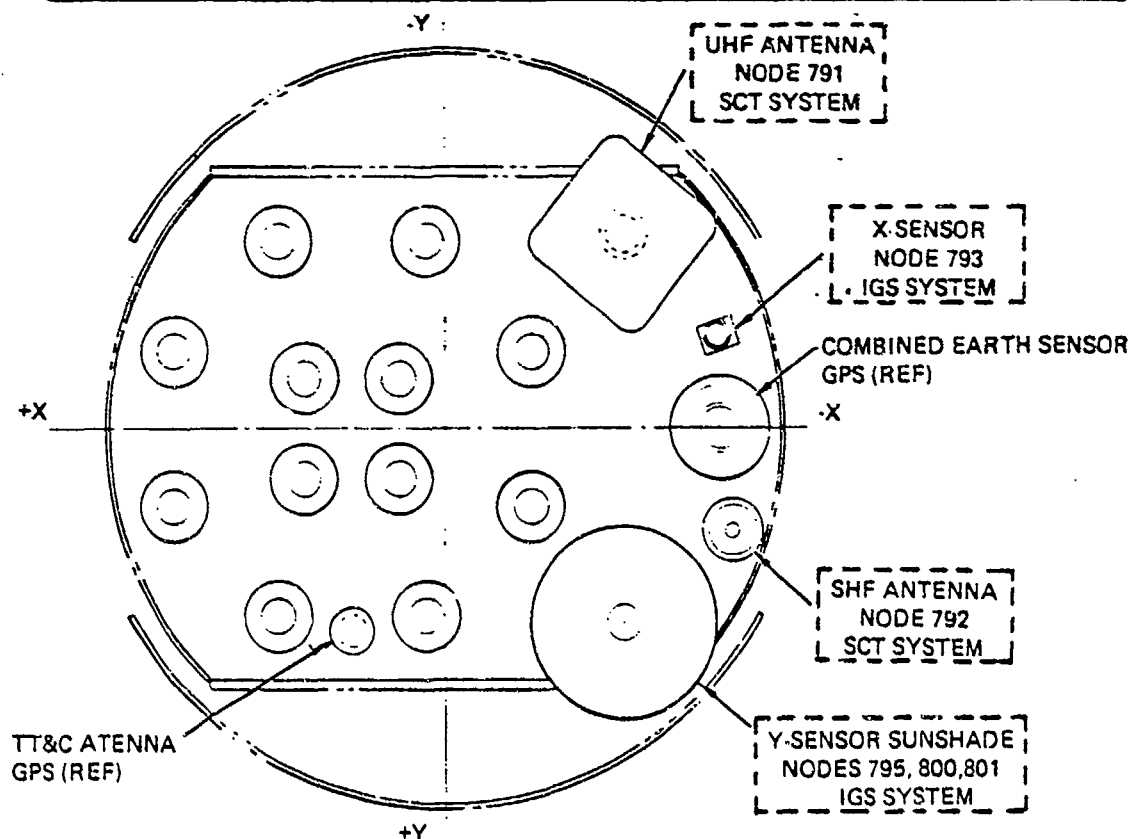


Figure 141. SPL Equipment Nodal Location - Forward Face, Forward Bulkhead

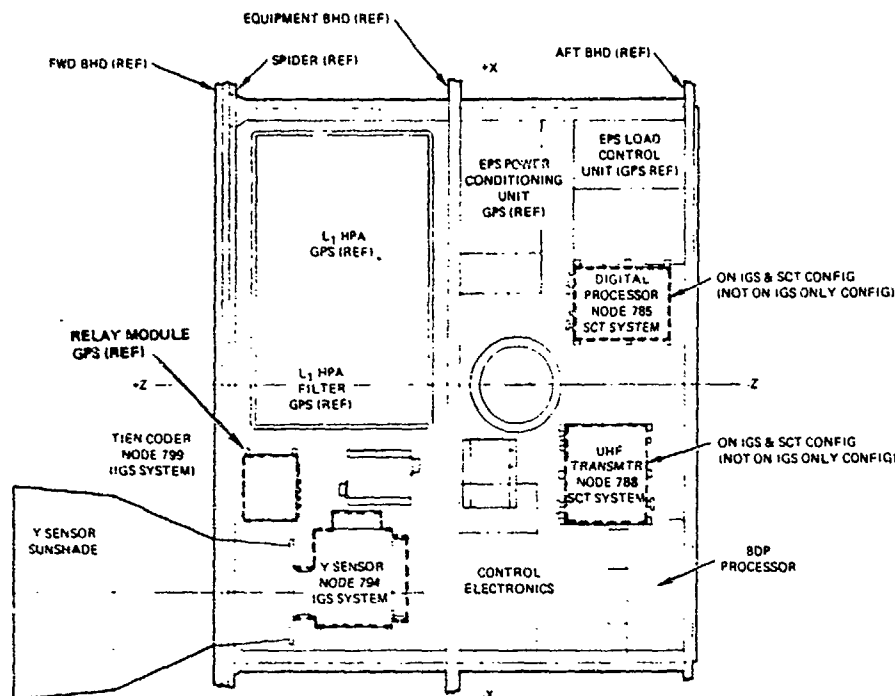


Figure 142. SPL Equipment Nodal Location - +Y Shear Panel

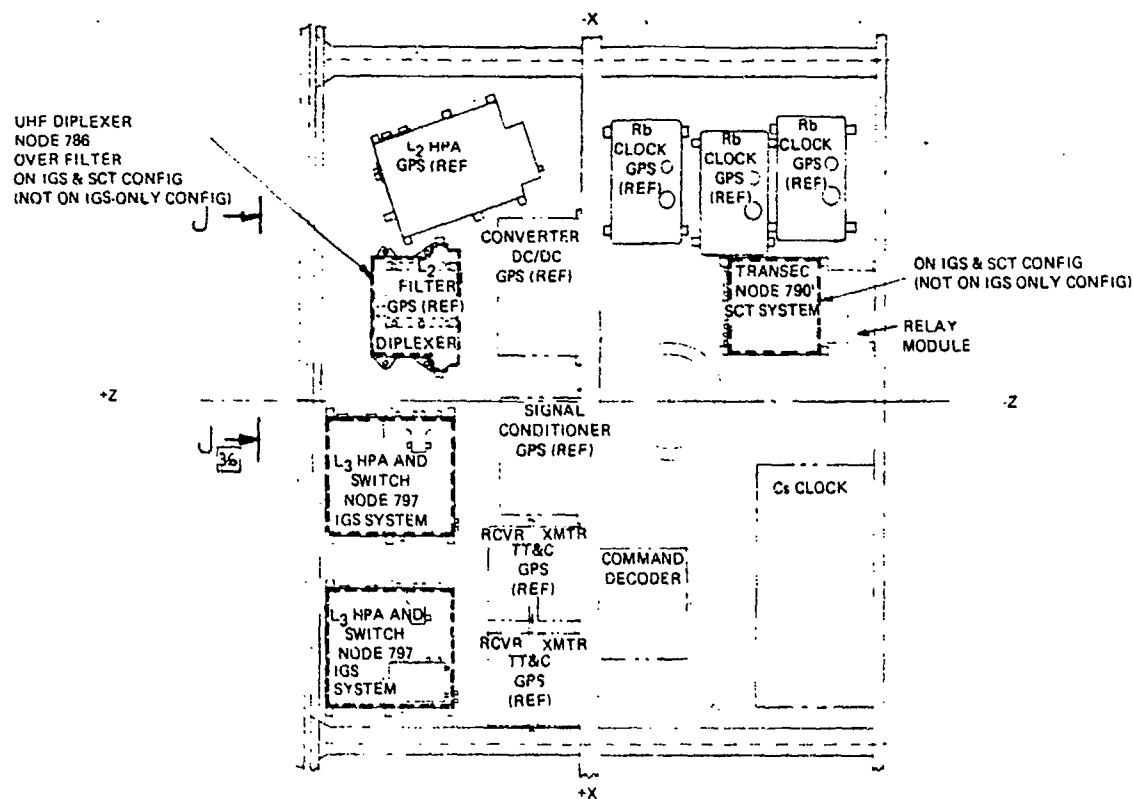


Figure 143. SPL Equipment Nodal Location - -Y Shear Panel

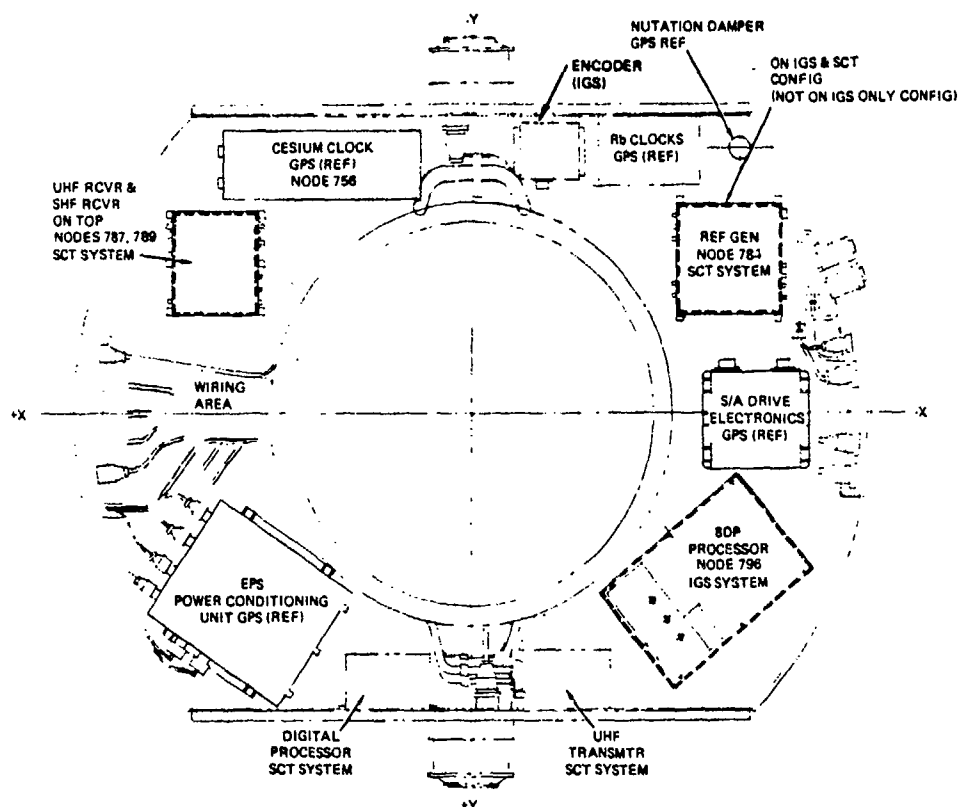


Figure 144. SPL Equipment Nodal Location - Forward Face, Aft Bulkhead

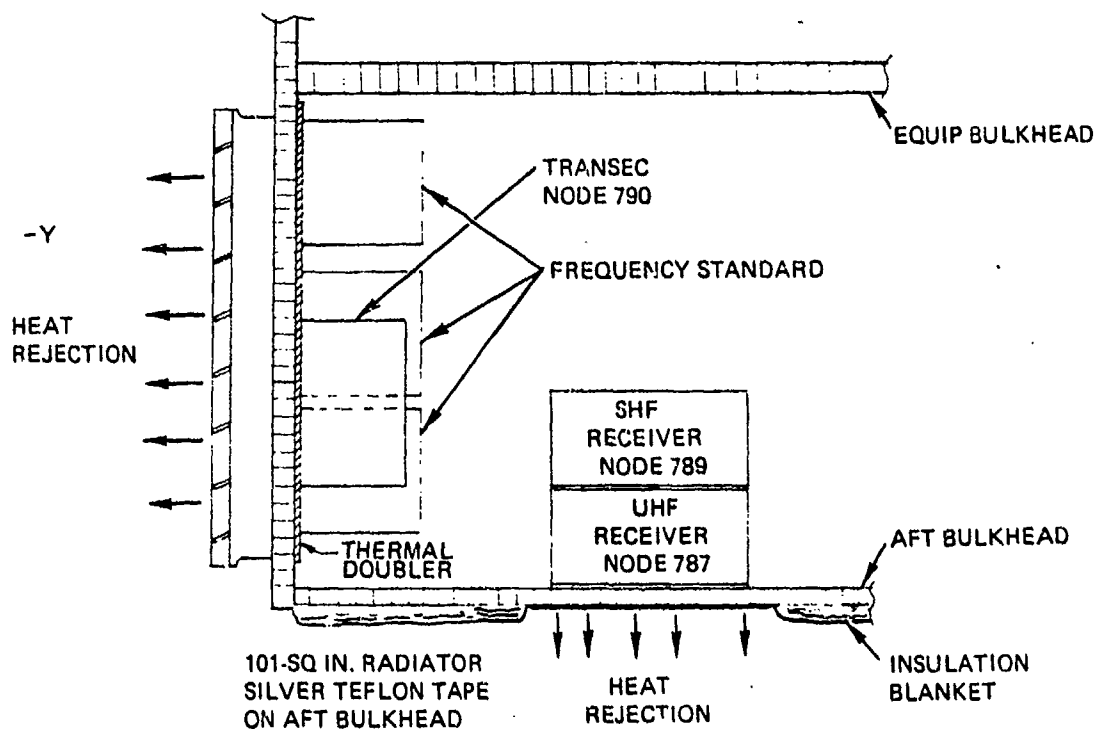


Figure 145. Proposed SPL Radiator Addition

Table 55. IGS Equipment Temperatures -
On-Orbit Steady-State Cold Case

Equipment	Temperature (°C)
X-sensor	14
Y-sensor	9
Triplexer	20
Data processor	16
L3 HPA transmitter + switch	8
L3 HPA transmitter	8
TIE	9

Table 56. IGS Equipment Temperatures - On-Orbit Steady-State Hot Case

Equipment	Power Steady-State Transient (w)	Temperature (°C)	
		Standby Steady-State	Transmit At 1 Hour
X-sensor	1.0	28	28
Y-sensor	1.5	21	21
Triplexer	5.8/7.5	31	34
Data processor	9.0	25	25
L3 HPA + switch	0.0/58.0	14	30
L3 HPA	0.0	14	25
TIE	3.2/6.2		

for the IGS payload impact. One was a steady-state orbit average analysis with the IGS equipment in a standby mode. The other was a transient analysis with the IGS, SCT, and IGS/SCT equipment in a transmit mode for one hour.

As shown in Table 53, the impact of adding the IGS payload results in minor GPS equipment temperature increases over the qualification test results. The noticeable exceptions are the PCU and EPS control electronics unit, which have 8°C and 9°C increases, respectively, over their qualification test results. A few GPS components actually operate at a lower temperature level than qualification test results due to math model inaccuracies or SPL thermal control design additions. Examples of this are the diplexer/triplexer, LCU, and PCM. In summary, the impact of IGS payload on GPS is minor, requiring no requalification of GPS equipment and few thermal control design changes.

The IGS/SCT payload addition also results in minor GPS equipment temperature increases over the qualification test results as shown in Table 56. The noticeable exceptions are Batteries 1 and 2, the PCU, and the EPS control electronics unit, which have respectively 7°C, 6°C, 11°C, and 11°C temperature increases over their qualification test results. Although the impact of the IGS/SCT payload on GPS is minor and requires no requalification of GPS equipment, it does require a few thermal control design changes, including additional radiator area on the aft bulkhead for heat rejection.

Table 57. GPS Component Temperatures - Hot Case (IGS Configuration)

Component	Accept. Spec	Allowable Pred	GPS Test Results	GPS and IGS-IGS Standby	GPS and IGS-IGS Transmit at 1 Hour
Navigation Subsystem					
Baseband processor	47	36	29	31	31
L1 HPA	60	49	45	44	45
L1 MOD/IPA	56	45	32	33	34
L1/L2 carrier synchronizer	49	38	26	25	26
L2 HPA	40	29	21	25	25
L2 MOD/IPA	50	39	29	31	32
Frequency standard 1 (Rb)	45	45	20	22	22
Frequency standard 2 (Rb)	45	45	32	34	34
Diplexer/triplexer	46	35	35	31	34
C1 clock	45	45	-	40	40
EPS					
DC/DC converter	60	49	29	32	32
Battery 1	30	30	3	7	7
Battery 2	30	30	3	7	7
Battery 3	30	30	7	4	4
PCU	60	49	27	35	35
LCU	60	49	29	25	25
Control electronics	60	49	15	24	24
AVCS					
Reaction wheel	60	49	36	36	36
Reaction wheel	60	49	36	36	36
Reaction wheel	60	49	36	36	36
Reaction wheel	60	49	36	36	36
Control electronics	48	37	27	27	27
CES	60	49	30	29	29
TT&C					
PCM	60	49	31	25	25
RF unit	60	49	23	25	25
Signal conditioner	60	49	24	26	26
KIR-23	60	49	29	25	25
KIR-23	60	49	24	25	25
Command decoder	60	49	21	25	25
Transmitter	55	44	21	24	25
Transmitter	55	44	22	24	24
Receiver/demodulator	55	44	23	25	25
Receiver/demodulator	55	44	23	25	25

The GPS model utilized for the hot orbital analyses was a hot bias spacecraft with a maximum solar constant (442 Btu/hr-ft^2) and a $\beta = 0$ -degree maximum eclipse environment. The GPS navigation subsystem was in the high-power mode, with the TT&C subsystem dissipation averaged for the entire orbit. The electrical power subsystem was at the average eclipse loads (charge/discharge), and the attitude and velocity control subsystem was at normal (hot bias) loads.

The GPS model utilized for the cold orbital analyses was a cold bias spacecraft with a minimum solar constant (415 Btu/hr-ft^2) and a $\beta = 90$ -degree full sun orbit. The navigation subsystem was in the L_1 and L_2 mode, and the EPS was at the trickle charge loads.

Table 58. SCT/IGS Equipment Temperatures -
On-Orbit Steady-State Cold Case

Equipment	Temperature (°C)
SCT	
Reference generator	9
Digital processor	5
UHF diplexer	12
UHF receiver	-2
UHF transmitter	6
SHF receiver	-2
Transec	16
IGS	
X-sensor	12
Y-sensor	8
Triplexer	19
Data processor	14
L3 HPA transmitter + switch	7
L3 HPA transmitter	7
TIE	9

Table 59. SCT/IGS Equipment Temperatures - On-Orbit Steady-State Hot Case

Equipment	Power Steady-State/ Transient (W)	Temp °C			
		Steady-State SCT/IGS Standby	IGS Transmit, SCT Standby at 1 Hour	SCT Transmit, IGS Standby at 1 Hour	SCT Transmit, IGS Transmit, at 1 Hour
SCT					
Reference generator	5.3	26	26	26	26
Digital processor	12.3	22	22	23	23
UHF receiver	8.7	43	43	43	43
UHF diplexer	0.0/1.3	19	19	20	21
UHF transmitter	0.1/49.4	14	14	29	29
SHF receiver	9.8	47	47	47	47
Transec	6.3	27	27	27	27
IGS					
X-sensor	1.0	26	26	26	26
Y-sensor	1.5	21	21	21	22
Triplexer	5.8/7.5	33	35	33	35
Data processor	9.0	27	27	27	27
L3 HPA + switch	0.0/58.0	14	30	14	30
L3 HPA	0.0	14	25	14	25
TIE	3.2/6.2	18	21	18	21

Table 60. GPS Component Temperatures - Hot Case (IGS/SCT Configuration)

Component	Accept. Spec	Allow. Pred	GPS Test Results	GPS and SCT/IGS— Standby SCT/IGS	GPS and SCT/IGS—IGS Transmit, SCT Standby	GPS and SCT/IGS—SCT Transmit, IGS Standby	GPS and SCT/IGS SCT Transmit IGS Transmit
Navigation Subsystem							
Baseband processor	47	36	29	32	32	32	32
L1 HPA	60	49	45	45	45	45	45
L1 MOD/IPA	56	45	32	34	34	34	34
L1/L2 carrier synthesizer	49	33	26	26	26	27	27
L2 HPA synthesizer	40	29	21	25	25	25	26
L2 MOD/IPA	50	39	29	32	32	32	32
Frequency Std 1 (Rb)	45	45	20	23	23	23	23
Frequency Std 2 (Rb)	45	45	32	33	33	33	33
Diplexer/triplexer	46	35	35	33	35	33	35
C1 clock	45	45	-	44	44	44	44
EPS							
DC/DC converter	60	49	29	33	33	33	33
Battery 1	30	30	3	10	10	10	10
Battery 2	30	30	3	9	9	9	9
Battery 3	30	30	7	5	5	5	5
PCU	60	49	27	38	38	38	38
LCU	60	49	29	26	26	26	27
Control electronics	60	49	15	26	26	26	26
AVCS							
Reaction wheel	60	49	36	36	36	36	36
Reaction wheel	60	49	36	36	36	36	36
Reaction wheel	60	49	36	36	36	36	36
Reaction wheel	60	49	36	36	36	36	36
Control electronics	48	37	27	28	28	28	28
CES	60	49	30	28	28	28	28
TT&C							
PCM	60	49	31	26	27	27	27
RF unit	60	49	23	26	26	26	26
Signal conditioner	60	49	24	27	27	27	27
KIR-23	60	49	29	27	27	27	27
KIR-23	60	49	24	26	26	26	26
Command decoder	60	49	21	26	26	26	26
Transmitter	55	44	21	25	25	25	26
Transmitter	55	44	22	25	25	25	25
Receiver/demodulator	55	44	23	26	26	26	26
Receiver/demodulator	55	44	23	26	26	26	26

7. CONCLUSIONS AND RECOMMENDATIONS

7.1 CONCLUSIONS

The validation test has verified that the SPL IGS/GPS operates as specified without impact to the basic GPS navigation mission.

The test program involved integration and testing of the complete SPL IGS system installed on the GPS vehicle. Anechoic chamber tests were run with both payloads operating and with all transmitters operating at full power. No detectable cross coupling of transmitter/receiver combinations was observed.

The following conclusions have been derived:

- Minimum modifications to GPS to accommodate IGS achieved
 - Timing, power, TT&C, and antenna interfaces provided without impact to the GPS navigation payload or mission
- The IGS system does not impact the navigation system performance
 - Tested using the GPS X-set receiver and no effect on the navigation system was verified
 - Antenna pattern testing verified no impact on navigation patterns with IGS added
 - Anechoic chamber tests with all transmitters operating at full power verified that there were no undesirable intermodulation products that affect the IGS/GPS mission
- IGS design goals achieved
 - L₁/L₃ handoff workable and proven
 - Weight and power within specifications and budget
 - Environmental levels verified and tested
 - Vibroacoustic and thermal levels established
 - EDM tested to qualification levels
 - Full qualification tests completed
 - L₃ should not impact the radio astronomy service due to low power and duty cycle. A radio astronomy filter is planned for extended duty cycle.



7.2 RECOMMENDATIONS

The performance of a full-up test on FSV 6 is recommended.

- EMI: The ETV survey indicated minor problems which were corrected; should have full-up test with all GPS and IGS systems operating.
- Thermal: Math model indicates no problem; needs augmented (performance versus design/workmanship) thermal-vacuum test on FSV 6 for verification.

APPENDIX. RADIO ASTRONOMY INTERFERENCE STUDY

The GPS space vehicle with the IGS secondary payload radiates three spread-spectrum modulated carriers designated L_1 (1575.42 MHz), L_2 (1227.6 MHz), and L_3 (1381.05 MHz) which contain spectra within two radio astronomy bands allocated worldwide. This appendix contains the background, requirements, measurements, and data analyses relevant to evaluating the potential radio astronomy signal interference levels.

BACKGROUND

Radio astronomy is primarily the passive observation of radio frequency sources in our own and distant galaxies at various frequencies ranging from a few megahertz to a few tens of gigahertz. The characteristics of these radio sources vary from broadband continuum-type radiation to narrow line emissions, all of which show practically no modulation other than random noise. Observations of these signals generally fall into two broad classes. Class A observations, often used in the study of cosmic emissions of relatively high intensity, are those in which the sensitivity of the equipment is not a primary factor. Many observations fall into this class, and continuity is a primary factor.

The nature of Class B observations is such that advanced low-noise receivers, long integration times, and wide receiver bandwidths are usually involved, and their significance is critically dependent on the sensitivity of the equipment used in making them. Potential interference with this latter class of observation is the primary emphasis of this appendix.

The sensitivity of a radio astronomy observation can be defined as the smallest power level change that can, with high certainty, be detected and measured. International Radio Consultative Committee (CCIR) Annex 7-1 notes that the smallest detectable change

depends on the bandwidth used for the observation, on the total effective noise temperature of the radiometer and antenna, and on the length of time over which the power in a single observation is integrated. In simple terms, the most sensitive observations are those made with the smallest system noise temperature, the largest bandwidth and the longest integration times. Good techniques can reduce the system temperature, integration times of a large fraction of a day can be used if the telescope tracks the source, but the bandwidth must be chosen to suit the experiment. For example, when an observation of a source spectrum is needed, and it is believed that the spectrum is regular, operation with large bandwidths and for long integration times is feasible when no harmful interference is present, with consequent increase in sensitivity. But when the spectrum of a fairly narrow line is being observed, the fine detail in the spectrum may only be observable if a narrow bandwidth is used; such observations are then less sensitive.

The observation of line emissions is one of the most difficult tasks in radio astronomy. High gain antennas, low-noise receivers, and complex electronic processing equipment are used, with integration times of many hours being common. Protection, therefore, is required from the harmful interference that can occur when an unwanted signal flux impinging on the antenna is so great that the background operating noise is increased by an amount comparable to the signal being observed.

If the Radio Astronomy Service (RAS) is to secure the advantage of low-noise receivers, the interference should not produce an error of more than 10 percent in the measurement of the desired signal. This raises the question of whether any harmful interference can be tolerated by the Radio Astronomy Service. Although the answer is somewhat subjective and many radio astronomers would reply that no harmful interference can ever be tolerated, many radio astronomers do excellent work in the presence of bursts of strong interference.

This led the authors of CCIR Annex 7-1 to conclude "that strong recognizable interference can be tolerated if it occurs in short bursts for a small fraction of the total time," while "an insidious danger to the Radio Astronomy Service lies in interference just below the power level at which it can be recognized, present for large fractions of the total time." Furthermore, the report states, "unless harmonic suppression much greater than 80 dB is provided in transmitter designs, services employing high transmitter powers will cause interference, if assigned to operate within the line-of-sight at frequencies sub-harmonically related to those employed by the Radio Astronomy Service."

For many sources, the best times of observation are controlled by natural phenomena and are limited to the time when the object is well above the horizon. Since these signals are weak in relation to typical high power transmitters and have no unique encoding to improve detectability, the Radio Astronomy Service is extremely susceptible to interference. To ensure continued progress in this field, a series of radio frequency bands have been set aside by international agreement to provide some protection for the observations. Two of these bands, 1400 to 1427 MHz for the observation of the hydrogen lines (1420 MHz, 1425 MHz) and 1664.4 to 1668.4 MHz for the observation of the OH radical lines (1666 MHz and 1667 MHz), are in the near vicinity of the L_1 , L_2 , and L_3 frequencies and are the major topics of this study. Although these are line spectra, they can exhibit a doppler shift or broadening in frequency depending on the relative velocity of the source and radio telescope. This can become especially significant for extragalactic quasi-stellar radio sources (quasars) which typically appear to be receding from the earth. In these cases, red shift, or apparent lowering of line frequency, occurs, shifting the H and OH lines toward the L_3 and L_1 frequencies.

Although the 1400- to 1427-MHz band has proved very satisfactory for neutral hydrogen in the past, the use of larger telescopes and more sensitive receivers has made possible the observation of more distant galaxies whose red shift moves the line to frequencies below 1400 MHz. An extension of some degree of protection down to 1390 MHz would be of considerable value for improving such observations, and such an extension down to 1350 MHz is being considered. Similarly, the basic hydroxyl frequencies are observable within a band extending from 1660 to 1670 MHz. Other hydroxyl lines, which occur near

1612 and 1721 MHz can be observed in a band of about 1 MHz centered on their rest frequency. For this reason, frequency administrators have been urged to give all practicable protection in the 1660- to 1670-MHz band for future research. An additional 20 MHz, up to 1690 MHz, are used by Albania, Bulgaria, Hungary, Poland, Romania, Czechoslovakia, and the USSR in their radio astronomy observations.

The IONDS payload for the GPS spacecraft is being developed under the guideline of no impact on the host vehicle's mission capability. In order to minimize cost, risk and vehicle impact, as many existing GPS components as possible are used to support the IONDS payload. The key area for using existing components is the downlink. Piggyback use of the existing GPS L-band navigation and S-band telemetry data links was considered for the IONDS data link. However, no existing link was available that could provide the required data rate and flexibility of receiving terminal to satisfy the IONDS users. The use of an L-band frequency between L_1 and L_2 was driven by the need for minimum impact to the GPS spacecraft. Using any other frequency would drive the need for an additional antenna, which would significantly impact the spacecraft and possibly degrade present mission capabilities.

Preliminary investigations emphasized the GPS L-band antenna performance, potential interference with the L_1 and L_2 navigation links (at either the satellite or the user receiver), potential intermodulation effects with GPS downlinks, and the existence of the protected Radio Astronomy Service band at 1400 to 1427 MHz. These results, when combined with preliminary FMO guidance (USAFFREQMGT/FC/DONF 071530 May 1976), resulted in five frequencies in the 1350- to 1400-MHz band being selected for evaluation. The IGS frequency selection criteria were as follows:

- Use navigation mission antenna
- Minimum interference to GPS L_1 and L_2 . (L_1 is more critical than L_2 .)
- Minimum interference to TT&C receive band
- Minimum interference to 1400- to 1427-MHz radio astronomy band
- L_3 synthesized from rubidium clock frequency
- Preliminary USAF/FMO guidance 1350 to 1400 MHz
 - USAF/FMO/DONF 071530Z May 1976
- Support secondary to radio location service

A tradeoff among these frequencies (Table A-1) indicated that 1350.36 and 1381.05 MHz were the best options available. Furthermore, subsequent antenna testing revealed a VSWR singularity that varied between 1365 and 1375 MHz, precluding the use of frequencies in that band. The key factor in selecting 1381.05 MHz over 1350.36 was the impact on L_2 . The triplexer design is affected by intercarrier isolation. The isolation between L_3 and L_2 using the three-pole filter design was approximately the same as the L_1/L_2 isolation, assuring

Table A-1. Frequency Selection Summary

Candidate Fc	L ₁ Isolation (39 dB)	L ₂ Isolation (39 dB)	TT&C Interference (1783.84 MHz)	Synthesizer Mechanization 10.23 Ratio
1381.05 MHz	-51 dB	-44 dB	1769.79 MHz	135
1375.935 MHz	-52.5 dB	-42 dB	1774.90 MHz	134.5
1370.82 MHz	-54.5 dB	-40.5 dB	1780.02 MHz	134
1364.0 MHz	-55.5 dB	-38 dB	1785.84 MHz	133-1/3
1350.36 MHz	-57 dB	-30.5 dB	1800.84 MHz	132
Note: Subsequent antenna testing identified VSWR singularity which essentially precludes use of 1365-1375 MHz band				

minimal L₃ impact on the navigation mission. The isolation at 1350.36 was almost 10 dB less than the -39-dB criteria that had been selected based on the GPS design to assure no impact on user equipment. Although 1381.05 MHz resulted in a signal level approximately 14 dB higher in the 1400- to 1427-MHz region, discussions with radio astronomers in the Los Angeles area indicated that the infrequent, short IONDS transmissions should provide negligible interference. In addition, a radio astronomy band filter should bring the L₃ signal level below the -238 dBW/m²/Hz criteria used in the GPS design. Similarly, frequency synthesis was not a major factor since 1381.05 and 1350.36 MHz are equally implementable. Using a frequency in the 1240- to 1290-MHz band was considered as requested (USAFFREQMGT OFC Wash DC/FMO 301800Z June 1977) but is not technically feasible because of its probable impact on L₂.

The L₃ selection process is outlined as follows:

- Five frequencies in preliminary guidance range
- Only 1381.05 MHz has attenuation at L₁ and L₂ equal to or better than L₁ at L₂ and L₂ at L₁
- 1350.36 MHz puts least energy in TT&C band. 1381.05 MHz nearly as good
- 1350.36 MHz puts least energy in 1400- to 1420-MHz band. 1381.05 MHz approximately 14 dB above radio astronomy threshold
- ITT proposes five-pole L₃ filter for radio astronomy protection (14-dB protection). Minor triplexer weight change. 1-dB L₃ impact
- 1381.05 and 1350.36 MHz equally synthesizable

Since the compatibility testing completed in August 1977 indicates there is no interference between the current 1381.05-MHz L₃ and the existing 1227.6-MHz L₂ downlinks, the use of 1350.36 MHz may be more technically feasible than

analytically estimated. The effort to validate the feasibility of using 1350.36 MHz would appear appropriate if the use of that frequency would significantly reduce limitations on the use of IONDS which would be imposed for 1381.05 MHz. Eliminating restrictions that would require a change in frequency after a relatively short time (i.e., 5 to 10 years) and/or effectively preclude the scientific community from deliberately using the system to observe severe weather may be worthy of consideration. Use of the system in a scientific lightning mode could result in 10 or more random triggers per day during certain weather conditions.

The IONDS system is designed to be dormant unless an event triggers the sensor system. The spacecraft system is being sized to permit up to 60 minutes of transmission per orbit under extreme (i.e., war) conditions. Normal operations would consist of scheduled calibration commanded from Continental U.S. (CONUS) ground stations and random triggers due to natural (i.e., lightning "superbolt") events. Memory for readout at prescheduled times for 1 to 5 minutes in CONUS may also be expected about once a week. Precoordinated tests of satellites in CONUS which would involve transmission periods of 60 to 90 minutes may be requested several times during the first few years of operation.

The predominate source of random triggers will be lightning "superbolts" which have been observed by similar sensors on the VELA and other satellites. The IONDS sensors will have multiple trigger criteria that will be both automated and selectable by command to control the random false trigger rate as near to zero as possible. The VELA satellite system with its unique worldwide full-time observation capability has recorded a large number of terrestrial lightning signals each year. A small number of these, estimated to be 10^{-8} of the worldwide flash rate of about 100 per second, could potentially cause random triggers that would not be rejected by trigger logics. Since there is a large probability that the direct line-of-sight between the satellite and the lightning flash will be obscured by clouds, the satellites would detect only a fraction of the lightning flashes. This fraction has been estimated from the number of single- and dual-satellite lightning observations in which two VELA satellites were within view of the lightning stroke.

From the ratio of dual- and single-satellite detections, one can estimate that only 20 percent of these intense lightning strokes will be detected by the satellite system. Since the VELA data indicates the number of superbolts generated per year to be about 25, there should be less than one superbolt per week that will generate random triggers even if the IONDS trigger rate is a factor of two or so greater than VELA. Also, since the VELA data indicates only a 0.2 probability of a dual observation, only one of the four to six GPS satellites that would be within the appropriate zenith angle of the lightning is likely to observe the bolt. Although these superbolts have been detected worldwide, their most frequent occurrence is over Japan and the northeast Pacific Ocean. They are located in regions of strong convective activity and have been correlated with severe thunderstorms.

STUDY OVERVIEW

The Rockwell investigation was conducted to ascertain the magnitude of potential interference introduced by the three GPS SV modulated carriers (L_1 ,



L₂, and L₃) into the two radio astronomy bands allocated worldwide. Theoretical spectrum power density levels referred to the earth's surface were calculated based on GPS transmissions and compared to harmful radio astronomy interference levels as defined by CCIR Annex 7-1. Actual spectral measurements made on the Engineering Test Vehicle (ETV) confirmed these computations.

Results indicated that both L₁ and L₃ exceed CCIR levels. Of these, the L₃ spectrum is of most concern since the calculated power levels within the radio astronomy bands can significantly exceed the desired minimum level if no specific filtering for the 1400- to 1427-MHz radio astronomy band is used. This potential detrimental effect of L₃ interference on the radio astronomy data is not only a function of the instantaneous energy levels, but also a function of the interference duty cycle (i.e., interference in band time to radio astronomy integration). Since less than five minutes of L₃ transmission per day per satellite, including both the normal and test and calibration modes is planned, L₃ interference is not expected to affect radio astronomers, who integrate over long periods of time.

In the event this is unsatisfactory to the RAS, two approaches to reduce power density, on a worst-case basis, below the specified harmful interference levels were pursued. They included using either an in-line eight-pole band reject filter or modifying the triplexer L₃ bandpass filter from a three- to a five-pole design for increased selectivity. The possibility of shifting the filter center frequency down from 1381.05 MHz to a point where the filter skirts reduce the 1400- to 1427-MHz spectral energy to the desired level was also considered. Since this approach must be consistent with maintaining specified code track sensitivity, experimental test data using a tunable five-pole filter was taken to demonstrate that sufficient tracking sensitivity could be maintained.

All three frequencies have received developmental approval. The GPS L₁ and L₂ navigation frequency assignment notifications, AF Forms 135, were transmitted to Rockwell on December 29, 1975, providing authority to radiate. The IGS L₃ frequency of 1381.05 ± 12 MHz was approved for developmental use by the Military Communications Electronics Board (MCEB), Joint Frequency enclosure 12/4607 on November 16, 1977. However, this approval of L₃ requires a coordinated test of the first IONDS/GPS vehicle with the Radio Astronomy Service to confirm minimal interference exists. To date, the L₃ transmitter has been operated at full power with the Navstar antenna only during RF compatibility tests within a shielded anechoic chamber at the Seal Beach Naval Weapons Station (NWS).

REQUIREMENTS

The MCEB approval of the L₃ frequency had four stipulations to be met before an operational frequency was approved. Two have been met. Based on actual measurements, the maximum L₃ power flux density at the earth's surface should be -203 dBW/m²/Hz which is below the -144 dBW/m²/4 KHz (-180 dBW/m²/Hz) level specified to aid in coordination with other nations. Furthermore, the L₃ RF downlink hardware is compliant with MIL-STD-461A. The spurious emission, which was the primary concern, of -73 dBc at the transmitter output is well within the -68.76 dBc (-57 dBW with 11.76 dBW transmitter) requirement, and is further reduced to -119 dBc by the triplexer filtering. A third stipulation, an ECAC survey of potential interference, is in progress and should be completed by

mid-1979. The fourth stipulation is the previously mentioned coordination, primarily with the RAS, during the flight of NDS 6.

Regulations relevant to Radio Astronomy Service with the associated frequency ranges and harmful flux densities are contained in Annex 7-1 of CCIR documents (February - March 1971). The basic information came from CCIR Report 224-2 which provided realistic calculations of the sensitivity of Class B observations. Table A-2 and A-3 are extensions of two tables from that report as provided in Annex 7-1. Table A-2 is typical of line observations and is the less stringent requirement. The annex states that the information in Table A-3 "covers the case of typical measurements of continuum radiation, with reasonable assumptions as to the bandwidth chosen. In both tables, it is assumed that a 2,000-second integration time is used. The quantitative assumptions which led to the tables are quite realistic and typical of very good present-day observations."

Signal levels causing harmful interference are specified as power flux densities for the adjacent bands of interest. Most notable are the 1400- to 1427-MHz and 1664.4- to 1668.4-MHz bands, which have exclusive and secondary worldwide allocations, respectively. The lines of highest importance within

Table A-2. Harmful Interference Levels (Line)*

Freq f (MHz)	Min Antenna Noise Temp T _a (°K)	Receiver Noise Temp** T _{eff} (°K)	Typ Bandwidth B (MHz)	Sensi- tivity ΔT _e (°K)	Min Harmful Power Input ΔP _H (dBW)	Signal Level Causing Interference (Isotropic Antenna)**		
						Power Flux		Field Strength E _H (dB(μV/m))
						S _H • B (dBW/m ²)	S _H (dBW/ m ² /Hz)	
20	32,000	200	0.1	1.6	-186	-199	-249	-53
40	6,200	200	0.1	0.32	-193	-200	-250	-54
80	1,000	200	1	0.02	-196	-196	-256	-51
150	200	200	2	0.0045	-199	-194	-257	-48
327	40	100	2	0.0016	-204	-192	-255	-46
408	26	100	2	0.0014	-204	-190	-253	-45
610	16	100	8	0.00065	-201	-184	-253	-39
1,420	10	20	27	0.00009	-205	-180	-254	-35
1,665	10	20	4	0.00024	-209	-183	-249	-37
2,700	10	20	10	0.00015	-207	-177	-247	-31
5,000	10	20	10	0.00015	-207	-171	-241	-16
10,680	12	20	20	0.00011	-205	-163	-236	-17
15,350	18	100	50	0.00026	-197	-152	-229	-6
30,000	20	100	100	0.00019	-196	-145	-225	+1
100,000	35	2,000	1,000	0.0010	-179	-118	-208	+28

*From CCIR Annex 7-1 (Table 7-1-1)
**See Table 10

Table A-3. Harmful Interference Levels (Continuum)*

Freq. f (MHz)	Min Antenna Noise Temp ¹ T _a (°K)	Receiver Noise Temp ² T _{eff} (°K)	Sensi- tivity ΔTe (°K)	Min Harmful Power Input ΔP _H (dBW)	Signal Level Causing Interference (Isotropic Antenna) ³		
					Power Flux		Field Strength (dB(μV/m))
					S _H · B (dBW/m ²)	S _H (dBW/ m ² /Hz)	
1,420	10	20	0.005	-222	-197	-237	-51
1,665	10	20	0.005	-222	-196	-236	-50
4,830	10	20	0.005	-222	-187	-227	-41
23,000	20	100	0.019	-216	-167	-207	-21
115,000	35	2,000	0.32	-207	-142	-182	+4

*From CCIR Annex 7-1 (Table 7-1-II); bandwidth 0.01 MHz, typical for single channel of multichannel or tunable receiver
¹Noise from the ground has, provisionally, been assumed to increase antenna temperature by 10°K
²Referred to antenna terminals
³For antenna of power gain G (dB) in the direction of any unwanted signal, reduce all values by G

Note: An integration time (or total time of observation) of 2000 s is used throughout. For longer integration times, the minimum detectable power flux will be lower and the unwanted signal will be harmful at correspondingly lower levels. For example, with a time of observation of ten hours the relevant figures in the tables should be reduced by 6 dB.

these bands are 1420.405 MHz, 1665.401 MHz, and 1667.358 MHz. This is consistent with Table A-4, reproduced from the Arecibo Observatory User's Manual, which includes 1420 MHz and 1667 MHz as two of the prime measurement frequencies.

Another aspect to be considered in determining interference with the RAS is the duty cycle of the transmitter. As previously mentioned, radio-telescope receivers typically integrate the observed signal over a large number of seconds since the receiver output noise decreases as integration time increases. The maximum length of time is generally determined by the degree of data smoothing that can occur without unacceptable loss of data. CCIR Annex 7-1 recognizes this aspect by permitting an increase in the instantaneous interference level as a function of duty cycle. This factor (k) is given as

$$k = 5 \log_{10} \frac{T_I}{B_T/B_R}$$

where T_I is the integration time, B_T is the number of bits transmitted, and B_R is the bit rate, which, for L_3 , is 200 bps.

ANALYSIS RESULTS

The broadcast spectra of L_1 , L_2 , and L_3 depend on which code is used to PRN-modulate the carrier since the data rates (75 bps for GPS and 200 bps [400 symbols/second] for IONDS) are insignificant compared to either the 10.23-MHz P code or 1.023-MHz C/A code. L_1 is quadrature phase shift key (QPSK) modulated with both the C/A and P codes and exhibits both the spread P spectrum and narrower C/A spectrum. L_2 and L_3 are normally biphase shift key (BPSK)

Table A-4. Arecibo Observatory Measurement Frequencies

Frequency (MHz)	Usual Location on Carriage House (note 1)	Feed Type	Polarization	Sens. (°K/f.u.)	3 db Beamwidth (arc min)	Receiver/Amplifier Type	Sys. Temp. (°K) (note 2)	Bandwidth (MHz)	Calibration Values (note 3)	Switching System (note 5)	L.O. System (note 4)	I.F. (MHz)	Remarks
430 (cont)	total power	96' line	right circ.	19.7	9.0	transistor	250°	10	same as LRR2	S	internal reference	30	30 MHz i.f. and detected outputs.
	CH1 UH 2	stacked yagis	linear	-	-	transistor	250°	10	same as LRR2	S	internal reference	30	reference antenna 30 MHz i.f. and detected outputs.
	CH2 LR	LPPF	linear or circ.	1.0	-	transistor	250°	10	51°	-	internal or phase locked	30	not tunable. 30 MHz i.f. and detected outputs.
600-1200	CH2 UR	16' line	linear	3.0	10.0	transistor	220°	60	1 step	F	external	260	760, 932, 1020-50 MHz. 16' in-pol. feeds exist.
	CH2 LR	LPPF	linear	1.5	10.0	paramp	250°	10	1 step	-	external reference	30	temporary.
606	CH1 UH	40' line	linear	5.5	9.2	paramp	120°	10	1 step	F	mult. ext. reference	30	not permanently installed.
611	CH1 UH	16' line	linear	2.5	12.7	transistor	250°	10	1 step	S	mult. int. or ext. ref.	30	temperature stabilized total power receiver 30 MHz i.f. and detected outputs.
830	CH1 UH	40' line 16' line	linear linear	~4 ~2	10.0 10.0	transistor	300°	10	1 step	F	multiplying	30	feed not permanently installed.
1420	CH2 UL	40' line 40' line 16' line	dual circ. linear linear	8.5 6.0 ~3	3.3 3.3 5.8	paramps	76°	40	6°, 6°	FM	multiplying	260	receiver and feed tunable 1380-1450 MHz. See Note 6 & 8.
1667	CH2 LC	40' line 16' line	dual circ. linear	8.0 ~3	3.1 5.0	paramp (single channel)	100° 110°	40 100	1 step	FM	multiplying	260	long line feed. See Note 7. Short line feed usable over ~100 MHz receiver tunable 1612-1720 MHz. See Note 6.
2380	CH2 UC	40' line	dual circ.	6.0	2.0	maser paramp	45° 90°	10 10	3° 3°	N N	heterodyned external ref.	30	dual channel radar receiver, will not frequency switch.
						maser	45°	25	3°	F.N	mult., phase locked	260	single channel.
	100' dish	horn casse-grain	linear rotatable	.13	-	maser	30°	10	3°	N	fixed, external reference	30	located at interferometer site, 10 km north of AO.
2695	CH2	16' line	linear	-	-	transistor	360°	10	1 step	-	-	30	not installed.
4830	CH2 LL	16' line horn	linear linear	-	-	paramp	225°	100	1 step	F.N D	multiplying external ref.	270	low efficiency due to surface roughness. See Note 6.

modulated with the P code and exhibit only the spread P spectrum characteristics. In either case the P code provides the basic spectra characteristics. L_2 can be BPSK-modulated with the C/A code alone and in this case has a spectrum that decreases on either side of the center frequency an order of magnitude faster than the P code. However, this mode of modulation is rarely used. L_3 does not use the C/A code. All of the spectra that may be broadcast are addressed in this section, with emphasis placed on the L_1 (P) and L_3 (P), which have the greatest potential for RAS interference.

Spectra Computations

Basic spectra plots analyzed consisted of L_1 (P, C/A), L_3 (P), and the composite L_1 (P, C/A), L_2 (P), and L_3 (P). L_2 (C/A) is also provided although it has considerably steeper slopes and is of secondary importance relative to an interference-level investigation. The spectra produced by spread-spectrum PRN modulation at either or both chip rates (10.23 and 1.023 Mbps for P and C/A baseband codes, respectively) are the basic source combinations. The output spectra are further modified by the triplexer in the GPS navigation assembly. Measured attenuation characteristics of the triplexer were available at 10 MHz discrete steps, from 1000 to 2000 MHz for this investigation.

Any PRN sequence modulated carrier exhibits a discrete power spectrum of form (for unit power) of

$$\left| s(f) \right|^2 = \frac{1}{M^2} \delta(f) + \frac{1}{M} \left(\frac{\sin(\pi f \Delta)}{\pi f \Delta} \right)^2 \sum_{k=-\infty}^{\infty} f - \frac{k}{T}$$

$k \neq 0;$

where

$$\frac{1}{M} = \frac{\Delta}{T}$$

with Δ being the chip period and T being the sequence repetition period.

For a long sequence, the discrete lines are very closely spaced, and a more useful representation becomes the continuous power spectral density

$$T \left| s(f) \right|^2 = \psi(f) = \frac{\Delta^2}{T} \delta(f) + \Delta \left(\frac{\sin \pi f \Delta}{\pi f \Delta} \right)^2$$

$f = 0$

For practical purposes, the $\frac{\Delta^2}{T} \delta(f)$ is ignored and the spectrum runs continuously through $f = 0$, using $\psi(f) = \left(\frac{\sin \pi f \Delta}{\pi f \Delta} \right)^2$, watts/Hz, for unit power.

In multiple source cases, the combined spectrum is written as

$$\psi(f) = \sum_i \sum_j P_{ij} A_{ij} \Delta_j \left(\frac{\sin \pi (f - f_i) \Delta_j}{\pi (f - f_i) \Delta_j} \right)^2$$

where

f_i is the i th carrier

Δ_j is the j th chip period

P_{ij} is the source power

A_{ij} is the attenuation, including antenna gain

Spectral plots were computed for the configurations listed in Table A-5 using a navigation antenna gain of 12 dB. The spatial spreading loss, $\frac{1}{4\pi R^2}$, was 157 dB ($R = 2 \times 10^7$ meters).

Table A-5. Carrier/Code Configurations

Figure	Carrier, Code	Power Level
A-1, A-5	L_1 (P, C/A)	15.85 W, 12 dBW (P) 39.81 W, 16 dBW (C/A)
A-6	L_2 (P)	10 W
A-9	L_2 (C/A)	10 W
A-2, A-10	L_3 (P)	17 W
A-11	L_3 (C/A)	17 W
A-12	$L_1 + L_2$ (P)	
A-3	$L_1 + L_2$ (P) + L_3 (P)	
A-13	$L_1 + L_2$ (P) + L_3 (C/A)	
$L_1 = 1575.42$ MHz $L_2 = 1227.6$ MHz $L_3 = 1381.05$ MHz		

Triplexer attenuation values were interpolated from the discrete network analyzer measured values shown in Table A-6 (refer to Figure A-1).

The L_1 bandpass, L_2 bandpass, and bandstop filter characteristics are identical for the current GPS diplexer and the GPS/IONDS triplexer. The L_3 bandpass filter is unique to the triplexer.

Figure A-2 shows the combined L_1 (P, C/A) plus L_2 (P) spectrum radiated from the GPS satellites for the basic navigation mission. The CCIR requirements for the 1420-MHz and 1665-MHz bands are provided for reference. This spectrum is a combination of the individual L_1 and L_2 spectra shown in Figures A-3 and A-4. The 1750-MHz to 1825-MHz notch in the spectrum is generated by the triplexer

Table A-6. Discrete Triplexer Values

Frequency (MHz)	Insertion Loss (dB)			Frequency (MHz)	Insertion Loss (dB)		
	J1 to J4	J2 to J4	J3 to J4		J1 to J4	J2 to J4	J3 to J4
1000	63.19	35.72	71.27	1530	0.71	40.94	44.31
1010	57.11	33.00	65.77	1540	0.66	40.67	44.98
1020	58.99	30.48	67.40	1550	0.53	40.86	45.72
1030	56.03	29.02	64.11	1560	0.46	40.74	47.01
1040	54.01	28.08	60.71	1570	0.50	41.57	48.15
1050	53.97	26.90	60.69	1580	0.54	42.06	49.22
1060	54.70	24.85	70.52	1590	0.48	43.17	50.33
1070	53.79	22.07	68.76	1600	0.41	44.13	51.41
1080	53.29	19.05	61.28	1610	0.41	45.01	54.94
1090	51.15	16.78	62.00	1620	0.52	45.92	54.59
1100	51.52	15.22	60.92	1630	0.61	47.12	56.46
1110	49.89	13.22	58.44	1640	0.77	48.42	59.69
1120	49.60	10.34	56.22	1650	1.43	48.10	48.94
1130	48.88	6.75	56.91	1660	2.99	48.36	60.65
1140	49.45	3.98	58.23	1670	4.76	47.65	59.20
1150	52.04	2.80	59.12	1680	6.22	46.51	59.25
1160	56.02	1.85	62.12	1690	7.67	45.08	57.65
1170	53.13	0.91	57.88	1700	9.55	45.07	57.27
1180	53.54	0.55	59.33	1710	10.92	44.42	57.94
1190	51.41	0.63	55.59	1720	9.84	41.50	54.61
1200	50.29	0.67	53.87	1730	7.04	37.17	49.44
1210	48.88	0.57	53.09	1740	19.89	48.24	59.63
1220	47.69	0.46	50.50	1750	30.84	58.05	65.82
1230	47.41	0.40	49.66	1760	42.50	63.35	71.33
1240	47.46	0.45	47.93	1770	56.71	69.42	71.20
1250	46.27	0.45	45.90	1780	73.90	74.87	70.70
1260	46.12	0.51	44.66	1790	64.52	69.17	77.80
1270	46.80	1.03	43.73	1800	60.75	69.00	81.55
1280	48.32	2.09	44.36	1810	57.72	81.53	73.73
1290	49.23	3.08	43.50	1820	52.43	66.89	77.91
1300	45.14	3.70	38.06	1830	31.80	52.25	68.77
1310	40.27	4.64	30.68	1840	36.03	55.98	71.01
1320	36.85	6.36	24.51	1850	36.43	55.42	66.83
1330	34.52	8.14	18.63	1860	35.56	53.92	72.21
1340	31.63	9.22	11.73	1870	34.96	52.23	69.43
1350	30.14	11.25	4.90	1880	35.46	52.21	67.08
1360	33.12	17.41	1.87	1890	36.08	52.53	61.24
1370	34.03	21.74	0.78	1900	36.24	52.83	72.64
1380	31.96	22.79	0.49	1910	36.13	51.76	67.36
1390	29.81	23.68	0.58	1920	36.51	52.58	64.82
1400	28.13	25.03	0.77	1930	38.14	52.74	67.75
1410	30.59	30.47	2.23	1940	39.60	53.70	68.93
1420	35.68	38.76	5.30	1950	40.48	53.35	65.69
1430	23.93	30.35	8.24	1960	40.84	52.90	63.71
1440	17.99	27.45	11.73	1970	41.45	54.94	68.92
1450	15.02	27.70	16.19	1980	42.42	54.74	64.62
1460	12.30	28.42	20.06	1990	43.60	56.62	65.55
1470	9.25	29.15	23.30	2000	45.58	58.60	71.68
1480	6.55	30.54	26.68				
1490	4.93	33.40	31.25				
1500	3.55	37.37	36.60				
1510	2.04	40.93	41.42				
1520	0.97	41.67	44.04				

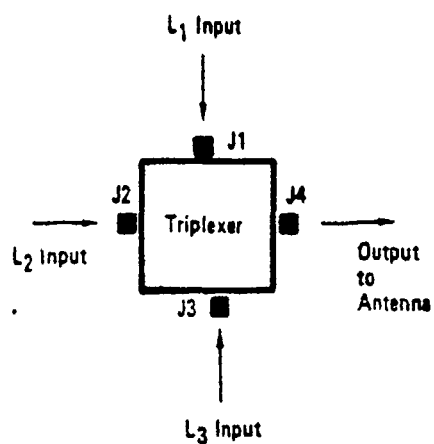


Figure A-1. Triplexer Diagram

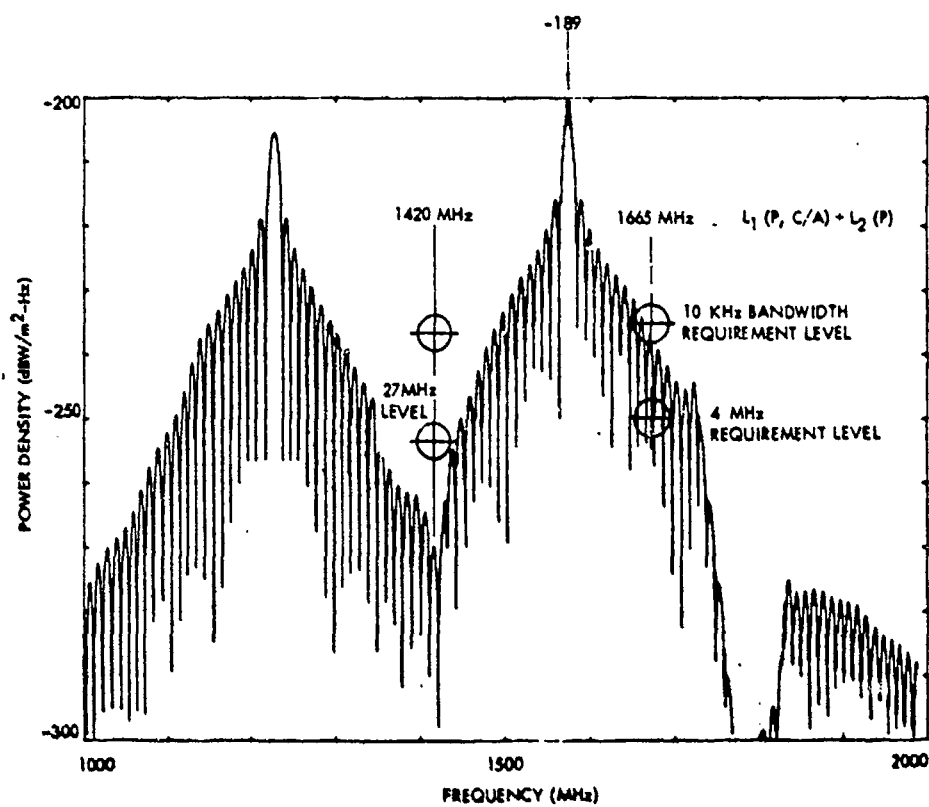


Figure A-2. L_1 , L_2 Spectra Plot

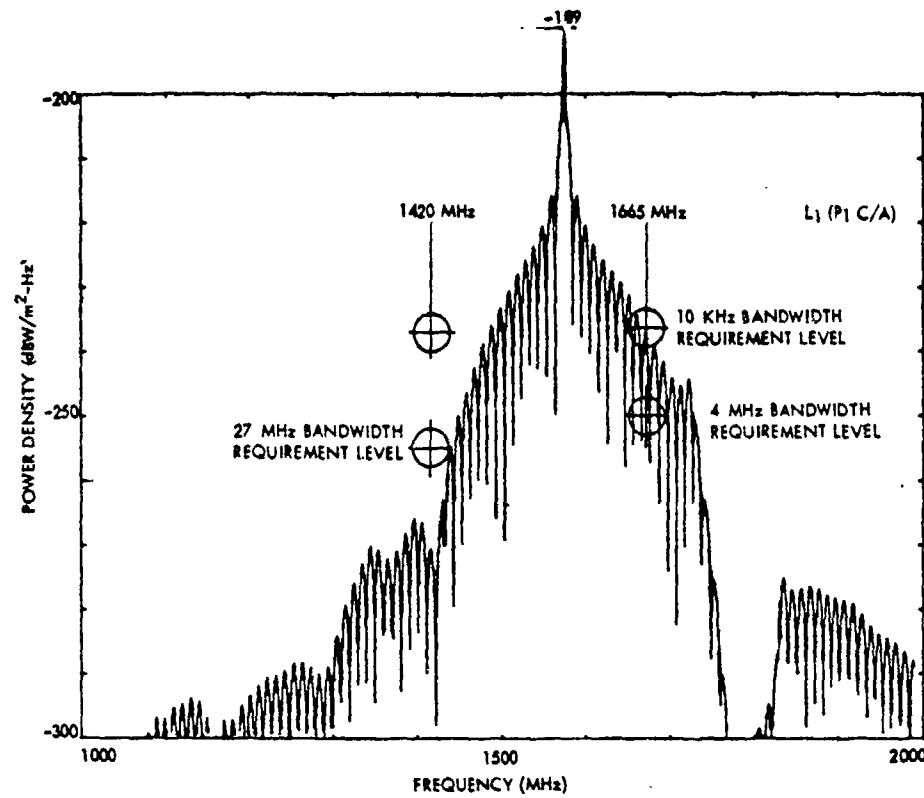


Figure A-3. L₁ Spectra Plot (P₁, C/A Codes)

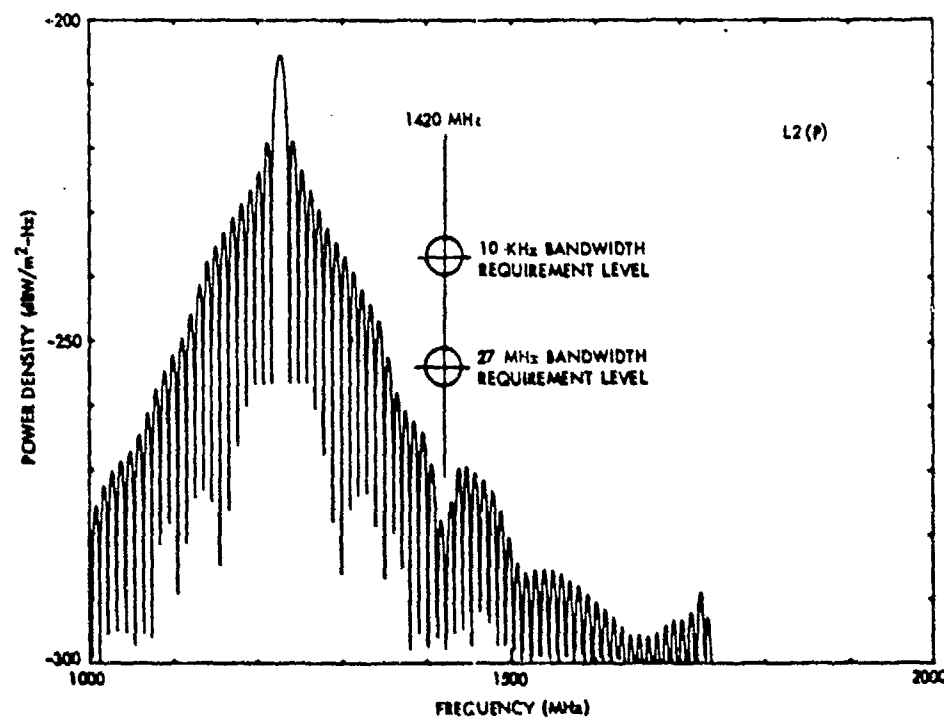


Figure A-4. L₂ Spectra Plot (P Code)

bandstop filter used to preclude L-band signal interference in the satellite S-band telemetry receiver. As stated previously, these spectra are basically the result of the P code, with the -18° dBW/m²/Hz spike on L₁ being the only obvious contribution from the C/A code. A similar spike at -195 dBW/m²/Hz would occur on L₂ as shown in Figure A-5 if the C/A code were used in lieu of the P code. In either case L₂ meets the CCIR 1420-MHz requirement and will, therefore, not be discussed further.

An L-band frequency was selected for IONDS to minimize the interface with and potential impact on the GPS satellite. By selecting a frequency between L₁ and L₂ the existing L-band antenna could be used. Furthermore, the basic GPS receiver could be used to receive L₁ and L₃, eliminating the necessity for an interface to provide the basic spacecraft data for the L₃ data link. This latter aspect of the design both reduces the amount of data that must be transmitted on L₃ and precludes the necessity for continuous L₃ transmission. The L₃ frequency was to be centered approximately between L₁ and L₂ to minimize L₃ spectra in the L₁ and L₂ regions. Of the several frequencies in this region that were reasonably achievable using the 10.23-MHz GPS clock, 1381.05 MHz provided the best protection for the 1420-MHz RAS. Minimal interference with GPS was assured by selecting a narrower bandpass filter for L₃ than used for L₁ and L₂ (≥ 60 MHz versus ≥ 150 MHz). The result was an L₃ (P) spectrum as shown in Figure A-6 which is similar to L₂ (P) but with a steeper spectral slope.

The triplexer frequency response characteristics are shown in Figure A-7. Figure A-8 presents a block diagram of the triplexer.

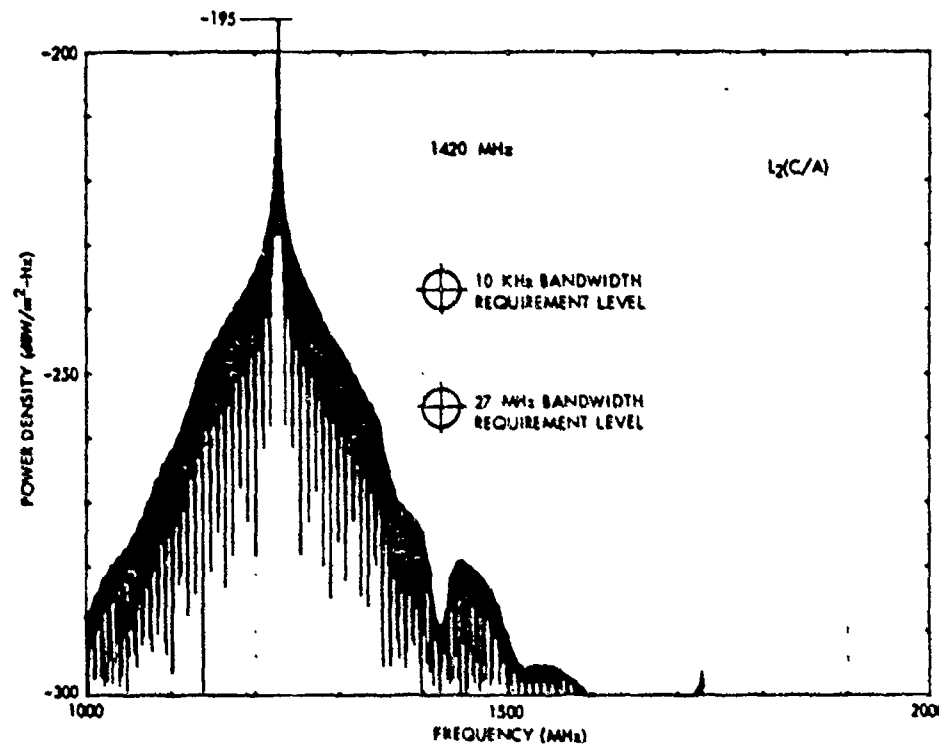


Figure A-5. L₂ Spectra Plot (C/A Code)

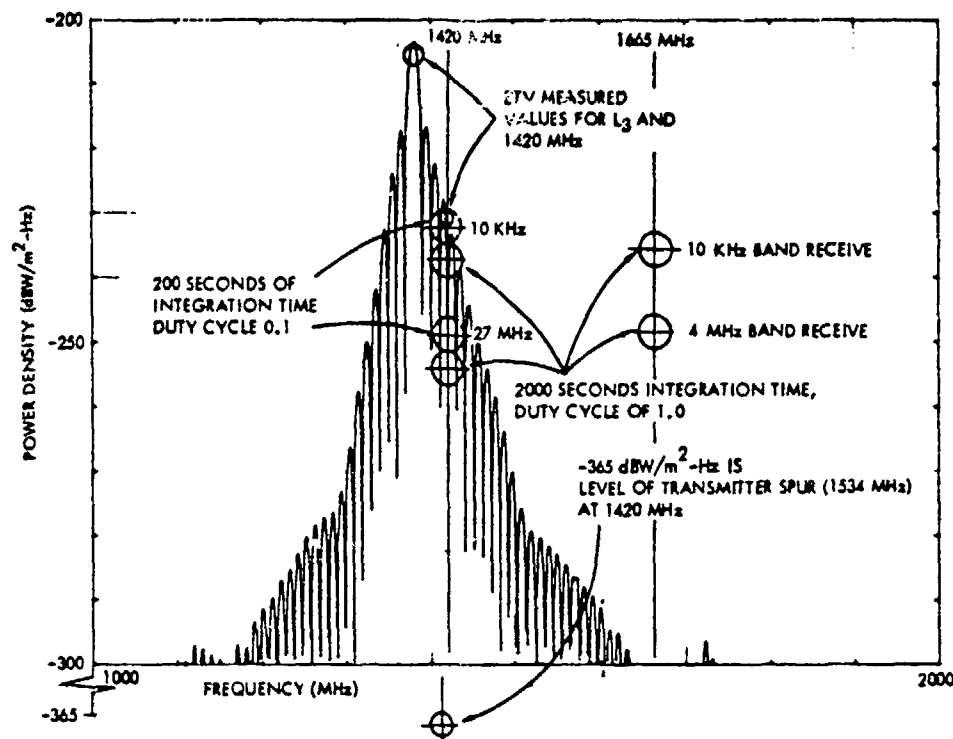


Figure A-6. IGS Phase II Radio Astronomy Spectra Study
(L₃ P Code)

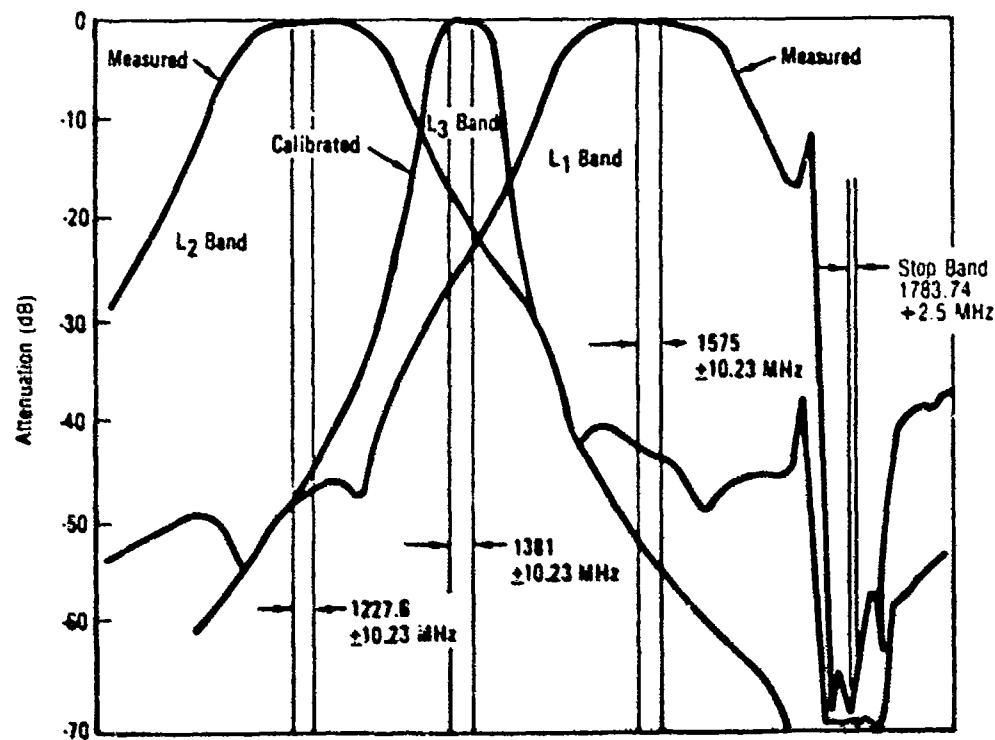


Figure A-7. Triplexer Frequency Response Characteristics

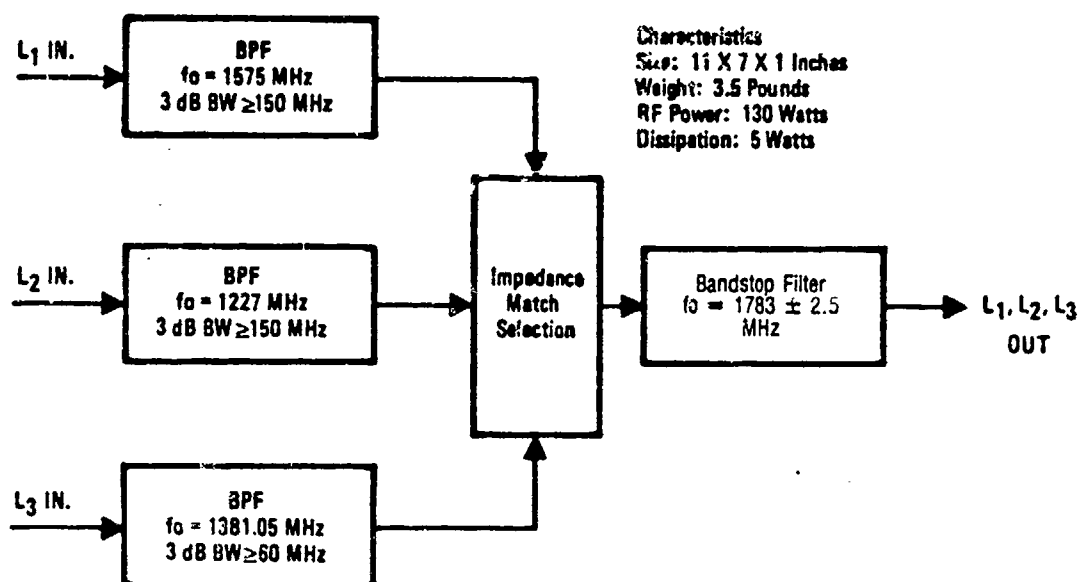


Figure A-8. Triplexer Block Diagram

The resulting L₃ (P) spectrum radiates less energy in the L₂ region than the L₁ signal, less energy in the L₁ region than L₂, and less energy in the 1665-MHz RAS band than L₁. However, continuous L₃ transmission clearly exceeds the CCIR limits for the 1420-MHz band. This would also be true, as shown in Figure A-9, if the C/A code were used on L₃ in lieu of the P code.

Since L₃ is not a continuously transmitting system, the apparent conflict with the CCIR 1420-MHz requirement is not as significant as Figure A-6 implies. The actual potential interference is a function of the L₃ transmission time (or number of data bits) and the integration time of the radio-telescope. This is depicted in Figure A-10 using a typical integration time of 2,000 seconds per CCIR Annex 7-1. Figure A-10 makes it clear that the average L₃ spectral level is clearly within the CCIR line interference level for both the typical random IONDS transmission of less than 2,000 bits and typical scheduled servicing, which should take less than five minutes. Although the typical L₃ random transmission still exceeds the CCIR continuum interference level for the 1420-MHz RAS band, taking its short transmission time into account reduces the potential interference to approximately the same relative level of L₁ in the 1665-MHz RAS band.

Two other factors that further decrease the probability of L₃ interference are the low probability that an L₃ transmission will occur within a beam of a radio-telescope and the probability that the entire L₃ transmission will not occur within one of the integration segments. The latter factor results from the fact that large integration times are typically obtained by combining multiple short segments taken over several days. However, these factors are beyond the scope of this investigation and will not be considered.

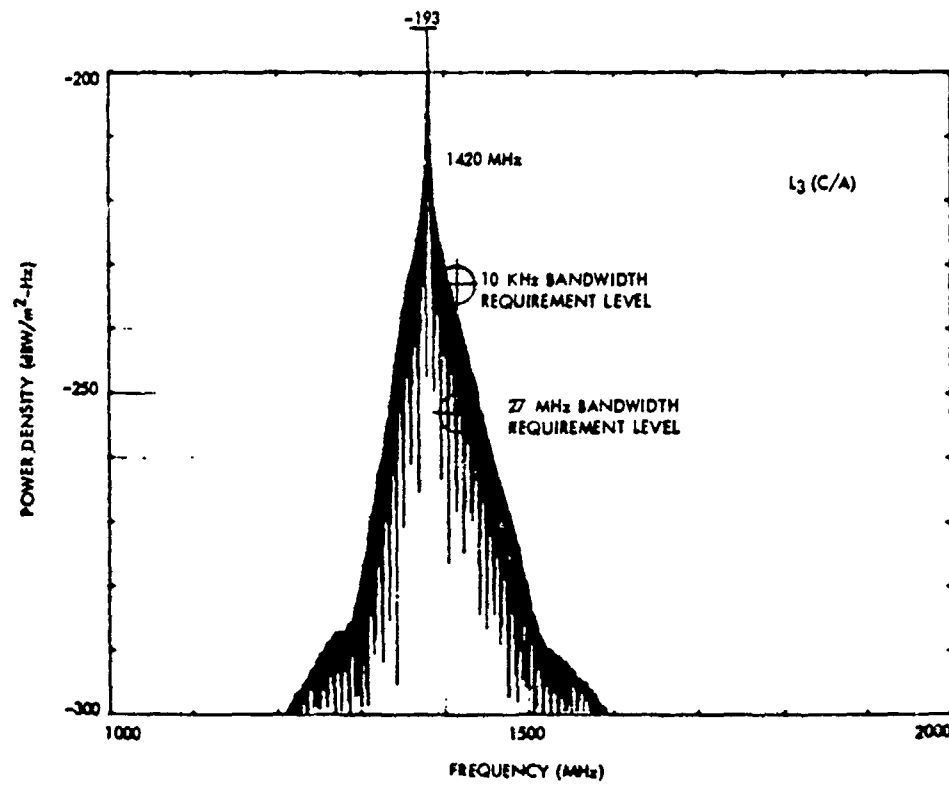


Figure A-9. L3 Spectra Plot (C/A Code)

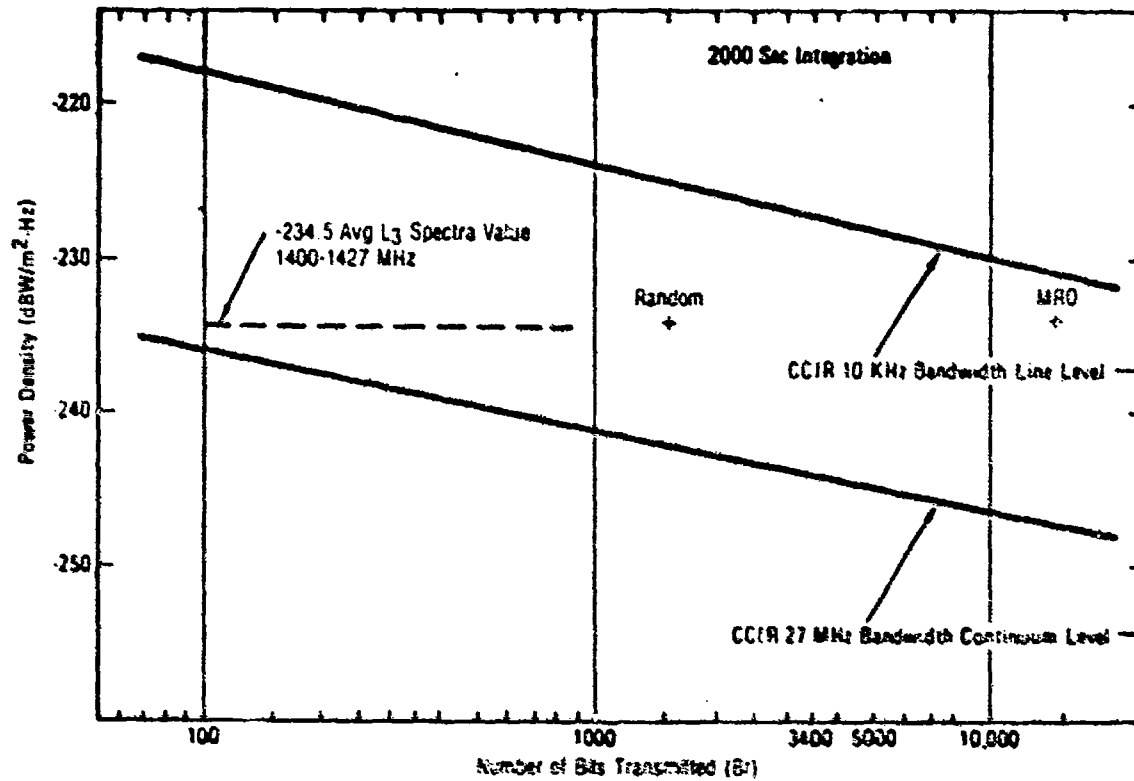


Figure A-10. Radio Astronomy Survey - Interference Levels
Versus Bits Transmitted

Naval Weapons Station (NWS) Spectra Measurements

During system compatibility tests of the ETV at the NWS anechoic chamber, a spectrum analyzer was used to measure RF signal responses of the GPS/IGS integrated vehicle. The downlink spectra were transmitted 158 inches (4 meters) from the ETV to a conical spiral pickup antenna and routed through 80 feet of cable to the spectrum analyzer, located outside the chamber (see Figure A-11).

The CRT display of the spectrum analyzer was calibrated from a known 30-MHz calibration signal within the intermediate frequency (IF) unit, so that the top graticule line of the display corresponded to -30 dBW. This calibration level, with known data for the pickup antenna, interconnecting cables, distance to the NAV antenna, etc., allowed calculation of equivalent power flux density at the earth's surface. The peak measured and corresponding theoretical levels, which agreed to within 0.3 dB, are listed in Table A-7.

Test results on the ETV at the NWS during the systems/EMC tests indicated spectra response similar to the analyses. Measured peak test levels within the anechoic chamber were extrapolated to compare with the predicted theoretical power flux density levels of the earth's surface. Measured points at the frequencies of interest also were extrapolated to the earth's surface and superimposed on the theoretical charts as shown for the L₃(P) and L₁(P, C/A), L₂(P), L₃(P) plots in Figure A-12. Worst-case variance of the measured spectra compared to theoretical was approximately 3 dB at 1665 MHz.

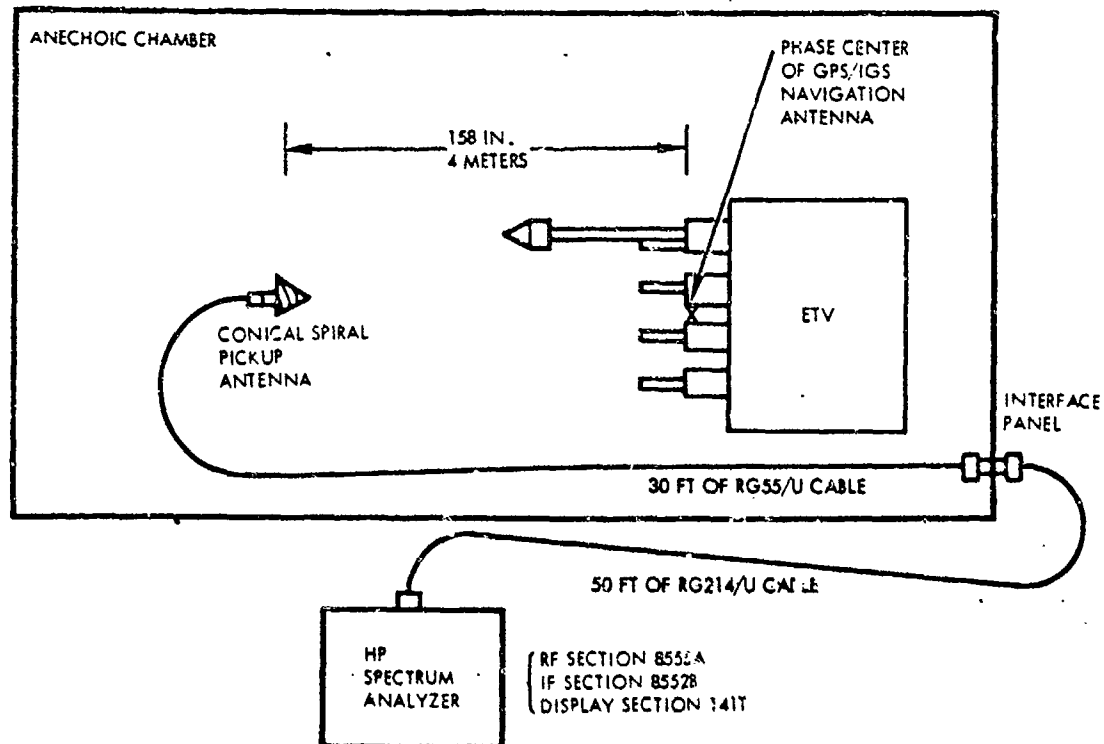


Figure A-11. Naval Weapons Station Measurement Setup

Table A-7. Comparison of Computed and Measured Peak Spectra Values

Parameters	Unit	Theoretical Analysis Values	NWS Measured Values
L ₁ chip rate and combo P + C/A transmitter power	dBW	-43.9	N/A
Navigation antenna gain	dB	12.0	N/A
Path loss $\left(\frac{1}{4\pi R^2}\right)$, R = 2 x 10 ⁷ meters	dB	-157	N/A
Level (P _x) of L ₁ (P + C/A) on spectrum analyzer	dBW	N/A	-30
Receive antenna gain (pick up spiral)	dB	N/A	-8
Spectrum analyzer antenna aperture $\left(\frac{\lambda^2}{4\pi}\right)$ meters	dB	N/A	25.4
Spectrum analyzer cable loss	dB	N/A	11.0
connector pair loss	dB	N/A	0.8
Spectrum analyzer antenna at $\frac{D^2}{\lambda}$	dB	N/A	0.1
Theoretical transmitter/antenna gain Δ over actual	dB	N/A	0.3
Space loss (2 x 10 ⁷ versus 4 meters)	dB	N/A	-134
Bandwidth Δ (300 kHz of spectrum analyzer versus 1 Hz theoretical)	dB	N/A	-34.8
			37.6
Power flux density $\frac{\text{dBW}}{\text{m}^2\text{-Hz}}$		-188.9 predicted at earth's surface	-189.2 measured extrapolated to earth's surface -0.3 dB less signal than predicted

Figures A-13 through A-19 show CRT displays of P and C/A modulation codes at L₁, L₂, and L₃ frequencies as taken at the Naval Weapons Station.

Radio Astronomy Filters

Since L₁ and L₃ spectra exceeded the allowed interference levels within the adjacent radio astronomy bands, an analysis was performed to determine the filters required. Incorporation of in-line band reject filters sufficiently

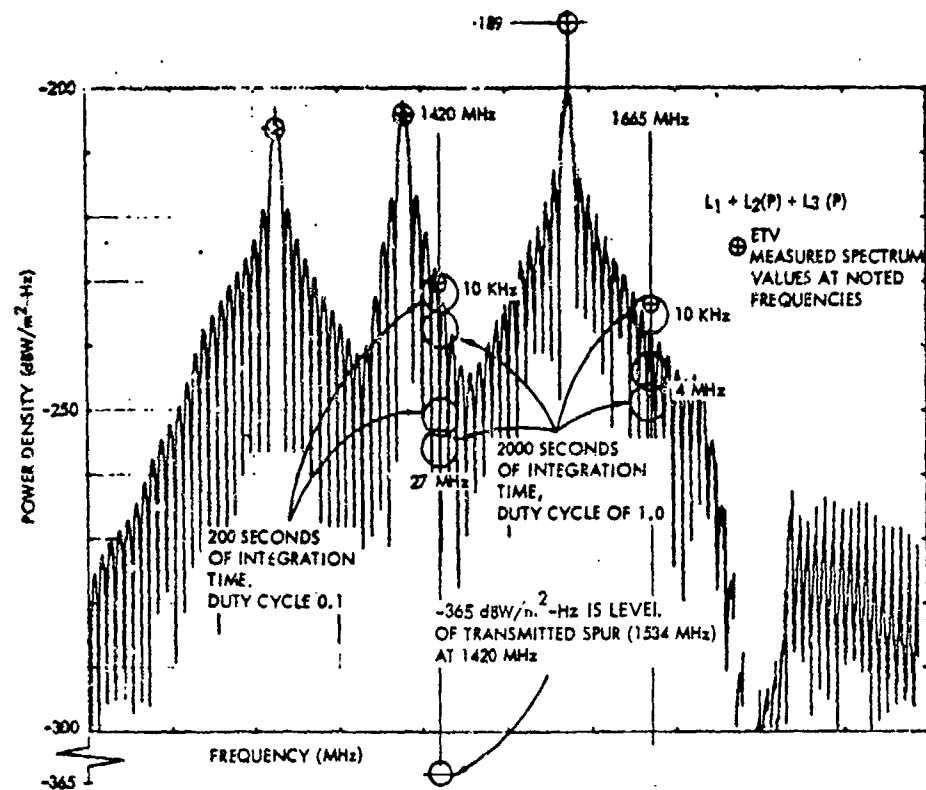


Figure A-12. IGS Phase IIA Radio Astronomy Spectra Plot

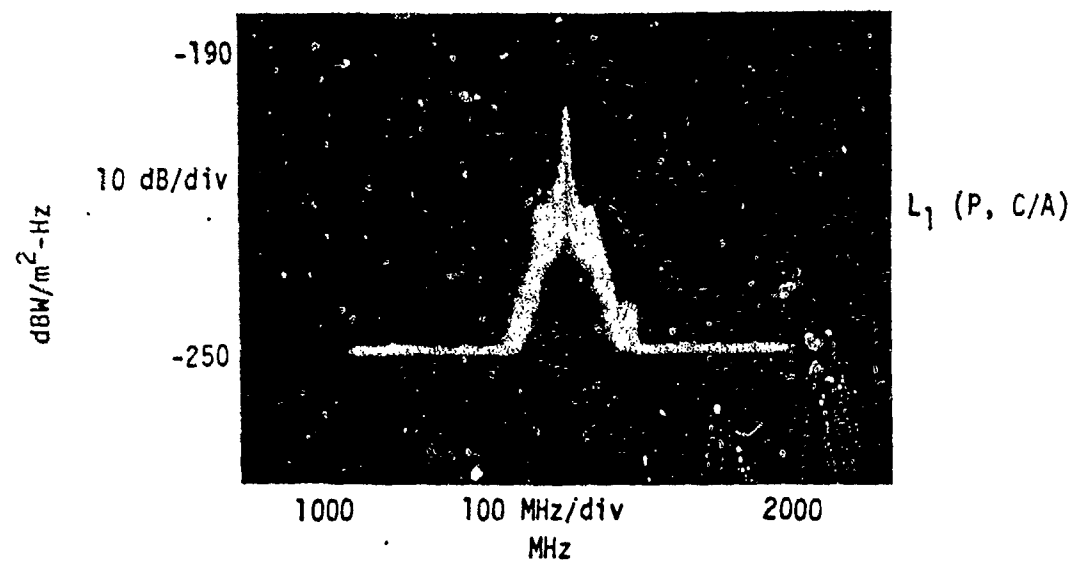


Figure A-13. L_1 (P, C/A) Spectra (CRT Display)

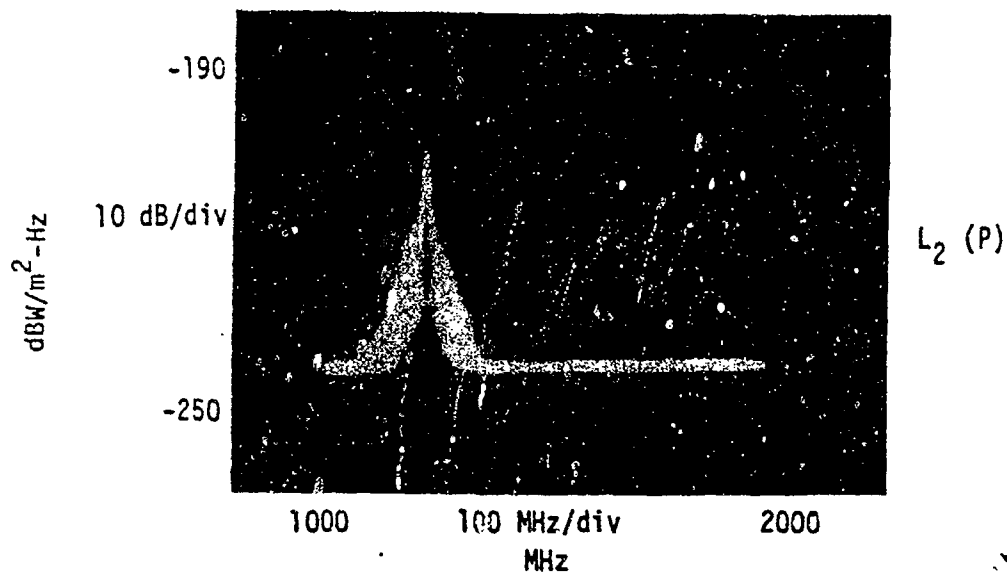


Figure A-14. L_2 (P) Spectra (CRT Display)

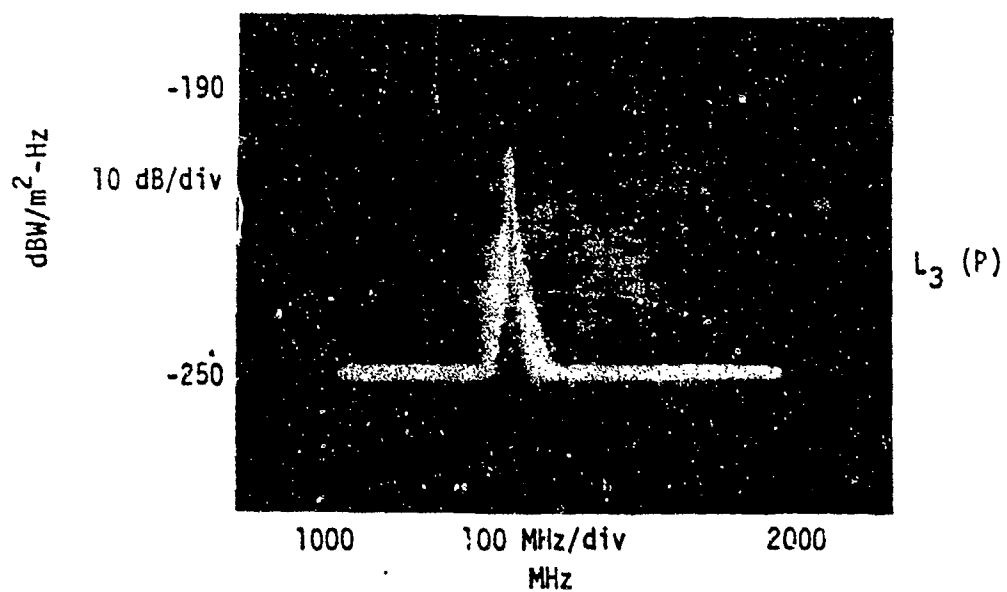


Figure A-15. L_3 (P) Spectra (CRT Display)

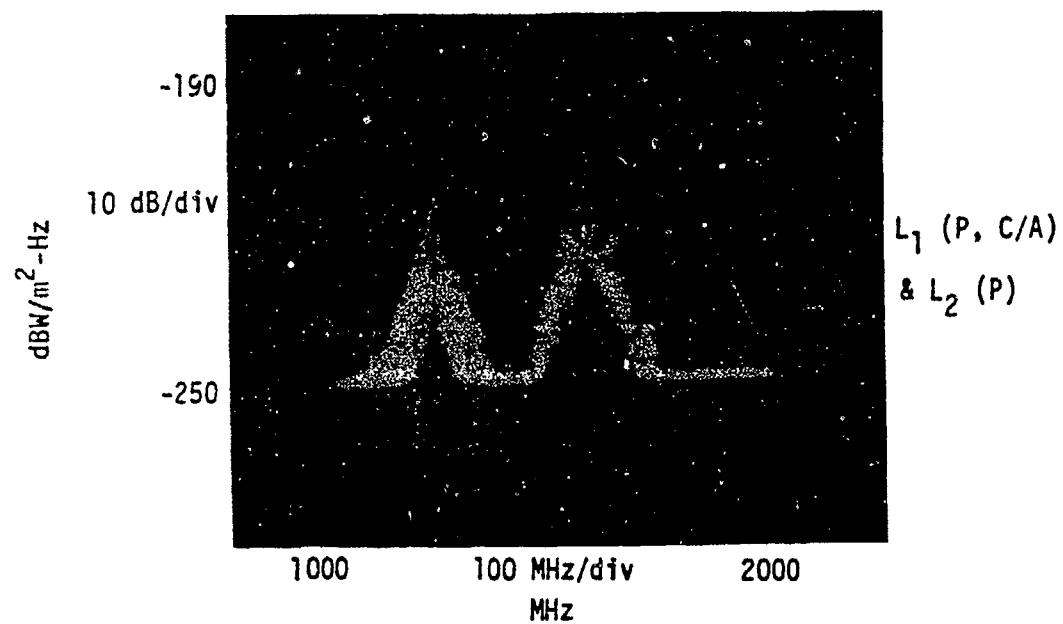


Figure A-16. L_1 (P, C/A) and L_2 (P) Spectra (CRT Display)

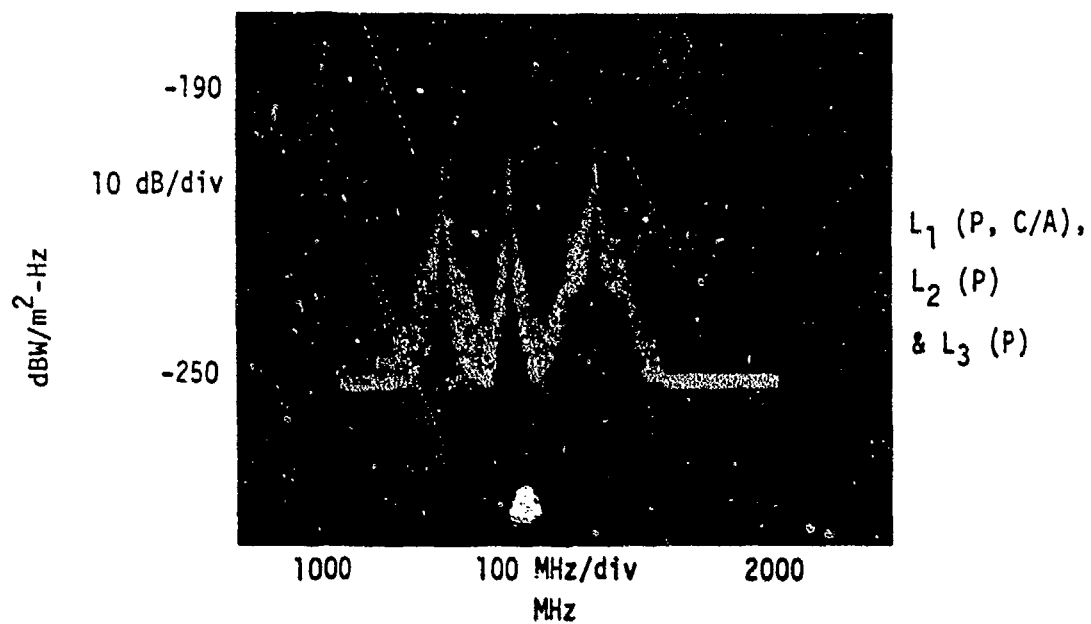


Figure A-17. L_1 (P, C/A), L_2 (P), and L_3 (P) Spectra (CRT Display)

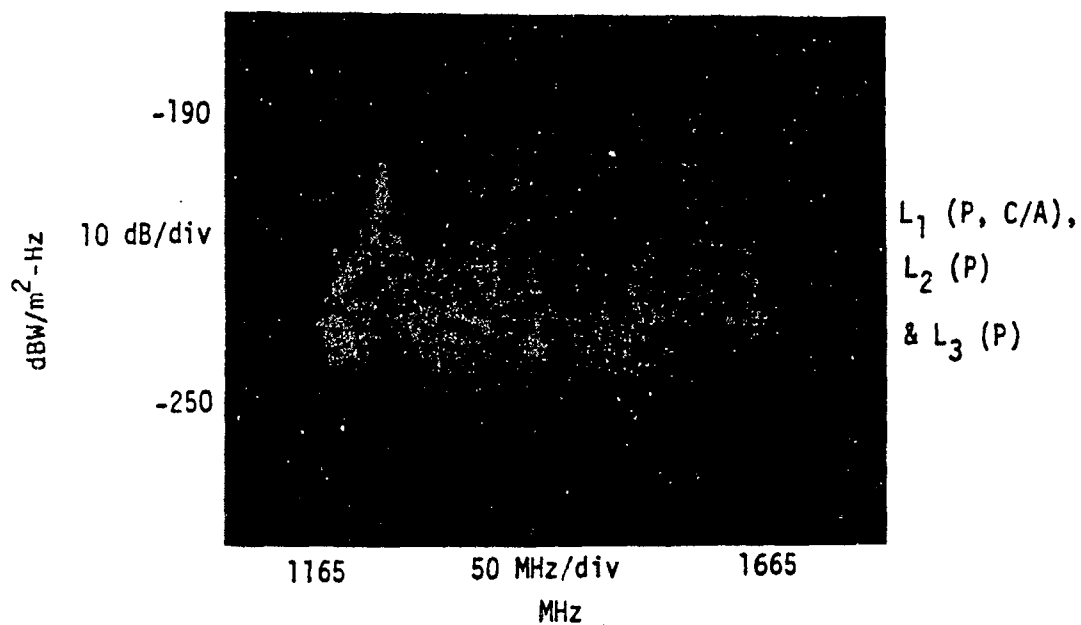


Figure A-18. L₁ (P, C/A), L₂ (P), and L₃ (P) 1165- to 1665-MHz Spectra (CRT Display)

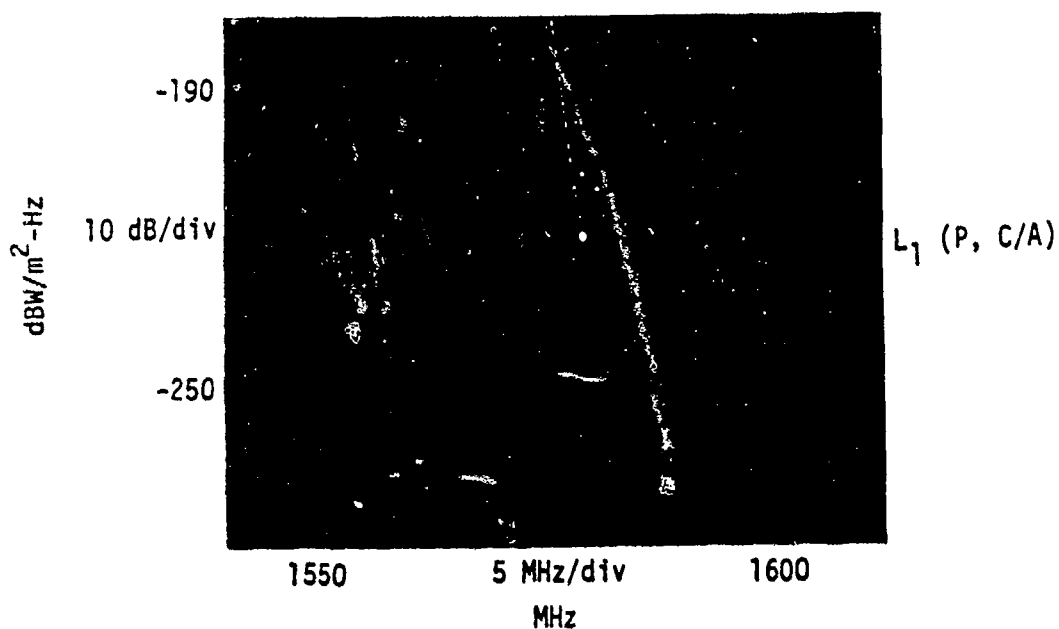


Figure A-19. L₁ (P, C/A) 1550- to 1600-MHz Spectra (CRT Display)

modifies the spectral output for compliance with the requirements levels over the appropriate bandwidths. For these computations the filter was placed in the antenna feed line between the triplexer stopband output and the helix antenna input. The filter would produce identical results if placed between the transmitter output and the input to the appropriate triplexer bandpass filter, which is the approach being considered for NDS 6. The characteristics of the radio astronomy filter used in the analysis are shown in the following listing.

- 1400 - 1427 MHz: 4 cascaded 2-pole (8 poles total)
- 1664.4 - 1668.4 MHz: single-pole
- Insertion loss: L_3 , 1381.05 MHz 0.8 dB
 L_1 , 1575.42 MHz 0.1 dB
- Total weight: 2 lb
- Total volume: 20 in.³

Ninety percent of the estimated weight and volume is attributed to the eight-pole 1420-MHz filter for L_3 with the remainder for the single-pole 1665-MHz filter for L_1 .

Figures A-20 and A-21 are expanded plots of the combined spectra in the region of the 1665-MHz RAS band. Figure A-20 shows the primary 1664.4-MHz to 1668.4-MHz RAS band as a shaded area and the secondary 1660-MHz to 1690-MHz RAS band as dashed lines. Figure A-21 shows that the spectra with the single-pole

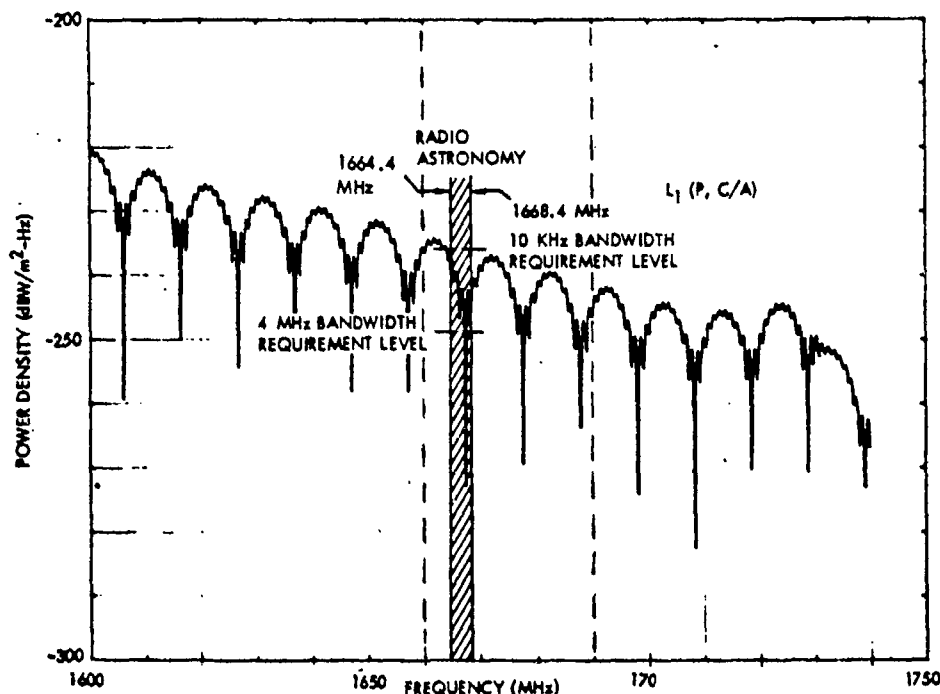


Figure A-20. L_1 Expanded Spectra Plot

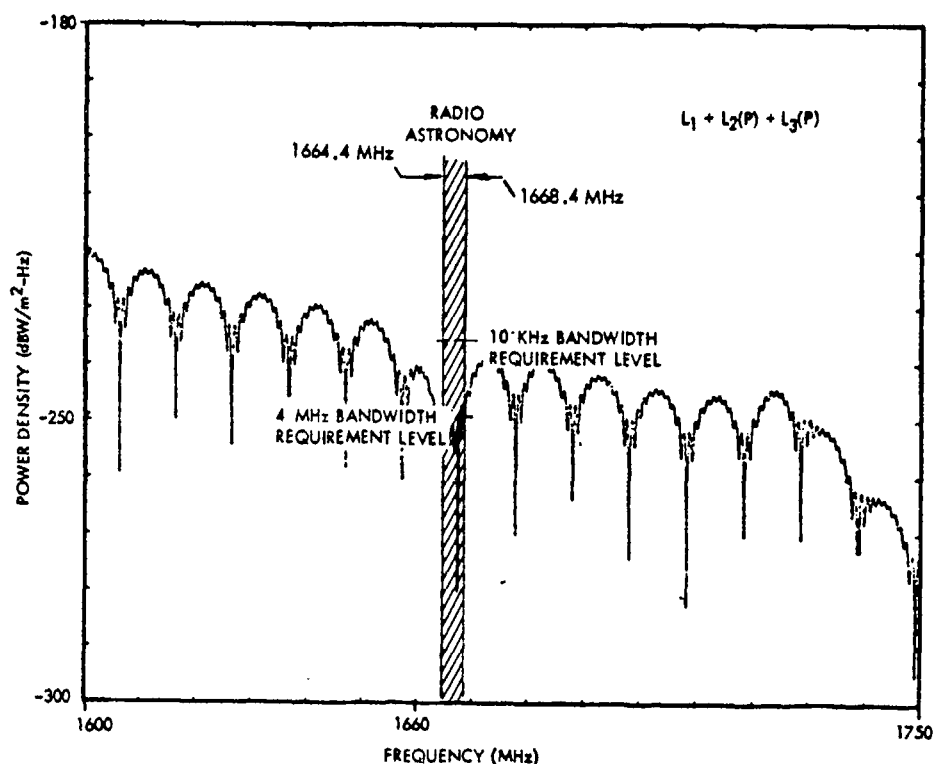


Figure A-21. L_1 Expanded Spectra Plot With 1664.8- to 1668.4-MHz Filter

radio astronomy filter (RAF) does fall below the CCIR 1665-MHz RAS band requirements. No computation was made for a filter that would protect the larger band since it is shared instead of being restricted to RAS use.

Figures A-22 and A-23 show similar combined spectra expanded in the region of the 1420-MHz RAS band. Again, use of the proposed filter reduces the power density below the CCIR RAS requirements. The net effect of these two band reject filters on the overall $L_1/L_2/L_3$ spectra is shown in Figure A-24.

An alternate approach to reducing spectral energy in the 1400- to 1427-MHz band is to consider modifying the triplexer L_3 bandpass filter. The initial concept was to increase the filter selectivity by adding several poles to the present three-pole design. However, this resulted in a significant increase in the size and weight of the triplexer. A variation in which only two poles were added and the bandpass center frequency lowered from L_3 was then considered. In this approach, the offset filter skirt would further reduce the 1400- to 1427-MHz spectral energy to the desired level, consistent with maintaining specified code track sensitivity. Figures A-25 and A-26, which show the computer predictions for this concept, indicate that offsetting the center frequency by 16 MHz should reduce the power density below the required level with only an additional 0.2-dB loss in L_3 signal power.

Since it was not economically practical to verify this approach by modifying a triplexer, a test was run with a 1- to 2-GHz tunable five-pole filter inserted between the transmitter and triplexer as shown in Figure A-27.

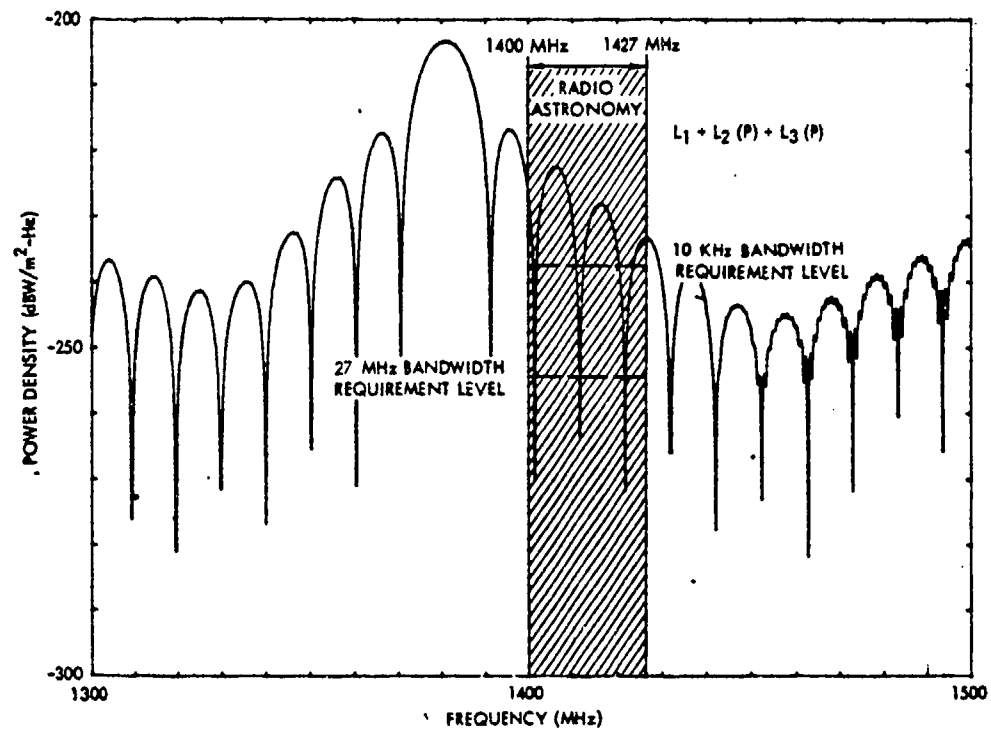


Figure A-22. L_3 Expanded Spectra Plot

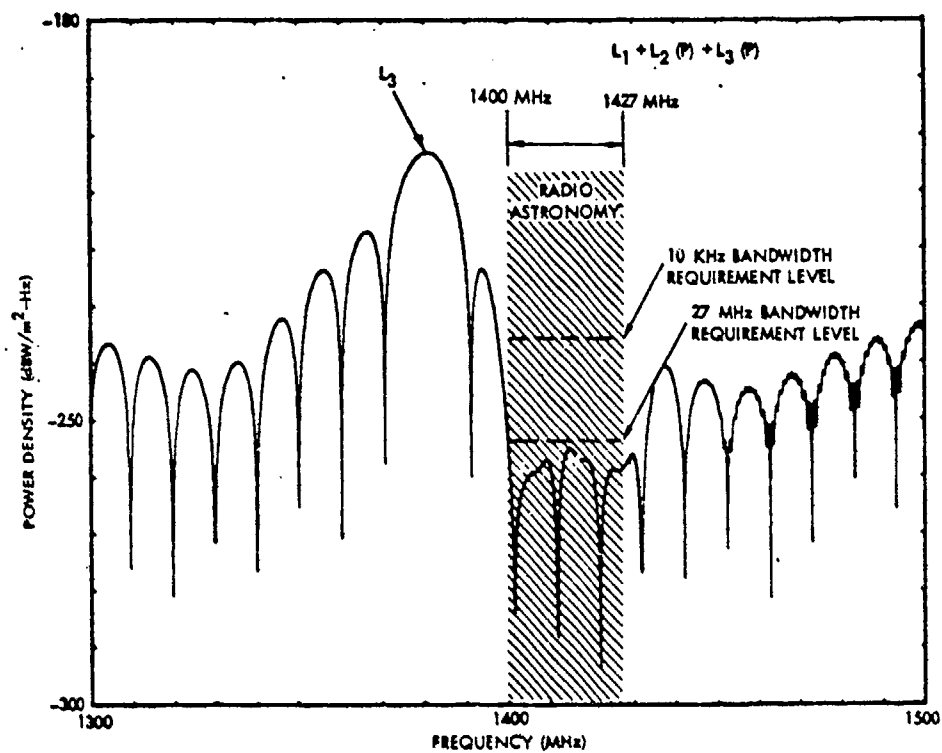


Figure A-23. L_1 , L_2 , L_3 Expanded Spectra Plot With 1400- to 1427-MHz Filter

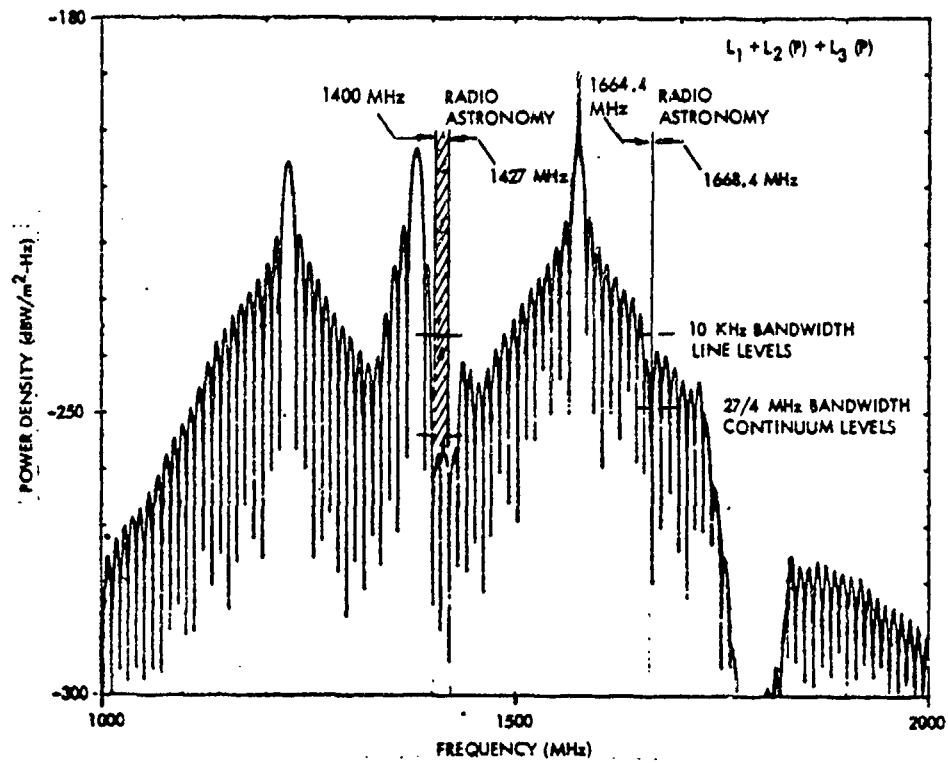


Figure A-24. L_1 , L_2 , L_3 Spectra With 1400- to 1427-MHz
to 1668.4-MHz Filters and 1664.8-

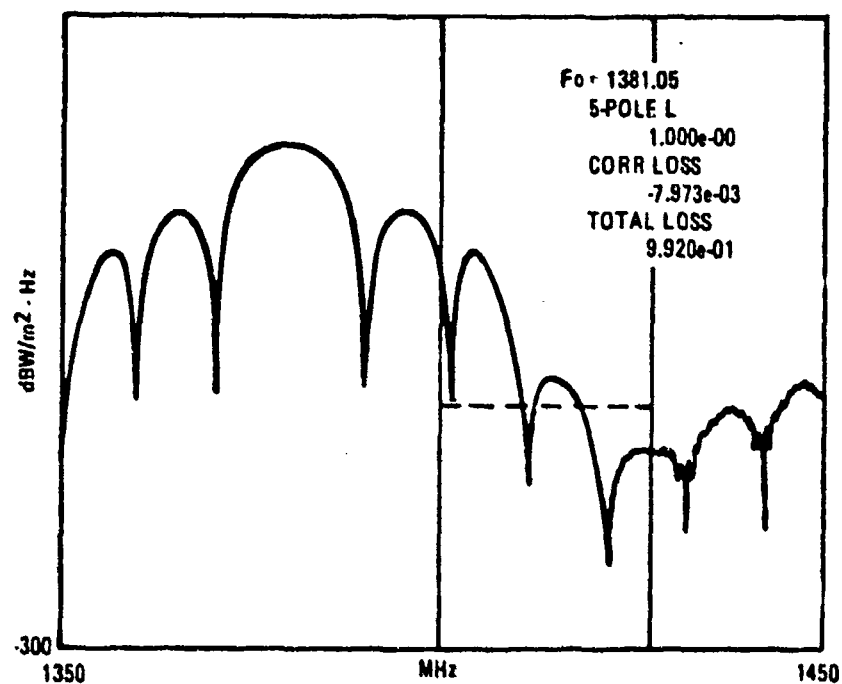


Figure A-25. Five-Pole Bandpass Filter Spectrum
(Computer Prediction)

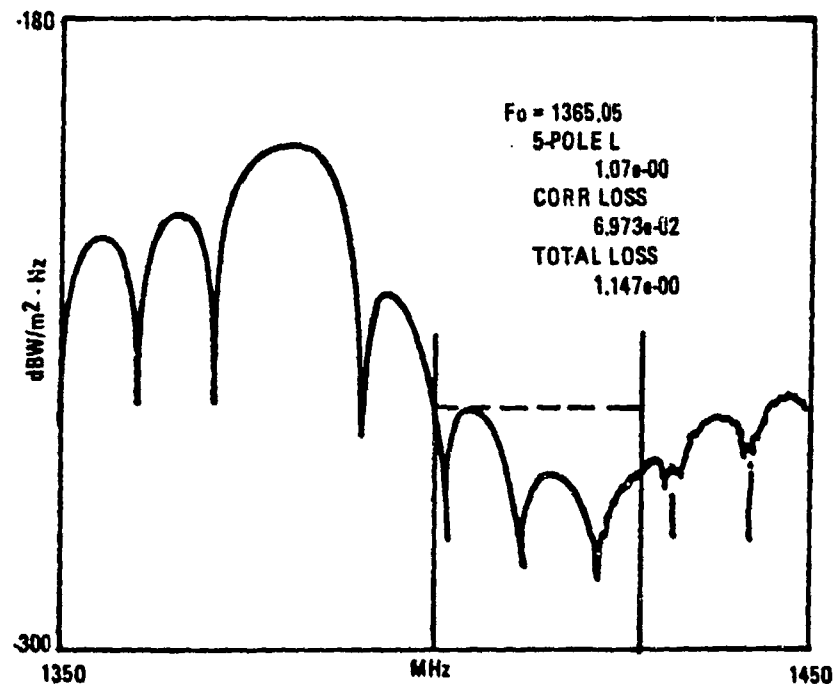


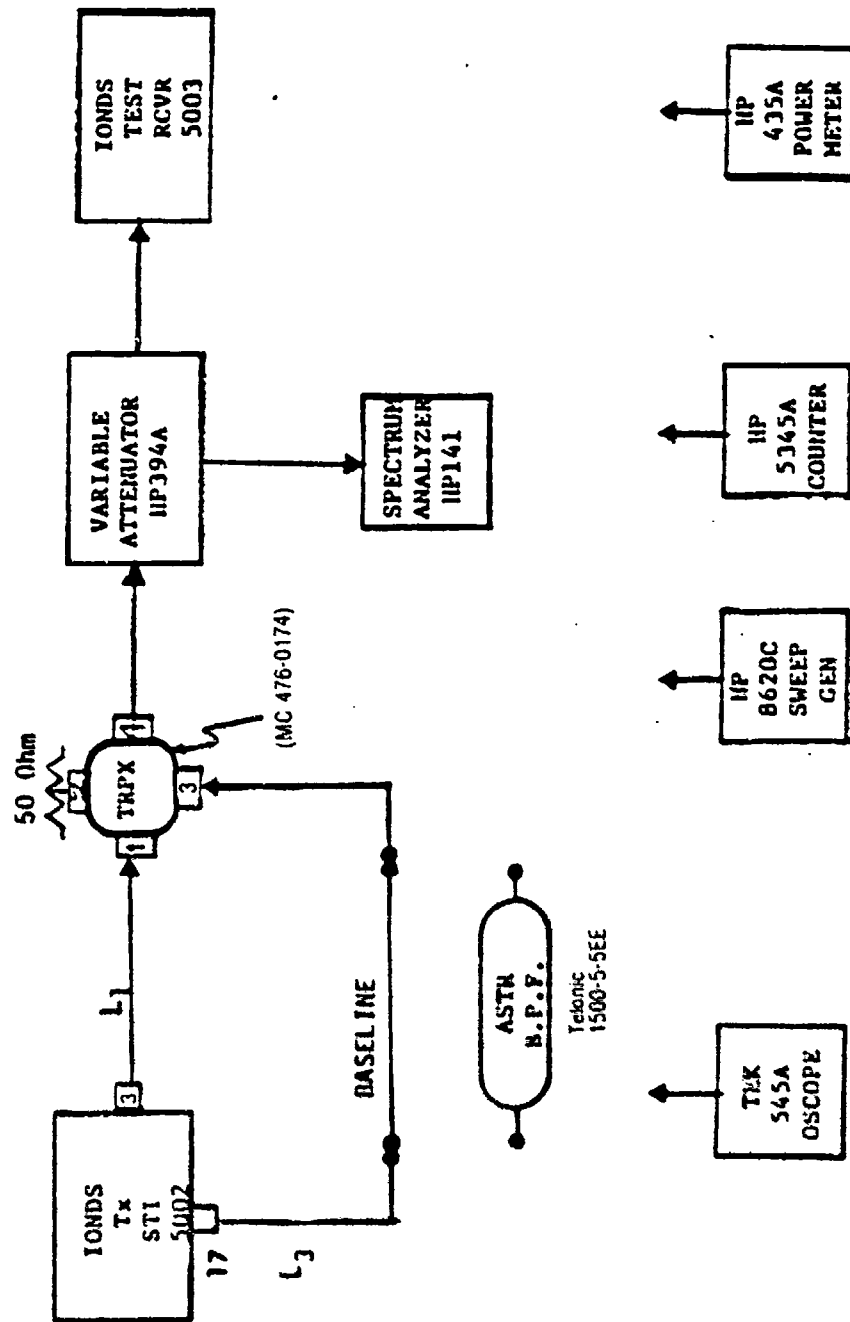
Figure A-26. Five-Pole Bandpass Filter Spectrum With Offset Center Frequency (Computer Prediction)

The IONDS receiver is used in the test to determine the change in tracking sensitivity due to correlation loss as the center frequency is offset. The filter, purchased from Telonic, has an approximate 79-MHz bandwidth and 0.8-dB insertion loss in the frequency range of interest. The filter's frequency response is shown in Figure A-28.

The test results are indicative of a five-pole bandpass filter design in the triplexer even though the triplexer three-pole design and the five-pole tunable filter were included in the testing. This can be seen by noting the approximate change of 1 dB in the second spectra side lobe level without the five-pole tunable filter (Figure A-29) and with the filter (Figure A-30).

The next series of CRT displays (Figures A-31 through A-34) are the data taken as the bandpass center frequency was lowered from the basic L_3 frequency of 1381.05 MHz to 1339.5 MHz. The effect on the L_3 spectrum is obvious, and the resulting correlation loss reduced the tracking sensitivity to as much as 2.5 dB below the -133 dBm specification level.

The data obtained from these tests are summarized in Table A-8 and Figure A-35. A significant change in tracking sensitivity clearly occurs around 1345 MHz, which is where the CRT display began showing a significant change in the center lobe of the L_3 spectrum. Therefore, the optimum bandpass, f_0 , for the five-pole filter appears to be around 1345.5 MHz, where the reduction of the highest spectral side lobe in the RAS band was 25 dB and an L_3 tracking sensitivity of -133.8 dBm was maintained. The spectral energy



ASTRONOMY BAND INTERFERENCE:

- 1400-1427 MHz

MEASUREMENT:

W/O BPF

Figure A-27. Measurement Block Diagram With Tunable Bandpass Filter

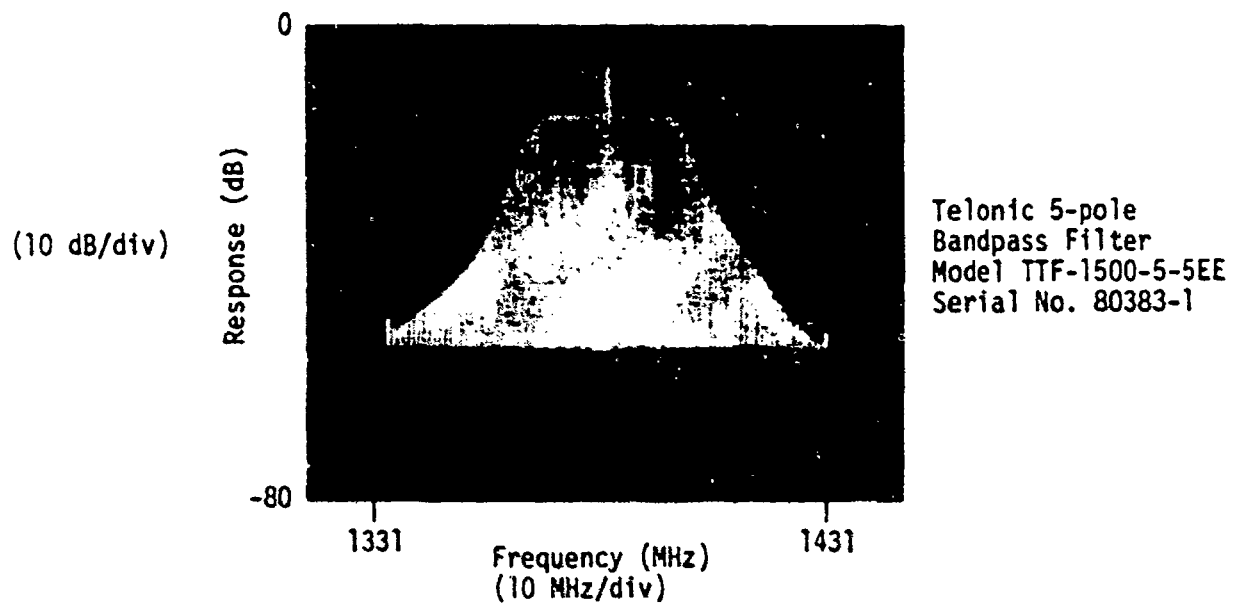


Figure A-28. Five-Pole Filter Pass Band

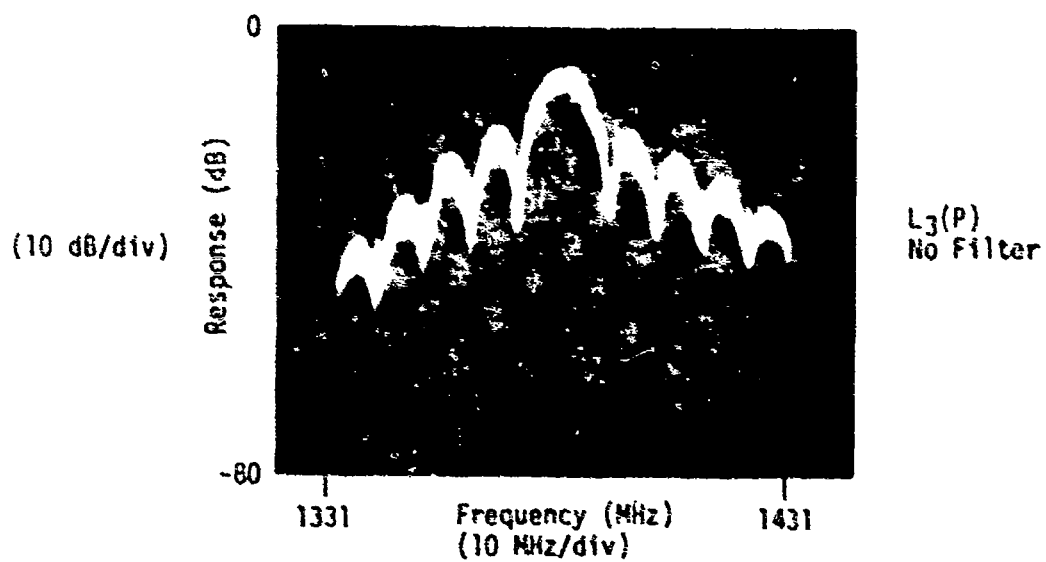


Figure A-29. $L_3(P)$ Spectra With No Filter

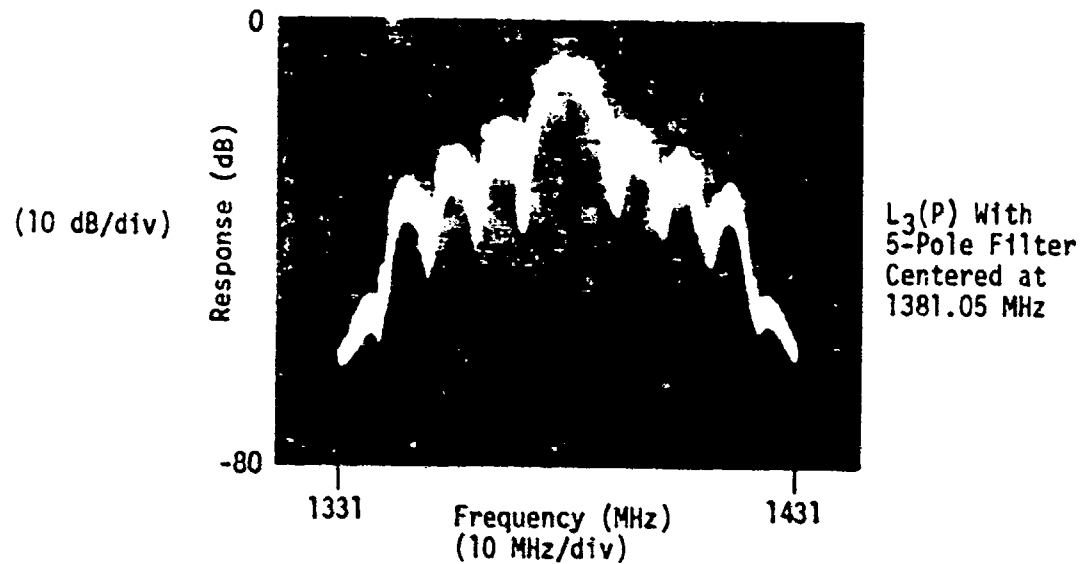


Figure A-30. $L_3(P)$ Spectra With Five-Pole Filter ($f_0 = 1381.05$ MHz)

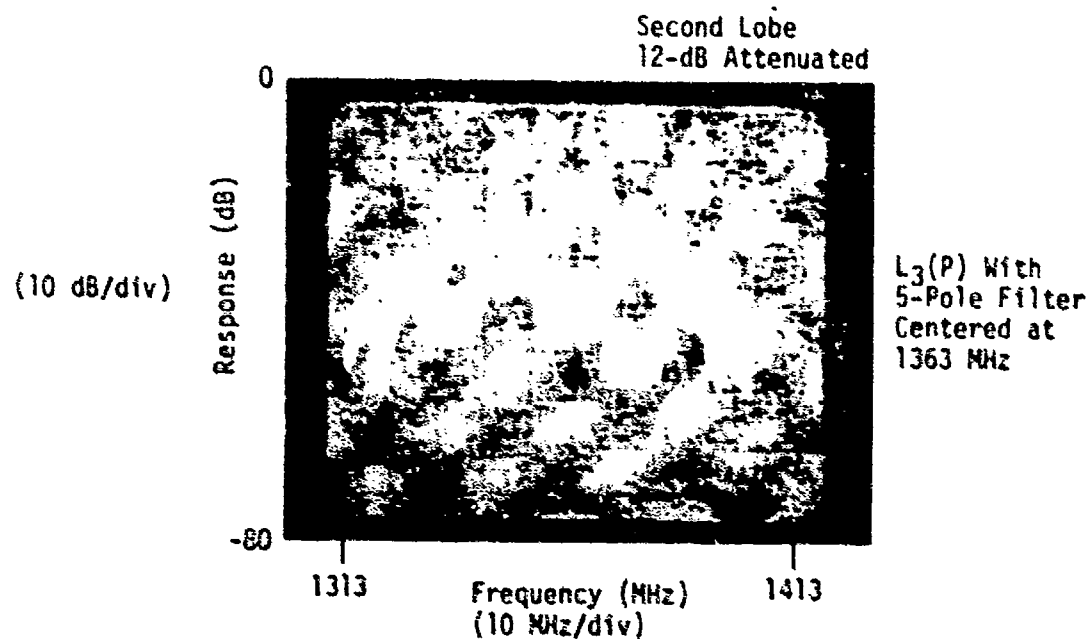


Figure A-31. $L_3(P)$ Spectra With Five-Pole Filter ($f_0 = 1363$ MHz)

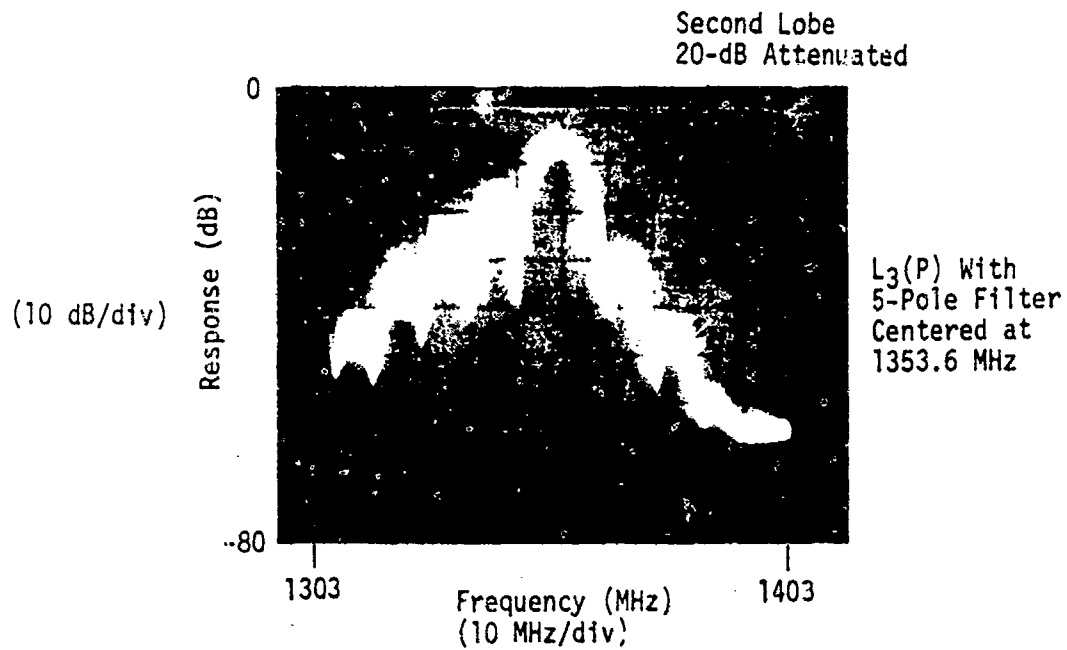


Figure A-32. $L_3(P)$ Spectra With Five-Pole Filter ($f_0 = 1353.6$ MHz)

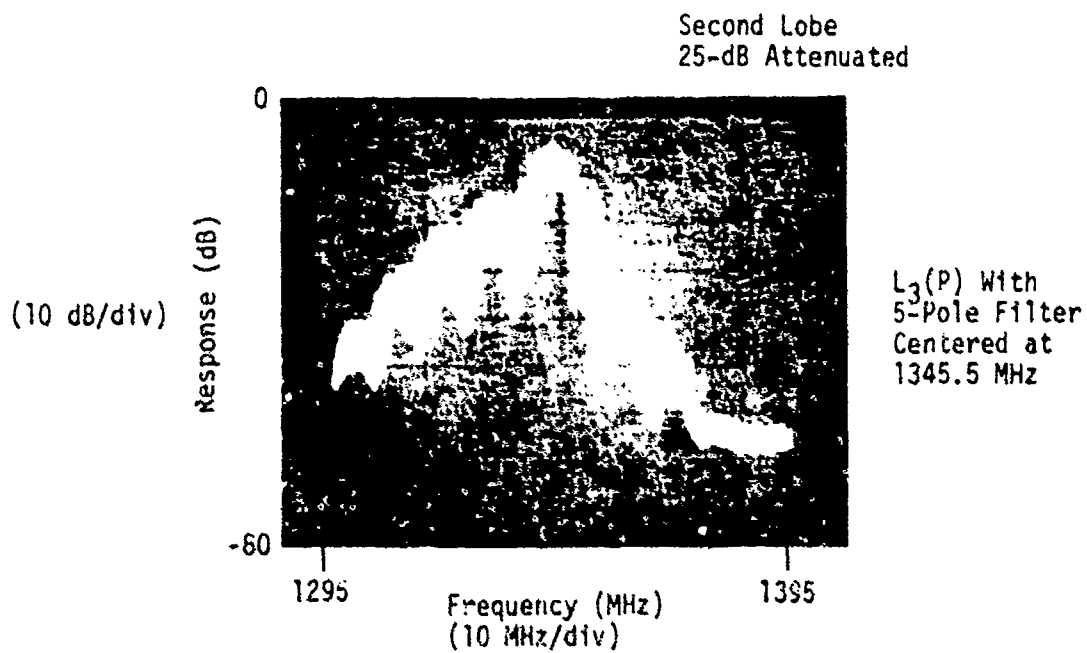


Figure A-33. $L_3(P)$ Spectra With Five-Pole Filter ($f_0 = 1345.5$ MHz)

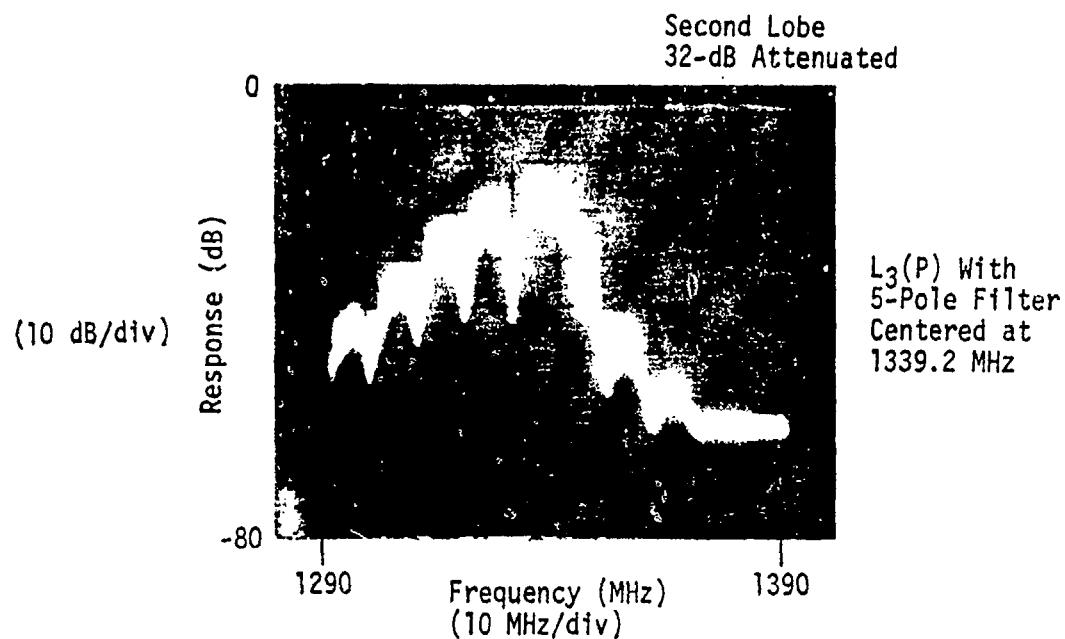


Figure A-34. L_3 (P) Spectra With Five-Pole Filter ($f_o = 1339.2$ MHz).

Table A-8. Tunable Filter Test Summary (Function of Filter Center Frequency)

Configuration (MHz)	Second Lobe Attenuation (dB)	Tracking Sensitivity	
		Measured (dBm)	Loss (dB)
No filter	0	-136.0	0
$f_o = 1381.05$	0	-135.2	0.8
$f_o = 1363.0$	12	-135.0	1.0
$f_o = 1353.6$	20	-134.5	1.5
$f_o = 1345.5^*$	25	-133.8	<u>2.2</u>
$f_o = 1339.5$	32	-130.5	5.5
*1345.5 MHz is acceptable			

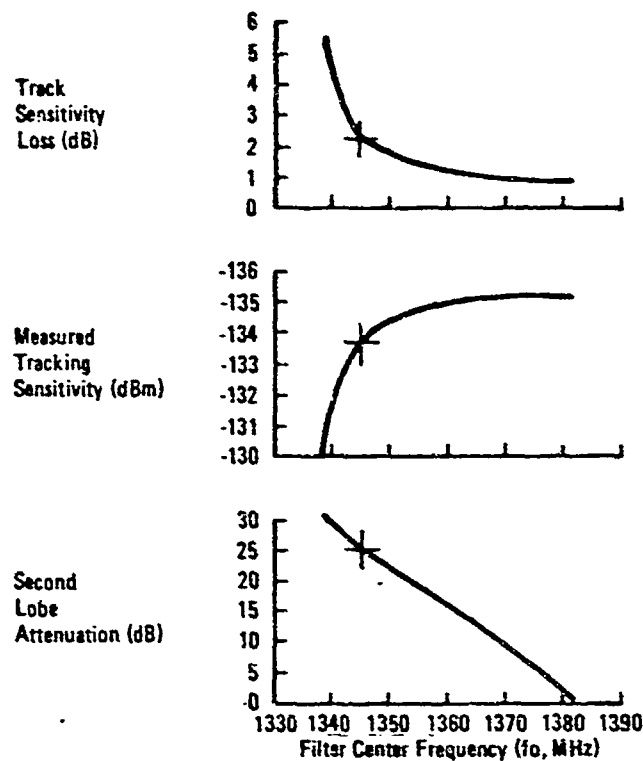


Figure A-35. Tunable Filter Performance
Summary (Function of Filter Center Frequency)

reduction in the 1427-MHz band is more than adequate using the integrated band level as a reference but is still 7 dB short from the worst-case 32-dB level.

Proposed NDS 6 RAS Filter

Following these analyses the decision was made to pursue a band reject filter as the best overall approach. This filter would be for the 1427-MHz band only and would be installed between the L3 transmitters and the triplexer. The selection of the band reject filter over the offset bandpass filter was based on several factors. First, a band reject design is less susceptible to multipacting, which is a major consideration in L-band filter design. Second, a band reject filter provides greater 1427-MHz band protection with less impact on L3 performance (insertion and correlation loss). And third, a reasonably small, low weight unit can be built based on an existing space-qualified design that has performed flawlessly on ATS 6 for more than four years on orbit. The specifications for the unit (Table A-9) are similar to the theoretical unit previously discussed and should have the characteristics shown in Figure A-36. This is a computed curve synthesized with series resonant cavities spaced at $1/4$ intervals on a transmission line. The cavities had the qualities listed in Table A-10 beginning at the input end.

Table A-9. Radio Astronomy Eight-Pole Band Reject Filter Characteristics

Power Handling Capability	25 Watts (Continuous rms Power)
Passband	1360-1390 MHz
Insertion loss at 1381 MHz	≤ 0.7 dB
Insertion loss at 1390 MHz	≤ 2.0 dB
Impedance	50 ohms
VSWR	$\leq 1.2:1$
Operating life	5 years, 7 years design goal
Group delay at 1381 MHz	\pm ns over operating temperature range
Weight	2 pounds
Size	2 x 3 x 7 inches
Connector type	TNC
Space-qualified unit	
Applicable MIL-STD	MIL-STD-1540A MIL-STD-1541A (USAF)
Acceptance test temperature range	-10° to $+61^{\circ}\text{C}$
Quality test temperature range	-20° to $+71^{\circ}\text{C}$

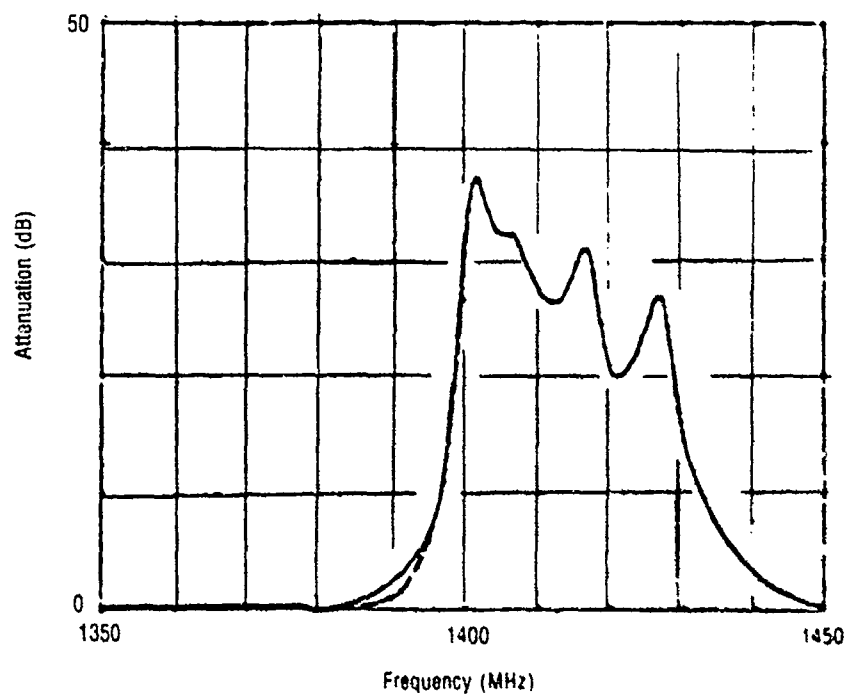


Figure A-36. Proposed Radio Astronomy Filter Attenuation Characteristic

Table A-10. Characteristics of Series-Resonant Cavities
(Eight-Pole Band Reject Filter)

n	f_n	Q_n	Normalized Conductance at f_n
1*	1401.00	450	4
2	1401.00	450	4
3	1407.00	350	5
4	1407.00	350	6
5	1417.05	350	5
6	1417.05	350	5
7	1427.05	350	4
8**	1428.05	350	5
*Input cavity **Output cavity			

RADIO ASTRONOMY SUMMARY AND CONCLUSIONS

Harmful interference power flux density values from Tables A-2 and A-3 do exist in the theoretical spectra plots corresponding to L_1 (P, C/A) and L_3 (P) modulation code conditions. It is evident that continuous transmission of the L_3 spectrum would be of most concern since it does exceed the desired level for the 1400- to 1427-MHz worldwide radio astronomy allocation continuum by as much as 32 dB on a worst-case basis (Figure A-22). Considerable improvement in the potential L_3 interference levels can be obtained by considering the L_3 duty cycle to radio astronomy integration time or using the integrated or average value of spectra energy over a band rather than peak levels or both (Figure A-10). Because of these factors, an in-line L_3 notch filter with a nominal 27-dB attenuation would be sufficient to fully protect the band.

In the normal mode, the L_3 transmitter operates only when it detects an event and then only long enough (normally much less than one minute) to get the data to the ground. Random triggers from cosmic particles and very powerful lightning strokes can trigger the system; however, operational transmissions will be quite infrequent. A test/calibrate mode will also be used approximately weekly once the system is established. Considering both modes there should be less than five minutes of transmission per day per satellite. Therefore, even without a radio astronomy filter, the infrequent, low-power transmissions of L_3 are not expected to affect radio astronomers, who integrate signals over long periods, which is the basis for the developmental frequency approval.

The L_1 spectrum has much less impact on the worldwide radio astronomy band of 1664.4- to 1668.4-MHz, as shown in Figure A-20. However, reduction in interference levels based on duty cycle is not possible since L_1 is transmitted continuously.

GPS L_1 transmission can be forecasted over the earth's surface and radio astronomy measurements appropriately eliminated or judged separately at 1665 MHz during interference periods. Announcements to the radio astronomy community concerning schedule and test periods with space vehicle coordinates could alleviate this potential interference.

One approach to reducing both the L_1 and L_3 interference is to use filters in the transmit lines to limit spectra to the desired levels. Band reject filters would result in an insertion loss at L_1 and L_3 of 0.1 and 0.8 dB, respectively. Another method of reducing spectral energy to the desired level is to modify the existing three-pole bandpass filter in the L_3 triplexer arm. Replacing the three-pole bandpass filter with a five-pole design and lowering the center frequency to approximately 1365 MHz should achieve the results as shown in the computer plot in Figure A-26. The additional insertion loss, compared to the three-pole design, is approximately 0.5 dB, for a total loss of approximately 1.2 dB.